

**Novel Graphene-modified Carbon Electrodes for
Trace Electroanalytical Determination of L-
Tyrosine, Dopamine and Uric Acid**

BY

NADEEM BAIG

A Dissertation Presented to the
DEANSHIP OF GRADUATE STUDIES

KING FAHD UNIVERSITY OF PETROLEUM & MINERALS

DHAHRAN, SAUDI ARABIA

In Partial Fulfillment of the
Requirements for the Degree of

DOCTOR OF PHILOSOPHY

In

CHEMISTRY

MAY 2017

KING FAHD UNIVERSITY OF PETROLEUM & MINERALS

DHAHRAN- 31261, SAUDI ARABIA

DEANSHIP OF GRADUATE STUDIES

This thesis, written by **NADEEM BAIG** under the direction of his thesis advisor and approved by his thesis committee, has been presented and accepted by the Dean of Graduate Studies, in partial fulfillment of the requirements for the degree of **DOCTOR OF PHILOSOPHY IN CHEMISTRY**.


5/6/2017

Dr. Abdulaziz Al-Saadi
Department Chairman

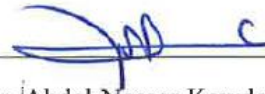


Dr. Salam A. Zummo
Dean of Graduate Studies



8/6/17

Date



Dr. Abdel-Nasser Kawde
(Advisor)



Dr. Abdalla Mahmoud
Abulkibash
(Member)



Dr. Anvarhusein A. Isab
(Member)



Dr. Saviour A. Umoren
(Member)



Dr. Mohammed A. Morsy
(Member)

© NADEEM BAIG

2017

| Dedicated to my beloved parent, brothers, sister and to my wife |

ACKNOWLEDGMENTS

First and foremost I want to thank Almighty Allah who is most Beneficent and Merciful for His countless blessings and giving me the courage to accomplish this work successfully. I want to pay my gratitude to our beloved Prophet Hazrat Muhammad (PBUH) for guidance us to the right path and providing the best teaching in every department of life. His life is a real source of light and knowledge. He taught us what the priority of knowledge is for a person.

A good research work could not be completed without a healthy supervision. I want to say thanks to all of my committee members for being a part of my thesis. I am very grateful to Dr. Abdel-Nasser Kawde for his active supervision, caring and excellent guidance. He tried his best to provide creative atmosphere. I really appreciate his behavior, time and all efforts he has made to arrange materials for completion of research. His knowledge, expertise and encouraging behavior help a lot to complete the work in short time. I am thankful to King Fahd University of Petroleum and Mineral for providing me the opportunity and support to excel my education career. Special thanks to KFUPM chemistry department for facilitating the healthy research environment and providing the well-equipped labs. All lab colleagues, the chemistry department staff, and my friends made the research more interesting. Their suggestions and conversation help me to further proceed in research

I want to pay my humble gratitude to my beloved mother and my late father. Their prayers help to achieve this goal. My father was passed during this period; he always has pleasing words for me. I want to say thanks for all of his efforts to reach this stage. Both of you pave the way for me to achieve success in life. Thanks to my brothers and sister

for supporting me. Finally, I want to say thanks to my wife for understanding the situation and supporting me to complete the research.]

TABLE OF CONTENTS

ACKNOWLEDGMENTS	V
TABLE OF CONTENTS	VII
LIST OF TABLES	XI
LIST OF FIGURES	XIII
LIST OF ABBREVIATIONS	XXI
ABSTRACT	XXII
ملخص الرسالة	XXV
CHAPTER 1 INTRODUCTION	1
1.1 Significance of L-Tyrosine, Dopamine and Uric Acid	2
1.2 Glassy Carbon and Graphite Pencil Electrodes	4
1.3 Graphene as a Modifying Material.....	5
1.4 Modified Carbon Electrodes for Electrochemical Sensing.....	6
CHAPTER 2 LITERATURE REVIEW	7
2.1 Challenges in the Individual and Simultaneous Sensing of Targeted Analytes.....	8
2.2 Characteristics and a Brief Overview of the Modification Materials.....	10
2.2.1 Carbon Nanotubes	10
2.2.2 Graphene.....	12
2.2.3 Polymer Films.....	15
2.2.4 Ionic Liquids.....	17
2.3 A Comparison of the Modified Electrodes for Simultaneous Sensing of AA,UA and DA.....	19
2.3.1 Carbon Nanotubes Modified Electrodes	19
2.3.2 Graphene Modified Electrodes	27
2.3.3 Polymer Films Modified Electrodes.....	39
2.3.4 Ionic Liquid Modified Electrodes	54
2.3.5 Other Electrodes	Error! Bookmark not defined.

2.4	Challenges in Modified Electrodes' Commercialization and Real Sample Application	62
-----	--	----

CHAPTER 3..... 68

A NOVEL, FAST AND COST EFFECTIVE GRAPHENE - MODIFIED GRAPHITE PENCIL ELECTRODE FOR TRACE QUANTIFICATION OF L-TYROSINE, DOPAMINE AND URIC ACID..... 68

3.1	Introduction.....	69
-----	-------------------	----

3.2	Materials and Methods.....	73
-----	----------------------------	----

3.2.1	Reagents.....	73
-------	---------------	----

3.2.2	Apparatus	73
-------	-----------------	----

3.2.3	Preparation of Modified GPEs.....	74
-------	-----------------------------------	----

3.3	Results and Discussion	75
-----	------------------------------	----

3.3.1	Characterization and Optimization of Synthesized Graphene Oxide.....	75
-------	--	----

3.3.2	Morphological and Electrochemical Characterization	75
-------	--	----

3.3.3	Ionic Medium Supported Graphene Oxide (IM-GO) Reduction on GPE.....	82
-------	---	----

3.3.4	Optimization of IM-GO.....	83
-------	----------------------------	----

3.3.5	A Novel, Fast and Cost effective Graphene – modified Graphite Pencil Electrode for Trace Quantification of L-Tyrosine	85
-------	---	----

3.3.6	A Single Step Fast and Facile Fabrication of the Single-use Ionic Medium Supported-reduced Graphene Oxide Sensor for Sensitive and Selective Determination of Dopamine.....	97
-------	---	----

3.3.7	A Cost Effective Single-use Disposable Electrodes Based on Acetate Medium Supported-reduced Graphene Oxide for Sensitive and Selective Detection of Uric Acid in Human Urine	114
-------	--	-----

CHAPTER 4..... 130

HIGHLY SENSITIVE PLATINUM NANOPARTICLES SANDWICHED IN GRAPHENE LAYERS MODIFIED GRAPHITE PENCIL ELECTRODE FOR TRACE LEVEL QUANTIFICATION OF DOPAMINE..... 130

4.1	Introduction.....	131
-----	-------------------	-----

4.2	Materials and Methods.....	133
-----	----------------------------	-----

4.2.1	Reagents.....	133
-------	---------------	-----

4.2.2	Apparatus	133
-------	-----------------	-----

4.2.3	Fabrication of Pt NPs Sandwiched Graphene Layers GPEs Sensor.....	133
-------	---	-----

4.3	Results and Discussions.....	134
-----	------------------------------	-----

4.3.1	Experimental Conditions Optimization	134
-------	--	-----

4.3.2	Characterization of Synthesized Graphene Oxide and Fabricated Sensor	135
-------	--	-----

4.3.3	Scan Rate Study	141
4.3.4	pH Study of the Electrolyte	144
4.3.5	Optimization of Sensing Technique.....	145
4.3.6	Detection of Dopamine, Reproducibility, and Limit of Detection	145
4.3.7	Real Sample Analysis and the Interferences Study	148
CHAPTER 5.....		152
A COST-EFFECTIVE DISPOSABLE GRAPHENE-MODIFIED ELECTRODE DECORATED WITH ALTERNATING LAYERS OF Au NPS FOR THE SIMULTANEOUS DETECTION OF DOPAMINE AND URIC ACID IN HUMAN URINE.....		152
5.1	Introduction.....	153
5.2	Materials and Methods.....	156
5.2.1	Reagents.....	156
5.2.2	Apparatus	156
5.2.3	Fabrication of GR/Au/GR/Au/GPE Sensor	156
5.3	Results and Discussion	156
5.3.1	Characterization of the Synthesized Graphene Oxide	156
5.3.2	Optimization of the Conditions for Fabrication of a Sensitive Sensor	157
5.3.3	Combination of Au NPs and Graphene Layers Patterned onto the Electrode Surface, and Stepwise Morphological Characterization of the Sensing Surface	162
5.3.4	Electrochemical and Kinetics Study of the Modified Electrode	165
5.3.5	Study of pH.....	174
5.3.6	Optimization of the SWV.....	176
5.3.7	The Simultaneous Detection of DA and UA, Reproducibility, and the Detection Limit	177
5.3.8	Comparison with Previously Described Graphene Composites and, Particularly, with Au NP Graphene Composites.....	181
5.3.9	Actual Sample and Interference Studies	182
CHAPTER 6.....		186
SINGLE STEP ELECTROCHEMICALLY FABRICATED OPTIMIZED EXTENDED GRAPHENE-METHYLENE BLUE LAYERED NANOCOMPOSITE MODIFIED DISPOSABLE COST-EFFECTIVE GRAPHITE PENCIL ELECTRODE FOR THE SIMULTANEOUS SENSITIVE SENSING OF DA, UA AND L-TYROSINE IN HUMAN URINE.....		186
6.1	Introduction.....	187
6.2	Materials and Methods.....	189

6.2.1	Reagents.....	189
6.2.2	Apparatus.....	190
6.2.3	Preparation of Modified GPE	190
6.3	Results and Discussion	190
6.3.1	Optimization of Various Parameters for Effective Reduction of MB-GO on GPE.....	190
6.3.2	Characterization by FE-SEM and Raman Spectroscopy.....	191
6.3.3	Electrochemical Investigation of the GPE Surface and its Interaction with MB-GO	196
6.3.4	Study of pH Effect.....	198
6.3.5	Optimization of the Sensing Technique	202
6.3.6	Simultaneous Sensing of Dopamine, Uric acid, L-Tyrosine, Limit of Detection, and Reproducibility.....	202
6.3.7	Distinguish Characteristics of MB-GR/GPE over other Graphene-Based Sensors.....	205
6.3.8	Application and Interference Study	209
CHAPTER 7	211
CONCLUSION	211
REFERENCES	215
VITAE	250

LIST OF TABLES

Table 2- 1: Comparison of figure of merits for simultaneous sensing of AA, DA and UA using CNTs modified electrodes	29
Table 2- 2: Figure of merits comparison for the simultaneous sensing of AA, DA and UA using various graphene and its composite modified electrodes	40
Table 2- 3: Figures of merits comparison for simultaneous detection of AA, DA and UA utilizing polymer film modified electrodes.....	55
Table 2- 4: Figures of merits comparison for simultaneous detection of AA, DA and UA using ionic liquid modified electrodes.	59
Table 2- 5: Figures of merits comparison for simultaneous detection of AA, DA and UA using pretreated, surfactant or nanoparticles modified electrodes.	63
Table 3- 1: Comparison of the GR-modified GPE properties to those of other modified electrodes for the determination of the L-tyrosine in a sample.	94
Table 3- 2: Determination of L-tyrosine in human urine samples.....	96
Table 3- 3: Comparison of the developed electrode with previously reported graphene and graphene composite electrodes.	109
Table 3- 4: Detection of dopamine in human urine sample.....	113
Table 3- 5: Comparison of the dERGO-GPE with the previously graphene and graphene composite modified electrodes.....	126
Table 3- 6: Study of the uric acid recoveries in the human urine sample.....	127
Table 4- 1: Comparison of the GR/Pt/GR/GPE with the reported graphene nanocomposite modified sensors	150

Table 4- 2: Determination of DA in the human urine sample	151
Table 5- 1: Comparison of the fabricated electrochemical sensor with previously reported graphene modified sensors	183
Table 5- 2: Determination of dopamine and uric acid in the human urine sample.....	185
Table 6- 1: Comparison of MB-GR/GPE with reported graphene-based sensors	207
Table 6- 2: Determination of dopamine, uric acid and L-tyrosine by MB-GR/GPE in the human urine sample	210

LIST OF FIGURES

- Figure 3- 1: (A) FTIR spectra of graphite (a) and GO (b), and (B) Raman spectra of graphite (a) and GO (b). Inset of B shows the graphite Raman spectrum.78
- Figure 3- 2: FE-SEM images at three different magnifications: 10 μm (A), 5 μm (B), and 500 nm (C) of bare (a) or GR-modified GPE (b).79
- Figure 3- 3: Cyclic Voltammograms obtained from a solution comprising 5 mM $\text{K}_3\text{Fe}(\text{CN})_6/\text{K}_4\text{Fe}(\text{CN})_6$ and 0.1 M KCl (A) Bare GPE and (B) dERGO-GPE at different scan rates of (a) 20 (b) 40, (c) 60, (d) 80, and (e) 100 mVs^{-1} . The insets in (A) and (B) show the linear relationship between current and the square root of the scan rates.80
- Figure 3- 4: (A) Nyquist and (B) bode phase plots of 5 mM $\text{K}_3\text{Fe}(\text{CN})_6/\text{K}_4\text{Fe}(\text{CN})_6$ in 0.1 M KCl solution on (a) IM-rGO/GPE, and (b) bare GPE upon application of frequency range from 0.01 Hz to 100 kHz. (C) CVs of (a) IM-rGO and (b) bare GPE were recorded at 0.1 V/s in a 1 mM dopamine 0.1M PBS buffer (pH 6.8).81
- Figure 3- 5: Cyclic voltammograms of 2 mM $\text{K}_3\text{Fe}(\text{CN})_6/\text{K}_4\text{Fe}(\text{CN})_6$ in 0.1 M KCl solution using (A) w-rGO/GPE, (B) pc-rGO/GPE, (C) pb-rGO/GPE, and (D) ac-rGO/GPE at scan rates of (a) 20, (b) 40, (c) 60, (d) 80, and (e) 100 mV/s . The insets in (A), (B), (C), and (D) show the linear relationship between current and the square root of the scan rates ($v^{1/2}$).84
- Figure 3- 6: Cyclic voltammograms of (a) the bare GPE, and (b) the GR-modified GPE in a 1 mM L-tyrosine PBS buffer (0.1 M, pH 6.7). Scan rate: 100 mV s^{-1} ...86
- Figure 3- 7: Square wave voltammograms of 50 μM L-tyrosine in 0.1 M PBS (pH 6.7) on the (a) bare GPE, (b) pretreated GPE, and (c) GR-modified GPE. The parameters of the SWV experiment: amplitude 0.03 V, frequency 50 Hz, and adsorption time 210 s.87
- Figure 3- 8: (A) Square wave voltammograms in a 50 μM L- tyrosine 0.1 M L^{-1} PBS solution at various pH values (a) 7.5 pH, (b) 7.0 pH, (c) 6.7 pH, (d) 6.0 pH, (e) 5.5 at GR-modified GPE. (B) Graphical representation of the peak current vs. pH. Inset: Relationship between the pH and the oxidation peak potential.89

Figure 3- 9: Plots of the current vs. amplitude (A) or frequency (B), and adsorption time (C) obtained from the square wave voltammograms collected from 50 μ M L-tyrosine in a PBS buffer (0.1 M, 6.7 pH).	91
Figure 3- 10: (A) Square wave voltammograms in PBS buffer (0.1 M, pH 6.7) at various concentrations of tyrosine: (a) 0, (b) 0.8, (c) 2, (d) 5, (e) 10, (f) 20, (g) 30, (h) 40, (i) 50, (j) 60 μ M. The graph (B) showed the linear relationship between I (μ A) and the concentration (μ M) of L-tyrosine ($R^2 = 0.9995$), with the error bars. The SWV parameters were: amplitude of 0.03 V, frequency of 50 Hz, and adsorption time of 210 s.	93
Figure 3- 11: CVs of (a) IM-rGO and (b) bare GPE were recorded at 0.1 V/s in a 1 mM dopamine 0.1M PBS buffer (pH 6.8).	98
Figure 3- 12: (A) Cyclic voltammograms of 1mM dopamine in PBS buffer (0.1 M, pH 6.8) using (A) IM-rGO/GPE at scan rates of (a) 50, (b) 100, (c) 150, (d) 200, (e) 250, and (f) 300 mV/s ; or using (B) the bare GPE at scan rates of (a) 50, (b) 100, (c) 150, (d) 200, and (e) 250 mV/s. (C) The cyclic voltammograms of 1mM dopamine using IM-rGO/GPE at higher scan rate (a) 500, (b) 600, (c) 700, (d) 800, and (e) 900 mV/s. (D) The linear relationship between $\log v$ vs. (a) anodic and (b) cathodic peak potential of the cyclic voltammograms at 500 to 900 mV/s. The insets in (A) and (B) show the linear relationship between current and the square root of the scan rates ($v^{1/2}$).....	99
Figure 3- 13: (A) Multiple cyclic voltammograms at 0.1 V/s scan rate on IM-rGO/GPE surface for 0.2 mM dopamine in 0.1 M PBS buffer (pH 6.8).	104
Figure 3- 14: (A) Square wave voltammograms in 0.1 M PBS solution containing 50 μ M dopamine at various pH values (a) 5.0, (b) 5.5, (c) 6.0, (d) 6.5, (e) 7.0, (f) 7.5, and (g) 8.0 pH at IM-rGO/GPE. (B) Graph indicated the relationship between pH and peak current and Inset is showing the relationship between the peak potential and pH of the sensing medium	105
Figure 3- 15: Plots of the oxidation peak current vs. amplitude (A), frequency (B), at 30s adsorption time and adsorption time (C) obtained from the square wave voltammograms collected from 20 μ M dopamine in a PBS buffer (0.1 M, 6.5 pH).	107

- Figure 3- 16: Square wave voltammograms at various concentrations of dopamine: (a) 0, (b) 0.4, (c) 0.5, (d) 1, (e) 3, (f) 5, (g) 10, (h) 15, (i) 25, (j) 30 μM . The inset shows the linear relationship between oxidation peak current (μA) and the concentration (μM) of dopamine ($R^2 = 0.998$).....108
- Figure 3- 17: Square wave voltammetric response of 15 μM dopamine in the presence of 1mM ascorbic acid. Inset showing the ascorbic acid peak current.112
- Figure 3- 18: CVs of (a) the bare GPE, and (b) the ac-dERGO/ GPE in PBS buffer (0.1 M, pH 6.8) containing 1 mM uric acid. Scan rate: 100 mV s^{-1}118
- Figure 3- 19: Cyclic Voltammograms obtained from a solution comprising 0.2 mM uric acid (A) Bare GPE, (B) w-dERGO/GPE, and (C) ac-dERGO/GPE at different scan rates of (a) 20 (b) 40, (c) 60, (d) 80, and (e) 100 mVs^{-1} . The insets in (A), (B) and (C) show the linear relationship between current and the square root of the scan rates.....120
- Figure 3- 20: (A) Square wave voltammograms in 0.1 M PBS solution containing 10 μM uric acid at various pH values (a) 8.0 , (b) 7.5 , (c) 6.8 , (d) 6.5 , (e) 6.0 at ac-dERGO/GPE. (B) Graphical representation of the peak current vs. pH. Inset is relationship between the pH vs. the oxidation peak potential.....121
- Figure 3- 21: The corresponding plots of the oxidation peak current vs. (A) amplitude, (B) frequency, and (C) adsorption time obtained from the square wave voltammograms collected for 10 μM uric acid in a PBS buffer (0.1 M, 6.8 pH).122
- Figure 3- 22: Square wave voltammograms in PBS buffer (0.1 M, pH 7.0) at various concentrations of uric acid: (a) 0, (b) 0.2, (c) 0.5, (d) 2, (e) 6, (f) 10, (g) 14, (h) 18 and (i) 22 μM . The inset shows the linear relationship between I (μA) vs. concentration (μM) of uric acid ($R^2 = 0.996$). The SWV parameters were: amplitude of 0.03 V, frequency of 50 Hz, and adsorption time of 120 s.....125

Figure 3- 23: (A) Square wave voltammograms of 500 μ M ascorbic acid in the presence of 50 μ M uric acid before (A) and after (B) optimization. Parameters for (A): amplitude 0.02V, frequency 25 Hz, and adsorption time 30s. Parameters for (B): the amplitude of 0.03 V, frequency of 50 Hz, and adsorption time of 120 s.....	128
Figure 4- 1: The corresponding histogram for the oxidizing peak current of cyclic voltammograms for 0.2 mM dopamine in 0.1 M PBS (pH 6.80) at various modified electrode surfaces.	136
Figure 4- 2: (A) Nyquist plot of 5 mM $K_3Fe(CN)_6/K_4Fe(CN)_6$ in 0.1 M KCl solution at the (a) bare GPE, (b) GR/Pt/GR/GPE, and (c) GR/GPE by applying of 5 mV potential in the frequency range 100 to 0.01 Hz. (B) CVs of 0.2 mM DA in 0.1 M PBS buffer (pH 5.5) at the (a) bare GPE, (b) GR/GPE, and (c) GR/Pt/GR/GPE at scan rate 0.15 V/s. Inset B is the histogram of the oxidation peak current (OP) and reduction peak current (RP) on various electrode surfaces.	138
Figure 4- 3: FE-SEM images at two magnifications (A) 1 μ m and (B) 500 nm of the (a) bare/GPE, (b) GR/GPE (c) GR/Pt/GR/GPE.....	139
Figure 4- 4: FE-SEM image of GR/Pt/GR/GPE by using (A) back scattering electron beam (BSE) and (B) secondary electron beam (SE).....	140
Figure 4- 5: Cyclic Voltammograms obtained from solution containing 0.2 mM dopamine in PBS buffer (0.1M, pH 5.5) using (A) GR/GPE and (B) GR/Pt/GR/GPE at scan rates of (a) 50, (b) 100, (c) 150, (d) 200 , (e) 250 mV/s. The insets in (A) and (B) shows the linear relationship between current and the square root of scan rates. (C) The cyclic voltammograms of 0.2 mM dopamine using GR/GPE at higher scan rate (a) 400, (b) 500, (c) 700, (d) 800, and (e) 900 mV/s. (D) The linear relationship between Log v vs. (a) anodic and (b) cathodic peak potential obtained by cyclic voltammograms from 400 to 900 mV/s.....	142

Figure 4- 6: (A) CVs obtained from solution containing 0.5 mM dopamine in 0.1 M PBS solution at various pH values (a) 5.0, (b) 5.5, (c) 6.0, (d) 6.5, (e) 7.0, (f) 7.5 pH at GR/Pt/GR/GPE. (B) Graphical representation of the peak current vs. pH for dopamine. Inset is showing the relationship between the pH and the oxidation peak potential.....	146
Figure 4- 7: Plots of the oxidation peak current of SWV vs. amplitude (A), frequency (B) collected at 20 μ M and 10 μ M dopamine, respectively (10 s adsorption time) and adsorption time (C) for 10 μ M dopamine obtained from the SWVs in a PBS buffer (0.1 M, 5.5 pH).....	147
Figure 4- 8: SWVs of various concentration of dopamine in PBS buffer (0.1 M, pH 5.5) at (a) 0, (b) 0.06, (c) 0.08, (d) 0.3, (e) 0.5, (f) 1, (g) 3, (h) 5, (i) 10, (j) 15, (k) 20 μ M. The inset shows the linear relationship between I (μ A) and concentration. SWV parameters: amplitude 0.06 V, frequency 80 Hz and adsorption time 120s.	149
Figure 5- 1: The CVs oxidation peak current response for 0.5 mM dopamine (a) and uric acid (b) in 0.1 mM PBS at various concentration of H ₂ AuCl ₄	158
Figure 5- 2: The CVs oxidation peak current response for 0.5mM dopamine (a) and uric acid (b) in 0.1 mM PBS at various scan rate for the reduction of Au ⁺³ on the electrode surface for Au NPs formation.	159
Figure 5- 3: The Scan window optimization for reduction of Au ⁺³ for 0.5mM dopamine and uric acid in 0.1mM PBS	160
Figure 5- 4: The different electrolyte behavior for Au ⁺³ reductions on GPE surface for 0.5 mM dopamine and uric acid in 0.1 mM PBS.....	161
Figure 5- 5: Oxidizing (a) and reducing peak currents (b) obtained during collection of the 0.2 mM dopamine and uric acid cyclic voltammograms, for a starting layer of the Au NPs (A) or graphene (B) on the GPE surface	163

Figure 5- 6: FE-SEM images of the bare (a) and GR-GPE (b) at 1 μm (A) and 500 nm (B).	166
Figure 5- 7: FE-SEM images collected at two magnification values: 1 μm (A) or 500 nm (B), for the Au/GPE (a), GR/Au/GPE (b), Au/GR/Au/GPE (c), and GR/Au/GR/Au/GPE (d).	167
Figure 5- 8: EDX spectrum obtained from the GR/Au/GR/Au/GPE electrode.	168
Figure 5- 9: Cyclic voltammograms obtained from a solution comprising 5 mM $\text{K}_3\text{Fe}(\text{CN})_6/\text{K}_4\text{Fe}(\text{CN})_6$ and 0.1 M KCl, using (A) the bare GPE, (B) GR/GPE, and (C) GR/Au/GR/Au/GPE at scan rates of (a) 20, (b) 40, (c) 60, (d) 80, or (e) 100 mVs^{-1} . The insets in (A), (B), and (C) reveal the linear relationship between the current and the square root of the scan rates. (D) EIS of the (a) GR/GPE, (b) Au/GPE, (c) GR/Au/GR/Au/GPE, and (d) bare GPE under an applied 5 mV potential over the frequency range 100 to 0.01 Hz in a KCl (0.1 M) solution comprising 5 mM $\text{K}_3\text{Fe}(\text{CN})_6/\text{K}_4\text{Fe}(\text{CN})_6$	171
Figure 5- 10: Cyclic voltammograms were obtained from a solution comprising 0.2 mM uric acid (A) and 1 mM dopamine (B) in 0.1 M PBS. The responses of the GR/GPE to uric acid (Aa) at scan rates of 50 (a), 100 (b), 150 (c), 250 (d), and 300 mVs^{-1} (e). The responses of the GR/Au/GR/Au/GPE to uric acid (Ab) at scan rates of 50 (a), 100 (b), 150 (c), 200 (d), 250 (e), 300 (f), and 350 mVs^{-1} (g). The responses of the GR/GPE (Ba) and GR/Au/GR/Au/GPE (Bb) at scan rates of 50 (a), 100 (b), 150 (c), 200 (d), 250 (e), 300 (f), and 350 mVs^{-1} (g). The insets in (A) and (B) reveal the linear relationship between the current and the square root of the scan rate.	172
Figure 5- 11: CVs of the bare GPE (a), Au NPs/GPE (b), GR/GPE (c), and GR/Au/GR/Au/GPE in 0.1 M PBS containing 0.5 mM dopamine and uric acid.	173
Figure 5- 12: (A) Cyclic voltammograms obtained from solutions comprising of 0.5 mM dopamine and uric acid in 0.1 M PBS at various pH values: (a) 7.5 pH, (b) 7.0 pH, (c) 6.5 pH, (d) 6.0 pH, (e) 5.5 pH, (f) 5.0 pH at GR/Au/GR/Au/GPE. (B) Graphical representation of the peak current vs. pH for uric acid (a) and dopamine (b). Inset: Relationship between the pH and the oxidation peak potential.	175

- Figure 5- 13: Plots of the oxidation peak current vs. the (A) amplitude or (B) frequency, collected at 20 μM after a 10 s adsorption time (C) adsorption time in the presence of 10 μM (a) uric acid or (b) dopamine, obtained from the SWV in a PBS buffer (0.1 M, 6.0 pH).....179
- Figure 5- 14: Square wave voltammograms of (A) dopamine and uric acid at various concentrations: (a) 0, (b) 0.09, (c) 0.1, (d) 0.3, (e) 0.5, (f) 1, (g) 5, (h) 10, (i) 15, (j) 20, and (k) 25 μM . The inset shows the linear relationship between I (μA) and the concentration. (B) Dopamine concentrations: (a) 5, (b) 8, (c) 10, (d) 12, (e) 15 μM in the presence of 8 μM uric acid. (C) Uric acid concentrations: (a) 2, (b) 4, (c) 6, (d) 8, (e) 10 μM in the presence of 5 μM dopamine. The inset shows the linear relationship between I (μA) and the concentration (μM).180
- Figure 6- 1: Effect of different sensing medium for 0.5 mM Dopamine, uric acid and L-tyrosine on MB-GR/GPE.192
- Figure 6- 2: FE-SEM images at two magnification (A) 1 μm and (B) 500 nm (a) bare/GPE, (b) MB/GPE, (c) GR/GPE, (d) MB-GR/GPE.194
- Figure 6- 3: Raman spectra of (a) bare GPE (b) GR/GPE, and (c) MB-GR/GPE.....195
- Figure 6- 4: Cyclic Voltammograms were acquired using (A, B, C) GR/GPE and (A', B', C') MB-GR/GPE from 0.1 M PBS solution comprising 0.2 mM (A, A') dopamine (B, B') Uric acid at scan rates of (a) 0.05, (b) 0.1, (c) 0.15, (d) 0.2, and (e) 0.25 v. The response of 0.5 mM L-tyrosine (C, C') at scan rates of (a) 0.01 (b) 0.02, (c) 0.04, (d) 0.05, (e) 0.08, and (f) 0.1 v. The insets in (A, A', B, B', and C, C') has shown the linear relationship between current and the square root of the scan rates.....199
- Figure 6- 5: (A) Nyquist plot of 5 mM $\text{K}_3\text{Fe}(\text{CN})_6/\text{K}_4\text{Fe}(\text{CN})_6$ in 0.1 M KCl solution on (a) bare-GPE, and (b) MB-GR/GPE (c) GR/GPE, and (d) MB/GPE upon application of frequency range from 0.01 Hz to 100 kHz. (B) CVs of (a) bare GPE, (b) MB/GPE, (c) GR/GPE, (d) MB-GR/GPE were recorded at 0.1 V/s in

0.1M PBS solution containing 0.2 mM dopamine, uric acid and 0.5 mM L-tyrosine.....200

Figure 6- 6: (A) Cyclic voltammograms in 0.1 M PBS solution containing 0.4 mM (Aa) L-tyrosine, 0.2 mM (Ab) uric acid and (Ac) dopamine at various pH values from 5 to 7.0 at MB-GR/GPE. (B) The graph indicated the relationship between pH and peak current of (Ba) L-tyrosine, (Bb) uric acid, and (Bc) dopamine. Inset is showing the relationship between the peak potential and pH of the sensing medium201

Figure 6- 7: Plots of the oxidation peak current vs. (A) amplitude scanned for 20 μM dopamine, uric acid and 40 μM L-tyrosine , (B) frequency scanned for 10 μM dopamine, uric acid, and 20 μM L-tyrosine, (C) adsorption time for 5 μM dopamine, uric acid and 40 μM L-tyrosine obtained in PBS buffer (0.1 M, 6.0 pH) using square wave voltammetry.203

Figure 6- 8: Square wave voltammograms of (A) dopamine, uric acid at various concentrations: (a) 0.05, (b) 0.1, (c) 2, (d) 4, (e) 6, (f) 8, (g) 10 μM , and L-tyrosine (a') 0.7, (b') 0.9, (c') 10, (d') 15, (e') 20, (f') 25, (g') 30 μM . The (B) graphs show the linear relationship between I (μA) and the concentration of (Ba) dopamine, (Bb) uric acid and (Bc) L-tyrosine. (C) Dopamine concentrations: (a) 2, (b) 4, (c) 6, (d) 8 μM in the presence of 4 μM uric acid and 20 μM L-tyrosine. (D) Uric acid concentrations: (a) 2, (b) 4, (c) 6, (d) 8, (e) 10 μM in the presence of 2 μM dopamine and 20 μM L-tyrosine. (E) L-tyrosine concentrations: (a) 10, (b) 15, (c) 20, (d) 25 μM in the presence of 2 μM dopamine and uric acid. The inset in (C), (D) and (E) shows the linear relationship between I (μA) and the concentrations (μM).....204

LIST OF ABBREVIATIONS

GPE:	Graphite Pencil Electrode
GCE:	Glassy Carbon Electrode
ESA:	Electroactive surface area
GO:	Graphene Oxide
GR:	Graphene
CV:	Cyclic Voltammetry
SWV:	Square Wave Voltammetry
LSV:	Linear Sweep Voltammetry
DPV:	Differential Pulse Voltammetry
MTLB:	Methylene Blue
FE-SEM:	Field Emission-Scanning Electron Microscope
FTIR:	Fourier Transform Infrared Spectrometer
AA:	Ascorbic Acid
UA:	Uric Acid
DA:	Dopamine
PBS:	Phosphate Buffer Saline
IM:	Ionic Medium

ABSTRACT

Full Name : [NADEEM BAIG]

Thesis Title : [Novel Graphene-modified Carbon Electrodes for Trace Electroanalytical Determination of L-Tyrosine, Dopamine and Uric Acid]

Major Field : [CHEMISTRY]

Date of Degree : [May 2017]

[Monitoring of biomolecules, typically L-tyrosine, dopamine, and uric acid is essential to perceive the health condition of an individual. For instance, L-tyrosine is a crucial amino acid. It acts as a precursor for several neurotransmitters, such as dopamine, and for some hormones. Dopamine in the body acts as a neurotransmitter and also involves in the regulation of heartbeat and blood pressure. Uric acid is produced in the body due to purine metabolism and excreted from the body by urine with the help of kidneys. The abnormal level of these biomolecules inside the body could cause some serious problems. The abnormal level of L-tyrosine, dopamine and uric acid could cause tyrosinemia, albinism, liver disease, lung disease, Parkinson's disease, schizophrenia, attention deficit hyperactivity disorder, gout and kidney issues. Various cost effective modified electrodes surfaces were introduced for sensing of these biomolecules. An inexpensive carbon material based graphite pencil electrode was used and modified by advance graphene material to achieve the high sensitivity and selectivity for the sensing of dopamine, uric acid, and L-tyrosine. It was found that ionic medium supported the direct reduction of graphene oxide on GPE was more effective to enhance the sensitivity and electroactive surface area of GPE. A satisfactory linear response was obtained using dERGO/GPE from 0.8 to 60, 0.4 to 30, and 0.2 to 22 μM for individual sensing of L-tyrosine, DA, and

UA, respectively. The modified electrode yielded a low LOD of 0.07, 0.095 and 0.037 μM for L-tyrosine, DA, and UA, respectively. The sandwich structure of graphene with Pt NPs was fabricated on GPE for trace level quantification of dopamine. This arrangement of the Pt NPs and the graphene layers enhanced the sensitivity, electroactivity and promoted the fast charge transfer on the electrode surface. The value of K_s and electroactive surface area for dopamine was found 8.99 s^{-1} and 0.81 cm^2 , respectively. The developed sensor was found very sensitive towards dopamine with a LOD of 9 nM. The sensor response was linear for dopamine concentration from 0.06 to 20 μM . The simultaneous sensing of DA and UA was done using alternating Au NPs and graphene layers fabricated GPE. The fabrication process of the disposable electrodes was simple, fast, and accomplished through the dERGO and Au(III) onto a graphite pencil electrode surface. Good linear sensitivity was obtained over the ranges of 0.1–25 μM for dopamine and 0.09–25 μM for uric acid under optimum conditions using square wave voltammetry. Very low LOD of 0.024 (DA) and 0.029 μM (UA) were attained from the fabricated electrochemical sensors. The dopamine and uric acid peak separation were 151 mV. Finally, the extended layers of methylene blue and graphene were fabricated using the facile method on GPE for the simultaneous sensing of DA, UA, and L-tyrosine. These extended wrinkled shape layers dramatically enhanced the electroactive surface area compared to merely GR layers on GPE. MTLB-GR/GPE surfaces have shown satisfactory linear ranges from 0.05 – 10 μM for dopamine and uric acid while for L-tyrosine was found 0.7 – 30 μM . The developed sensor was found very sensitive with very low LODs of 0.015, 0.027, and 0.247 μM was achieved for dopamine, uric acid, and L-tyrosine, respectively. The various graphene modified GPE surfaces behave well in the

presence of potential interferences such as alanine, adenine, glucose, L-methionine, fructose, some ionic species Na^+ , K^+ , Ca^{+2} , Co^{+2} , Cl^- and satisfactory recoveries were obtained in the human urine sample. |

ملخص الرسالة

الاسم الكامل: نديم بيح

عنوان الرسالة: أقطاب مبتكرة من الجرافيت المعدل بالجرافين للتقدير التحليلي الكهربائي لتركيزات منخفضة من التيروزين و الدوبامين و حمض البوليك

التخصص: الكيمياء

تاريخ الدرجة العلمية: مايو 2017

يعتبر رصد الجزيئات الحيوية مثل التيروزين، الدوبامين، وحمض اليوريك عملية ضرورية لإدراك الحالة الصحية للفرد. حيث أن التيروزين هو حمض أميني حاسم فهو بمثابة مقدمة للعديد من الناقلات العصبية مثل الدوبامين وبعض الهرمونات. يعمل الدوبامين في الجسم كناقل عصبي ويشارك أيضا في تنظيم ضربات القلب وضغط الدم. وفي نفس الوقت يتم إنتاج حمض البوليك في الجسم بسبب الأيض لمركبات البيورين والذي يخرج من الجسم عن طريق البول بمساعدة الكلى. إن المستوى غير الطبيعي من هذه الجزيئات الحيوية داخل الجسم يمكن أن يسبب الكثير من المشاكل الخطيرة. يمكن أن يسبب المستوى غير الطبيعي من التيروزين، والدوبامين وحمض اليوريك التيروزينيميا، المهق، وأمراض الكبد، وأمراض الرئة، ومرض باركنسون، والفصام، و قضايا اضطراب عجز الانتباه فرط النشاط، والنقرس والكلى. وأدخلت العديد من أسطح الأقطاب المعدلة الفعالة والمكلفة للاستشعار من هذه الجزيئات الحيوية. واستخدم قطب قلم رصاص الجرافيت المصنع من مادة الكربون غير المكلفة والمعدلة مسبقا لتحقيق الحساسية العالية والانتقائية للاستشعار من الدوبامين وحمض اليوريك والتيروزين. وقد وجد أن الوسط الأيوني يدعم الاختزال المباشر لأكسيد الجرافين على سطح قلم رصاص الجرافيتي وكان أكثر فعالية لتعزيز حساسية والنشاط الإلكتروني لمساحة سطح القطب. تم الحصول على استجابة خطية مرضية باستخدام dERGO/GPE من 0.8 إلى 60، 0.4 إلى 30، و 0.2 إلى 22 ميكرومولار للتقدير الفردي من التيروزين والدوبامين و حمض البوليك على التوالي. وأسفر القطب المعدل انخفاض LOD من 0.07، 0.095 و 0.037 ميكرومولار لمركبات التيروزين، والدوبامين وحمض البوليك على التوالي. تم تطوير هيكل ساندوتش للجرافين مع جسيمات البلاتين المتناهية في الصغر (Pt NPs) على سطح قطب الكربون الجرافيتي (GPE) لتقدير مستوى أثر الدوبامين. هذا الترتيب من جسيمات البلاتين المتناهية في الصغر و طبقات الجرافين عزز الحساسية، النشاط الإلكتروني وترقية سرعة نقل الشحنة على سطح القطب. وقد وُجدت أن قيمة K_s ومساحة السطح الإلكتروني للدوبامين 8.99 s^{-1} و 0.81 cm^2 على التوالي. وُجد أن أجهزة الاستشعار المتطورة هذه حساسة جدا تجاه الدوبامين مع LOD تساوي 9 نانومولار. كانت استجابة أجهزة الاستشعار خطية لتركيز الدوبامين من 0.06 إلى 20 ميكرومولار. تم إجراء التقدير المتزامن في آن واحد من الدوبامين و حمض البوليك باستخدام التناوب جسيمات الذهب المتناهية في الصغر (Au NPs) وطبقات الجرافين على سطح قطب الكربون الجرافيتي (GPE). كانت عملية تصنيع الأقطاب الكهربائية القابل

للتصرف بسيطة وسريعة، وانجزت من خلال dERGO و Au(III) على سطح قطب الرصاص الجرافيتي. تم الحصول على حساسية خطية جيدة على مدى من 0.1-25 ميكرومولار للدوبامين و 0.09-25 ميكرومولار لحمض اليوريك تحت الظروف المثلى باستخدام موجة فولتاميتري المربعة. تم الحصول على LOD منخفض جدا من 0.024 (DA) و 0.029 ميكرومولار (UA) من أجهزة الاستشعار الكهروكيميائية المفتعلة. وكانت قمة فصل الدوبامين و حمض اليوريك عند 151 ملي فولت. وأخيراً، تم إفتعال الطبقات الممتدة من الميثيلين الأزرق والجرافين باستخدام طريقة فاسيل على GPE للاستشعار في أن واحد من الدوبامين وحمض البوليك والتيروزين. تعد هذه الطبقات الممتدة المتجددة الشكل هي المعززة بشكل كبير لمساحة السطح الكهربائي مقارنة بطبقات GR على GPE. وقد أظهرت الأسطح MB-GR/GPE مداً خطياً مرضياً من 0.05 - 10 ميكرومولار للدوبامين وحمض اليوريك بينما وُجد لل التيروزين 0.7، 30-0 ميكرومولار. وُجد أن أجهزة الاستشعار المتقدمة حساسة جدا مع LOD منخفضة جدا من 0.015، 0.027، 0.247 ميكرومولار للدوبامين وحمض البوليك، و التيروزين، على التوالي. وجد ان هذه الأقطاب المعدلة بالجرافين تتصرف بشكل جيد في وجود التداخلات المحتملة مثل ألانين، الأدينين، الجلوكوز، ميثيونين، الفركتوز، بعض الأنواع الأيونية Na^+ ، K^+ ، Ca^{+2} ، Co^{+2} ، Cl^- وتم الحصول على استردادات مرضية في عينة من البول البشري.

CHAPTER 1

INTRODUCTION

Monitoring of bio-molecules in human body has great significance to observe the health status of the human being

1.1 Significance of L-Tyrosine, Dopamine, and Uric Acid

L-tyrosine is one of the crucial amino acids in the human body. It helps to upkeep the positive nitrogen balance in the body [1]. It is an important precursor for certain neurotransmitters. L-tyrosine is acting as a precursor for L-dopa, dopamine, L-noradrenaline and L-adrenaline [2]. L-tyrosine is converted into L-dopa with the help of enzyme tyrosine hydroxylase, L-dopa into dopamine by L-aromatic amino acid decarboxylase, dopamine further transferred into the L-noradrenaline by dopamine- β -hydroxylase and finally, phenyl ethanolamine-N-methyl transferase enzyme converts L-noradrenaline into L-adrenaline. Likewise, L-tyrosine acts as precursors for some hormones like thyroxine and also for the melanin [3]. The dark color of the skin is appeared due to the melanin and it protects the skin from ultraviolet light which could cause skin cancer. In the body, L-tyrosine is formed from the phenylalanine with the help of phenylalaninase enzyme. If the phenylalaninase enzyme is absent, it causes the production of phenyl pyruvic acid instead of L-tyrosine. The accumulation of this acid may cause the problem for the CNS and prompts mental retardation [4]. Likewise, Nicotinic acetylcholine receptors metabolic stability in the muscles controlled by the phosphotyrosine level [5].

The unusual concentration of L-tyrosine in the body causes the number of serious problems. Sister chromatid exchange in the culture medium affected by the high concentration of the L-tyrosine [6]. The low concentration of L-tyrosine could cause

depression [7]. In a number of studies it has been reported, the doses of the L-tyrosine could improve the condition of fatigue, stress, and cold [8]. The abnormal level of the L-tyrosine in the body may cause tyrosinemia, albinism, alkaptonuria, liver problems, lung disease and mental illness [9]. In the case of renal failure or the diabetes mellitus patients, the tyrosine excretion was increased in the urine [10]. L-tyrosine is being added into the foodstuffs, pharmaceutical, and the dietary products to overcome the deficiency of L-tyrosine [11].

Dopamine is an amine and belongs to the catecholamine family [12]. Dopamine and L-tyrosine co-related with each other as L-tyrosine is acting as a precursor for dopamine. The dopamine in the body is generated by the removal of the carboxyl group from the L-dopa. Dopamine is also precursors for other two neurotransmitter noradrenaline and adrenaline. Dopamine produced in the brain and in the adrenal glands. Dopamine performs certain functions in the body. It acts as a neurotransmitter and facilitates the smooth functions of the cardiovascular, hormonal, and renal system [13]. Dopamine plays a vital role in the brain activity like motivational and reward base behavior. The attention, sleep, movement, behavior, memory, learning and mood somehow depend upon the dopamine level. Dopamine is also involved in the motor control system in which it controls the coordination and movement of the muscles [14]. The number of diseases could result due to the absolute absence or the low concentration of the dopamine. A serious Parkinson's disease results due to the dopamine low level in basal ganglia [15]. Dopamine low concentration also causes some other neurological disorders like Attention Deficit/Hyperactivity disorder [16], schizophrenia and epilepsy [13]. It

could be the reason of the restless leg syndrome. Dopamine is also the reward of abusive drugs which makes a person drug addictive [17, 18].

The metabolic breakdown of the purine produces uric acid [19]. Like L-tyrosine and the dopamine, it is a vital biomarker for certain diseases and its concentration in the body directly related to the health of the person. Uric acid is distributed in the serum, blood and the urine. The body gets rid of extra uric acid with the help of the kidney to clear the blood from the uric acid by excreting it with urine. The uric acid abnormal level in the blood and urine is an indicator for certain diseases like gout and Lesch-Nyhan syndrome [20]. The risk of diabetes mellitus is much more in the people with higher level of the uric acid [21]. Moreover, an elevated level of uric acid may cause kidney and cardiovascular problems [22].

1.2 Glassy Carbon and Graphite Pencil Electrode

Glassy carbon due to its interesting behavior has become the widely used electrode material. Glassy electrode considered as a good inert electrode due to low pore size, less liquid or gas permeability, chemical inertness, mechanical stability and low oxidation rate [23]. Due to these properties, the GCE is extensively used in the electrochemical sensing.

Another carbon electrode is the emerging graphite pencil electrode. Graphite pencil electrode could be proved a good electrochemical sensor due to its some key features which make it distinctive among other electrodes.

- It could be used as disposable or single use electrode due to the facile removal of the surface and the very low cost of the pencil. It makes the surface foul free due

to a single use. The multiple time use non-disposable electrode such as GCE, the cleaning of the surface is really challenging to get rid of by-products of the electrochemical reactions which adsorb on the surface.

- In the case of GCE, the surface polishing is required while GPE it is not mandatory.
- As the graphite pencil is being used for the writing purposes, it is easily available.
- GPE sensitivity is enhanced due to the presence of porosity on the surface.
- GPE could be disposable like screen printed carbon electrode. However, it is cost effective compared screen printed carbon electrode.
- The extruded pencil length of the electrode could be adjusted to desired sensing surface area which is difficult with other electrodes.

All these features make the GPE a fascinating electrode for sensing [24]. We tried to improve the sensitivity of the surface using graphene as a basic modification material.

1.3 Graphene as Modifying Material

Graphene is an attractive two-dimensional single layered sp^2 hybridized hexagonally arranged carbon material. After isolation in 2004, it is widely being explored in the field of supercapacitors, batteries, fuel cells, transparent conductors, field emission display and the development of electrochemical sensors [25]. Graphene is an exceptional material due to the large theoretical surface area ($2630 \text{ cm}^2\text{g}^{-1}$). Graphene could be proved a remarkable electrode material due to the huge electroactive surface area, fast charge transfer, low charge transfer resistance and wide potential window. Due to these

exceptional characteristics, the graphene is widely being explored for the development of various electrochemical sensors [26].

1.4 Modified Carbon Electrodes for Electrochemical Sensing

Various modified carbon electrodes are being used for the individual and the simultaneous sensing. Md. Rahman et al. determined L-tyrosine in the existence of AA, DA and UA by poly (thionine) modified GCE [27]. Similarly, dopamine and uric acid were determined by poly (L-lysine)/GO/GCE [28]. Mesoporous silica nanoparticle and pyrogallol red modified CPE was applied for the sensing of l-tyrosine, DA and UA [29 ,30]. Screen printed CE is used as a disposable electrode. It is also considered for determination of L-tyrosine, dopamine and uric acid to develop disposable sensor and the pretreated surface of the screen printed carbon electrode was used for simultaneous analysis [31].

CHAPTER 2

Literature Review

2.1 Challenges in the Individual and Simultaneous Sensing of Targeted

Analytes

The simultaneous or individual sensing of ascorbic acid (AA), dopamine (DA), L-tyrosine and uric acid (UA) is of a great interest among researchers and it has following benefits.

- As these biomolecules co-exist in the physiological fluid, their individual or simultaneous measurement provides timely information.
- Small sample consumption in case of in-vitro study.
- Accurate and real-time measurements of these analytes may help to deal with the health issues and the drug treatment in right direction.

The investigation of these molecules is a subject under intensive study in the field of medical and neurochemistry and considered as a diagnostic tool in pathogenic research. Several analytical techniques are continuously being explored for sensitive sensing of these analytes such as capillary electrophoresis, HPLC, UV- visible spectroscopy, chemiluminescence and electrochemical methods [32]. The electrochemical methods are considered as a good choice over other sensing techniques due to good sensitivity, simplicity, cost effectiveness, and rapid response [33]. Despite all these facts, electrochemical methods are facing serious problems for simultaneous or individual sensing of AA, UA, and DA:

- The major challenge is their close electro-oxidation potentials [34] and conventional electrodes surface unable to resolve peak potential of these analytes.

- Individual sensing is also a difficult task as these biomolecules typically coexist in the extracellular fluid and serum in the human body.
- Managing reproducibility and stability at the conventional electrodes is a tedious job due to the formation of by-products during an electrochemical analysis.

To overcome these issues, a number of electrochemical sensors have been reported in which different modification materials were used to enhance the electrode sensitivity. Most of the electrodes fabricated for simultaneous or individual measurements of AA, UA, L-tyrosine, and DA were being modified using carbon nanotubes (CNTs), graphene, conductive polymer, ionic liquids (IL) and their composites. These modifications improved peak separation, enhanced the electroactive surface area and reduced the charge transfer resistance. Incorporation of metal NPs in these advanced materials further improves the sensitivity. As a result, a wide linear range and very low limit of detection (LOD) were achieved. The real challenges in the development of modified sensors to make them applicable in the field of medical and diagnostic laboratories should have following characteristics:

- The modification should be simple and completed in short time.
- The fabricated surface should be foul free as the biological matrix is really complex which could easily affect the electrode surface.
- The developed sensor should have acceptable reproducibility and the repeatability.
- Development of the portable devices.
- The developed sensor should have good shelf life.
- Modification material and the fabrication process should be cost effective.

Substantial efforts are being put to develop sensors for individual or simultaneous measurement of AA, UA, L-tyrosine and DA. There is a need to consolidate the work for future progress and real development in this area. We have tried to provide a brief overview of the modification materials followed by a comprehensive comparison of various modified sensors for simultaneous measurements. The modified electrodes were being assessed in terms of their measuring techniques, sensing medium, dynamic range, LOD, limit of quantification (LOQ) and their practical applications. The specific characteristics of modified electrodes were debated. This review has shown the significant improvement in modification materials to improve the sensitivity of the sensor for the individual or simultaneous recognition of AA, UA, L-tyrosine and DA. Although most of these sensors are still far away from practical applications due to short shelf life, complex modification process, indispensable and surface fouling after single measurement.

2.2 Characteristics and a Brief Overview of the Modification Materials

2.2.1 Carbon Nanotubes (CNTs)

Pure CNTs are not displaying any voltammetric response in the generally applied potential window [35]. However, carbon and metallic nanoparticles and amorphous carbon are introduced into CNTs as impurities during their synthesis [36, 37]. Afterward, the raw CNTs are purified by utilizing chemical or thermal treatment; several electroactive oxygen-containing groups are introduced on the open ends and defects along sidewalls of CNTs. As a result, dramatic change in electronic and structural characteristics of CNTs can be observed, which make them electroactive for many

species [38-40]. CNTs exhibit a different kind of electrochemical behavior as compared to other forms of carbon-based materials [41]. CNTs contain two groups of carbon atoms

- At edges of CNTs, carbon atoms act as edge plane of highly orientated pyrolytic graphite (HOPG).
- At sidewall of CNTs, carbon atoms resemble basal plane of HOPG.

If CNTs are examined by the mechanistic point of view there is no difference in both type of carbon atoms, however, edge plane carbon atoms contain higher electron transfer kinetics as compared to basal plane carbon atoms of CNTs due to the presence of different sort of chemical bonding [42]. Compton et al. comprehended that activity of MWCNTs and graphite modified basal plane pyrolytic graphite (BPPG) electrode is similar when electroactivity of both materials was related towards redox reaction of NADH, epinephrine, and norepinephrine. Their further study disclosed that electrochemical response at the ends of CNTs look like edge plane sites of pyrolytic graphite, while walls of CNTs turn like the basal plane of carbon and their constant for heterogeneous electron transfer limit is zero. That's why the higher electrocatalytic activity of the CNTs directly related to the edge plane components [43–45].

Development of electrochemical sensors by exploiting carbon-based materials is amongst most explored area in biosensing [46]. Numerous fascinating properties of carbon nanotubes such as rapid electron relocation kinetics and facile chemical functionalization make them more compatible for the fabrication of electrochemical sensors [47]. The electrode surface can be modified by dispersing CNTs in an appropriate solvent and then directly casting on the surface of the electrode. Other methods for depositing the CNTs on the electrode surface include by detrition of the electrode on a filter paper containing

CNTs or casting mixture of nafion and CNTs dispersion on the electrode surface [46, 48]. However, these methods might introduce unwanted impurities that can decrease the electroactivity and sensitivity of modified electrode. Most effective method to overcome above-mentioned drawbacks is the direct development of CNTs on electrode surface which result in better electrical contact, less chance of impurities, fast electron transmission and requisite arrays of CNTs can be achieved on the surface of the electrode. Through applied electric field and van der Waals self-assembly forces, the growing nanotubes orientation can be controlled [49, 50]. Due to their unique surface characteristics and inconsequential maculating of electrode surface comprising CNTs they can be combined with other modifying materials to get the composite electrode of higher sensitivity. While looking at published literature, this fact can be realized that most of the work included a composite of CNTs with other materials like metal nanoparticles, polymer films, graphene, ionic liquids etc [51–56]. It is unjust to determine sensitivity by only looking at the limit of detection of a particular sensor. However, the other factors also contribute a lot in the practical application such as ease of modification, the time required for sensor fabrication, cost-effectiveness, linear dynamic range, robustness etc.

2.2.2 Graphene

Graphene is a fascinating material discovered in 2004 by Geim and Novoselov. Graphene is a thinnest two-dimensional sp^2 planner material which has a honeycomb like structure. Graphene is the recent member of the carbon family. The carbon nanomaterial family, previously, consists of zero-dimensional fullerene material, 1-D CNTs nanomaterial, and 3-D graphite material and the gap of 2-D is filled by the most efficient graphene material

[57]. Graphene considered as revolutionary material in the field of transparent conductors, energy storage devices, field emission display, high-frequency electronics and bioscience. The graphene got rapid attention due to its following key features [57-61]:

- Large surface area (theoretical surface area of graphene is $2630 \text{ m}^2/\text{g}$ which is much greater than carbon nanotubes surface area $1315 \text{ m}^2/\text{g}$)
- Extraordinary electrical and thermal conductivities
- High elasticity
- Unprecedented impermeability
- Tunable band gap
- Tunable optical properties
- Strong mechanical strength
- Low-cost synthesis

Graphene is also being explored widely in the field of electrochemical sensing for various electroactive analyte. Graphene emerged as promising modification material due to the following reasons:

- High electrical conductivity (64 mS/cm)
- Fast charge transfer
- Low charge transfer resistance
- Huge electroactive surface area
- Wide electrochemical working window (in 0.1 mM PBS solution the electrochemical working window was observed 2.5 V)

- Excellent electrochemical activity
- Small amount of graphene is enough for the surface modification of the electrodes
- Good biocompatibility

These entire exceptional characteristics make it worthy material for electrode fabrications. Moreover, the fast charge transfer between graphene and electroactive analyte facilitate the mediator-less sensing [59]. The graphene is produced by numerous methods such as metal substrate based (Cu, Ni, or Ru), or substrate free chemical vapor deposition, micromechanical exfoliation of graphite, the opening of carbon nanotubes, and decomposition of SiC at high temperature. Recently, 3D graphene was prepared on macroporous Ni foam scaffolds using chemical vapor deposition. 3 D structure was built from Ni-coated porous carbon by annealing and etching with FeCl₃ to eliminate Ni [62]. In electrochemical sensing process, the reduced GO is obtained from the GO reduction. GO is different from the pristine graphene due to oxygen-containing hydroxyl and the epoxy group on the basal plane of SP₃ hybridized carbon while carboxyl and the carbonyl groups are present on the SP₂ carbon at the sheet edges [63]. Generally, the graphene oxide is prepared from the oxidation of graphite by the mixture of oxidizing agents and the strong acid by Hummers method [64]. Although, the graphene oxide and graphite oxide have similar functional groups however graphene oxide is a single layer material. The synthesized graphene oxide could be easily dispersed by sonication in water due to its hydrophilic nature. The suitable sonication could give a single layer graphene oxide solution. GO is rich in oxygen-containing functional groups and have C/O ratio ~2. It contains many defects and displaying non-conductive behavior. Due to poor conductivity, the GO has not considered a good electrode modification material. The electrical

behavior and the conductance could be restored by reducing the GO [65]. For electrode modification process, the RGO is commonly obtained by two methods:

- Chemical reduction of GO
- Electrochemical reduction of GO

In chemical reduction, the reducing agents like hydrazine and sodium borohydrate generally used for the reduction of GO into RGO. The hydrophilic behavior of the RGO is decreased due to the elimination of oxygen groups and it starts precipitating out. The electrochemical reduction of the GO on the electrode surface to get RGO has been a frequently used method in literature for graphene-based sensors. In this method normally certain amount of GO is deposited on the electrode surface and later on reduced electrochemically. In addition to this, few methods also described in which direct electrochemical reduction of GO was done on electrode surface [66].

2.2.3 Polymer Films

The aromatic heterocyclic compounds like benzenoid can be electrochemically oxidized on the electrode surface to formulate conducting polymer film with good electrical contact and adhesion. Polymer films can be produced by cycling the potential between oxidized state and neutral state, by dipping the electrode into the solution comprising monomer [67, 68]. For this purpose, various sort of organic molecules can be utilized such as azulene, benzenoid, neon benzenoid, carbazole, fluoranthene, thiophene, triphenylene, thionaphthene and pyrene [69–74]. The partially filled molecular orbitals of the polymer overlap to form delocalised pi (π) molecular orbitals and the electrons move all over the orbitals of polymer structure. Resonances of alternate single and double bonds result in conduction of charge carriers and stabilization of polymer structure [75].

Due to the higher electronic conductivity of the organic polymers, they are named as 'synthetic metals' [76].

The structure of monomer, the composition of the electrolytic solution and applied potential determine the features of polymer film [77]. The key characteristics of polymer films must be evaluated before utilizing for the biosensing applications include:

- Ability of polymer films to change the electrical conductivity
- Mechanical configuration of films
- Interaction of the polymer films with target analyte

The suitable and homogenous polymer coating result in distinctive non-faradic signals for the target analyte, effective pre-concentration, higher electron transfer rate and exclusion of interfering species [78, 79]. The polymer films on the electrode provide multilayered three-dimensional reaction zones that improve surface area and reaction sites on the surface of the electrode. Consequently, the intensity of reaction occurring on the surface of electrode dramatically amplify, which in turn positively affect the sensitivity [80]. The surface of the polymer film can be derivatized chemically to carry out complexation, precipitation, and ion exchange reactions [81, 82].

Like semiconductors, conducting polymers develop energy gaps and Fermi energy levels in between them due to charge interactions and structural (conformational and structural) factors [83]. Until the introduction of suitable dopants, some polymers are not stable and very poor conductors. As a result of doping, charge carriers are produced that carry the charge throughout the polymer. Electrochemical polymerization is the chief source of dopant ions introduction into the polymer system. Type of dopants determines the morphology of the resulting polymer and also charge distribution on the backbone of the

polymer [84]. The area of the polymer containing unequally distributed charge interacts with a free radical as a result unstable polaron is produced which on further polymer oxidation form a bipolaron. Dopant ions and bipolaron play important role in the electrical conduction mechanism of conducting polymer [85]. When delocalized electrons of one polymer backbone interact with nuclei in neighboring unit leads to conduction and this phenomenon is outspread to all directions due to three-dimensional structure of polymer [86].

The dopant ions inserted into the semiconducting polymer can change the conformational, electrical, magnetic and conducting features are called primary dopants, while those dopants applied to the polymer already containing primary doped ions are called secondary dopants. Secondary dopants can also change the features of the polymer as primary dopant [87, 88]. Possible interaction between the polymer and secondary dopant can occur by covalent bonding and intermolecular forces that lead to variation in conformation and charge transfer. The target analytes detected by the polymer modified electrodes are considered as secondary dopants and a charge transfer complex arises between polymer and target species [89–91].

2.2.4 Ionic Liquids

Ionic liquids are consisting of positive and negative ions, and free of molecular solvent.

The cations are bulky organic in nature such as *N,N'*-dialkylimidazolium and *N*-alkyl pyridinium and a number of anions like NO_3^- , BF_4^- , AlCl_4^- , CF_3COO^- , Cl^- , Br^- , I^- , PF_6^- , etc. Ionic liquids remain liquid at room temperature due to asymmetric nature of ions. The bulky cations put hindrance in lattice packing. The organized packing of the cations and anions could not take place which results in decrease their melting point and most of

them remain liquid at room temperature. The properties of the ionic liquids depend upon the nature of cations and anions. The behavior of the ionic liquid could be tuned to some degree for a specific application by varying the cations and anions for optimum results [92]. Similarly, the miscibility or immiscibility with other solvents can also be controlled by varying the cations and anions [93]. Ionic liquids are showing enormous potential for the development in the field of advanced batteries, solar cells, super-capacitors, fuel cells, actuators, hydrogen generation by water splitting, thermo-electrochemical cells, thermal storage applications and in the field of electrochemical sensors [94, 95]. Ionic liquids have a number of unique properties which make them promising material in the field of electrochemistry. Ionic liquids have high electrochemical and chemical stability. The ionic liquids considered safe due to low volatility and flammability. The ionic liquids could be spread very easily by casting method on the electrode surface using a mixture containing volatile solvent. Moreover, the viscosity of the ionic liquid matched with nujol or n-alkane which is commonly used binders in CPE. Instead of these binders, the ionic liquid could be used [96]. Ionic liquids displayed a wide stability window almost from 2-6 V. The wide electrochemical window is attributed to the poor electrochemical oxidation and reduction of the ionic liquid ions. However, the stability window could varied as various materials are being used as a working electrode and different references are being used [95]. Due to a number of attractive features, it is extensively being used for the fabrication of various modified electrodes using various methods such as casting, rubbing, direct electrodeposition, physical adsorption and direct mixing [97].

2.3 A Comparison of the Modified Electrodes for Simultaneous Sensing of AA, UA and DA

2.3.1 Carbon Nanotubes Modified Electrodes

Carbon Nanotubes are members of the fullerene structural category and immensely used in electrochemical sensing owing to eminent electrical conductivity, chemical stability and rapid electrode kinetics [98, 99]. CNT-based sensors proved to be much superior as compared to conventional carbon electrodes and demonstrate low detection limits and higher sensitivity [100]. CNT-based sensors display diverse performance depending on preparation methods, surface alteration of CNTs and addition of electron mediators [101–103]. CNTs can channelize high currents over longer distances because electron propagates substantially along CNTs owing to one-dimensional structure of SWCNTs or MWCNTs. This property makes CNTs suitable for application of electrocatalyst [104].

With high structural flawlessness, there are two chief types of CNTs. Single-walled carbon nanotubes, (SWCNTs) comprise of seamless graphene sheet in which carbon is sp^2 hybridized, while multiwalled carbon nanotubes (MWCNTs) constitute set out of homocentric nanotubes similar to rings of tree bole. Other types of CNTs include double-walled carbon nanotubes [105], helical carbon nanotubes [106] and Single-walled carbon nanohorn (SWCNH) [107].

Assorted methods are employed for the synthesis of CNTs like chemical vapor deposition, electrolysis, laser ablation, and arc discharge [108]. Arc discharge methods employ higher temperature more than 1700°C , higher current application over graphite electrodes ensued in deposition of CNTs on the cathode [109], with the help of this

method SWCNTs, DWCNTs and MWCNTs can be produced by altering the applied conditions. Laser extirpation is done by pulsing high energy laser beam on the surface of graphite target to vaporize carbon in a chamber filled with buffer gas; as a consequence CNTs are generated. Characteristics of CNTs produced largely depends on energy flux of laser, pulse rate of the laser, physical and chemical properties of the target material, composition and pressure of the buffer gas [110]. Laser ablation usually yields MWCNTs but the use of metal nanoparticles as a catalyst can afford high quality and purity SWCNTs [111]. CVD now become the standard method for production of CNTs at commercial scale, in which gas phase molecules like hydrocarbons are decomposed to reactive species succeeded in shaping of CNTs. Properties of CNTs can be operated by altering nature of reacting gas, flow rate, catalysts and reaction temperature [112, 113]. A comparatively new method for development of CNTs is electrolysis in which carbon dioxide act as a precursor for carbon nanomaterial is introduced to melted chloride salts. As a result of the electrolytic reaction, CNTs are produced at the cathode with very high purity. The only factor that can affect the % yield of this method is the pressure of CO₂ due to the fact the CO₂ has very low solubility in melted chloride salts [114].

2.3.1.1 CNTs Mixed with Graphite Powder

The synthesized CNTs are widely used for the electrochemical sensing of various analytes. The scope of this review is simultaneous espial of AA, DA and UA, therefore, we focused the CNTs applications to these biomolecules. Many studies have been reported for simultaneous detection of these analytes by using CNTs in different ways, like M. S. Ghoreishi et al. intermingled consistent suspension of MWCNT with graphite powder to form a paste that was crammed into polyethylene tube to get CPE. After

comparison of differential pulse voltammetric, (DPV) response of regular CPE and MWCNT modified CPE revealed that MWCNT/CPE exhibit improved electro-oxidation of UA, AA, and DA but still not appropriate for simultaneous recognition of these electroactive biomolecules. That's why anionic surfactant i.e. sodium dodecyl sulfate (SDS) was added to the mixture containing target analytes to get well-resolved peaks of UA, AA, and DA. They practiced the above-described method for measurement of DA in injection, UA, and AA in urine. The recovery of target compounds was very high i.e. 98.6 – 101.2 % for DA and 99.6 – 100.0 % for AA and UA with a high tolerance for intrusive entities [103].

2.3.1.2 Direct Deposition of CNTs on Electrode Surface

Single wall carbon nanotubes can also be utilized as a platform for sensitive detection of biomolecules. S. Zhu et al. employed SWCNH on the polished surface of GCE to sense AA, DA, and UA. The coating of SWCNH on GCE surface was probed by Scanning electron microscopy. The modified electrode showed extraordinary sensitivity with LOD of 5, 0.06 and 0.02 μM for AA, DA and UA, respectively [107]. The proposed method has shown sensitive response and significantly resolved peaks were achieved. The SWCNH modified GCE was used to 1000 times diluted urine samples and recoveries were attained in the range of 94 – 109 %. In a similar fashion, H. Bi et al. geared up a MWCNT modified GCE for the contemporaneous recognition of analytes. Primarily, upshot of functional groups on the electroactivity of transformed electrode was canvassed. The outcomes demonstrated that MWCNT treated with acid (MWCNT-T) show most eminent efficiency toward electro-oxidation of target analytes as compared to pristine MWCNT (MWCNT-P), MWCNT with the carboxylic group (MWCNT-COOH),

and hydroxyl- holding MWCNT (MWCNT-OH). The high electroactivity of MWCNT-T towards oxidation of DA was ascribed to π - π interaction amongst carboxyl functional group of MWCNTs and hexagonal carbon fabrication of analyte that results in high electron transfer rate. This result remains same when analysis of a ternary solution containing AA, DA, and UA was analyzed [115].

2.3.1.3 Metal and CNTs Nanocomposite

Metal nanoparticles possess extraordinary surface area and exhibited fast charge transfer kinetics which results into a substantial improvement in the fabricated sensor sensitivity. Z. Dursun et al. lodged platinum nanoparticles on the MWCNT surface and cast on GCE for the concurrent detection of UA, AA, and DA. SEM images and XRD scan confirmed the existence of PtNPs on the surface of MWCNTs, whereas electrochemical impedance spectroscopy exhibited that PtNPs/MWCNT/GC electrode has lower resistance for charge transfer as related to bare GCE and MWCNT/GCE. DPV was used for recognition of analytes at the same time in 0.1 M phosphate buffer, well-separated peaks of the analyte with peak separation 190, 180 and 370 mV for AA-DA, DA-UA and AA-UA were obtained, respectively [116]. As the PtNPs/MWCNT/GCE display, low detection limits and estimable steadiness of results but this method was not utilized for the real sample application. Similarly, to boost the electrocatalytic properties of the CNTs H. Filik et al deposited gold nanoparticle on the surface of N',N'-dimethylphenothiazin-5-ium-3,7-diamine (AzA) that act as a binder to attach NPs with CNTs. Nafion/AuNPs/AzA/MWCNTs/GCE nanocomposite electrode efficaciously detect DA, AA, and UA. The linear ranges were obtained from 300–10,000, 0.5–50 and 0.5–50 μ M,

correspondingly. The limit of detection for AA, DA and UA was 16, 0.014 and 0.028 μM respectively [117].

Similarly, Zhang et al. fabricated a La-MWCNTs nanocomposite electrode to detect DA, AA, and UA. The increased sensitivity of La/MWCNTs/GCE was attributed to the porous behavior of the surface. The modified electrode has shown the excellent chronoamperometric response of various concentrations of the UA, DA, and AA. The modified electrodes were stored over a period of one and two weeks, they displayed satisfactory current stability of 96% and 92.7%, respectively [118]. Deng and coworkers modified the GCE by utilizing covalently bonded carbon nanotube with prophyrinoid nickel (II) norcorrole complex (CNT-NiNC). Attachment of NiNC with CNT surface not only accelerated the electron transfer but also improves the peaks separation of the analytes [119]. Another nickel-based complex was recently used for the modification of GCE surface by utilizing single-walled carbon nanotubes. Characterization of $[\text{Ni}(\text{phen})_2]^{2+}/\text{SWCNT}/\text{GCE}$ was done by using CV and EIS, that demonstrated higher electron transfer and decrease in resistance as compared to bare GCE, $[\text{Ni}(\text{phen})_2]^{2+}/\text{GCE}$ and SWCNT/GCE. Fabricated electrode displayed highly consistent up shots for DA and UA and rationally comparable reproducibility for AA. The developed technique was employed to real samples including urine, dopamine hydrochloride injection and vitamin C tablets [120].

2.3.1.4 Graphene and CNTs Nanocomposites

Graphene is a zero-gap semimetal with the ballistic mobility of electrons. These characteristic stimulate graphene an ideal material in surface modification of electrode for detection of diverse significant analytes. To enhance electric properties of graphene

Huixiang et al. commingled mesocellular graphene foam with MWCNTs and lodged on the surface of GCE for concurrent recognition of DA, AA, and UA. As compared to GS/MWCNTs/GCE the MGF/MWCNTs/GCE displayed amply split peaks and higher response due to the greater surface area of MGF ($2581 \text{ m}^2 \text{ g}^{-1}$) related to graphene nanosheets ($466 \text{ m}^2 \text{ g}^{-1}$) and MWCNTs ($240.1 \text{ m}^2 \text{ g}^{-1}$). Differential pulse voltammetric study for sensing of UA, AA, and DA revealed a good correlation amongst voltammetric current and concentration of target analytes [121]. Although, MGF/MWCNTs/GCE displayed low detection limit with good stability over two weeks, notwithstanding the 6.5 % reproducibility of the sensor was not appropriate. Likewise, not enough interference study was done and this method was not employed to any existent biological sample. Interestingly, Sun and coworkers derived graphene nanoribbons from commercially available MWCNTs by simple treatment in microwave reactor in the presence of KMnO_4 . Optimization of microwave power concluded that at 250 W a fully flat carbon structure was generated; formation of graphene was confirmed by FTIR spectroscopy. MWCNT/GONR/GC electrode was employed to simultaneously sensing of a ternary solution of targeted analytes and enhanced efficiency was observed for the electro-oxidation of above-mentioned biomolecules. X-ray absorption near-edge structure spectroscopy employed to observe electronic arrangement of GONR/MWCNTs, high compactness of unfilled electronic states over the Fermi level accompanied by enriched oxygen-based functional groups at the edge of heterostructure held responsible for high efficiency of nanocomposite towards the electrochemical properties [102]. Although described method is sensitive but not well established, none of the figures of merit for the

MWCNT/GONR/GCE was investigated and the sensor was not tested for any real samples.

2.3.1.5 CNTs Immobilized on Monolayer Platform

Xu et al. employed choline as a platform to attach double wall CNTs on the GCE surface. Choline contains $-N^+(CH_3)_3$ polar head that covalently attached on the carbon electrode and then it interacts with DWCNT containing negative charge in the form of the carboxyl group. Amperometric response of DWCNTs/Ch/GCE was studied for DA, AA, and UA individually; wide linear ranges and low LOD for target analytes were observed. The simultaneous response of AA, DA, and UA was ascertained in a ternary solution, where a linear correlation between concentration and peak current was found. The stability of oxidation currents for 3000s was examined and the maximum decrease was observed for UA i.e. 1.86%. Satisfactory long-term stability was observed for 20 days. Different figures of merit proved DWCNTs/Ch/GCE were highly reproducible [105]. The proposed method is not only applicable to urine sample for finding of UA and DA but also utilized for AA in daily life products like vitamin C tablets, orange and lemon juices.

2.3.1.6 Polymer Incorporated CNTs

Functionalization of CNTs with the hydrophilic polymer was proved a successful strategy for the simultaneous detection. Poly (diallyl dimethyl ammonium chloride) (PDDA)/helical carbon nanotubes (HCNTs) modified GCE shows enhanced electrocatalytic behavior and prominently separated peaks for target analytes. DPV was employed to detect targeted analytes simultaneously in 0.1 M PB. The developed strategy exhibited

satisfactory outcomes when applied to fetal bovine serum samples to detect target analytes [106].

In another example, flavin adenine dinucleotide (FAD) and poly(3,4-ethylenedioxythiophene) (PEDOT) were co-deposited by cyclic scanning potential ranges on the surface of GCE and then amino functionalized MWCNTs were cast on the modified electrode surface. In the case study, it was realized that deposition of PEDOT–FAD composite on the surface of GCE before or after casting MWCNTs can produce a pronounced effect on the electroactive behavior of sensor. MWCNTs/PEDOT–FAD/GCE showed lower potential and higher electrocatalytic activity for the DA, AA, and UA in the existence of hydrogen peroxide. Developed multifunctional electrode showed good stability over a period of two weeks, higher tolerance for interferences and nearly 100 % retrieval of target species in human urine samples [122]. To take the advantage of active site of porphyrins, that can be used for redox reaction of biologically crucial biomolecules. Wang et al. modified GCE by casting composite of metalloporphyrin i.e. Fe(III)P/MWCNTs. Fe(III)P/MWCNTs/GCE provide excellent electrocatalytic response and well-distinguished peaks for AA, DA and UA in ternary solution with LOD i.e. 3.0, 0.09 and 0.3 μM respectively. Although very promising results were obtained for Fe(III)P/MWCNTs/GCE, however, the detection of target species was done on pH 4.0 that is not a physiological pH [55].

Noroozifar et al. tried to overcome the interference from anionic species and large biomolecules present in a real sample containing AA, DA, and UA using iron ion-doped natrolite zeolite, chitosan and MWCNTs modified sensor (MWCNTs/FeNAZ/CH/GCE). The modified electrode not only increase the peak current for targeted analytes but also

resolved the coincided peaks of target species as compared to bare GCE, MWCNT/CH/GCE, MWCNT/NAZ/CH/ GCE and MWCNT/FeNAZ/CH/GCE [56]. In another method, GC electrode surface was modified by in-situ produced vanillic acid functionalized MWCNTs. The developed sensor was used to study the interference effect on signal strength and peak separation of target analytes. When DA, AA, and UA were targeted simultaneously in the presence of serotonin, MWCNT/poly-VA /GCE seems unable to resolve the peak for UA. Although the modified transducer can easily resolve the signals for DA, AA, and UA but the LOD for this method not meet the required level [123].

2.3.1.7 CNTs-Ceramic Electrode

A new class of composite carbon-silica material derived from sol-gel used as the electrode was showing higher porosity, rigidity, and stability over other electrodes. Habibi and his co-workers tried to use the unique properties of the composite ceramic material as a platform for the MWCNTs, to detect AA, DA, and UA simultaneously. Sol-gel material methyltrimethoxysilane-tetraethoxysilane (MTMOS) was mixed with graphite powder in the presence of hydrochloric acid and methanol to form a carbon-ceramic electrode, afterward MWCNTs were cast on the surface to get MWCNTs/CCE. DPV in PB (pH 4.5) indicated highest response for concurrent determination of targeted analytes with excellent peak separation and the developed sensor was applied to analyze pharmaceuticals and human blood serum samples [124].

2.3.2 Graphene Modified Electrodes

The key characteristics of a material are being used as electrode modification; it should have better electrical conductivity, huge electroactive surface area, fast charge transfer.

Graphene and its composites are displaying all these characteristics. The graphene-based sensors have shown excellent selectivity and the sensitivity for the concurrent determination of targeted analytes. The large surface area of graphene sheets provide the attachment of analyte high densities and facilitate the miniaturization of highly sensitive sensors [59]. As discussed, mostly reduced graphene oxide are being used instead of graphene in electrochemical sensing. The extensive use of RGO in electrochemical sensing is due to its facile and cost effective preparation, easy functionalization and electrode surface modification [66]. Reduced graphene oxide has slight difference compared to graphene. Graphene is exactly polycyclic aromatic network and has only carbon and hydrogen while RGO most of the part consist of the polycyclic aromatic network but it may have around 10 % oxygen fraction. However, its characteristics resemble with graphene in terms of mechanical, electrical and thermal properties [125].

Table 2- 1: Comparison of figure of merits for simultaneous sensing of AA, DA and UA using CNTs modified electrodes

Sr#	Electrode	Analyte	Technique	Medium/pH	Linear range (μM)	LOQ (μM)	LOD (μM)	Peak separation (mV)	Application	Ref.
1.	MWCNT/CPE	AA DA UA	DPV	0.2 M PB solution/ pH 3.0	300-900 20-50 40-140	300 20 40	18.85 1.07 2.86	AA-DA=108 DA-UA=150 AA-UA=260	Dopamine hydrochloride injection and human urine	[103]
2.	SWCNH/GCE	AA DA UA	LSV	0.1 M PB/ pH 7.0	30-400 0.2-3.8 0.06-10	30 0.2 0.06	5 0.06 0.02	AA-DA=211 DA-UA=152 AA-UA=363	Human urine	[107]
3.	MWCNTs/GCE	AA DA UA	DPV	0.1 M PBS/ pH 7.4	-	-	-	AA-DA=188.8 DA-UA=164.3 AA-UA=353.1	-	[115]
4.	PtNPs/MWCNT/ GCE	AA DA UA	DPV	0.1 M PB/ pH 7.0	24.5-765 0.061-7.03 0.455-50	24.5 0.061 0.455	20 0.0483 0.35	AA-DA=190 DA-UA=180 AA-UA=370	-	[116]
5.	AuNPs/AZA/M WCNTs/ GCE	AA DA UA	DPV	0.1 M PB / pH 7.0	300–10,000 0.5–50 0.5–50	300 0.5 0.5	16 0.014 0.028	-	Human urine	[117]
6.	La– MWCNTs/GCE	AA DA UA	CA	0.1 M PBS/ pH 6.0	0.4–710 0.04–890 0.04–810	0.4 0.04 0.04	0.14 0.013 0.015	AA-DA=150 DA-UA=150 AA-UA=300	Human urine and serum	[118]
7.	CNT-NiNC/GCE	AA DA UA	DPV	0.1 M PB/ pH 6.5	7.5–2000 0.3–7.0 1–45	7.5 0.3 1.0	2.0 0.1 0.4	AA-DA=270 DA-UA=180 AA-UA=450	Human urine and serum	[119]
8.	[Ni(phen) ₂] ²⁺ / SWCNTs/GCE	AA DA UA	DPV	0.1 M PB/ pH 4.0	30–1546 1–780 1–1407	30 1.0 1.0	12.0 1.0 0.7	AA-DA=204 DA-UA=152 AA-UA=356	Human urine, Dopamine hydrochloride injection and vitamin C tablets	[120]
9.	MWNTs/MGF/ GCE	AA	DPV	0.1 M PB /	100–10,000	100	18.28	AA-DA=141	-	[121]

	GCE	DA UA		pH 7.3	0.3–50 5.0–1000	0.3 5.0	0.06 0.93	DA-UA=132 AA-UA=273		
10.	MWCNT/ GONRs/GCE	AA DA UA	A	0.1 M PB/ pH 7.0	0.1-8.5 0.15-12.15 0.15-11.4	0.1 0.15 0.15	0.06 0.08 0.07	AA-DA=229.9 DA-UA=126.7 AA-UA=356.6	-	[102]
11.	DWCNTs/Ch/ GCE	AA DA UA	DPV	0.1 M PBS/ pH 7.0	0.10–777 0.06–314 0.25–344	0.10 0.06 0.25	0.03 0.03 0.05	AA-DA=182 DA-UA=146 AA-UA=328	Pharmaceuticals , fruit juices and human urine	[105]
12.	PDDA@HCNTs/ GCE	AA DA UA	DPV	0.1 M PB/ pH 7.4	25–1045 2.5–10 5.0–175	25 2.5 5.0	0.12 0.08 0.22	AA-DA=211 DA-UA=152 AA-UA=363	fetal bovine serum	[106]
13.	MWCNT/PEDO T-FAD/GCE	AA DA UA	LSV	0.05 M PB/ pH 7.0	400–8000 6.0–75 2.0–40	400 6.0 2.0	400 6.0 2.0	AA-DA=163 DA-UA=132 AA-UA=295	Human Urine	[122]
14.	Fe(III)P/ MWCNTs/GCE	AA DA UA	CV	0.1 M PB/ pH 4.0	14-2500 0.7-3600 5.8-1300	14 0.7 5.8	3.0 0.09 0.3	AA-DA=300 DA-UA=160 AA-UA=460	Human urine and serum	[55]
15.	MWCNTs/ FeNAZ/CH/GCE	AA DA UA	LSV	DCAAB buffer/ pH 1.0	7.77–833 7.35–833 0.23–83.3	7.77 7.35 0.23	1.11 1.05 0.033	AA-DA=270 DA-UA=150 AA-UA=420	Human urine and serum	[56]
16.	MWCNT/ poly-VA /GCE	AA DA UA	A	0.1 M PB/ pH 7.0	5–120 5–120 5–120	5 5 5	3.5 4.5 1.2	AA-DA=225 DA-UA=75 AA-UA=300	Human Urine	[123]
17.	MWCNT/CCE	AA DA UA	DPV	0.05 M PB / pH 4.5	15-800 0.50-100 0.55-90	15 0.50 0.55	7.71 0.31 0.42	AA-DA=188 DA-UA=163 AA-UA=351	Pharmaceuticals and human serum	[124]

2.3.2.1 Electrochemical Reduction of GO on Electrode Surface

Few methods have been reported in which GO directly reduced on the electrode surface. B. Yang et al. directly electrodeposited the GO on carbon fiber electrode surface by applying potential -1.2 V for 5000s in 0.1 M Lithium perchlorate. Electrochemically reduced graphene oxide was observed by SEM images. Prior to analysis, the fabricated sensor was dipped for 30 minutes to remove the adsorbed GO. The electrochemically reduced graphene oxide remarkably improved the electron transfer kinetics of the electrode surface for electrooxidation of the DA, AA, and UA. The stability of the fabricated electrode was studied by keeping the ErGO/CFE at 25 °C for a week and a small decrease in current 4.6 % (AA), 3.1 % (DA) and 3.8 % (UA) was observed [126]. However, the behavior of the ErGO/CFE sensor for real sample and the presence of interferences needs to investigate. Similarly, in another method instead of direct electrochemical reduction by dipping GO solution, a small amount of GO solution was cast on the GCE surface and then reduced in 0.1M Na-PBS (pH 4.12) at constant potential -0.9 V for 1000s. RGO/GCE was displayed good peak separation, satisfactory dynamic range, good recoveries from real samples (Urine and serum) and low LODs. A small decrease in current observed over a week storage of the sensor at room temperature [127]. A partially reduced graphene oxide sensor was fabricated by controlled reduction of graphene oxide on GCE by two potentiodynamic cycles in 0.1 M PB. The partial reduction of graphene oxide improved the conductivity, sensitivity and the selectivity. The excellent electrocatalytic activity of the sensor gave a wide linear range, good peak separation and low limit of detection. The fouling of the electrode surface is a common issue during the determination of biomolecules especially dopamine. The fouling effect

was found at pH 7.0 while it did not appear at pH 3.0 regardless of the electrode material. The fouling at pH 7.0 could be due to the formation of poly DOPA at neutral or basic pH which decreases the sensitivity of the modified electrode as the number of scans increased. The developed sensor showed good recoveries of the spiked serum sample which make it a good candidate for real sample analysis [128]. Similarly, the L-lysine was electropolymerized by successive direct electrochemical reduction of GO on the surface of GCE. The limit of detection was achieved 2, 0.1 and 0.15 for AA, DA, and UA with satisfactory linear range [129].

2.3.2.2 Nitrogen-Doped Graphene Modified Electrodes

As we discussed the graphene is highly effective material to increase the electroactive surface area, facilitate the rapid charge transfer and have excellent electrical conductivity. These extraordinary properties of graphene are operative if the graphene layers are well separated. The graphene layers generally agglomerate irreversibly and sometimes converted back into graphitic structure due to their van der Waals interaction [130]. This is also one reason which is acting as an obstacle to paving its way towards real practical applications. Some graphene modified electrodes have been reported for simultaneous sensing of targeted analytes in which spacer molecules or metal nanoparticles have been used to prevent the graphene converting back into graphitic form.

Hollow nitrogen doped carbon spheres recently got consideration due to their low cost, high surface permeability, good surface area and conductivity. H. Zhang et al separate the graphene layers by using electrostatic self-assembled hollow nitrogen doped carbon spheres as spacers on the glassy carbon electrode. HNCS hollow spheres were prepared by removing the SiO₂ template using HF. The Figure 3 is demonstrating the schematic

formation of HNCS-RGO. The HNCS hollow sphere has a uniform diameter and shell thickness 475 nm and 15 nm, respectively. The hollow spheres spacers between the graphene layers significantly improved the electrocatalytic activity for the simultaneous perceiving of the targeted analytes compared GCE and the RGO/GCE. Moreover, HNCS improved the peak separation between ascorbic acid and dopamine to 252 mV whereas on RGO/GCE is 205 mV which indicate the kinetics of the graphene improved by the presence of HNCS spacer [131]. Although, the number of steps was involved in the preparation of HNCS-RGO, the developed electrode showed good stability, reproducibility, and recoveries in the spiked urine sample.

In another work, the nitrogen doped graphene was produced from melamine-graphene oxide mixture by combining the covalent transformation and the ultrafast thermal exfoliation. The various ratio of nitrogen doped configuration (graphitic-N pyridinic-N, pyrrolic-N, and pyridinic-N) graphene synthesized by varying the temperature of ultrafast thermal exfoliation. The C/O ratio was found less than graphene in nitrogen doped graphene which indicated some carbon replaced by the nitrogen. The highest current was achieved by the nitrogen doped graphene which was fabricated at high temperature (600 C° & 900 C°) thermal exfoliation. This technique gave a porous structure and large active surface area to nitrogen doped graphene [132]. Similarly, NG/GCE was used for the simultaneous determination of targeted analytes [133]. The nitrogen doped graphene modified electrodes could be promising electrodes for electroanalytical application but still, there is a need to establish them for real sample sensing.

2.3.2.3 Metal and Metal Oxide Based Graphene Nanocomposite Modified

Electrodes

The combination of various metals and metal oxide nanoparticles with graphene further improve the catalytic activity, and the sensitivity of the electrodes for the concurrent recognition of DA, AA, and UA. The noble metals unique physical and chemical properties made them an attractive candidate for the chemical and biochemical sensor developments [134]. X. Wang et al. fabricated the Pd NPs/GR/CS/GCE used for the detection of targeted analytes. The chitosan was used to enhance the stability of the nanoparticles on the electrode surface. It was fabricated in two steps, in a first step, the graphene-chitosan cast on the GCE and later on it was dried up to 24 hours. In a second step the Pd NPs formed electrochemically on the GR/CS/GCE by immersing the electrode in the palladium chloride and Sodium dodecyl sulfate mixture. The Pd NPs GR nanocomposites significantly improved the current and well-resolved peaks compared the GR or Pd NPs modified electrodes. The developed electrode showed excellent stability and small decrease in current observed after 30 days storage in the refrigerator [135]. However, the real sample application and the inferences effect on the behavior of the electrode were not investigated. Silver nanowires reduced graphene oxide nanocomposite (Ag NW/rGO) was also used for the simultaneous sensing of the analytes. In two steps the Ag NWs covalently embedded on the rGO surface. For covalently grafting of AgNWs on the rGO surface, in a first step, the cysteamine through thiol group adsorbed on the Ag-NWs and its amino group react with an epoxide of the GO to give Ag-NWs/GO. In the second step, the microwave assisted hydrothermal method was used to reduce Ag-NWs/GO into Ag-NWs/rGO nanocomposite. The Ag-NWs not only act as the nano-

spacer which prevented the agglomeration of the rGO layers and also facilitate the electron mobility between the layers by providing the conductive pathway. Moreover, the positively charged amino group on the N-AgNWs also prevented them from agglomeration by repulsion and was provided hierarchically three-dimensional conductive pathways. The fabricated electrode was exhibited good selectivity, reproducibility and the stability for the concurrent sensing of targeted analytes [136]. However, the sensitivity of the developed AgNWs/rGO is not so good and its behavior in real samples needs to establish. Similarly, AgNPs/rGO/GCE was also used for the simultaneous determination of targeted analytes. The highly dispersed Ag NPs on the rGO ease the transfer of electrons. The developed electrode was used in a number of real samples and satisfactory recoveries were obtained [137]. In another method, the Au NPs simultaneously reduced and dispersed on the graphene nanosheets (GNS) surface using single step solvothermal method. The ethylene glycol was used as reducing agent and the solvent. The homogenous dispersion of Au NPs on GNS was achieved by the solvothermal process. The charge transfer resistance (R_{ct}) decreased and the electrochemical activity was enhanced for AuNPs/GNS/GCE compared GNS/GCE and GCE. Moreover, well-resolved peaks were observed for the simultaneous detection of targeted analytes with negative peak shift compared GNS/GCE [138]. Q Zhu et al. was fabricated a three-dimensional graphene hydrogel (3DGH) and gold nanoparticles hybrid electrocatalyst on the GCE. The 3DGH and Au NPs have a synergistic effect on the electroactivity of each other for sensitive and selective determination of targeted analytes. Very low LOD in nM range was achieved for targeted analytes [139].

H. Imran et al described the green synthesis of the GO by electrochemical exfoliation of GP. The graphene oxide synthesized without out any ionic liquid by applying the DC potential +7.0 V between two GPE. The aqueous solutions of hydrochloric acid, sodium hydroxide, and the phosphate buffer have been used for the electrical exfoliation of graphene oxide. The various amount of graphene oxide obtained using different mediums. The CVs for 1mM $[\text{Fe}(\text{CN})_6]^{3-/4-}$ showed higher current with HGO (HCl medium) and NGO (NaOH) compared PGO (phosphate buffer saline) modified GCE. The functional group like epoxide and the hydroxyl group repel the $[\text{Fe}(\text{CN})_6]^{3-/4-}$ and the relative response revealed the PGO have more functional groups whereas HGO and NGO have a fewer functional group. However, the few layer and the high-quality graphene oxide obtained by phosphate buffer (pH 7.4) compared another medium. The maximum PL peak intensity, the smaller crystal size and the highest I_D/I_G ratio for PGO endorse the more hydrophilic nature compared other medium prepared GO. The poor peak separation was observed for simultaneous sensing of targeted analytes by Au NPs/PGO/GCE while Au NPs/ErGO/GCE showed well-resolved peaks. The developed sensors showed a good response in the real samples. The sensor was highly sensitive towards dopamine and 10 nM detection limits was achieved [140].

The catalytic activity of the monometallic modified electrode surfaces could be improved by doping with another noble metal. The use of graphene as a support for bimetallic nanostructure further improves the sensing capability of the sensors due to their synergistic effect. L. Chen et al. synthesized the porous alloyed Pd-Ag nanoflower composite supported on the rGO by using in situ reduction method with the support of CTAB. The developed PdAg NFs/rGO/GCE showed better sensitivity towards the

simultaneous detection of the analytes due to a huge surface area that was contributed by the porous structure of the Pd-Ag NFs and the surface area was further improved due to the well organized distribution of the Pd-Ag NFs on the surface of the rGO sheets. The sensor exhibited good anti-interfering capability, reproducibility, and stability after one-month storage of the sensor in the refrigerator, the current was decreased in the range of 6 to 10 % for the analytes [141]. Similarly, Au@Pd-RGO/GCE showed the promising result for the sensing of targeted analytes [142]. In another method, a one-step in situ reduction process was used for the anchoring of Pd and Pt nanoparticles on the surface of the functionalized RGO. The major problem during the co-reduction of the GO and the metal ions for the formation of the metal-graphene nanocomposite, the metal ions nucleate at the GO defective sites which are generated during the synthesis of GO from graphite and it causes the poor distribution of metal NPs on the rGO surface. The GO was functionalized with PDDA to obtain a uniform distribution of the Pd and the Pt NPs. The PDDA is the positively charged long chain cation; the Pd and the Pt ions ($[\text{PtCl}_6]^{2-}$, $[\text{PdCl}_4]^{2-}$) randomly gathered on PDDA-GO surface due to the electrostatic force of attraction. Later on, the metal ions and the GO reduced to obtain PDDA-anchored uniformly distributed Pd-Pt NPs. PDDA effectively stabilized and facilitate the dispersion of Pd-Pt NPs on the RGO surface. The EIS study revealed the charge transfer resistance was significantly decreased compared the bare electrode. The ternary mixture of target analytes was investigated on the graphene nanocomposite fabricated GCE surface and well-resolved peaks were obtained. Furthermore, the developed sensor was used for the analytes spiked samples of the urine and the serum samples. The satisfactory recoveries were obtained in the range of 98 to 104% [143, 144].

Recently, few works are reported in which metal oxide and sulfide was used for the miniaturization of the sensitive electrode for the simultaneous detection of targeted analytes with the combination of graphene. The graphene/SnO₂ nanocomposite was used for the sensing of targeted analytes. Graphene/SnO₂ nanocomposite was formed by reducing the graphene oxide by SnCl₂ in acidic medium containing HCl. Although Graphene/SnO₂ nanocomposite-modified electrode has shown well-separated peaks of targeted analytes, yet its sensitivity was not so good. The detection limit was found 100, 1, 3 μM for AA, DA and UA, respectively [145]. Similarly, Fe₃O₄-NH₂@GS modified GCE has shown the fast charge transfer and well-resolved peaks for the concurrent sensing of DA, AA, and UA were achieved [146]. MoS₂ based materials just like graphene have 2 D structure, edge defective sites, and the tunable energy gaps. It exhibited excellent performances in the fields of electrocatalysis, lithium ion battery and the supercapacitors [147]. H. Bagheri et al. has introduced a carbon paste electrode incorporated by ternary nanocomposite. The synergistic effect of Fe₃O₄, SnO₂, and graphene was used to attain a very sensitive surface for the simultaneous analysis. A very low limit of detection 62.0, 7.1 and 5.0 nM was observed for AA, DA, and UA. Moreover, Fe₃O₄-SnO₂-Gr/CPE performed well in various real samples including human serum as well as urine and satisfactory recoveries were obtained [148]. MoS₂ based materials have been used for the sensing of bioactive molecules like Proteins, mRNA, and DNA [149–151]. Liwen Xing & Zhanfang Ma synthesized the MoS₂/rGO nanocomposite by one spot hydrothermal treatment. The prepared nanocomposite has porous nanostructure, good electrical conductivity, and huge electrical surface area. The MoS₂ surface area was found 23.6 m² g⁻¹ and rGO effectively improved the area to 96.5

$\text{m}^2 \text{g}^{-1}$. Only the MoS_2 on the GCE electrode has shown a huge background current not capable to fully resolve the peaks of the ascorbic acid, dopamine and the uric acid. However, the combination of MoS_2 and rGO on GCE electrode has significantly improved the sensitivity and the peak separation for AA-DA and DA-UA was 232 and 152 mV, respectively. In the presence of interferences, the small current variation was observed. The devolved electrode was used for the sensing in human urine by standard addition method. Moreover, it has shown good selectivity, reproducibility and wide linear range [152].

2.3.3 Polymer Films Modified Electrodes

Polymer films in recent years turned out to be versatile platforms that are widely utilized for catalytic, photovoltaic, biological and sensor development applications. The incisively operating surface of the polymer film can be employed for the specific application depending on its chemical composition, steadiness, linkage, functional groups attached and morphology. Polymer films offer many advantages for tailoring a surface utilized as a sensitive electrochemical sensor. The performance of polymer film electrodes depends on its composition and coating method [164].

Table 2- 2: Figure of merits comparison for the simultaneous sensing of AA, DA and UA using various graphene and its composite modified electrodes

Sr#	Electrode	Analyte	Technique	Medium/pH	Linear range (μM)	LOQ (μM)	LOD (μM)	Peak separation (mV)	Application	Ref.
1	MFGSs/GPE	AA DA UA	DPV	0.1 M PBS/7.0	0.05-9.0 0.03-13 0.03-5.5	0.05 0.030.0 03	0.02 0.01 0.01	AA-DA= 136 DA-UA= 232 AA-UA= 368	-	[153]
2	ErGO/CFE	AA DA UA	DPV	0.1M PBS/7.0	8-2016.45 1.5-224.82 6-899.3	8 1.5 6	4.5 0.77 2.23	AA-DA= 198 DA-UA= 167 AA-UA= 361	-	[126]
3	H-GO/GCE	AA DA UA	DPV	B-R/6.0	1-100 0.5-40 0.5-50	1 0.5 0.5	0.3 0.17 0.17	AA-DA= 180 DA-UA= 180 AA-UA= 360	Human serum and urine	[154]
4	pRGO-GCE	AA DA UA	DPV	0.1 M PB/3.0	40-1000 0.1-100 0.8-800	40 0.1 0.8	4.2 0.08 0.6	AA-DA= 300 DA-UA= 170 AA-UA= 460	Human serum	[128]
5	RGO/GCE	AA DA UA	DPV	0.1 M PBS/7.0	0.7-100 0.1-400 2-600	0.7 0.1 2	0.7 0.1 1	AA-DA= 220 DA-UA= 160 AA-UA= 380	Serum and urine	[127]
6	NG/SPCE	AA DA UA	LSV	0.1 M PBS/7.4	600-1200 120-220 100-250	- - -	- - -	- - -	-	[132]
7	HNCS-RGO/GCE	AA DA UA	DPV	0.1 M PBS/7.0	50-1200 0.5-90 1-70	50 0.5 1	0.65 0.012 0.018	AA-DA= 252 DA-UA= 132 AA-UA= 650	Urine sample	[131]
8	NG/GCE	AA DA	DPV	0.1 M PBS/6.0	5-1300 0.5-170	5 0.5	2.2 0.25			[133]

		UA			0.1-20	0.1	0.045			
9	SPGNE	AA DA UA	DPV	0.1 M PBS/7.0	4-4500 0.5-2000 0.8-2500	4 0.5 0.8	0.95 0.12 0.20	AA-DA= 200 DA-UA= 150 AA-UA= 350	Vitamin C & DA hydrochloride injection and Urine samples	[32]
10	MoS ₂ /rGO/GCE	AA DA UA	DPV	0.1 M PB/7.0	12-5402 5-545 25-2745	12 5 25	0.72 0.05 0.46	AA-DA= 232 DA-UA= 152 AA-UA= 384	Human serum	[152]
11	AgNW/rGO/ SPCEs	AA DA UA	LSV	0.1 M PBS/7.4	45-1550 40-450 35-300	45 40 35	0.81 0.26 0.30	AA-DA= 198 DA-UA= 134 AA-UA= 332		[136]
12	CTAB/rGO/ZnS/ GCE	AA DA UA	DPV	0.1 M PBS/7.0	50.0-1000 1.0-500 1.0-500	50 1.0 1.0	30 0.5 0.4	AA-DA= 190 DA-UA= 100 AA-UA= 290	Urine sample	[155]
13	AuNCs/AGR/M WCNT/GCE	AA DA UA	SWV	0.1 M PBS/7.0	10-150 1.0-210 5.0-100	10 1 5	0.27 0.08 0.1	AA-DA= 210 DA-UA= 140 AA-UA= 350	Human urine	[156]
14	MgO/Gr/TaE	AA DA UA	DPV	0.1 M PBS/5.0	5-350 0.1-7 1-70		0.03 0.15 0.12	AA-DA= 300 DA-UA= 147 AA-UA= 447	Human serum	[157]
15	Graphene/SnO ₂ / GCE	AA DA UA	DPV	0.05 M PBS/6.8	100-1000 1-20 3-21	100 1 3	100 1 3	AA-DA= 240 DA-UA= 180 AA-UA= 420	-	[145]
16	RGO/PAMAM/ MWCNT/AuNP/ GCE	AA DA UA	DPV	0.1 M PBS/4.0	20-1800 10-320 1-114	20 10 1	6.7 3.3 0.33	AA-DA= 260 DA-UA= 120 AA-UA= 380	-	[158]

17	PdAg NFs/rGO/GCE	AA DA UA	DPV	0.1 M PB/6.0	1-4100 0.05-112 3-186	1 0.05 3	0.185 0.017 0.654	AA-DA= 204 DA-UA= 128 AA-UA= 332	-	[141]
18	Fe ₃ O ₄ - NH ₂ @GS/GCE	AA DA UA	DPV	0.1 M PBS/7.0	5.0-1600 0.2 – 38 1.0-850	5 0.2 1.0	0.074 0.126 0.056	-	Urine samples	[146]
19	Ni/sG/GCE	AA DA UA	DPV	0.1 M PBS/4.0	50-450 0.44-11 2-50	50 0.44 2	30 0.12 0.46	AA-DA= 219 DA-UA= 161 AA-UA= 380	Human serum and urine	[159]
20	Trp-GR/GCE	AA DA UA	DPV	0.1 M PBS/	200-12900 0.5-110 10-1000	200 0.5 10	10.09 0.29 1.24	-	Vitamin C injection, Multivitamin tablet, Dopamine hydrochloride injection, urine and serum samples	[160]
21	Au@Pd- RGO/GCE	AA DA UA	DPV	0.1 M PBS/7.0	1-800 0.1-100 0.1-350	1 0.1 0.1	0.28 0.024 0.02	AA-DA= 178 DA-UA= 164 AA-UA= 342	Urine samples	[142]
22	Au/RGO/GCE	AA DA UA	DPV	0.1 M PBS/7.0	240-1500 6.8-41 8.8-53	240 6.8 8.8	51 1.4 1.8	AA-DA= 200 DA-UA= 110 AA-UA= 310	Serum samples	[161]
23	Pd3Pt1/PDDA- RGO/GCE	AA DA UA	DPV	0.1 M PBS/7.4	40–1200 4–200 4–400	40 4 4	0.61 0.04 0.10	AA-DA= 184 DA-UA= 116 AA-UA= 300	Human urine and serum samples	[144]
24	Pd NPs/GR/CS /GCE	AA DA	DPV	0.1M PBS/4.0	100-4000 0.5-15&20- 200	100 0.5	20 0.1	AA-DA= 252 DA-UA= 144	-	[135]

		UA			0.5-200	0.5	0.17	AA-UA= 396		
25	AgNPs/rGO/ GCE	AA DA UA	LSV	PB/3.5	10-800 10-800 10-800	10 10 10	9.6 5.4 8.2	AA-DA= 260 DA-UA= 124 AA-UA= 384	-	[137]
26	GS-PTCA/GCE	AA DA UA	DPV	0.1 M PBS/3.0	20-420 0.4-374 4-544	20 0.4 4	5.60 0.13 0.92	-	-	[162]
27	Pt-Gr/CNT/GCE	AA DA UA	DPV	0.1 M PBS/7.0	200-900 0.1-30 0.1-50	200 0.1 0.1	50 0.01 0.1	AA-DA= 208 DA-UA= 140 AA-UA= 360	Vitamin C, Urine, serum samples	[163]

For electrode modification, electroactive polymer films are required and their three major classes can be described as follow [165].

- The polymer films in which electrical conduction arises due to the mobility of charge bearing particles alongside the chains are categorized as electronically conducting polymers e.g. polypyrrole.
- Type of polymer films in which conduction of electrical current is because of redox reaction at active sites are named redox polymers e.g. polyvinyl ferrocene.
- Class of polymer films in which conduction is a consequence of the movement of ions within the film is called electrolyte polymers e.g. nafion.

Since the development of first biosensor [166], numerous sensors were developed. Most of the target analytes in real life samples exists in a complex mixture and at trace level; therefore the sensitivity and selectivity of the biosensor need more attention. The functional group rich surface of polymer films can help to immobilize different sort of biomolecules on its stable platform, that can give the enhanced signal and help to avoid interferences from surrounding chemical environment for the target analyte. As a result, the high selectivity and sensitivity can be achieved by using polymer film electrodes [167, 168]. Polymer film electrodes show unique properties like easy to fabricate, low-cost materials, ease of doping various entities into polymer film (ions, molecules, nanoparticles) and liberty in the choice of platform for a deposition that make them best choice for real life sensor applications. The electroactive polymer film on the surface of inorganic platform can be done in different ways like

- Electropolymerization method, the working electrode is dipped into the solution containing monomer and polymer layer is formed on the surface by electropolymerization [169, 170]. For this type of polymerization very small volumes of the monomers, solutions are required, that is a big advantage in term of cost and safety.
- Screen printing, after preparation of required polymer, a film is coated on the surface of the electrode by screen printing process. By the use of this method multiple layers can be deposited in a well-defined pattern and at the end, pattern is settled by exposure to UV light or heat annealing [171, 172].
- For Spin coating, a solution containing microsphere suspension of the polymer is added to the spinning surface, as a result, they cross-linked to each other and form a hydrogel, later on, solvent is evaporated [173].

Out of all above methods discussed, the electropolymerization method is proved to be the best for polymer immobilization on the electrode surface. This method provides better control of homogeneity of film breadth, infusion, and charge transfer features. Once an unwavering and consistent layer is acquired on the surface of electrode then following advantages can be encountered [165].

- The polymer films have a large number of catalytic sites compared to other chemically modified electrodes, as a result, high catalytic currents can be observed.
- Required active sites can be designed to target a particular analyte by precisely choosing the chemical composition of the polymer. It gives a chance to mimic the

interaction between the polymer film and its redox counterpart. Therefore, high selectivity can be achieved for various analytes.

- The polymer film can entrap various substances to improve the charge transfer kinetics.
- Polymer films are highly selective in their interaction so they can avoid fouling by undesirable species or side reactions.

It is very difficult to categorize the signal with specific class due to a variety of materials and physical/ chemical interaction phenomena involved during sensing of target analytes [174, 175]. Therefore, the electrical signal obtained from the modified electrode is a combined effect of the physical and chemical interaction of the analyte with a polymer film. The unique characteristics of polymer films made them a famous contender for detection of biomolecules and it is widely applied for simultaneous sensing of targeted analytes.

2.3.3.1 Thiadiazole Based Polymer Film Modified Electrodes

The materials used for modification should have the capability to overcome the opposite charges for the concurrent detection of analytes. To fulfill this requirement the 5-amino-2-mercapto-1,3,4-thiadiazole functionalized film was used to GCE. p-AMT/GCE not only variate peak potentials to give well-defined peaks but also increase the peak current of each peak two to three folds, compared to broad peaks obtained from bare GCE. The response of p-AMT/GCE towards AA, DA and UA proved that AMT film consists of heteroatoms attached to positively charged backbone of the polymer film. This characteristic made it easier to interact positively charged analyte (DA) and the

molecules with a negative charge (AA and UA) [176]. In another study same authors utilized 1 mM 2-amino-1, 3, 4-thiadiazole solution in 0.1 M H₂SO₄ for the formation of poly ATD film on the surface of GCE. Atomic force spectroscopic studies confirm the presence of ultrathin film with a thickness of 25 nm on average. The modified electrode was employed to sense AA, DA and UA at the same time, linear range obtained was 30-300, 5.0-50 and 10-100 μM and the detection limit was 2.01, 0.33 and 0.19 μM respectively [177].

2.3.3.2 Azo Dye Based Polymer Film Modified Electrodes

Eriochrome black T (EBT) is an azonaphthol dye well distinguished complexometric indicator. The structural characteristic like -SO₃ groups and oxygen rich structure make it suitable choice for development of polymer film to modify the surface of the sensor [178]. A pH indicator sulfonazo III was utilized as a monomer for the development of polymer film GCE. The resulting sensor showed high sensitivity and selectivity towards the target analytes and usability was proved by determination of targeted analytes in actual samples [167]. Zhang et. al. utilized complexometric indicator acid chrome blue K as a building block of polymer film form on the surface of GCE and they utilized this modified surface for recognition of targeted analytes. It likewise showed the ability to eliminate the effect of interferences at high concentrations of interfering species like biomolecules and metallic ions [179]. Evans Blue is an azo dye which is widely used for the sustainability evaluation of the living cells and measure the penetrability of the blood-brain obstacle to macromolecules. Lin and co-workers employed evans blue for simultaneous detection of targeted analytes. First, the GCE was stimulated by application of repeated potential cycles between -0.2 to 1.8 V in PBS (pH=9) then under same

conditions polymer film of Evans Blue was produced on the activated surface of GCE. During the polymerization of Evans blue, the amino group oxidized to $-NH$ which on oxidation produce hydrazobenzene sulfonic acid and finally reduced to hydrazobenzene sulfonic acid. The reactions on electrode surface were due to redox process between hydroazo and azo groups [180]. Similarly, PCDDA film modified electrode was used for the concurrent assay of targeted analytes. The characterization of electrode surface showed that PCDDA film was restrained on the surface of GCE and also displayed higher catalytic activity [181]. para-Phenylenediamine is an azo dye used in tattoo designs and hair dyes, employed for formation of poly para-phenylenediamine (PPD) on GCE. The modified electrode showed the higher electroactive area as compared to the bare electrode and greater catalytic activity for electro-oxidation of targeted analytes. The designed electrode showed satisfactory recovery of the added analytes in human serum samples with very small error [182].

2.3.3.3 Biomolecule Based Polymer Film Modified Electrodes

Biomolecules like amino acids when electropolymerized on the surface of the electrode, they form a thin film that shows electrocatalytic properties. 4-aminobutyric acid is an important part of the mammalian central nervous system and acts as a repressive neurotransmitter to lessen neuronal irritability. Zheng and coworkers used 4-ABA to synthesize the polymer film p-4-ABA for sensitive and discriminatory sensing of targeted analytes simultaneously. Polymer film not only helped to get higher peak current for the analytes but also exhibited substantially distinguished peaks of targeted analytes in ternary solution. The prepared electrode showed a stable signal when stored for a week and high tolerance for various interfering agents [183]. DNA composite of the amino acid

polymer film can also help to obtain better electrocatalytic properties as compared to the only amino acid acting as a modifier. The presence of p-electrons in double helical backbone in DNA can make a conductive layer to increase the surface area of the electrode and interfacial conductivity. The opposite charges on DNA and poly L-Leucine help to develop a strong interaction between two layers and form a composite layer with high electrocatalytic activity ascribable to greater electron transferal kinetics. The biomolecule composite modified electrode was applied for coincident sensing of AA, DA and UA with a detection limit of 2.0, 0.04 and 0.2 μM , respectively [184]. In another method, a polymer film of tyrosine on GCE was produced and immobilized the functionalize MWCNT on its surface. The presence of MWCNT on poly (tyrosine) heightened the electro-oxidation peak currents of analytes as compared to only poly (tyrosine) surface and also increase the peak separation. The developed electrode showed satisfactory recoveries of analytes when applied to the human urine samples [185]. Similarly, carbon nano-horns were deposited on the GCE, later on, glycine was electropolymerized to get CNHs/PGLY/GCE. Polyglycine produced synergistic effect along with carbon nano-horns and well-separated peaks of targeted analytes were observed [186].

2.3.3.4 Metal Nanoparticles Incorporated Based Polymer Film Modified Electrodes

The unique chemical, physical and mechanical properties of nanomaterial's make them highly suitable for electrode modification. Nanoparticle produced from metals are the widely used due to higher electroactivity, large surface area, easy to crop and encourage quicker electron transferal kinetics. Metal nanoparticles (MNPs) can form a composite

with conductive polymers due to their strong interaction, consequently, electrocatalytic characteristics and conductivity of polymers could be boosted. MNPs most probably act as makeweights to transform the polymer film or to design nanocircuits on the surface of polymers. Various conducting polymers can act as a base to support MNPs including polypyrrole, polydopamine, poly(N-isopropylacrylamide), nafion film etc. Polypyrrole is a conducting polymer and widely used in various bioanalytical applications due to greater environmental and thermal stability, higher conductivity and facile synthesis. Due to good adhesive properties of polypyrrole, it can be used to form a composite with MNPs like ZnO–Cu_xO. FE-SEM, XRD and Raman characterization revealed the formation of nanoparticles of metal oxides on the surface of polypyrrole modified GCE, also it was confirmed that ZnO nanosheets were lodged on the top of Cu_xO nanowires. The resultant ZnO–Cu_xO–PPy/GC electrode showed improved sensitivity and selectivity towards detection of targeted analytes in an assortment [187].

There is a chance that polypyrrole can lose its conductivity with the passage of time. However, the nanoparticles attached to the surface of polypyrrole remain conducive for a long time. To utilize this property of nanoparticles Khadijeh et al. form a nanocomposite of silver nanoparticles with electropolymerized pyrrole film to heighten the electrocatalytic activity of GCE. The resulting sensor showed the desirable characteristics (i.e. outside surface area, greater selectivity, superior electrical conductivity) [188]. A highly stable layer of poly 3-Amino-5-mercapto-1,2,4-triazole (p-TA) have many coordination sites like exocyclic –SH group, one exocyclic –NH₂ group and three N cyclic atoms. Overoxidation at higher potential resulted in the introduction of more functional groups in addition to coordination sites already present in p-TA. The resulting

overoxidized poly(3-Amino-5-mercapto-1,2,4-triazole) (p-TA_{OX}) displayed large surface area, better reproducibility, increased reaction rate and lower background current. The combination of copper nanoparticles resulted in the synergetic effect on the salient features of the overoxidized film, that helped in a sensitive and selective sensing of target analytes in human blood and urine samples [189]. Wang et al modify the p-TA by depositing gold nanoclusters as a result better sensitivity and lesser detection limits for target analytes were obtained. The permeability of p-TA for both positive and negative ions and better electrocatalytic activity of Au nanoclusters accumulatively created superior peak currents, lesser overpotential and improved peak separation for target organic analytes [190].

The polydopamine film was found effective for the reduction of gold metal into gold nanoparticles via functional groups present on its surface. The HAuCl₄ act as an oxidant to prompt DA polymerization and gold nanoparticles formation, Zhang and coworkers utilized the hybrid of pDA and gold nanoparticles for instantaneous sensing of targeted analytes. In situ electro-polymerization procedure was adopted to get the GCE modified with pDA and AuNPs composite. SEM images verified the presence of gold nanospheres with a diameter of 100 nm. The resulting electrode displayed higher sensitivity and good separation of peaks for the target analyte. Moreover, the developed sensor has shown 5 % relative error for very high concentration of metal ions (500 times Na⁺, K⁺ and Cl⁻, 100 times Mg⁺² and Ca⁺²) and biomolecules (30 times for glycine, chitosan, glutamic acid, glucose, and L-cysteine) as interfering species [191]. The gold nanoclusters were used for simultaneous sensing of target analytes due to fast charge transfer compared to gold nanospheres. Various parameters were optimized to control the thickness of pDA film

which contributes a crucial role to obtain the desired size of AuNCs. Small size AuNCs was not providing sufficient area for the reaction whereas a tremendous decrease in charge transfer rate was observed by large size AuNCs. Polydopamine supported AuNCs on Fluorine doped Tin Oxide (FTO) proved to be helpful for detection of DA with adequate sensitivity in existence of 10 times larger quantity of AA and UA [192]. A composite of polytyramine (Pty) and tris(2,2'-bipyridyl)Ru(II) complex was employed on the surface of the electrode. The improved electron transfer kinetics and higher electroactivity of the composite were attributed to the Ru redox centers and π -conjugated mainstay of Pty. The resultant electrochemical detector found to be suitable towards simultaneous sensing [193].

2.3.3.5 Three-Dimensional Structure Based Polymer Films Modified Electrodes

To exploit the unique properties like large surface area, low cost, smaller size and mechanical strength of three-dimensional structures, Shiji and coworkers electropolymerized ethylene dioxythiophene on Ni/silicon microchannel plate for simultaneous determination of targeted analytes. The better peak separation of the target analytes was achieved by PEDOT-modified Ni/Si MCP compared PEDOT-modified GCE electrode. The improved electroactivity of Ni/Si MCP electrode was ascribed to larger surface/volume ratio. The PEDOT-modified Ni/Si MCP electrode was applied to the dilute urine sample. However, the limited interferences effect was investigated [194]. Ordered mesoporous carbon possesses three-dimensional structure was utilized for determination of AA, DA, and UA in solution. Detection was done at physiological pH that makes it highly appropriate to apply for sensing of target analytes in existent samples [195]. Similarly, exfoliated MoS₂ nanosheets were embedded into PEDOT by

electrodeposition on the surface of GCE. The fabricated sensor has shown good selectivity for target analytes in the presence of potential interferences and displayed adequate recoveries of spiked analytes in real samples [196].

2.3.3.6 Acrylamide-Based Polymer Films Modified Electrode

Poly (N-isopropylacrylamide) (PNIPAAm) is a polymer that responds to temperature changes in its surroundings. The volume decreases about 90% reversibly when it is heated above 32°C. It can support electroactive materials to modify the surface of the electrode. Shieh et al. applied aqueous solution mixture of PNIPAAm and functionalized CNTs on the surface of GCE. The modified surface has shown good electrocatalytic behavior towards target analytes. CNT/PNIPAAm composite displayed different behavior depending on nature of CNTs, composite preparation temperature and temperature at which redox reactions of $\text{Fe}(\text{CN})_6^{3-/4-}$ was investigated [197].

2.3.3.7 Aniline Based Polymer Films Modified Electrodes

Polyaniline (PANI) is another polymer showing conducting properties but PANI is not much sensitive for bioanalytes. This issue could be resolved by suitable modification of PANI film with other highly conductive materials. Manivel et al. are prepared in situ composite of PANI and graphene oxide (GO) and cast on the surface of the electrode. PANI-GO nanocomposite displayed better electroactivity as compared to GO or PANI alone on the surface of GCE. The mass ratio of aniline and graphene oxide played a crucial role in attaining considerably separated signals for targeted analytes. The best ratio of aniline and graphene oxide for sensitive sensor fabrication was 100:3 [198]. Ion exchange characteristic of PANI helps to produce a composite with iron, consequently,

the electrocatalytic activity of the PANI enhance prominently. The resulting electrode Fe-Meso-PANI enhanced the oxidation peak current of the AA, DA, and UA. It also showed high resistivity towards foreign substances spiked to the solution containing target analytes [199].

2.3.4 Ionic Liquid Modified Electrodes

Ionic liquids are extensively being used for the modification of the electrodes to give them certain characteristics. Ionic liquids are basically the molten salts which have melting points close or less than room temperature. The ionic liquids composed of asymmetric cations and the anions. The ionic liquids are considered attractive electrode fabrication material due to their ionic conductivity, ionic structure, low volatility, high viscosity, biocompatibility and the hydrophobicity [96]. Due to these characteristics, many sensors have been reported based on ionic liquids. However, very few works have been reported in which simultaneous analysis of targeted analytes has been done by using ionic liquid modified electrodes. Carbon ionic liquid electrodes have some certain advantages over conventional carbon paste electrode where the nonconductive organic material was used as binding material. CILE have advantages like antifouling properties, fast charge transfer, and high conductivity. A pyridinium-based ionic liquid was used for the fabrication of the CILE and used for the simultaneous measurement of the targeted analytes. A wide linear range was obtained [203], however, the sensitivity of the electrode needed to improve. The sensitivity and the peak separation of the ionic liquid-based electrodes were further improved by using the ionic liquids in combination with other highly effective electroactive materials like graphene [204], CNTs [205], and metal NPs.

Table 2- 3: Figures of merits comparison for simultaneous detection of AA, DA and UA utilizing polymer film modified electrodes.

Sr#	Electrode	Analyte	Technique	Medium /pH	Linear range (μM)	LOQ (μM)	LOD (μM)	Peak separation (mV)	Application	Ref.
1.	p-AMT/GCE	AA DA UA	DPV/A	0.2 M PBS/ pH 5.0	30-240 5.0-40 10-80	30 5.0 10	0.075 0.040 0.060	AA-DA=130 DA-UA=150 AA-UA=280	dopamine hydrochloride injection samples	[176]
2.	p-ATD/GCE	AA DA UA	DPV	0.2 M PB solution/ pH 5.0	30-300 5.0-50 10-100	30 5.0 10	2.01 0.33 0.19	AA-DA=110 DA-UA=152 AA-UA=262	Human Urine	[177]
3.	PEBT / GCE	AA DA UA	DPV	0.05 M PBS / pH 4.0	150-1000 0.1-200 10-130	150 0.1 10	10 0.02 1.0	AA-DA=210 DA-UA=170 AA-UA=380	-	[178]
4.	PSF / GCE	AA DA UA	DPV	0.2 M PB solution / pH 3.0	0.5-1300 0.05-470 0.2-100	0.5 0.05 0.2	0.17 0.03 0.11	AA-DA=180 DA-UA=150 AA-UA=330	Human urine, Vitamin C tablets	[167]
5.	p-ACBK / GCE	AA DA UA	DPV	0.05 M PB solution / pH 4.0	50-1000 1.0-200 1.0-120	50 1.0 1.0	10 0.5 0.5	AA-DA=193 DA-UA=166 AA-UA=359	dopamine hydrochloride injection, Human urine, Vitamin C tablets	[179]
6.	PEB / GCE	AA DA UA	DPV	0.05 M PB solution / pH 4.5	1.0-30	1.0	0.3 0.25 2.0	AA-DA=182 DA-UA=180 AA-UA=362	dopamine hydrochloride injection and Human Urine	[180]
7.	PCDDA / GCE	AA DA UA	DPV	0.20 M PB solution / pH 4.0	50-240 50-280 0.1-18	50 50 0.1	1.43 0.29 0.016	AA-DA=160 DA-UA=170 AA-UA=330	Vitamin C, Human urine and Fruits	[181]
8.	p-PPD/GCE	AA DA UA	DPV	0.1 M PB solution/ pH 5.0	2.0-2000 10-1250 50-1600	2.0 10 50	0.4 1.0 2.5	AA-DA=200 DA-UA=145 AA-UA=345	Human blood serum	[182]

9.	P-4-ABA/GCE	AA DA UA	DPV	0.2 M PB solution/ pH 4.5	20-800 5.0-100 1.0-80.0	20 5.0 1.0	5.0 1.0 0.5	AA-DA=208 DA-UA=136 AA-UA=344	Human urine	[183]
10.	P _L -LEU/DNA/ GCE	AA DA UA	DPV	0.2 M PB solution/ pH 4.5	5-750 0.1-100 0.5-100	5.0 0.1 0.5	2.0 0.04 0.2	AA-DA=217 DA-UA=160 AA-UA=377	Human Urine	[200]
11.	poly(Tyr)/ MWCNTs- COOH/GCE	AA DA UA	DPV	0.067 M PB solution/ pH 7.4	-		2.0 0.02 0.3	AA-DA=160 DA-UA=150 AA-UA=310	Human serum	[185]
12.	CNHs/PGLY/ GCE	AA DA UA	DPV	0.1 M PB/ pH 6.0	30-450 1.0-280 2.0-350	30 1.0 2.0	0.34 0.03 0.18	AA-DA=130 DA-UA=120 AA-UA=250	Human Urine	[186]
13.	PDAox- PTCA/GCE	AA DA UA	DPV	0.1 M PBS/ pH 3.0	76-3900 0.6-253 1.8-238	76 0.6 1.8	25.3 0.2 0.6	AA-DA=150 DA-UA=180 AA-UA=330	-	[201]
14.	HNCMS/GCE	AA DA UA	DPV	0.1 M PB solution	100-1000 5.0-70 3.0-30	100 5.0 3.0	0.91 0.02 0.04	AA-DA=212 DA-UA=136 AA-UA=348	Human Urine	[202]
15.	ZnO-Cu _x O-PPy/GCE	AA DA UA	DPV	0.1 M BR solution/ pH 4.0	200-1000 0.1-130 0.5-70	200 0.1 0.5	25 0.04 0.2	AA-DA=150 DA-UA=154 AA-UA=304	Hydrochloride Injection and human urine	[187]
16.	AgNPs/PPy/ GCE	AA DA UA	DPV	0.1 M BR solution/ pH 4.0	10-580 0.5-155 2.0-100	10 0.5 2.0	1.8 0.1 0.5	AA-DA=120 DA-UA=170 AA-UA=290	Hydrochloride Injection and human urine	[188]
17.	CuNPs/p- TA _{ox} /GCE	AA DA UA	DPV	0.1 M PB solution/ pH 4.0	240-750 0.6-21.6 4.0-103	240 0.6 4.0	5.0 0.03 0.16	AA-DA=205 DA-UA=165 AA-UA=370	Human blood serum and urine	[189]
18.	nano-Au/ p-TA/GCE	AA DA UA	DPV	0.1 M PB solution/ pH 4.0	2.1-50.1 0.6-340.0 1.6-110.0	2.1 0.6 1.6	1.1 0.05 0.08	-	Human blood serum and urine	[190]

19.	PDA-AuNPs/GCE	AA DA UA	SWV	0.1 M PB solution/pH 7.0	40-1000 1.0-80 0.8-100	40 1.0 0.8	5.0 0.08 0.06	AA-DA=180 DA-UA=150 AA-UA=330	Human blood serum and urine	[191]
20.	AuNCs/PDA/FTO	AA DA UA	CV and DPV	0.01 M PB solution/pH 7.5	-	-		AA-DA=110 DA-UA=240 AA-UA=350	-	[192]
21.	Ru/Pty/GCE	AA DA UA	LSSV	0.1 M PB solution/pH 4.1	-	-	0.31 0.08 0.58	AA-DA=202 DA-UA=153 AA-UA=355	Human blood serum	[193]
22.	PEDOT-modifiedNi/Si MCP electrode	AA DA UA	DPV	0.1 M PBS/ pH 7.4	20-1400 12-48 36-216	20 12 36	10 1.5 2.7	AA-DA=220 DA-UA=140 AA-UA=360	Human urine	[194]
23.	OMC/Nafion/GCE	AA DA UA	DPV	PBS/ pH 7.4	40-800 1.0-90 5.0-80	40 1.0 5.0	20 0.5 4.0	AA-DA=190 DA-UA=150 AA-UA=340	Human Urine	[195]
24.	MoS ₂ /PEDOT/GCE	AA DA UA	DPV	PBS/ pH 7.4	20-140 1.0-80 2.0-25	20 1.0 2.0	5.83 0.52 0.95	AA-DA=210 DA-UA=150 AA-UA=360	Human Urine	[196]
25.	fCNT/PNIPAAm/GCE	AA DA UA	CV	0.1 M PB solution/pH 7.4	2000-10000 200-1000 600-1400	2000 200 600	-	AA-DA=200 DA-UA=150 AA-UA=350	Human blood serum and urine	[197]
26.	PANI-GO/GCE	AA DA UA	DPV	0.05 M PBS/ pH 7.0	25-200 2.0-18 2.0-18	25 2.0 2.0	20 0.5 0.2	AA-DA=320 DA-UA=230 AA-UA=550	-	[198]
27.	Fe-Meso-PANI/GCE	AA DA UA	LSV	PB solution/pH 3.5	10-300 10-300 10-300	10 10 10	6.5 9.8 5.3	AA-DA=150 DA-UA=160 AA-UA=310	Human blood serum and urine	[199]

A sensitive and selective sensor was fabricated by combining the properties of graphene platelet nanofibres and the ionic liquid. The developed sensor SGNF/IL/CS/GCE has shown excellent electrocatalytic activity and reduced the overpotential for the sensing of targeted analytes. The exceptional peak separation was observed between AA-DA (213 mV), DA-UA (151 mV) and AA-UA (364 mV). The sensor has shown long term storage capability, after two weeks the current signal was achieved 94.6 % and for 4 weeks 87.2 % [204]. A. Afraz et al. fabricated a carbon paste electrode (CPE) consist of graphite (60 %), paraffin (14.2 %), MWCNTs (10.8 %) and IL (15 %). The proper concentration of the ILs and the MWCNTs is necessary to control the background current as they could lead to the deceptive limit of detection due to overlapping of the signal with the background current. Statistical software was used to optimize the composition of the CPE. The Au NPs electrodeposited on the surface of GPE in the shape of cauliflower by potentiostatic double pulse technique. The fabricated electrode was found very sensitive for AA, DA and UA and limit of detections were achieved 120, 30 and 30 nM, respectively. The sensor was applied for the sensing of biomolecules in the human urine and the serum sample [205]. Similarly, in other work, the Pd NPs were electrodeposited on the CPE (graphite powder+ paraffin + pretreated MWCNTs+ IL). However, the Pd NPs was found not as much effective as Au NPs and limit of detections were acquired 200, 30, 150 nM for AA, DA and UA, respectively.

Table 2- 4: Figures of merits comparison for simultaneous detection of AA, DA and UA using ionic liquid modified electrodes.

Sr#	Electrode	Analyte	Technique	Medium /pH	Linear range (μM)	LOQ (μM)	LOD (μM)	Peak separation (mV)	Application	Ref.
1	CILE	AA DA UA	DPV	0.1 M PB/6.8	50-7400 2-1500 2-220	50 2 2	20 1 1	AA-DA= 160 DA-UA= 135 AA-UA= 295	Human serum and urine	[203]
2	SGNF/IL/CS -GCE	AA DA UA	DPV	0.1 M PB/6.0	30-350 0.05-240 0.12-260	30 0.05 0.12	14.8 0.05 0.1	AA-DA= 213 DA-UA= 151 AA-UA= 364	Human urine	[204]
3	Au-NP/CPE (MWCNTs/IL/G)	AA DA UA	DPV	PB/4.0	0.3-285 0.08-200 0.1-450	0.3 0.08 0.1	0.12 0.03 0.03	AA-DA= 152 DA-UA= 166 AA-UA= 318	Human serum and urine	[205]
4	Pd-NP/CPE (MWCNTs/IL/G)	AA DA UA	DPV	PB / 4.5	0.6-112 0.1-151 0.5-225	0.6 0.1 0.5	0.2 0.03 0.15	AA-DA= 180 DA-UA= 200 AA-UA= 380	Human serum and urine	[206]

2.3.5 Other Electrodes

Apart from graphene, polymeric, CNTs, ionic liquids modified electrodes; other methods were also being used to enhance the sensitivity of the electrodes.

2.3.5.1 Pretreated Electrodes

One of the simple methods is pretreatment method. The electrochemical and the chemical pretreatment of the carbon electrodes has shown the significant effect to improve the fast charge transfer and help to overcome the overlapping of the peak potential of the various analytes. The GCE was electrochemically pretreated in the 0.5 M NaOH over 40 CV cycles from 0.0 to +0.90 V. This electrochemical treatment has given unique characteristics and it overcomes the overlapping problem of the bare GCE for sensing of targeted analytes. It also significantly enhanced the oxidation peak currents. This characteristic attributed to the formation of some functional groups like carboxyl, hydroxyl and the carbonyl on the electrode surface. The developed sensor was applied to the samples of injections, urine, and the serum to find out AA, DA, and UA [207].

2.3.5.2 Surfactant Modified Electrodes

The surfactant-modified electrodes are also getting attention in the electroanalysis due to their unique physical and chemical properties. Some certain surfactant decreases the overpotential of the electrochemical redox reaction to make them kinetically possible. The surfactant-modified electrodes also improved the reversibility of some analytes which was poor on the bare electrode. S. Shankar et al has used an anionic surfactant for the fabrication of Sodium dodecyl benzene sulfate modified CPE and applied for the determination of targeted analytes [208].

2.3.5.3 Nanoparticle Modified Electrode

Few works were also reported in which metal nanoparticles were also used for the determination of AA, DA, and the UA. As discussed before the metal nanoparticles are frequently being used in combination with other highly effective electroactive materials like graphene [209] and CNTs. AuNPs in combination with MoS₂ has shown good electrochemical activity compared to the individual behavior of Au NPs and MoS₂. MoS₂ is a two-dimensional structure like graphene and considered its analogs when having single or fewer layers. These layers could be decorated easily with the noble metal NPs. AuNPs@MoS₂ film modified GCE exhibited a good sensitivity and wide linear range for targeted analytes [210]. In another work, the PtCu alloy hierarchical nanoporous structure was fabricated by dealloying and annealing of the PtCuAl precursor. The modified GCE of PtCu alloy has shown good electroactivity and the peak separation for targeted analytes [211]. Similarly, the NPs of NiCo alloy was implanted in the N-doped carbon nanoplates structure hierarchically. Similarly, M Li et al. has introduced a very sensitive method for the simultaneous sensing of targeted analytes. One-dimensional MgO various nanostructure morphologies were synthesized using Mg(NO₃)₂·6H₂O as a precursor. Three different forms such as nanorods, tadpole, and nanobelts of 1 D MgO were obtained by controlling the certain conditions and reaction time. 1 D MgO nanostructured GCE was fabricated by preparing the dispersed sonicated suspension of 1-D MgO and chitosan. 1-D MgO was electrodeposited by applying the -5V potential for 20 minutes and dried. Among all these forms the MgO nanobelt has shown excellent electrocatalytic activity for the sensing of targeted analytes. This excellent electrocatalytic activity was observed due to the presence of surface defects and surface electronic properties have a

strong dependence on the low coordination sites (steps, corners, and kinks). The resistance of MgO nanobelts was decreased attributed to electron tunneling between surface defects. The electron transfer rate was significantly accelerated and the very low limit of detection 0.2, 0.05, 0.04 μM for AA, DA and UA was achieved using CV [212].

2.4 Challenges in Modified Electrodes' Commercialization and Real Sample Application

DA is a major part of mammalian central nervous system related to catecholamine category of neurotransmitters with low concentration in the human brain. DA is formed in adrenal glands and numerous zones of encephalon and necessitated for brain–body consolidation [213]. Various electrochemical methods have been utilized to distinguish the DA in the occurrence of AA and UA due to their electroactivity, but with some exceptions, most of them are restricted to the in-vitro study or study under controlled conditions [214–216]. There is a great interest for the *in-vivo* study of above-mentioned analytes by utilizing chemically modified electrodes and microelectrodes due to the fact that it can help in understanding chemical changes occurring in the brain and consequently the function of the brain. The capability to directly monitor dopamine changes could provide information that might be beneficial for confronting diseases associated with dopamine-like Parkinson's disease [217]. There is also a lot of interest in commercialization due to a great deal of financial benefits.

Table 2- 5: Figures of merits comparison for simultaneous detection of AA, DA, and UA using pretreated, surfactant or nanoparticles modified electrodes.

Sr #	Electrode	Analyte	Technique	Medium/pH	Linear range (μM)	LOQ (μM)	LOD (μM)	Peak separation (mV)	Application	Ref.
1	pGCE	AA DA UA	DPV	0.1 M PB/7.0	25-300 3-30 5-70	25 3 5	23.38, 2.67, 4.70	AA-DA= 165 DA-UA= 135 AA-UA= 300	Injections, serum, urine, multivitamin tablet	[207]
2	DDBSMCPE)	AA DA UA	DPV	0.2 M PB/7.4	-	-	-	AA-DA= 189 DA-UA= 133 AA-UA= 322	Injection	[208]
3	AuNPs@ MoS ₂ /GCE.	AA DA UA	DPV	0.1 M PB/7.0	1000 – 70000 0.05 – 4000 10 – 7000	1000 0.05 10	100, 0.05, 10	-	Human serum	[210]
4	Hnp Pt-Cu alloy/GCE	AA DA UA	DPV	0.1 M PB/7.0	25 – 800 4 – 20 10 – 70	25 4 10	17.5, 2.8, 5.7	AA-DA= 150 DA-UA= 140 AA-UA= 290	-	[211]
5	NiCo-NPs-in-N/C electrode	AA DA UA	DPV	0.1 M PBS/7.0	50 – 1500 0.5 – 900 10 – 500	50 0.5 10	0.091, 0.080, 0.014	AA-DA= 178 DA-UA= 122 AA-UA= 300	Human urine	[33]
6	MgO nanobelts/GCE	AA DA UA	CV	0.1 M PBS/5.0	(2.5–15, 25–150) 0.125–7.5 (0.5–3, 5–30)	2.5 0.125 0.5	0.2, 0.05, 0.04	AA-DA= 111 DA-UA= 161 AA-UA= 272	-	[212]

Most of the methods developed in last decade deal with detection of DA cell cultures; even though the data obtained from cell cultures could be ambiguous and do not give actual insight for the true quantity and function of DA in an organism brain. The in-vitro results should be verified by real-time animal experiments. So in-vivo recognition of DA in the incidence of coexisting interferents is a big challenge. The human brain is complicated and most sensitive part of the body, thus detection of DA and its coexisting compounds can harm the brain tissues. That pose irreversible effects in the form of toxicity on the brain and consequently on the body. These issues have a great impact not only on biochemistry or neurochemistry but also on investigative and pathological research [218]. For the in-vivo electrochemical detection of DA the following prime challenges are present:

- The miniaturized electrode well-matched with brain environs and should not interfere with brain tissues and their functions.
- The material utilized for modification of electrode surface should not be toxic to brain tissues.
- Highly sensitive and selective strategy is needed for the *in-vivo* study of DA in the presence of complex matrix.
- In the brain, the complex matrix is present that can foul the surface of the electrode and decrease its sensitivity.
- Fast response of electrode is needed for the *in-vivo* application to decrease the contact time of electrode surface with biological tissues.

DA coexist with a high concentration of AA in the brain and has overlapping oxidation potential on the electrode surface; these coexisting species pose a problem in the

resolution of signals when these are detected simultaneously [200]. Other than AA, extracellular matrix of the brain consists of saccharides, proteins, lipids, etc. This indicates that there are innumerable factors that can enhance or suppress the response of DA considerably in different ways. During the simultaneous sensing of AA, DA, and UA, the following issues may arise:

- On the surface of customary electrodes, oxidation potential could overlap.
- The oxidation products of targeted analytes accumulate on the surface of the electrode, as a result sensitivity, selectivity and response time of the electrode decrease.
- The current signal for AA increases due to homogeneous catalytic oxidation in the presence of DA at the electrode surface.

Different approaches are utilized to overcome the above-mentioned issues for simultaneous detection of targeted analytes like pretreatment of sample and miniaturization of electrochemical sensors. Dilution of the sample by several folds containing target analyte is another way to tackle the matrix effect. Due to this reason, the reported work in literature describes far less amount of AA, DA, and UA compared to quantity present in the real sample. To overcome the effect of the matrix, following approaches are being applied:

- The real sample is pretreated to reduce the matrix in a real sample.
- Recovery of the spiked amount of analyte is measured.
- Real samples like blood or urine are diluted to several folds.
- Target analyte is extracted before analysis.
- The electrode surface is modified using the suitable material.

- Miniaturization of the electrode.

The miniaturized electrode has several advantages over traditional large scale electrodes likewise low signal to noise ratio, fast response time and minimal IR drop. But the major issue for small-scale sensors is a fabrication of sensor-solution interface and its response towards target analyte. Although, very little research has been done to study and design the sensor solution interface for the miniature electrode, however, most of the research in literature emphasize on the development of the electrochemical strategies to detect the targeted analytes simultaneously. It is very important to mention that state-of-the-art electrochemical techniques combined with miniature electrodes cannot be applied to in-vivo studies, but mostly restricted to the cell cultures or small motionless organism. However, ultra-microelectrodes and microfabricated electrode arrays can be utilized both in-vivo and in-vitro. Aggarwal et al. developed a gold microelectrode arrays for quantification of DA under the physiological concentration of AA and have potential in-vivo application. For this purpose, oxidoreduction reaction of DA was done by application of the suitable potential. Consequently, signals for the target analyte were amplified and detection limit $0.454 \mu\text{M}$ was obtained for dopamine in the occurrence of $100 \mu\text{M}$ AA in mocked cerebrospinal fluid buffer without background subtraction [219]. Zachek et al. developed pyrolyzed photoresist film (PPF) carbon microarrays to detect DA and oxygen simultaneously by applying fast scan cyclic voltammetry, later on, the same group applied fast scan cyclic voltammetry compatible microelectrode array for real-time observation of DA in the striatum of mouse brain under standard and pharmacological conditions [220, 221].

Although there are many methodologies available including miniaturized electrodes, for the individual and simultaneous recognition sensing of targeted analytes such as sensor arrays to detect specific analytes. However, a lot of improvements are requisite to develop highly sensitive and fast electrochemical arrays for in-vivo simultaneous detection of AA, DA, and UA.

CHAPTER 3

A Novel, Fast and Cost Effective Graphene - modified Graphite Pencil Electrode for Trace Quantification of L-Tyrosine, Dopamine, and Uric acid

3.1 Introduction

L-tyrosine is an essential amino acid with significant importance in the body. Its presence is crucial to regulating protein synthesis. L-tyrosine assists the maintenance of a positive nitrogen balance in the body. Tyrosine is a precursor to several neurotransmitters, such as norepinephrine, dopamine, and epinephrine [222, 223], and to hormones such as thyroxin, a critical thyroid hormone [224]. L-tyrosine is added to the foods, pharmaceuticals and dietary products [11]. The metabolic stability of the nicotinic acetylcholine receptor in the muscles is controlled by the phosphotyrosine level [5]. Tyrosine is produced in the body by phenylalaninase from phenylalanine. The absence of this enzyme favors the production of phenyl pyruvic acid, which can cause mental retardation [225]. Sister chromatid exchange in the culture medium may increase at high concentrations of L-tyrosine [226]. The absence of tyrosine causes depression [227], and several investigations have reported that L-tyrosine is useful for treating fatigue, cold, stress, and wakefulness [8]. L-tyrosine is involved in several diseases such as alkaptonuria, albinism, mental illness, lung disease, liver disease, and tyrosinemia [9]. L-tyrosine excretion in the urine increased in patients suffering from diabetes mellitus [10]. The importance of L-tyrosine in the body has motivated a need to develop a sensitive, rapid, reproducible, and low-cost detection method.

Dopamine belongs to the catecholamine family. Dopamine being a neurotransmitter plays a vital role in the CNS. It also regulates the heart beat and the blood pressure [13]. The abnormal metabolism or change in concentration of dopamine causes a number of serious problems. The abnormal concentration in the brain could result in Parkinson's disease, schizophrenia, senile dementia, restless legs syndrome, and attention deficit hyperactivity

disorder [16]. Besides the nervous system, it also plays a role in the control of the various functions of the renal [13] and the digestive system.

In the human body, UA is produced by the purine oxidation. It is an important biomarker for certain diseases. Uric acid present in the urine, serum and also in the blood. It is mainly excreted from the body with the help of kidneys. The abnormal level of uric acid in the body is responsible for a number of diseases like Lesch /Nyhan syndrome and hyperuricemia which could cause gout [20]. Higher concentration of uric acid causes cardiovascular disease and kidney damage [22]. The risk of diabetes mellitus is high in the people have a high concentration of UA [21]. The measurement of UA is highly important to know the health condition of the individual. The major problem in the electrochemical measurement of UA is the interferences of AA due to close electrooxidation potentials [228]. Due to the high importance of the UA in the body, reliable, sensitive, rapid and cheap methods are required for its measurement in the body.

Several methods have been designed and reported for the determination of the targeted analytes in biological samples and pharmaceutical products. These methods are mainly based on liquid chromatography tandem mass spectrometry [229, 230], gas chromatography, chemiluminescence [231], HPLC-fluorescence or UV detection [3, 232–236] fluorimetry, spectrophotometric and capillary electrophoresis [237–239]. Although all these methods display a good accuracy, most of them are tedious, require several preparatory steps prior to testing are time-consuming, and require a skilled practitioner. Electrochemical methods are advantageous in that they are low in cost, rapid, highly sensitive, selective, and provide good reproducibility.

Graphene is an exciting material since its isolation in 2004. It is a two-dimensional sp^2 hybridized material [240, 25]. Although graphene has a short history, yet its characteristics in a different field are widely explored. Due to its attractive features, the graphene has shown promising results in the field of biotechnology, electronics, and energy storage [241]. Graphene considered as a unique material due to excellent conductance, extremely low resistance and wide theoretical surface area ($2630 \text{ m}^2\text{g}^{-1}$). Moreover, graphene has very good electron mobility at room temperature and has exceptional mechanical strength [242]. Graphene display extraordinary electrochemical properties due to fast charge transfer, wide potential window, and high electrical conductance [26, 66]. All these characteristics make graphene an excellent material for electrode modification.

Several previous reports have described electrochemical methods that are useful for determining L-tyrosine, dopamine and uric acid concentrations. A nafion- CeO_2 modified GCE [243], an iron(III) doped zeolite-CPE [244], and an AuNP-MWCNT-GCE [245] have been used for L-tyrosine detection in human blood, and a multi-wall carbon nanotubes GCE [225], a thiolated- β -cyclodextrins gold electrode [246] and a B-doped diamond electrode [247] have been used to detect L-tyrosine in a pharmaceutical product. A p-AMT GCE [248] has been tested for its utility in detecting L-tyrosine in human urine. Graphene is not new for the detection of DA and UA. A number of modified electrodes were used for determination of dopamine. Kim et al and X. Ma et al cast the graphene on the GCE and estimated detection limits were $2.64 \mu\text{M}$ and $0.5 \mu\text{M}$, respectively [249, 250]. Y. Wang et al dispersed the graphene in CS and have dried overnight on GCE surface. The limit of quantification was obtained $5 \mu\text{M}$ [251]. The

graphene nanosheet paste electrode showed 0.6 μM limit of detection [252]. The 3D reduced graphene oxide GCE has 5 μM quantification limit and 0.17 μM detection limit [253]. The pristine graphene-based GCE has detection limit 2 μM . In addition to this, various graphene composite was also used to enhance the sensitivity of the electrodes towards dopamine. Overoxidized Polypyrrole graphene modified GCE has a limit of quantification and limit of detection 0.5 μM and 0.1 μM , respectively [254]. S. Pruneanu et al has fabricated Au/Graphene AuAg and Au/Graphene-Au electrode for dopamine sensing with a limit of detection 0.205 μM and 30.3 μM , respectively [255]. Similarly, several graphene-based work reported for uric acid determination. X. Wang et al; fabricated palladium nanoparticle/graphene/chitosan modified GCE for uric acid detection with a limit of detection 0.17 μM and the preparation of the electrode took 24 hours [135]. Y. Xue et al; introduced poly(diallyldimethylammonium chloride)-graphene nanosheets modified GCE which is also involved number of steps and time consuming with detection limit 0.1 μM [256]. Z. Zhang and J. Yin have prepared sensitive partially electro-reduced graphene oxide modified GCE electrode which took 12 hours before use and has a detection limit 0.05 μM [257]. All these developed electrodes involved a number of steps while our proposed electrode for L-tyrosine detection is easy to modify.

The graphite pencil has many advantageous over the other carbon base electrodes (CPE and GCE). The carbon paste electrode required a certain time for its preparation. The glassy carbon electrode is the most extensively used carbon electrode. Despite being widely used the glassy carbon electrode has some disadvantages. The surface of the glassy carbon electrode is easily fouled. The cleaning process of the glassy carbon electrode is also time-consuming. Moreover, the glassy carbon electrodes are expensive.

The graphite pencil electrode has great attraction for analysis due to cost effective, easy to handle and disposability [258].

The objective of the present work is to develop a sensitive and convenient method for detecting L-tyrosine, DA, and UA in biological samples. We report on the fabrication and characterization of a GR-modified GPE. The modification of GPE compared to GCE is rapid and simple. The electrochemical activity of the fabricated electrode increased markedly in the presence of targeted analytes in contrast with the corresponding activity of a bare GPE. To the best of our knowledge, this is the first example of L-tyrosine, dopamine and uric acid determination using a GR-modified GPE.

3.2 Materials and Methods

3.2.1 Reagents

L-Tyrosine, Dopamine, L-methionine, ascorbic acid, fructose, uric acid, potassium chloride and sodium chloride were supplied by Sigma-Aldrich (USA). Solutions of copper, nickel, zinc (1000 ppm), phenylalanine and alanine were received from Fluka (USA). Di-potassium hydrogen orthophosphate and sodium phosphate monobasic were purchased from BDH (England). Graphite was obtained from Fischer Science Education (USA). Double distilled water was used throughout the experiments and for solution preparation. The water was obtained directly from Water Still Aquatron A 4000 D (UK).

3.2.2 Apparatus

EIS, CV and SWV experiments were performed using an electrochemical workstation (Auto Lab, Netherland), coupled with a conventional three-electrode system. The working electrode was a GR-modified GPE or a bare GPE, the reference electrode was an

Ag/AgCl (in 3 M KCl, CHI 111, CH Instruments Inc.) and a platinum wire (CHI 115, CH Instrument Inc.) was an auxiliary electrode. The GPE pencil mounted vertically such that 7mm of the pencil lead was outside the pencil holder and dipped in the measuring solution. The pencil electrode is already described in detail [56]. The three-electrode system was inserted through plastic Teflon into a 3 mL glass cell. All weights were measured using an electrical balance (GR-200). During the experiments, different pH buffers (5.5, 6.0, 6.7, 7.0, 7.5) were prepared, and the pH was controlled using a pH meter (accumet® XL50). A Raman spectrum was obtained by HORIBA Scientific LabRAM HR Evolution (Japan). FE-SEM images were recorded using TESCAN LYRA 3 (Brno, Czech Republic) at the Center of Research Excellence in Nanotechnology, KFUPM.

3.2.3 Preparation of Modified GPEs

The GO (2, 3 or 4 mg/mL) was dispersed in a 0.1 M acetate buffer at pH 4.8 and the uniform dispersion was obtained by sonicating the solution for 2 hours. The GO solution was then transferred into 3 mL cell. The graphite pencil electrode and the Pt counter electrode and Ag/AgCl reference electrode were immersed into the GO solution. The GO was electrochemically reduced on the surface of the GPE under a cyclic sweeping potential from -1.4 V to +0.3 V applied at a scan rate of 20 mV/s over 2 or 5 cycles. All experiments were conducted at room temperature.

3.3 Results and Discussion

3.3.1 Characterization and Optimization of Synthesized Graphene Oxide

GO was prepared by Hummers method. Synthesized GO was characterized by FTIR and Raman spectra (Fig. 3- 1). The spectrum of GO (Fig. 3- 1Ab) showed alkoxy –C-O stretching at 1050 cm^{-1} , epoxy –C-O stretching at 1225 cm^{-1} , carboxylic acid –C-O stretching at 1383 cm^{-1} , aromatic carbon double bond absorbance at 1625 cm^{-1} , carboxyl carbonyl absorbance at 1733 cm^{-1} and hydroxyl group stretching at 3425 cm^{-1} [260]. On the other hand, no prominent absorbance was observed for the graphite FTIR spectrum (Fig. 3- 1Aa). The presence of these functional groups confirmed the formation of the GO from the graphite. The graphite Raman spectra (Fig. 3- 1Ba) showed a weak D band at 1344 cm^{-1} and a strong prominent peak of G band at 1567 cm^{-1} which are E_{2g} first order scattering and 2D band was observed at 2693 cm^{-1} . In GO Raman spectra (Fig.3- 1Bb) a prominent D band appeared at 1350 cm^{-1} compared to the graphite D band. This is may be due to the extensive oxidation of the graphite which reduced the size of the in-plane sp² domain. G band appeared at 1594 cm^{-1} and 2D band at 2670 cm^{-1} [128]. Id/Ig ratio was 0.98. The FTIR and Raman spectra confirmed the formation of GO from the graphite.

3.3.2 Morphological and Electrochemical Characterization

The surface morphologies of the bare and GR-modified GPEs were analyzed using the FE-SEM. Prior to analysis, the electrode was modified by directly reducing GO (4 mg/mL) on the surface of the GPE over two CV scans from - 1.4 V to 0.3 V.

The FE-SEM images were collected from the bare and the GR-modified GPEs at three different magnifications to optically image the surface (Figs. 3- 2 A, B, and C). Figures 3- 2a and 3- 2b show the bare GPE and GR-modified GPE, respectively. A comparison of the bare 10 μm SEM image with the modified GPE clearly reveals the formation of the graphene layer on the GPE surface. Figure 3- 2Ab (10 μm) reveals that a small uncovered region was present on the GPE whereas the rest of the GPE was covered by the graphene layer. High magnification images further revealed the structure of the nm thick wrinkled sheets of the graphene on the surface of the graphite pencil electrode (Fig. 3- 2Cb). The wrinkled graphene sheet is extremely valuable for enhancing the surface area of the electrode because these wrinkled shapes are much more stable and do not easily revert to the graphitic form.

The electroactive surface area of the bare and GR-modified GPE could be calculated with the help of the Randles-Sevcik equation [261]:

$$I_p = 2.69 \times 10^5 \text{ C n}^{3/2} \text{ A D}^{1/2} \gamma^{1/2}, \quad 1$$

Where n is electrons number participating in the redox reaction, C is analyte concentration in molL^{-1} , A is electrode electroactive surface area in cm^2 , γ is the scan rate in Vs^{-1} and D represents diffusion coefficient in cm^2s^{-1} . The insets in figure 3-3 showed the direct relation of peak current (I_p) and the square root of scan rate ($\gamma^{1/2}$). All other parameters n , C , and D in the Randles-Sevcik equation are constant. The electroactive surface area of bare GPE and dERGO/GPE was also analyzed for 5 mM $\text{K}_3\text{Fe}(\text{CN})_6/\text{K}_4\text{Fe}(\text{CN})_6$ using equation 1 by sweeping different scan rates from 20 mVs^{-1} to 100 mVs^{-1} in a solution containing 0.1 M KCl. The electroactive surface area of bare

GPE and dERGO/GPE was 0.0628 cm^2 and 0.372 cm^2 , respectively. The electroactive surface area values revealed the graphene layers have an enormous effect on the electroactive surface area of the GPE and it is improved significantly.

Electrochemical behavior of the bare and the modified electrode was further investigated by EIS. The EIS characterization was done in 0.1M KCl solution comprising 5 mM $\text{K}_3\text{Fe}(\text{CN})_6/\text{K}_4\text{Fe}(\text{CN})_6$ and the frequency range was scanned from 0.01 Hz to 100 kHz. The Nyquist plots consist of two portions. The one is linear and other is consisting of semicircle part. The semicircle part appeared at a higher frequency directly related to the electron transfer limited process and at a lower frequency, the linear part corresponds to the diffusion control process. The EIS spectra revealed the extensive change in the behavior of the GPE surface after modification with graphene. The charge transfer resistance (R_{CT}) values calculated from a semicircle of the Nyquist plot of the bare GPE (Fig. 3-4Ab) was 2746Ω and the IM-rGO/GPE (Fig. 3-4Aa) almost demonstrated a straight line and no semicircle was observed. The charge transfer resistance values of the bare and the modified electrode indicated the resistance was significantly reduced by the graphene layer on the electrode. The same phenomena were also demonstrated by the Bode phase plot (Fig. 3-4B). At higher frequencies, the bare GPE (Fig. 3-4Bb) has Bode phase angle 62.5° and IM-rGO/GPE (Fig. 3-4Ba) phase peak disappeared at higher frequencies. This revealed the high charge transfer of the modified surface due to low charge transfer resistance [262].

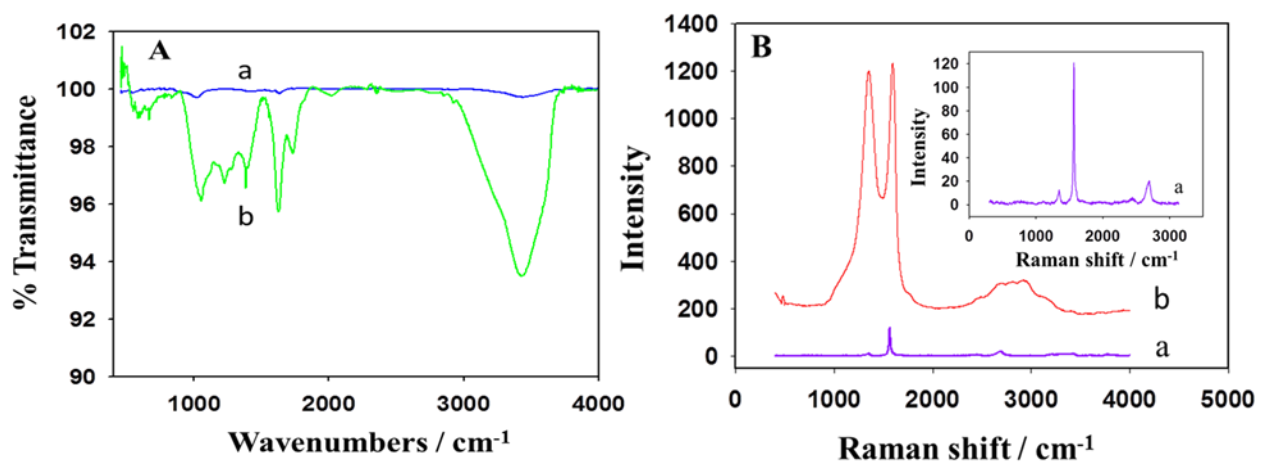


Figure 3- 1: (A) FTIR spectra of graphite (a) and GO (b), and (B) Raman spectra of graphite (a) and GO (b). Inset of B shows the graphite Raman spectrum.

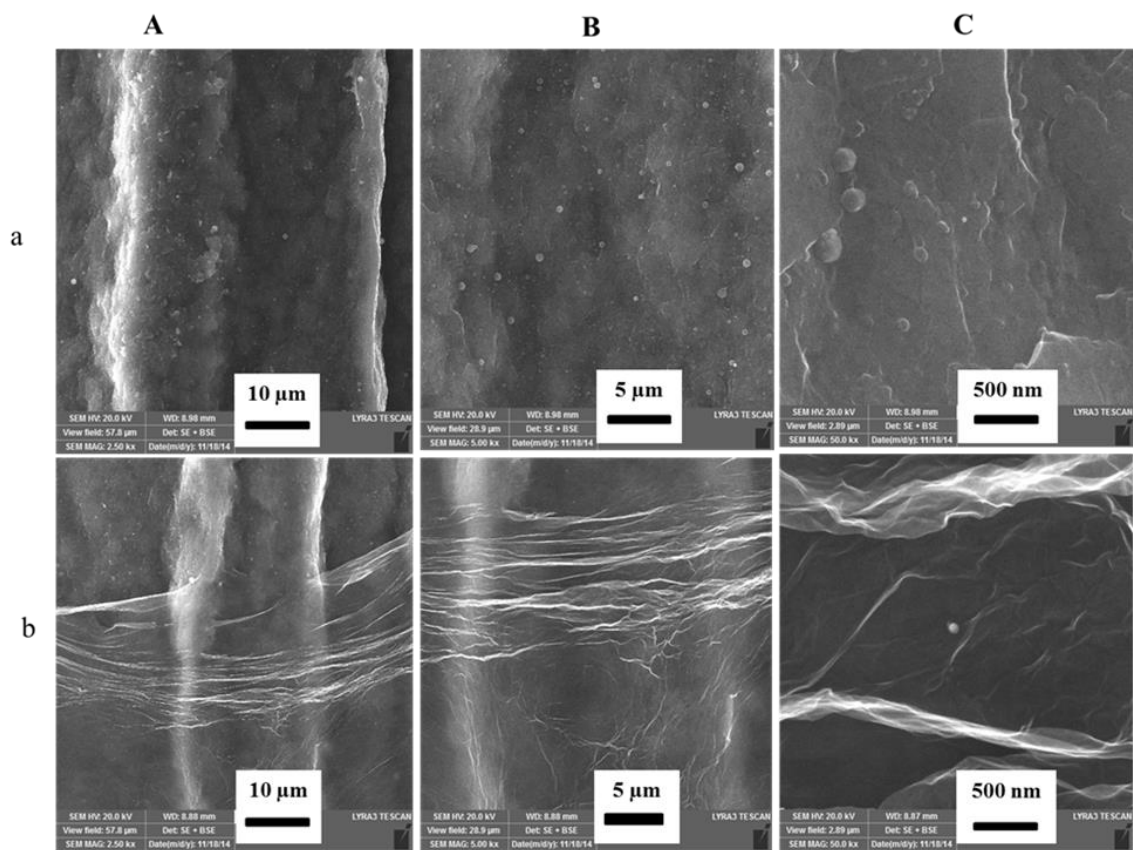


Figure 3- 2: FE-SEM images at three different magnifications: 10 μm (A), 5 μm (B), and 500 nm (C) of bare (a) or GR-modified GPE (b).

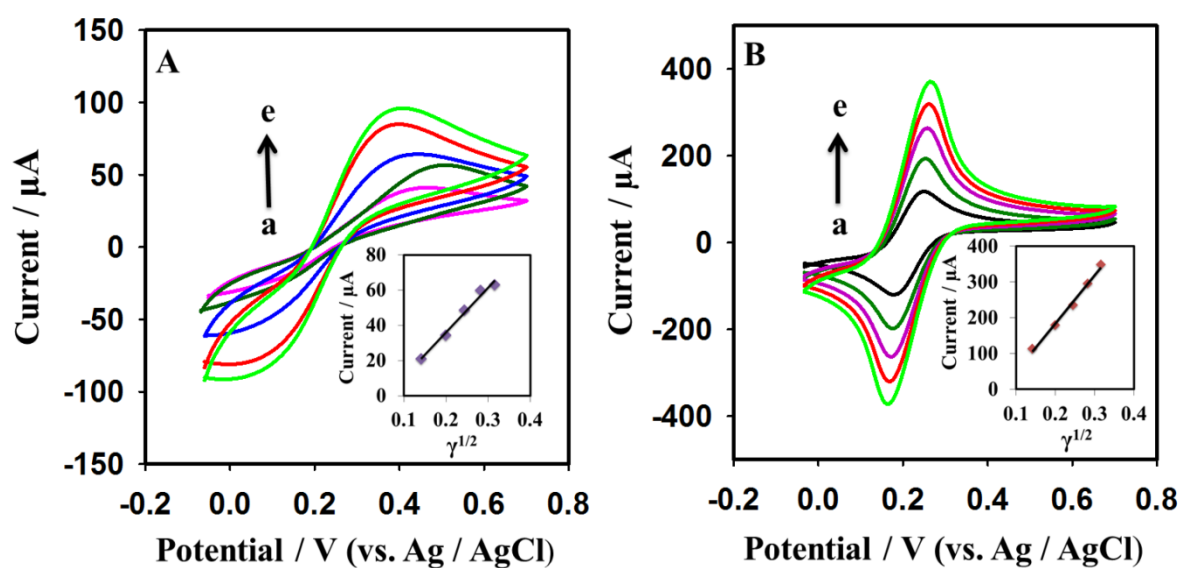


Figure 3- 3: Cyclic Voltammograms obtained from a solution comprising 5 mM $K_3Fe(CN)_6/K_4Fe(CN)_6$ and 0.1 M KCl (A) Bare GPE and (B) dERGO-GPE at different scan rates of (a) 20 (b) 40, (c) 60, (d) 80, and (e) 100 mVs^{-1} . The insets in (A) and (B) show the linear relationship between current and the square root of the scan rates.

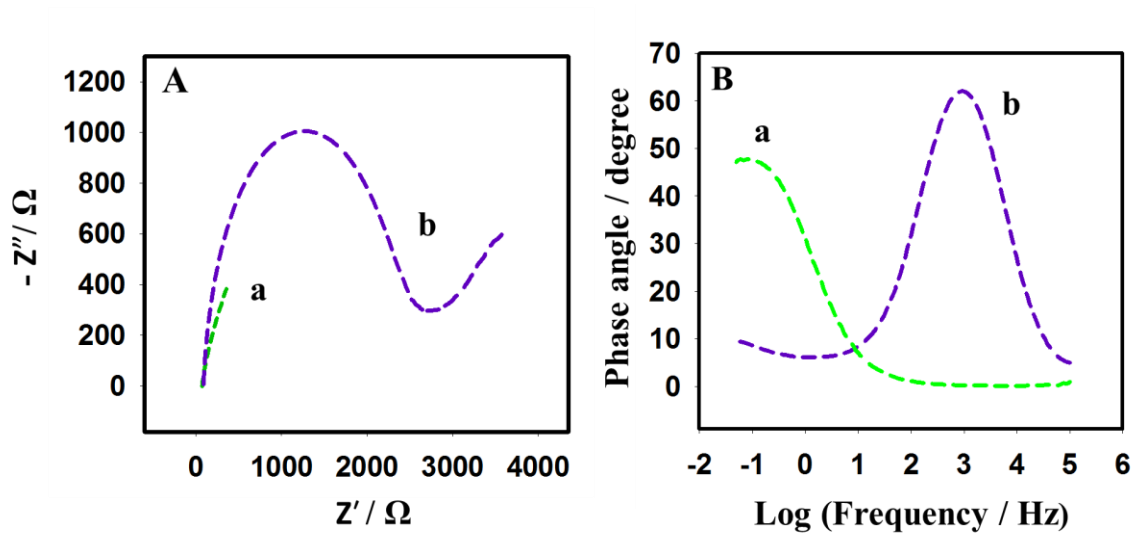


Figure 3- 4: (A) Nyquist and (B) bode phase plots of 5 mM $K_3Fe(CN)_6/K_4Fe(CN)_6$ in 0.1 M KCl solution on (a) IM-rGO/GPE, and (b) bare GPE upon application of frequency range from 0.01 Hz to 100 kHz. (C) CVs of (a) IM-rGO and (b) bare GPE were recorded at 0.1 V/s in a 1 mM dopamine 0.1M PBS buffer (pH 6.8).

3.3.3 Ionic Medium Supported Graphene Oxide (IM-GO) Reduction on GPE

The elongated shape of the graphite pencil electrode is assisting the facile direct electrochemical reduction of graphene oxide. For the fabrication of single-use surface, it is necessary the modification process should be fast and achieved in a couple of minutes. GO is easily dispersed in the water. It was observed, the few CV cycle reduction of the water dispersed GO was not enough to enhance the sensitivity of the GPE to the optimum level. The ionic medium supported graphene oxide has shown the dramatic effect on the sensitivity of the sensor. The sensitivity of the various GPE surfaces was analyzed using 2 mM $K_3Fe(CN)_6/K_4Fe(CN)_6$ in 0.1 M KCl solution. The effect of various ionic medium was investigated by reduction of 2 mg/mL GO on GPE surface. The electrochemical reduction was accomplished by scanning of CV from -1.4 – 0.3 V over 2 cycles. The study of the CV behavior of the reduced graphene oxide on GPE in the presence of ionic medium has shown the great impact on the peak current and peak shape (Fig. 3-5). The peak current and reversibility of $K_3Fe(CN)_6/K_4Fe(CN)_6$ was significantly improved using IM-rGO/GPE compared rGO/GPE. Furthermore, the electroactive surface area of the GPE was considered using GO in double distilled water (w-GO) and various ionic medium such as 0.1 M KCl (pc-GO), 0.1 M PB (pb-GO) and 0.1 M acetate buffer (ac-GO) by recording CV scans from 20 to 100 mV/s in 0.1 M KCl containing 2 mM $K_3Fe(CN)_6/K_4Fe(CN)_6$. The electroactive surface area was calculated 0.112, 0.185, 0.219 and 0.246 cm^2 using w-rGO/GPE, pc-rGO/GPE, pb-rGO/GPE and ac-rGO/GPE, respectively. The surface area study revealed the ionic medium supported GO (IM-GO) could be used for facile and rapid fabrication of disposable GPE sensor. The direct

electrochemical reduction of IM-GO could be more valuable to achieve required sensitivity in the short time. Acetate medium has shown more effective result compared another medium. For further study, ac-GO was used for the modification of GPE (Fig. 3-5).

3.3.4 Optimization of IM-GO

The synthesized graphene oxide was dried in the open air. The dried graphene oxide was dispersed in 0.1M acetate buffer and sonicated for 2 hours to get a uniform and stabilized the dispersion. The various concentrations of graphene oxide solutions were prepared from 1mg to 10 mg/mL to observe the response of the IM-rGO on the GPE surface. The best response was obtained with 4 mg/mL GO solution. The number of cycles was optimized from 1 to 6 cycles and maximum response was observed at 2 cycles and effective scan window for graphene oxide reduction was found -1.4 - 0.3 V. The scan rate for GO electrochemical reduction was optimized from 0.005 to 0.05 V/s, the current was enhanced till 0.02 V/s and decreased gradually as the scan rate was further increased. All these parameters were optimized for the the 1 mM concentration of dopamine. Various electrolytes were also scanned for 1mM dopamine and most suitable one were found PBS due to a sharp and high peak current for dopamine. The different voltammetric technique like CV, DPV, LSV and SWV were studied and the SWV was found much more sensitive for dopamine sensing.

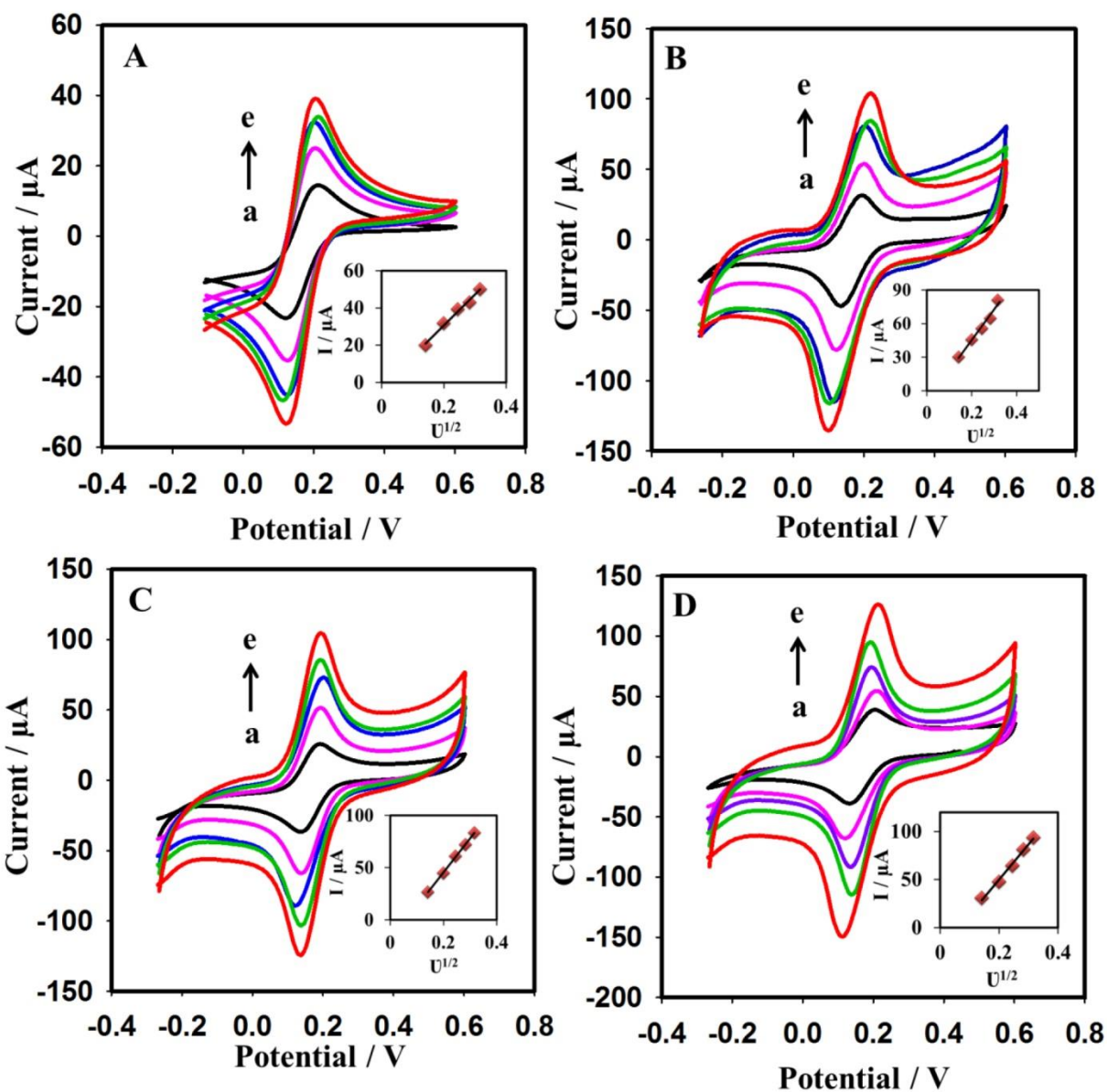


Figure 3- 5: Cyclic voltammograms of 2 mM K₃Fe(CN)₆/K₄Fe(CN)₆ in 0.1 M KCl solution using (A) w-rGO/GPE, (B) pc-rGO/GPE, (C) pb-rGO/GPE, and (D) ac-rGO/GPE at scan rates of (a) 20, (b) 40, (c) 60, (d) 80, and (e) 100 mV/s. The insets in (A), (B), (C), and (D) show the linear relationship between current and the square root of the scan rates ($v^{1/2}$).

3.3.5 A Novel, Fast and Cost Effective Graphene – modified Graphite Pencil Electrode for Trace Quantification of L-Tyrosine

3.3.5.1 L-Tyrosine Behavior on Modified GPE

Electrochemical studies of L-tyrosine were performed by collecting the CV and SWV curves in a tyrosine PBS buffer (0.1 M, pH 6.7). The oxidation peak current response at the surface of the GR-modified GPE in the 1 mM L-tyrosine solution (Fig. 3- 6b) was increased dramatically as compared to the corresponding response on the bare GPE (Fig. 3- 6a). Similar results were obtained using square wave voltammetry. The electrochemical responses in the presence of the 50 μ M L-tyrosine solution were much stronger at the GR-modified GPE than at the bare GPE in a 0.1M PBS buffer (pH, 6.7) (Fig. 3- 7). The current at the GR-modified GPE was 104 times the current measured at the bare GPE (Fig. 3- 7). The graphene solution was prepared in a 0.1 M acetate buffer (pH 4.8), and it is possible that the acetate pretreatment may have affected the electrochemical properties of the GPE. This possibility was tested by the pretreating the bare GPE between - 1.4 and 0.3 V under the same set of conditions as the graphene reduced on the surface of the GPE, over 2 cycles. Figure 3- 7b shows that only the 0.1 M acetate buffer did not affect the peak current in the presence of L-tyrosine. GO acts as an insulator rather than as a conductor, whereas in its reduced form, it is an excellent conductor [263]. The morphological and electrochemical results agreed well with one another, and the GO appeared to be successfully reduced on the GPE surface, yielding enhanced electroactivity, sensitivity, and an increase in the electroactive surface area compared to the bare GPE.

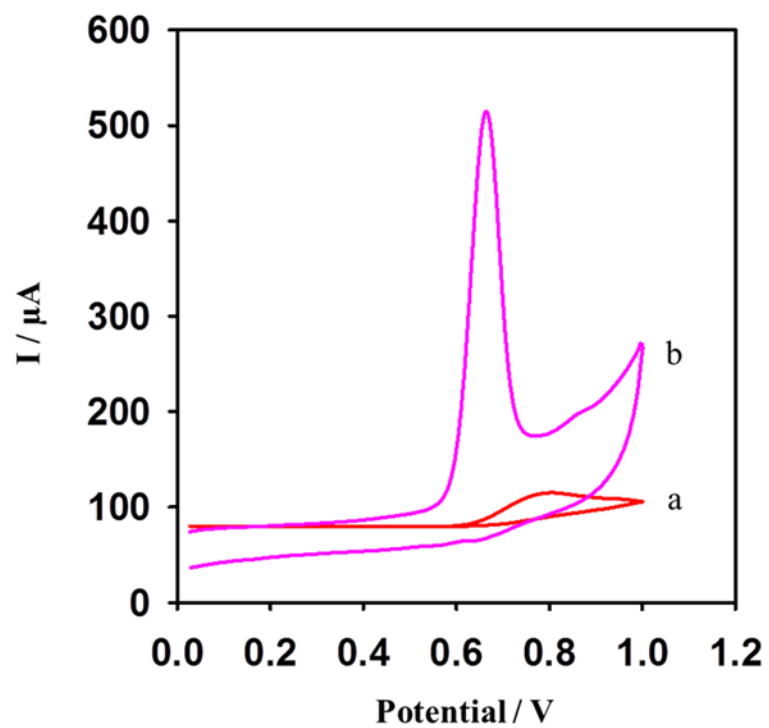


Figure 3- 6: Cyclic voltammograms of (a) the bare GPE, and (b) the GR-modified GPE in a 1 mM L-tyrosine PBS buffer (0.1 M, pH 6.7). Scan rate: 100 mV s⁻¹.

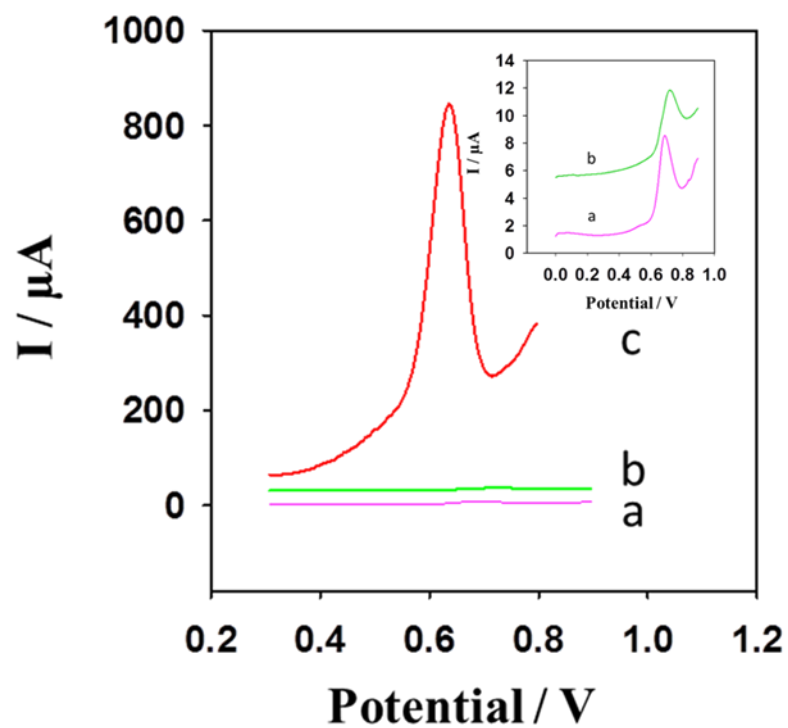


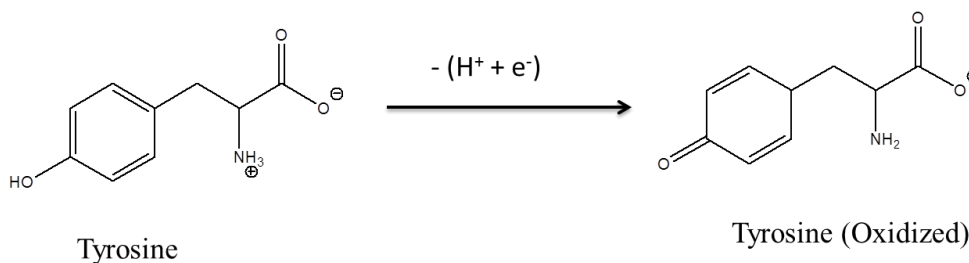
Figure 3- 7: Square wave voltammograms of 50 μM L-tyrosine in 0.1 M PBS (pH 6.7) on the (a) bare GPE, (b) pretreated GPE, and (c) GR-modified GPE. The parameters of the SWV experiment: amplitude 0.03 V, frequency 50 Hz, and adsorption time 210 s.

3.3.5.2 Effect of pH

The effect of the pH was examined using SWV in a PBS buffer (0.1 M) comprising 50 μM L-tyrosine at a pH ranging from 5.5 to 7.5 (Fig. 3- 8). The pH affected the peak current of the L-tyrosine oxidation reaction. In addition to the current variations, the oxidation peak potential was observed to shift with the pH. The oxidation peak current increased as the pH increased and reached its maximum value at pH 6.7. Further increases in pH reduced the current (Fig. 3- 8B). The peak position of the L-tyrosine oxidation reaction shifted linearly as the pH increased (Fig. 3- 8B, inset). The negative shift in the oxidation potential of L-tyrosine established that protons were directly involved in its oxidation. The slope of a linear plot ($R^2 = 0.9938$) of the oxidation peak potential vs. pH (Fig. 3- 8B, inset) was - 59.6 mV, near the theoretical value of - 59 mV. This slope indicated that the equal numbers of protons and electrons were involved in the process of charge transfer on the surfaces of the GR-modified GPE (Eq. 2).

$$E \text{ vs. Ag/AgCl} = 1.0356 - 0.0596[\text{pH}] \quad 2$$

The electrooxidation of tyrosine at the GR-modified GPE was a one-electron and one-proton process, in agreement with previous reports [224, 225, 243]. The electrochemical reaction took place on the electrode surface shown in Scheme 1.



Scheme 1: The electrochemical mechanism of L-tyrosine oxidation

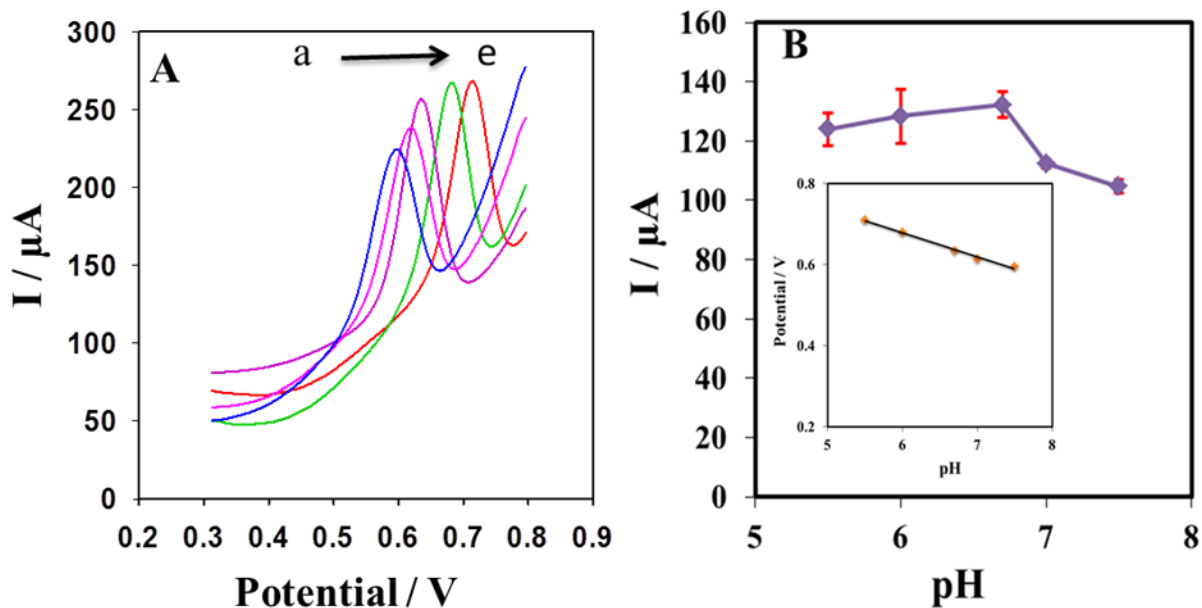


Figure 3- 8: (A) Square wave voltammograms in a 50 μM L- tyrosine 0.1 M L⁻¹ PBS solution at various pH values (a) 7.5 pH, (b) 7.0 pH, (c) 6.7 pH, (d) 6.0 pH, (e) 5.5 at GR-modified GPE. (B) Graphical representation of the peak current vs. pH. Inset: Relationship between the pH and the oxidation peak potential.

3.3.5.3 Optimization of the SWV Parameters

In an effort to develop a highly selective and sensitive electroanalytical method, we optimized each instrumental variable that could affect the L-tyrosine oxidation response under SWV measurements at a GR-modified GPE.

The amplitude of the square wave potential was first optimized between 0.02 V and 0.06 V as this parameter significantly impacted the oxidation signal of L-tyrosine. As the amplitude increased, the current also increased. A maximum current was obtained at 0.03 V above which the value decreased continuously (Fig. 3- 9A). Next, the frequency was optimized between 25 and 80 Hz. The frequency affected the L-tyrosine oxidation signal strength. The highest current obtained at 50 Hz (Fig. 3- 9B). Finally, the L-tyrosine adsorption time on the GR-modified GPE surface was optimized. The adsorption time significantly influenced the sensitivity and the strength of the signal. The oxidation peak current increased as the adsorption time increased. The increase in current indicated that L-tyrosine adsorbed onto the modified electrode surface. The electrode surface became saturated at 210 s, after which peak current became constant (Fig. 3- 9C). The optimized square wave potential was characterized by amplitude of 0.03 V, a frequency of 50 Hz, and an adsorption time of 210 s.

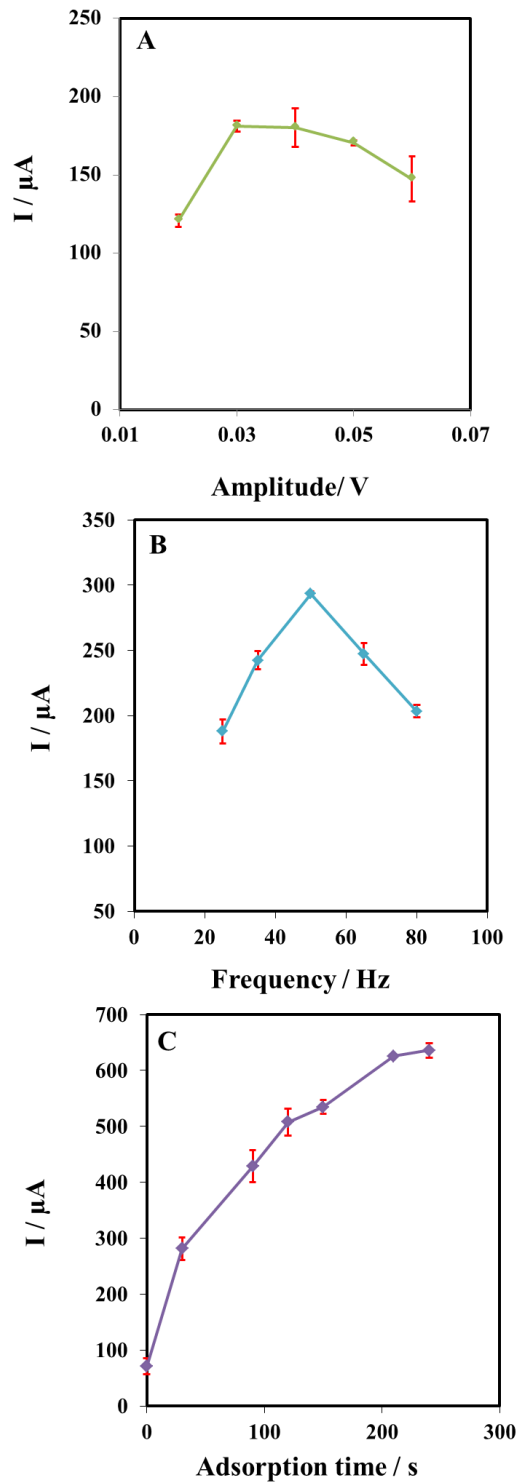


Figure 3- 9: Plots of the current vs. amplitude (A) or frequency (B), and adsorption time (C) obtained from the square wave voltammograms collected from 50 μM L-tyrosine in a PBS buffer (0.1 M, 6.7 pH).

3.3.5.4 Calibration Curve and the Detection Limit

A calibration curve was constructed using the optimized square wave parameters, including the amplitude of 0.03 V, frequency of 50 Hz, and the adsorption time of 210 s. The current and L-tyrosine concentration were linearly related between 0.8 μM and 60 μM ($n = 3$). A linear regression of the calibration curve yielded the equation: $I (\mu\text{A}) = 12.441 C_{\text{Tyr}} (\mu\text{M}) - 1.8942$, with a regression constant (R^2) of 0.9995 (Fig. 3- 10). The detection limit obtained using the GR-modified GPE was 0.07 μM . The sensitivity and the lower LOD of the modified electrode indicated that the electroactivity of the graphene on the GPE surface towards L-tyrosine was significantly enhanced. The LOD and the LOQ GR-modified GPE are much better or comparable with the other modified reported electrodes (Table 3- 1).

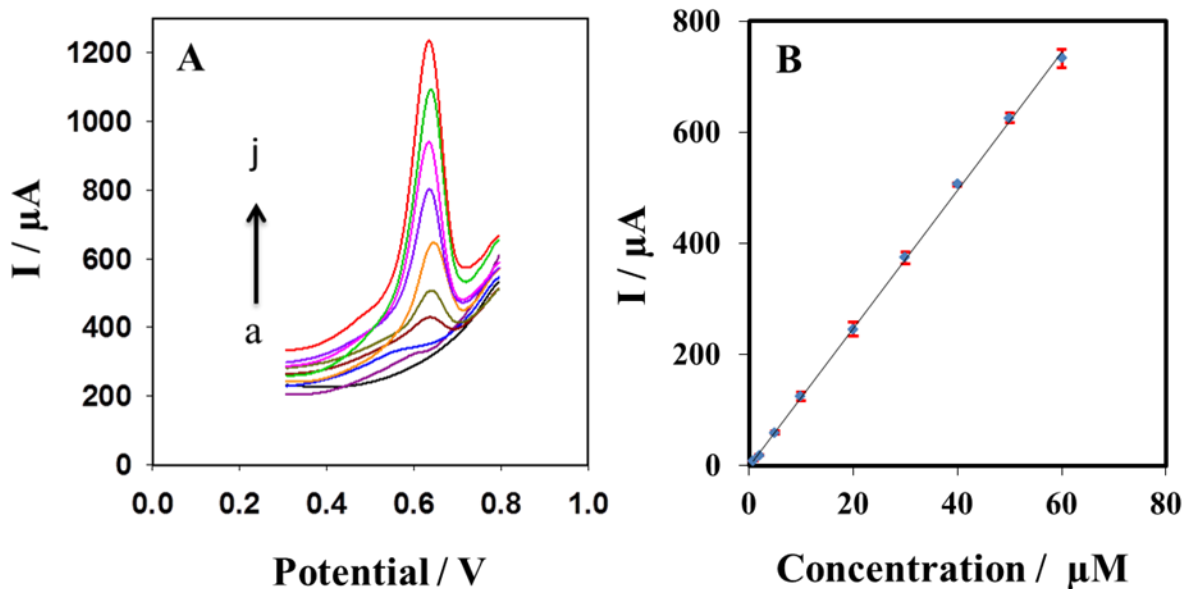


Figure 3- 10: (A) Square wave voltammograms in PBS buffer (0.1 M, pH 6.7) at various concentrations of tyrosine: (a) 0, (b) 0.8, (c) 2, (d) 5, (e) 10, (f) 20, (g) 30, (h) 40, (i) 50, (j) 60 μM . The graph (B) showed the linear relationship between I (μA) and the concentration (μM) of L-tyrosine ($R^2 = 0.9995$), with the error bars. The SWV parameters were: amplitude of 0.03 V, frequency of 50 Hz, and adsorption time of 210 s.

Table 3- 1: Comparison of the GR-modified GPE properties to those of other modified electrodes for the determination of the L-tyrosine in a sample.

Electrode	LOD (μM)	Electrode Modification Time	Linear Range (μM)	Correlation coefficient	Ref.
Nafion-TiO ₂ -GR-GCE	2.3	C*	10-160	0.9941	[224]
Nafion-CeO ₂ -GCE	0.09	C*	2-160	0.9973	[243]
BuCh-GCE	0.4	65 min	4-100	-	[1]
CNF-CPE	0.1	C*	0.2-109	0.9985	[264]
MWNTs-GCE	0.4	12 hr	2-500	0.9967	[225]
Fe ³⁺ /ZMCPE	0.32	24 hr	1.2-90	0.9989	[244]
B-doped diamond electrode	1	-	100-700	0.9972	[247]
MWCNTs-GNS/GCE	0.19	C*	0.90–95.4	0.9900	[227]
Ag/Rutin/WGE	0.07	100 min	0.3-10	0.9850	[265]
SWCNT arrayed-Pt	0.1	-	0.1-100	0.9996	[266]
Thiolated/ β -cyclodextrins /gold electrode	12	6 hr	36-240	0.9970	[246]
GR-modified GPE	0.07	5 min	0.8-60	0.9995	This work

C*= Casting method is used and electrode dried at room temperature. Time is not mentioned

3.3.5.5 Reproducibility Study

The reproducibility of the L-tyrosine detection properties was characterized by fabricating five GR-modified GPEs under the same set of conditions. Small deviations in the currents were observed using a 50 μM L-tyrosine solution in 0.1 M PBS (pH 6.7), with an RSD of 4.95% ($n = 5$). This small RSD value indicated the excellent reproducibility of the electrode developed here.

3.3.5.6 Applications and Interference Studies

The sensitivity of the L-tyrosine measurements to interference from other analyte was examined. Biomolecules such as phenylalanine, alanine, glucose, fructose, L-methionine, uric acid, ascorbic acid, and some common ions Na^+ , K^+ , Li^+ , Ni^{+2} , SO_4^{-2} and Cl^{-1} were tested for their interference effects on the measurement. Most interference agents introduced small variations in the current, on the order of 0.3 - 12 %. This fabricated electrode was then tested in a real sample. A urine sample was collected from a healthy person. Prior to analysis, the sample was diluted to 200 times in 0.1 M PBS buffer (pH 6.7). Urine samples spiked with 40, 50, or 60 μM L-tyrosine were measured under optimized conditions. The voltammograms yielded two well-defined peaks, one corresponding to uric acid and the other at +0.63 V corresponding to tyrosine. The signal recovered 89 to 95% at its initial value (Table 3- 2). These results suggested that the GR-modified electrode may be useful for L-tyrosine detection in urine, which tends to include impurities and interfering species.

Table 3- 2: Determination of L-tyrosine in human urine samples

Sr#	Added (μM)	Found (μM)	Recovery (%)
1	40	37.2	93
2	50	47.4	95
3	60	53.4	89

3.3.6 A Single Step Fast and Facile Fabrication of the Single-use Ionic Medium Supported-reduced Graphene Oxide Sensor for Sensitive and Selective Determination of Dopamine

3.3.6.1 Behavior of Modified Surface towards Dopamine

The electrochemical behavior of the bare and modified electrode towards the analyte was further examined by CV (Fig. 3-11). The CVs were obtained for 1mM dopamine in PBS buffer (0.1 M, pH 6.8). The graphene layer significantly improved the peak shape and current for dopamine electrochemical reaction compared to the bare electrode where a broad peak of dopamine appeared.

3.3.6.2 Study of the Electroactive Surface Area and Scan Rate Effect on Dopamine

The fabricated electrode kinetics for dopamine was further investigated by the cyclic voltammetry study. The effect of the scan rate on dopamine was examined by CV. The scan rate has a significant effect on the peak currents of the analytes. On the modified electrode surface, the current increased linearly as the scan rate increased for 1mM dopamine (Fig. 3-12A). The same effect has been observed for the bare electrodes (Fig. 3-12B). However, at higher potentials, the current response was dramatically decreased on the bare electrode surface. At higher scan rate the short time is available for the completion of the electrochemical reaction on the electrode surface; the bare electrode may not support the fast charge transfer compared to the modified electrodes. The Randles-Sevcik equation was used for the calculation of electroactive surface area for bare and IM-rGO/GPE.

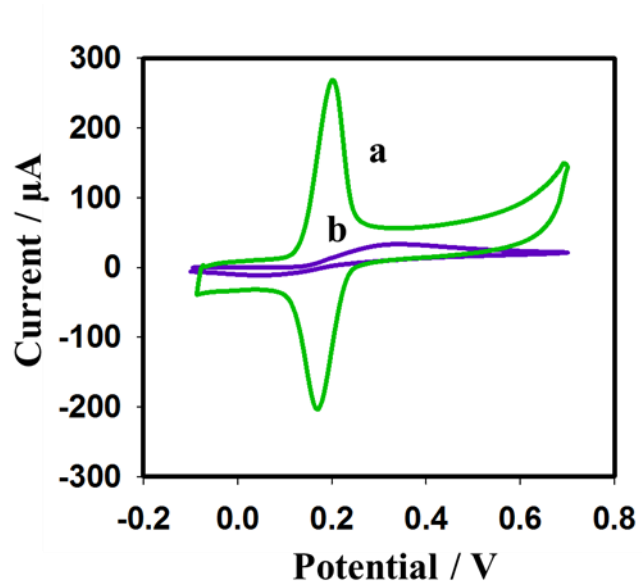


Figure 3- 11: CVs of (a) IM-rGO and (b) bare GPE were recorded at 0.1 V/s in a 1 mM dopamine 0.1M PBS buffer (pH 6.8).

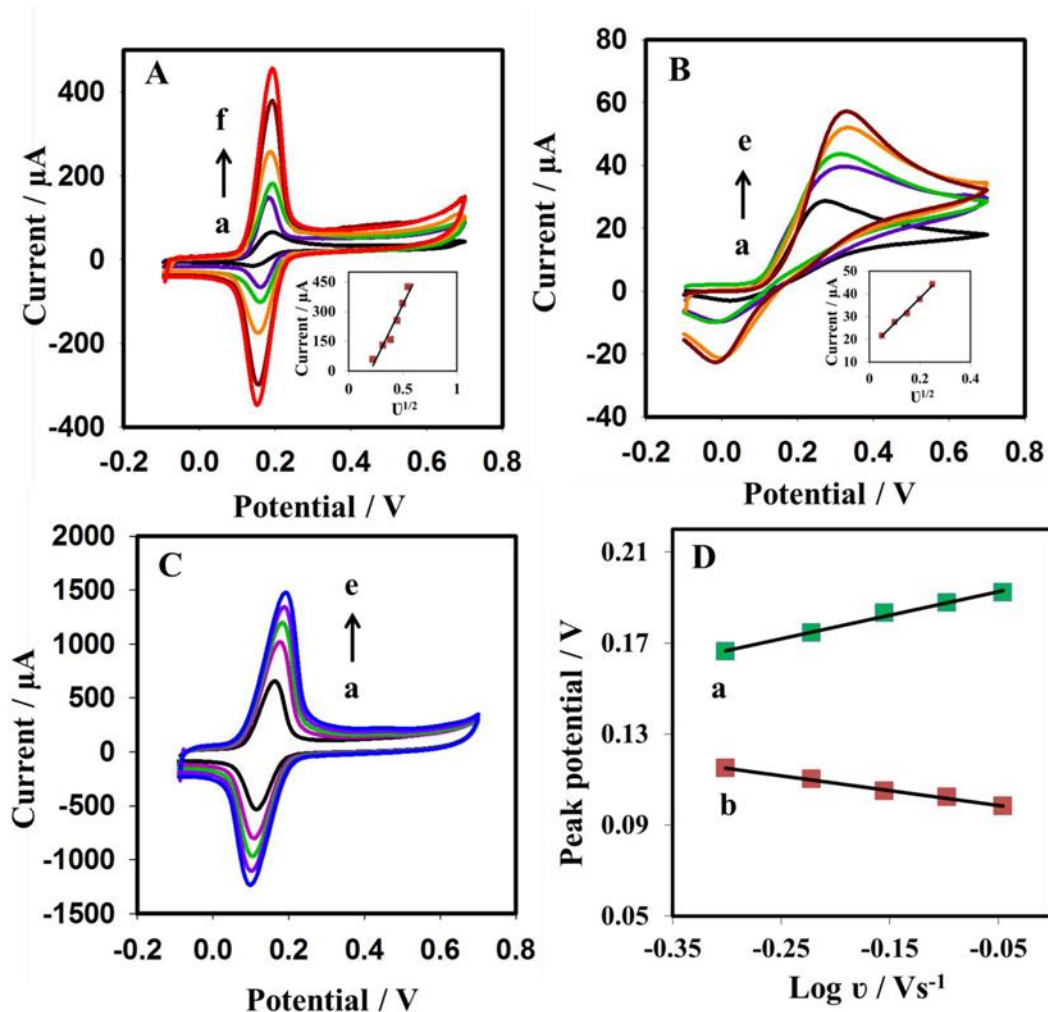


Figure 3- 12: (A) Cyclic voltammograms of 1mM dopamine in PBS buffer (0.1 M, pH 6.8) using (A) IM-rGO/GPE at scan rates of (a) 50, (b) 100, (c) 150, (d) 200, (e) 250, and (f) 300 mV/s ; or using (B) the bare GPE at scan rates of (a) 50, (b) 100, (c) 150, (d) 200, and (e) 250 mV/s. (C) The cyclic voltammograms of 1mM dopamine using IM-rGO/GPE at higher scan rate (a) 500, (b) 600, (c) 700, (d) 800, and (e) 900 mV/s. (D) The linear relationship between $\log v$ vs. (a) anodic and (b) cathodic peak potential of the cyclic voltammograms at 500 to 900 mV/s. The insets in (A) and (B) show the linear relationship between current and the square root of the scan rates ($v^{1/2}$).

The electroactive surface area was calculated using bare GPE or rGO-GPE from the CV scanned between 20 mV and 120 mV from a solution containing 5 mM $\text{K}_3\text{Fe}(\text{CN})_6/\text{K}_4\text{Fe}(\text{CN})_6$ in 0.1 M KCl solution. It has been observed the graphene layer on the graphite pencil electrode significantly increased the ESA. The ESA calculated for the bare GPE and the ionic medium supported graphene modified GPE were 0.0628 cm^2 and 0.372 cm^2 , respectively. The electroactive surface area also calculated for 1mM dopamine in 0.1 M PBS buffer on bare and modified surfaces were 0.063 cm^2 and 0.631 cm^2 , respectively. The value of dopamine diffusion coefficient was used $5.40 \times 10^{-6} \text{ cm}^2 \text{ s}^{-1}$ [267]. The huge increase of surface area for dopamine compared to the $\text{K}_3\text{Fe}(\text{CN})_6/\text{K}_4\text{Fe}(\text{CN})_6$ solution is indicated the ac-rGO on the GPE surface has great attraction and adsorption capability for the dopamine. However, the bare electrode surface area almost comparable for the dopamine and the $\text{K}_3\text{Fe}(\text{CN})_6/\text{K}_4\text{Fe}(\text{CN})_6$ solution. It is revealed the bare electrode did not have any specific attraction for dopamine. The possible attractions for dopamine on the modified electrode surface compared to the bare electrode may be due to the partial reduction of ionic medium supported GO on the GPE surface and few carboxylic group still retain by the ac-rGO which have a negative charge. This negative charge may be having electrostatic attraction for dopamine which is not present on the bare electrode surface

The electrode surface plays a key role in controlling the kinetics and the reversibility of the electrochemical reaction [268]. The information of the reversibility of the electrochemical reaction could be obtained from the cyclic voltammetry. The potential difference between the anodic and cathodic peak potential of the reversible reaction is represented by Equation 3.

$$\Delta E = E_{pa} - E_{pc} = 59/n \quad 3$$

Where E_{pa} is anodic peak potential (mV), E_{pc} is cathodic peak potential (mV) and n is the number of electrons. The value of ΔE for the reversible reaction is $59/n$ mV while for quasi-reversible reaction greater than $59/n$ and the only single peak is appeared in the case of an irreversible reaction. The ΔE calculated from CV (Fig. 3-11) on modified surface for dopamine was 33.8 mV. The value was close to $2.3RT/nF$ or $59/n$ mV which indicated the electrochemical reaction of dopamine on modified surface is quasi-reversible. The value of n calculated from equation 3 was 1.745 and this value suggested two electrons are participating in dopamine electrochemical reaction.

The surface coverage (Γ) [269] for dopamine on the electrode surface was calculated by using equation 4.

$$\Gamma = I_p / 4RT / n^2 F^2 A v \quad 4$$

Where I_p is the peak current, A is the surface area, and v is scan rate. The equation 3 showed the surface coverage has a direct relation with peak current. The surface coverage calculated for bare and modified GPE for 1mM dopamine in 0.1 M PBS buffer were 4.721×10^{-14} and 6.179×10^{-10} mol cm^{-2} , respectively. This high surface coverage of the modified GPE is attributed due to the presence of the IM-rGO on the surface.

In addition to this, at higher scan rate from 500 to 900 mVs^{-1} a linear relation has been observed between the logarithm of the scan rate ($\text{Log } v$) and peak potential of the dopamine (Fig. 3-12). The peak shift was observed for both oxidation and the reduction peak potential. The positive peak shift was observed for the oxidation and negative shift

for the reduction peak potential of the dopamine (Fig. 3-12D). For anodic (E_{pa}) and cathodic peak potential (E_{pc}) shift two straight line equations 5 & 6 was yielded.

$$E_{pa} \text{ (V)} = 0.1033 \log v + 0.1977 \quad (R^2 = 0.9919) \quad \mathbf{5}$$

$$E_{pc} \text{ (V)} = -0.0652 \log v + 0.0953 \quad (R^2 = 0.9956) \quad \mathbf{6}$$

According to Laviron's theory, [270] the slope of the anodic and cathodic peak potential vs. $\log v$ are $2.3 RT/(1-\alpha)nF$ and $-2.3 RT/\alpha nF$, respectively. The charge transfer coefficient value (α) was calculated 0.61 using the following equation 7.

$$\log k_a/k_c = \log \alpha/1-\alpha \quad \mathbf{7}$$

Moreover, the apparent heterogeneous electron transfer rate constant (k_s) on the single use graphene-modified electrode by using another Laviron's equation 8 for a surface controlled transfer model [270]:

$$\log k_s = \alpha \log (1-\alpha) + (1-\alpha) \log \alpha - \log (RT/nFv) - \alpha (1-\alpha)nF\Delta E_p/2.3RT \quad \mathbf{8}$$

where R , T , F , v and ΔE_p are gas constant, temperature, Faraday constant, scan rate and the peak potential separation of the redox pair. The n is the number of electrons. The value of n for dopamine is 2 (Eq. 3). The value of k_s was found 5.81 s^{-1} using equation 8. The k_s value is high compared reported values 0.25 s^{-1} [270] and 0.77 s^{-1} [271] for dopamine. The kinetics study of modified electrode is indicated the presence of IM-rGO on the GPE surface facilitate the fast charge transfer and considerably assist the electrochemical reaction of the dopamine.

The presence of ionic medium supported graphene not only enhanced the conductivity of the GPE but also its attraction towards the dopamine. The dopamine molecules attracted

towards the graphene layer on the GPE surface and the current enhancement was observed for multiple cyclic voltammograms scanned for 0.2 mM dopamine solution in 0.1 M PBS buffer (Fig. 3-13).

3.3.6.3 Effect of pH

The pH effect on dopamine was probed from 5.0 to 8.0 pH for 50 μ M dopamine in 0.1 M PBS buffer. The supporting electrolyte pH has shown a great impact on the oxidation peak potential of dopamine. The current was increased with pH till 6.5 (Fig. 3-14). The current decreased with further increase in pH. The pH also displayed a significant effect on the peak potential of dopamine and shifted from 298 mV to 122 mV as pH increased from 5.0 to 8.0. The peak potential was moved to a negative potential with an increase of pH. Moreover, a linear relationship has been observed between peak potential and pH (Fig. 3-14B inset). The regression constant (R^2) obtained from linearity equation 9 was 0.9994. The slope was -58.6 mV/pH and it was almost equal to the theoretical value -59 mV/pH.

$$E \text{ vs. Ag/AgCl} = 58.97 - 58.6[\text{pH}] \quad 9$$

The slope of the Eq. 9 describes the same quantity of electrons and protons were involved in the electrochemical process of the dopamine. The number of electrons obtained from Eq. 3 was 2. It has been confirmed the two protons and two electrons participated in the electrochemical process of dopamine.

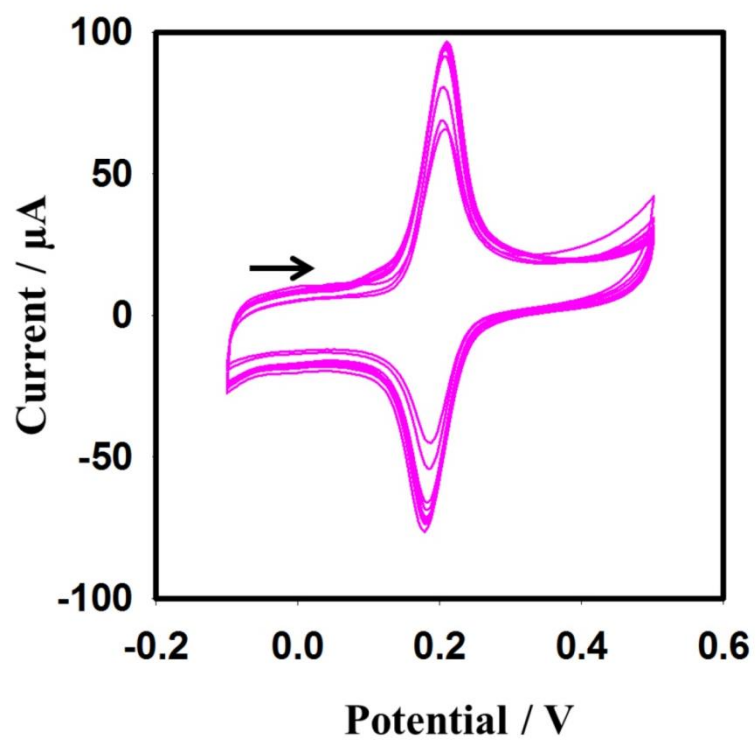


Figure 3- 13: (A) Multiple cyclic voltammograms at 0.1 V/s scan rate on IM-rGO/GPE surface for 0.2 mM dopamine in 0.1 M PBS buffer (pH 6.8).

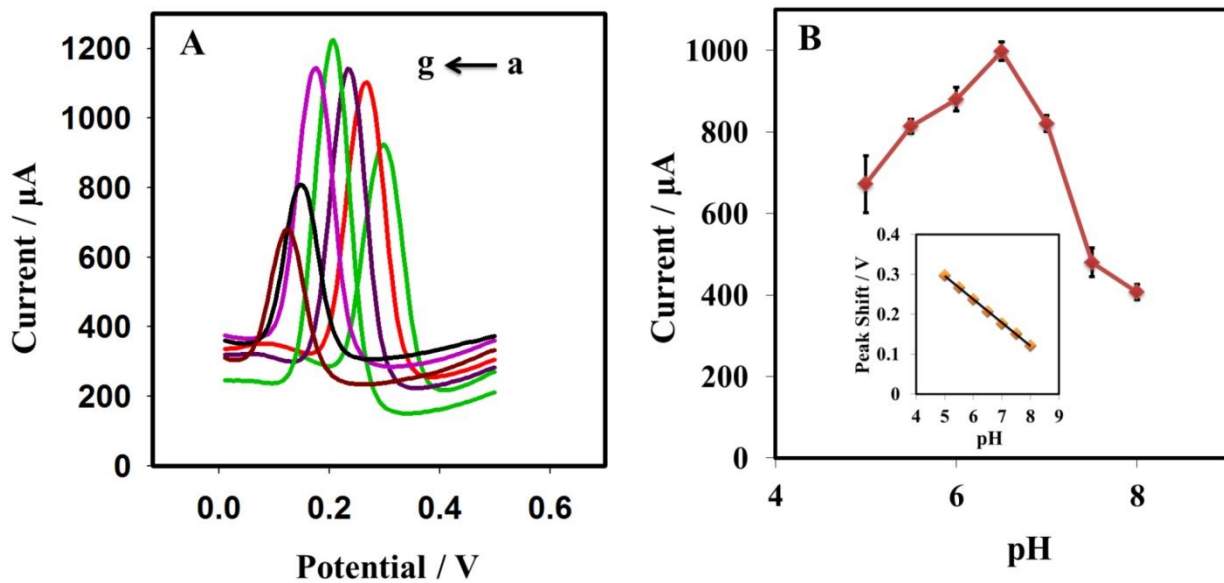


Figure 3- 14: (A) Square wave voltammograms in 0.1 M PBS solution containing 50 μM dopamine at various pH values (a) 5.0, (b) 5.5, (c) 6.0, (d) 6.5, (e) 7.0, (f) 7.5, and (g) 8.0 pH at IM-rGO/GPE. (B) Graph indicated the relationship between pH and peak current and Inset is showing the relationship between the peak potential and pH of the sensing medium

3.3.6.4 Optimization of SWV for Dopamine

The sensitivity of the electrode for dopamine was further enhanced by optimizing the square wave voltammetry parameters. The amplitude was optimized from 0.02 V to 0.1 V. The amplitude showed a great impact on the oxidation peak current strength and optimum amplitude was found 0.08 V (Fig. 3-15A). The frequency was scanned from 20 to 70 Hz and the highest response was obtained at 50 Hz (Fig. 3-15B). The ionic medium reduced graphene oxide modified electrode has shown some attraction or greater adsorption capability for dopamine which was cleared from Fig. 3-13 and Fig. 3-15C. The current was significantly enhanced with the adsorption time. The sharp increase in the peak signal was observed 0 to 120s and after this almost became constant. The constant current behavior indicated that the surface has become saturated with dopamine and no effect on the current strength with further increase of adsorption time.

3.3.6.5 Calibration Curve and Detection Limit

Fig. 3-16 has shown SWV for various concentration of dopamine on modified surface of GPE in 0.1 M PBS (pH 6.5). Under the optimum conditions of SWV, a linear relation was observed between dopamine concentrations and the peak current. A satisfactory linear relation has been observed for dopamine from 0.4 to 30 μM . The linear regression equation obtained was $I (\mu\text{A}) = 134.77 C_{\text{dopamine}} (\mu\text{M}) - 87.594$ and regression constant was 0.998. The limit of detection calculated by $S/N=3$ was 0.095 μM . The developed electrode was compared with other graphene modified electrodes that were previously used for the detection of the dopamine (Table 3- 3).

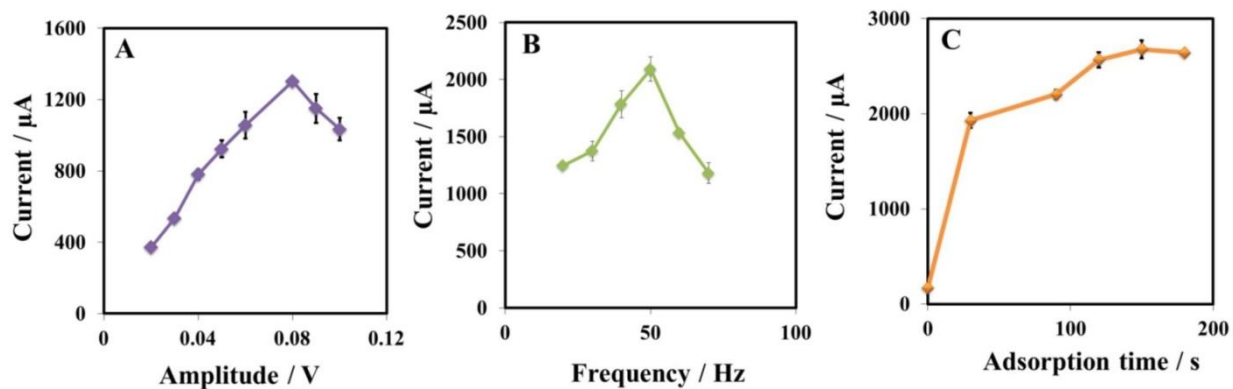


Figure 3- 15: Plots of the oxidation peak current vs. amplitude (A), frequency (B), at 30s adsorption time and adsorption time (C) obtained from the square wave voltammograms collected from 20 μM dopamine in a PBS buffer (0.1 M, 6.5 pH).

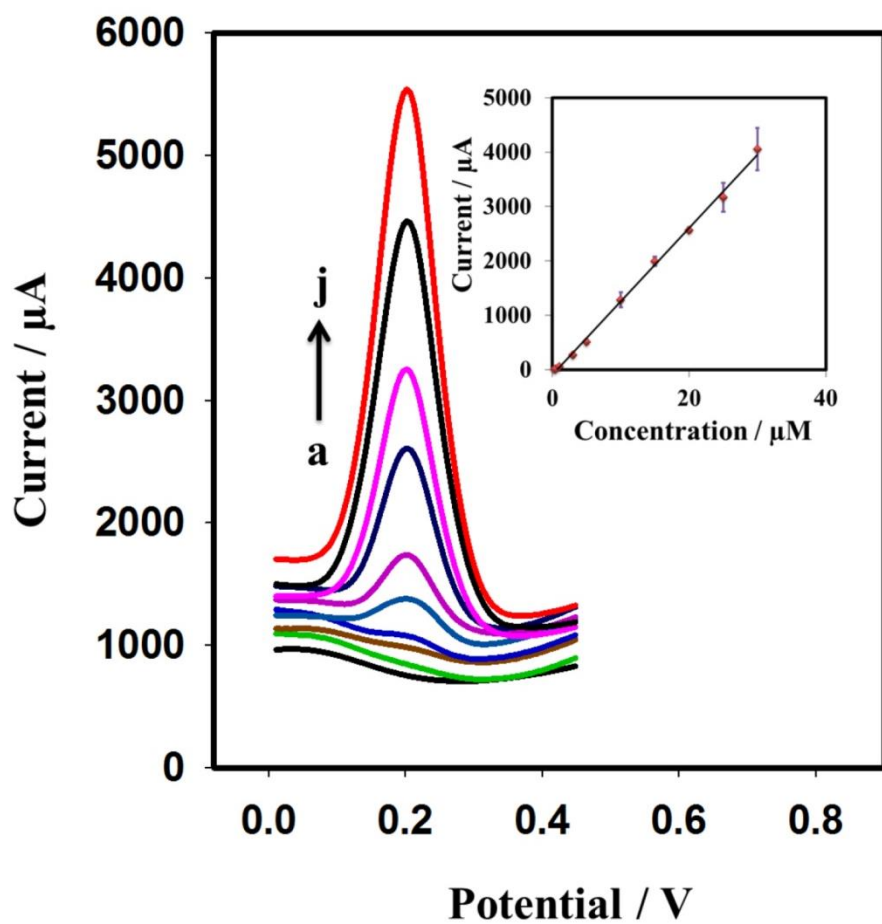


Figure 3- 16: Square wave voltammograms at various concentrations of dopamine: (a) 0, (b) 0.4, (c) 0.5, (d) 1, (e) 3, (f) 5, (g) 10, (h) 15, (i) 25, (j) 30 μM . The inset shows the linear relationship between oxidation peak current (μA) and the concentration (μM) of dopamine ($R^2 = 0.998$).

Table 3- 3: Comparison of the developed electrode with previously reported graphene and graphene composite electrodes.

Electrode	Technique	LOQ (μM)	LOD(μM)	Ref.
GR-CS/GCE	DPV	5		[251]
GR-GCE	DPV	4	2.64	[249]
GR-modified GCE	CV	2.50	0.5	[250]
GR-SnO ₂ /CILE	DPV	0.5	0.13	[272]
PPy/graphene/GCE	CV	0.5	0.1	[254]
GNS/paste electrode	DPV	4	0.6	[252]
PAM/rGO/GCE	CV	0.3	0.1	[273]
GR-AuNPs-CD-CS modified GCE	DPV	0.1	0.08	[274]
PGR/GCE	Amperometry	5	2	[275]
3D-rGO/GCE	DPV	5	0.17	[253]
Pt/RGO/GCE	DPV	10	0.25	[134]
MgO/Graphene/tantalum	DPV	0.1	0.15	[157]
mp-GR/GCE	DPV	4	0.15	[276]
Au/Gr-AuAg	SWV	0.3	0.205	[255]
Au/Gr-Au	SWV	100	30.3	[255]
IM-rGO/GPE	SWV	0.4	0.095	This work

3.3.6.6 Comparison of the Developed Sensors with Reported Graphene Modified Sensors

From Table 3-3, it is clear that reduced graphene oxide is not new in the sensing of dopamine. It is always being applied in different ways to enhance the limit of quantification and detection. Few methods have been reported in which the graphene was only used for the sensing of dopamine. Y. Wang has fabricated GR-CS/GCE by using casting method and achieved a limit of quantification $5\mu\text{M}$ [251]. Similarly, graphene was cast on the GCE and LOD was obtained $4\mu\text{M}$ [249]. The similar limit of quantification $5\mu\text{M}$ was achieved by using pristine graphene (PGR/GCE) [275] and 3D reduced graphene oxide (3D-rGO/GCE) [253] were also prepared by a casting method. In another method, graphene modified GCE was used and LOQ was attained $2.5\mu\text{M}$ [250]. The limit of quantification was obtained $4\mu\text{M}$ by using multi nanopore graphene modified GCE [276]. All these electrodes only used graphene for modification. In comparison all these methods, the developed electrode is very sensitive and limit of quantification was achieved successfully $0.4\mu\text{M}$ which is even better compared to many complex graphene composite electrodes (Table 3-3). The developed electrode is very simple and modification process is very fast compared to the casting method. The possible improvement of the LOQ and the LOD was due to the effective reduction of GO in the presence of ionic medium typically acetate buffer and control of the thickness of the layer by the optimized parameters of the directly reduced graphene oxide on the surface of GPE. It is difficult in casting method. The direct electrochemical reduction considerably improved by acetate medium and completed in short time while water dispersed graphene oxide the number of cycles required to improve the sensitivity. The

reusability of the modified electrodes was drastically affected by the electropolymerization of the dopamine on the electrode surface. The developed electrode coup this challenge very easily due to the fast fabrication process and very low cost compared to most of the reported methods in which multiple steps are involved in sensor fabrication.

3.3.6.7 Detection of Dopamine in Real Sample and Interferences Study

The modified electrode was also tested for the real sample. Healthy person urine was collected and diluted with 0.1 M PBS buffer. The various concentrations of dopamine spikes (5, 10, 15 μM) and oxidation peak current was measured. The recoveries were found between 96 to 107 %. The good recoveries indicated the developed electrode could be applied to real samples (Table 3- 4). The major interfering species in the determination of DA is UA and the AA. The well-separated peak observed in the presence of uric acid and the ascorbic acid. The 10 % variation in current was observed for 15 μM dopamine in the presence of 1 mM AA. Moreover, a weak response of the ascorbic acid was observed at 0.046 V which further endorse the rGO-GPE is more specific towards dopamine (Fig. 3-17). It could be due to the still presence of few negative carboxylate ions after the IM-rGO on the GPE surface which reduces the adsorption capability of the ascorbic acid due to less attraction. Moreover, the optimized parameters of the SWV are more sensitive and selective for dopamine. The high concentration of other biomolecules like L-methionine, adenine, glucose, L-tryptophan and presence of K^+ , Na^+ , SO_4^{-2} , and Cl^{-1} ions has shown current variations from ± 1.85 to ± 8.83 .

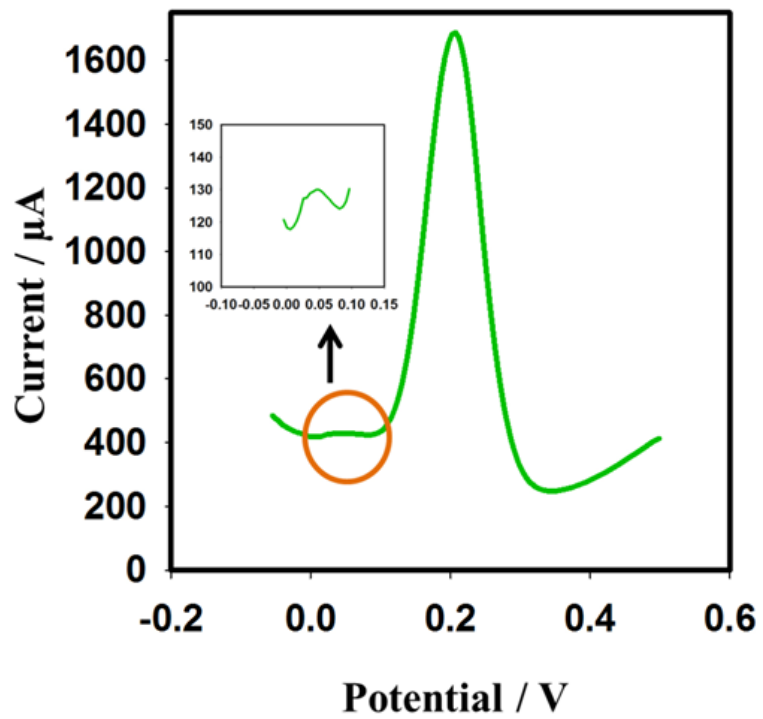


Figure 3- 17: Square wave voltammetric response of 15 μM dopamine in the presence of 1mM ascorbic acid. Inset showing the ascorbic acid peak current.

Table 3- 4: Detection of dopamine in human urine sample

Sr#	Found (μM)	Added (μM)	Recovered (μM)	%cent recovery
1	0	5	4.82	96.4
2	0	10	10.64	106.4
3	0	15	15.27	101.8

3.3.6.8 Developed Method Reproducibility

The common problem with the electrodes is the surface fouling after the first measurement of the dopamine. The same surface is normally used and many methods have been adopted to clean the surface prior to use for the second measurement because the renewal of the bare electrode surface is not so easy. In our case, the electrode is disposable and after each measurement, the new modified surface could be prepared very easily and in short time using ionic medium supported GO. The renewability of the surface makes it foul free for the dopamine measurement. The renewed surface just obtained in less than 6 minutes. The RSD obtained in six repeating ASSWV was 4.1%. The electrode surface was renewed prior to each measurement of dopamine.

3.3.7 A Cost Effective Single-use Disposable Electrodes Based on Acetate Medium Supported-reduced Graphene Oxide for Sensitive and Selective Detection of Uric Acid in Human Urine

3.3.7.1 Behavior of Uric Acid on Modified Surface

Fig. 3-18 has compared the behavior of the bare GPE and ac-dERGO/GPE for 1mM UA in 0.1 M PBS buffer (pH 6.8) by CV. A prominent sharp peak was observed on modified electrode compared to the bare electrode a broad peak appeared. A significant increase in current was obtained by ac-dERGO/GPE compared to the bare GPE. The uric acid oxidation peak on the bare and modified GPE appeared at 0.40 and 0.35 V, respectively. Moreover, no reversible peak appeared on the bare GPE while partially reversible peak could be observed on the ac-dERGO/GPE.

The electrode surface plays important role in the reversibility and the kinetics of the electrochemical reaction. The cyclic voltammograms reveal the reversibility of the electrochemical reaction [268]. The equation 3 was used to calculate the potential difference between E_{pa} and E_{pc} of the CVs of uric acid in 0.1 M PBS [234].

In the case of an irreversible reaction, the only single peak appears. The reaction is considered as reversible when the value of ΔE is $59/n$ mV and quasi-reversible if the value is greater than $59/n$ mV. The ΔE value calculated for the uric acid was 37 mV. The value was greater compared to the theoretical value $59/n$ mV which indicated the electrochemical reaction on the electrode surface was quasi-reversible. The CVs of bare electrode revealed the electrochemical reaction of the uric acid on the surface was irreversible and no reduction peak observed on bare GPE. It means the reversibility of the uric acid somehow has become feasible on the modified electrode surface. Moreover, the value of n calculated from equation 3 was 1.6. This value has revealed the two electrons contributing in the electrochemical reaction of uric acid

Study of the ESA of the dERGO-GPE modified from water dispersed or acetate buffer dispersed graphene oxide

3.3.7.2 Study of the Electroactive Surface Area of the dERGO-GPE Modified from Water Dispersed or Acetate Buffer Dispersed Graphene Oxide

Graphite pencil proved a good electrode material for direct electrochemical reduction due to an elongated shape. Graphene oxide was dispersed in water (w-GO) and in acetate buffer (ac-GO). It was observed, the acetate medium showing a more facile electrochemical reduction of GO and imparts more sensitivity to the GPE surface. To

elucidate the effect of acetate on the dERGO, the ESA was calculated using Randles-Sevcik equation 1 for bare GPE, w-dERGO/GPE and ac-dERGO/GPE for uric acid. Cyclic voltammograms were recorded at different scans rates from 20 to 100 mVs⁻¹ in 0.2 mM uric acid solution (Fig 3-19). The ESA was found 0.089, 0.481 and 0.821 cm² using bare GPE, w-dERGO/GPE, and ac-dERGO/GPE, respectively. The acetate medium dispersed GO almost showing the two-time increase in the electroactive area surface area of GPE compared water dispersed GO.

3.3.7.3 Effect of pH on the Oxidation Peak of Uric Acid at ac-dERGO/GPE

The supporting electrolyte pH has shown a significant effect on the peak shift and also on peak current of the uric acid. The pH effect was scanned from 6.0 to 8.0 in a 0.1 M PBS buffer comprising of 10 µM uric acid (Fig. 3-20). The oxidation peak current was slightly increased as the pH increased till 6.8 and after that, it was started decreasing. A linear negative shift in oxidation peak potential was observed as the pH increased from the 6.0 to 8.0 (Fig. 3-20B, inset). The slope of the linear relation ($R^2 = 0.991$) between pH and uric acid oxidation peak potential was -64.3 mV (Eq. 10) that was very close to the theoretical value -59 mv. It is indicated that the same number of protons and electrons participate in the electro-oxidation of the uric acid which is in agreement with reported work [78].

$$E \text{ vs. Ag/AgCl} = 756.5 - 64.3[\text{pH}] \quad 10$$

3.3.7.4 Optimization of the SWV Parameters

All the possible parameters of the square wave voltammetry that could affect the electrochemical oxidation of the uric acid on the ac-dERGO/GPE surface were

optimized. The amplitude was first optimized between 0.020 and 0.060 V. The oxidation peak current was maximum at 0.03 V and then continuously dropped with further increase of the amplitude (Fig. 3-21A).

Frequency also showed great influence on the oxidation signal of the uric acid when it was optimized from 15 to 70 Hz. The maximum response was obtained at 50 Hz (Fig. 3-21B). Finally, the adsorption time was optimized. The adsorption time has a substantial effect on the strength of the oxidation signal. The current was increased rapidly as the adsorption time increased and level off at 120 s (Fig. 3-21C). This huge increase in current revealed that acetate supported-graphene layer on GPE surface has substantially enhanced the adsorption capability for uric acid.

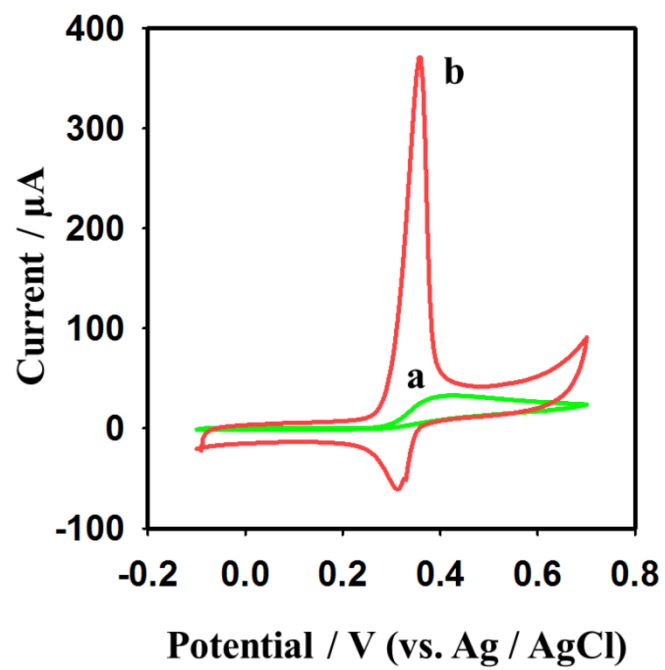


Figure 3- 18: CVs of (a) the bare GPE, and (b) the ac-dERGO/ GPE in PBS buffer (0.1 M, pH 6.8) containing 1 mM uric acid. Scan rate: 100 mV s^{-1} .

3.3.7.5 Calibration Curve and Detection Limit

A linear relation has been observed between the concentration and the oxidation peak current of the uric acid under the optimum conditions of the SWV, including 0.03 V amplitude, 50 Hz frequency and 120 s adsorption times. A linear relation has been observed between 0.2 and 22 μM with regression constant 0.996 (Fig.3-22). A linear equation was yielded by the calibration curve: $I (\mu\text{A}) = 136.08 C_{\text{UA}} (\mu\text{M}) - 29.914$. The LOQ was 0.2 μM and LOD obtained by ac-dERGO-GPE was 0.037 μM which is better compared to most of the graphene and graphene composite modified electrode (Table 3-5). It is elucidated from the results that acetate supported-graphene oxide more efficiently reduced on the GPE surface compared to the other electrode. Generally, the casting method is adopted for the graphene oxide reduction on the surface of the other electrode; the control of the thickness of the graphene layer is problematic while in GPE it is comparably easier due to the direct reduction of the graphene oxide.

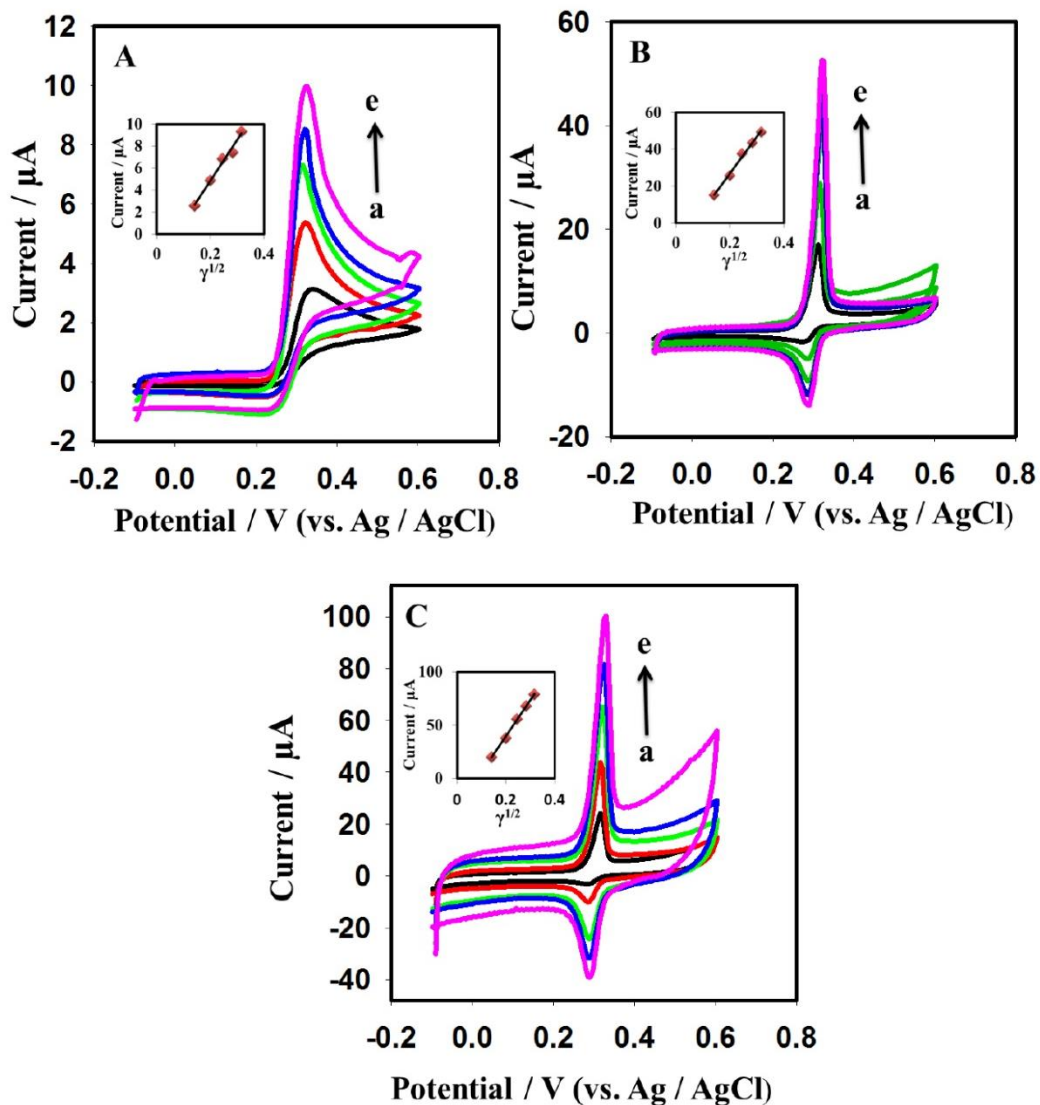


Figure 3- 19: Cyclic Voltammograms obtained from a solution comprising 0.2 mM uric acid (A) Bare GPE, (B) w-dERGO/GPE, and (C) ac-dERGO/GPE at different scan rates of (a) 20 (b) 40, (c) 60, (d) 80, and (e) 100 mVs^{-1} . The insets in (A), (B) and (C) show the linear relationship between current and the square root of the scan rates.

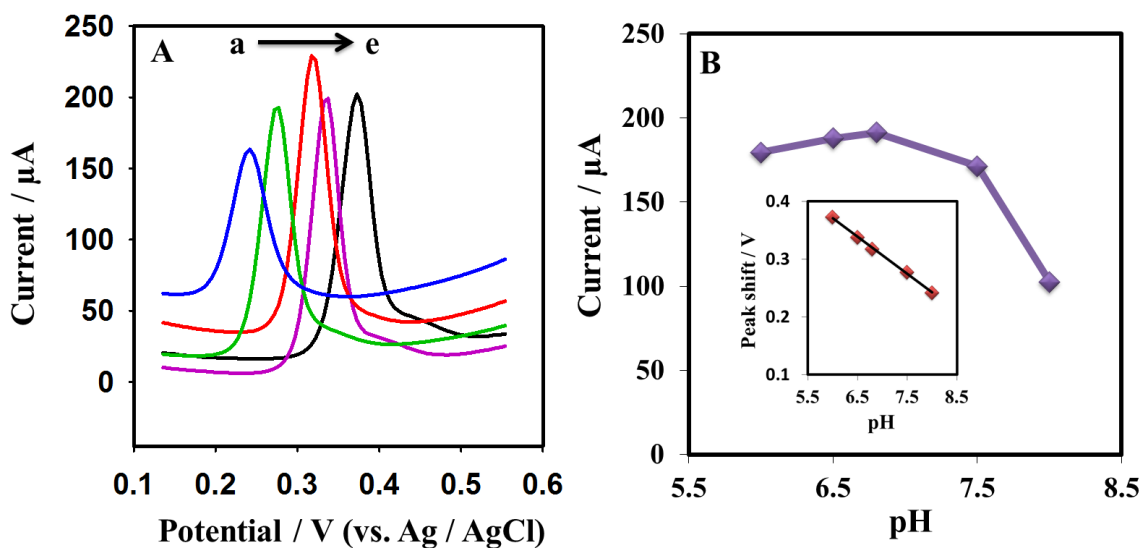


Figure 3- 20: (A) Square wave voltammograms in 0.1 M PBS solution containing 10 μM uric acid at various pH values (a) 8.0, (b) 7.5, (c) 6.8, (d) 6.5, (e) 6.0 at ac-dERGO/GPE. (B) Graphical representation of the peak current vs. pH. Inset is relationship between the pH vs. the oxidation peak potential.

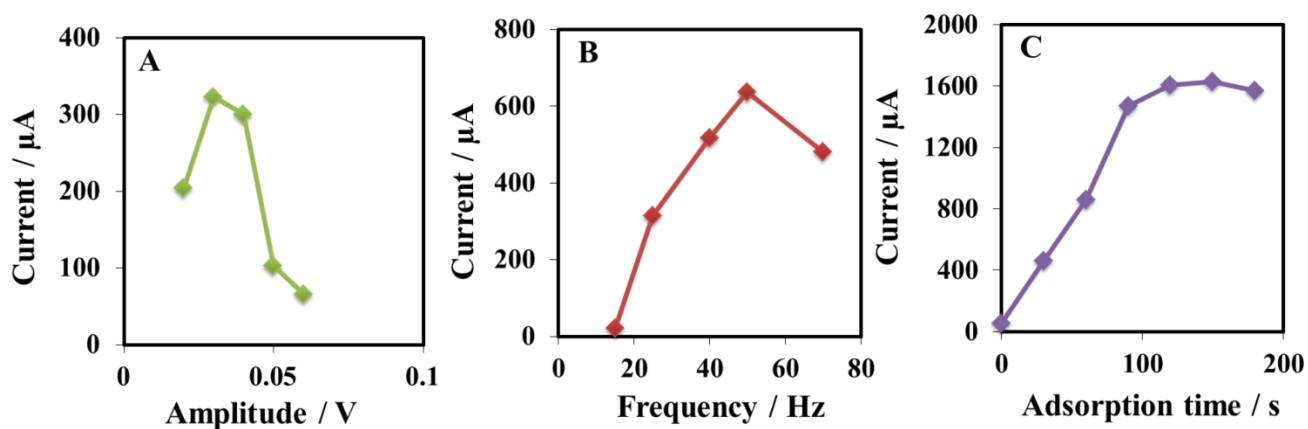


Figure 3- 21: The corresponding plots of the oxidation peak current vs. (A) amplitude, (B) frequency, and (C) adsorption time obtained from the square wave voltammograms collected for 10 μM uric acid in a PBS buffer (0.1 M, 6.8 pH).

3.3.7.6 Application and Interferences

The developed sensor was applied to real samples. Urine samples were collected from the healthy person and diluted with 0.1 M PBS to bring in the linear range of the sensor. A sharp peak was observed at 0.327 V. It was confirmed by spiking 8, 10, 12 μM of uric acid and the peak current was increased linearly. The recoveries of the spiked uric acid were between 98.2 and 105 % (Table 3-6). The real sample has a number of ions, proteins and interfering species. The good recoveries indicated that the developed electrode is foul free and could cope with real sample interferences. AA is the most commonly observed interfering species during the determination of uric acid. The oxidation potential of the ascorbic acid is very close to the UA. It has been observed under un-optimized conditions of SWV 25 Hz frequency, 0.02 V amplitude, and 30 s adsorption time a prominent well-defined peak of the 200 μM ascorbic acid was observed (Fig 3-23 A). It seems the optimized conditions for uric acid were not facilitating the oxidation of the AA and small peak of AA was observed (Fig 3-23 B). The 50 times higher concentration of ascorbic acid has just displayed 6 % variation in the oxidation peak current. Moreover, other interferences 50 μM L-methionine, 50 μM L-alanine, 20 μM L-phenylalanine, 10 μM fructose and glucose were also studied for 10 μM concentration of uric acid. The current variation was observed from 5 to 12 %. This small variation of current is indicated that ac-dERGO/GPE has the capability to behave well in the presence of interfering species and foul free even at a much higher concentration of the ascorbic acid.

3.3.7.7 Comparison with Clinical Methods

Common methods that are being applied for the determination of uric acid mostly based on the spectrometric determination of UA. In few methods, uric acid is determined by the colorimetric methods. In first method uric acid is reduced the phosphotungstic acid into tungsten blue in an alkaline solution that is measured photometrically [278]. This method is highly sensitive in the presence of other reducing agents. In the second colorimetric method, the sample is first incubated with the ascorbate peroxidase. Uricase oxidizes the uric acid and the resulted peroxide in the presence of peroxidase is reacted with N-ethyl-N-(2-hydroxy-3-sulfopropyl)-3-methylaniline and 4-aminoantipyrine and formed a red colored quinone-imine dye which is determined by photometrically [279]. The AA is severely interfering the results and its removal prior to analysis is necessary. In another method, the uricase enzyme is applied which oxidize the UA. The determination of UA could be done by the UV measurement or by using another enzyme which provides colorimetric assay. Chromatographic methods like HPLC-UV or HPLC-MS with reverse phase column are also used for the determination of the uric acid [280]. HPLC is an expensive instrument and high purity solvents are required which further increase the cost of the analysis. Moreover, in spectroscopic methods normally uricase enzyme is being used to break down the uric acid into a detectable product which also makes the process more delicate, costly and complex. The sensing through aforementioned method is a little bit tedious and sometimes expertise is required. The introduced method is very simple and the cost effective compared the previous clinical methods that are being used. Moreover, no enzyme is required for the sensing of uric acid. The fabricated sensor also behaves well in the presence of high concentration of ascorbic acid.

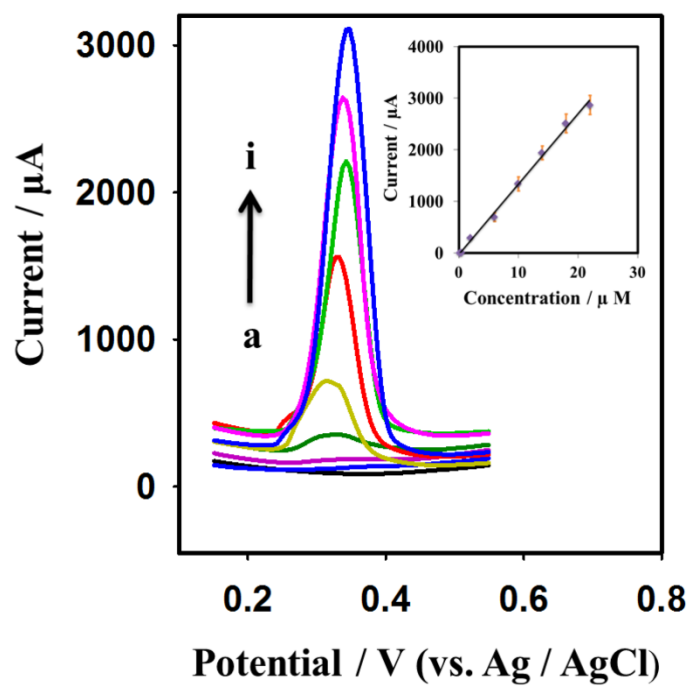


Figure 3- 22: Square wave voltammograms in PBS buffer (0.1 M, pH 7.0) at various concentrations of uric acid: (a) 0, (b) 0.2, (c) 0.5, (d) 2, (e) 6, (f) 10, (g) 14, (h) 18 and (i) 22 μM . The inset shows the linear relationship between I (μA) vs. concentration (μM) of uric acid ($R^2 = 0.996$). The SWV parameters were: amplitude of 0.03 V, frequency of 50 Hz, and adsorption time of 120 s.

Table 3- 5: Comparison of the dERGO-GPE with the previously graphene and graphene composite modified electrodes

Electrode	Technique	Electrode modification Time (h)	LOQ (μM)	LOD (μM)	Ref.
Screen-printed graphene electrode	DPV	1.16	0.8	0.2	[32]
Pd NPs/graphene/chitosan / GCE	DPV	24	0.5	0.17	[135]
Au NPs- β -cyclodextrin graphene / GCE	SWV	1.2	0.5	0.21	[281]
Graphene Sheet–PTCA/GCE	DPV	C*	4	0.92	[162]
Neutral red-functionalized graphene nanosheets /GCE	Amperometry	C*	0.12	0.062	[282]
partially electro-reduced graphene oxide /GCE	SWV	12	0.1	0.05	[257]
Graphene poly(acridine red) /GCE	DPV	C*	0.8	0.3	[283]
Pd ₃ Pt ₁ /PDDA-Reduced Graphene Oxide/GCE	DPV	C*	4	0.1	[144]
PDDA–Graphene nanosheets/GCE	DPV	-	0.5	0.1	[256]
ac-dERGO/GPE	SWV	0.46	0.2	0.037	This work

C*= certain amount of the graphene oxide composite cast on the surface of the GCE and dried but time is not mentioned.

Table 3- 6: Study of the uric acid recoveries in the human urine sample

Sr #	Found (μM)	Added (μM)	Recovered (μM)	Percent recovery
1	5.15	8	7.90	98.75
2	5.15	10	9.82	98.2
3	5.15	12	12.71	105

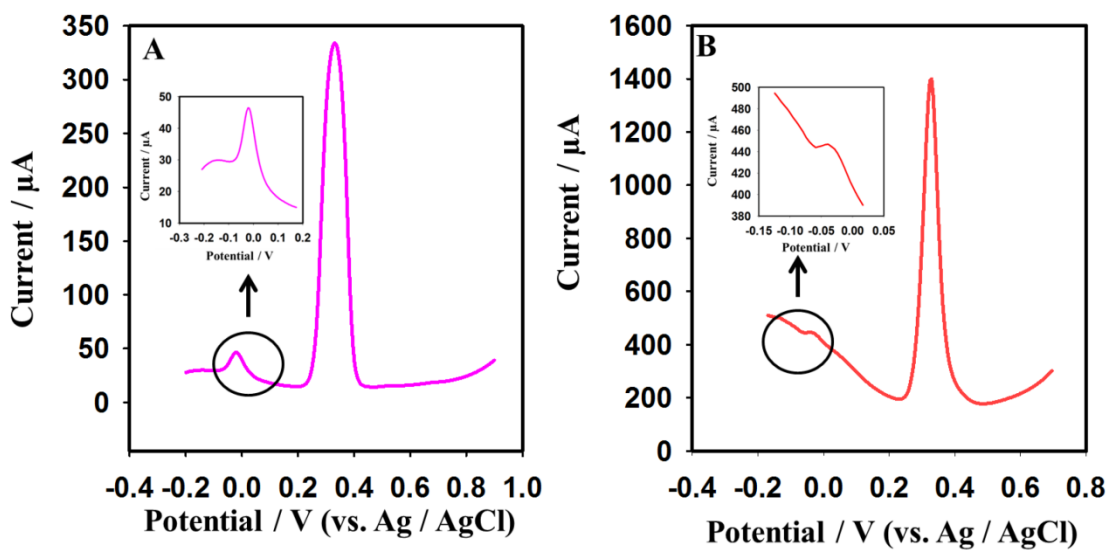


Figure 3- 23: (A) Square wave voltammograms of 500 μM ascorbic acid in the presence of 50 μM uric acid before (A) and after (B) optimization. Parameters for (A): amplitude 0.02V, frequency 25 Hz, and adsorption time 30s. Parameters for (B): the amplitude of 0.03 V, frequency of 50 Hz, and adsorption time of 120 s.

It could be a valuable tool for the sensing of the uric acid and the monitoring of various uric acid based problems like hyperuricemia. Very low cost and the facile fabrication of the electrode have given a disposable character to the electrode.

CHAPTER 4

Highly Sensitive Platinum Nanoparticles Sandwiched in Graphene Layers Modified Graphite Pencil Electrode for Trace Level Quantification of Dopamine

4.1 Introduction

The sensing of dopamine in the human body has great importance. DA is a vital neurotransmitter which belongs to the catecholamine family. Dopamine also contributes to the regulation of heart beat and the blood pressure [13]. Dopamine involved in the mobility, mood and the behavior of the individual. The abnormal level of the dopamine could cause some serious problems in the human body like restless leg syndrome, Parkinson's disease, senile dementia, attention deficit hyperactivity disorder [16] and schizophrenia. The monitoring of catecholamine in the human urine could be used as a biomarker for the renal and the cardiovascular disease in the patients. Due to the importance of the dopamine, the developments of the new sensors for dopamine sensing are highly appreciated for clinical purposes [284].

Numerous methods were reported for the sensing of DA. Most of these methods are based on capillary electrophoresis, liquid chromatography-electrospray mass spectrometry [285], HPLC-fluorescence based sensing [13], and fluorescence [286]. Although these methods are sensitive, yet some of them are consuming a lot amount of environment unfriendly chemicals, costly and most of the time the pretreatment of the sample is required [287]. Electrochemical techniques compared to the other techniques are considered simple, fast, cost-effective, less complex and easy to handle. Apart from their simplicity, the sensing of dopamine by electrochemical methods is always challenging due to the close electrooxidation to ascorbic acid and uric acid. This serious issue is addressed by modifying the electrode surface with various materials to achieve a well-resolved peak of dopamine. The modified electrodes like MgO nanobelts/GCE [212], PA6/PAH_MWCNTs nanofibers/ITO [288] and Flake shaped CuO nanoparticles/MCPE [289] were used for sensing of dopamine.

The modifying material that is widely being used to improve the selectivity, sensitivity and decrease the charge transfer resistance are CNTs, noble metal nanoparticles, graphene and their nanocomposite. Among these, the graphene-based nanocomposite has gained great attraction due to its unique behavior. Graphene is a hexagonal honeycomb-like sp^2 bonded two-dimensional carbon atoms [290]. Graphene due to its excellent thermal and the electrical conductivity, huge surface area, and the mechanical strength, it is continuously being studied in various fields like field emission displays, energy storage devices, conductors, and sensors fabrication. Graphene considered as excellent materials for electrode modification due to the wide potential window, large electroactive surface area and fast charge transfer [26]. The graphene-based sensors like NiO–CuO/GR/GCE [291], rGO–Cu₂O/GCE [292], Fe₃O₄-NH₂@GS/GCE [146], and CoTPP-CRGO/GCE [293]. The Pt-based nanocomposite is exhibiting a great potential for fabrication of the sensitive electrochemical sensors due to their outstanding biocompatibility, high conductivity, electrocatalytic behavior and chemical stability [294, 295].

Few works have been reported based on Pt and graphene nanocomposite modified GCEs for the determination of DA. T. Xu et al. has introduced the Pt/RGO/GCE for concurrent determination of DA and UA. It has shown good electrocatalytic activity towards dopamine and the LOQ, and LOD was obtained by the fabricated sensors was 10 and 0.25 μ M [296]. The sensitivity of the Pt-based nanocomposite was further improved by J. Yan et al. by using Pd-Pt nanoparticles anchored graphene sensor Pd₃Pt₁/PDDA-RGO/GCE. The LOQ and LOD were improved for dopamine to 4 and 0.04 μ M [144]. The casting was the method used in this Pt-based rGO nanocomposite on the GCE surface.

In this work, we have improved the sensitivity and the selectivity of the graphite pencil electrode by fabricating the Pt NPs based sandwich structure having upper and a lower layer of reduced graphene oxide. This specific arrangement of the Pt NPs reduced graphene oxide nanocomposite has significantly improved limit of quantification and detection to 0.06 μM and 0.009 μM for dopamine compared the previously Pt-based graphene composite. Moreover, the dERGO and Pt^{+2} on the electrode surface made the electrode fabrication fast, and no additional steps are involved. GPE electrode itself very cheap and renewability of the surface after a single use is very easy, and no surface polishing is required compared the glassy carbon electrode.

4.2 Materials and Methods

4.2.1 Reagents

The materials and reagents are same as stated in 3.2.1 subsection.

4.2.2 Apparatus

The instrumentation and apparatus are same as stated in 3.2.2 subsection.

4.2.3 Fabrication of Pt NPs Sandwiched Graphene Layers GPEs Sensor

The manufacture of the sensor was done by dipping the seven-millimeter tip of the graphite pencil electrode in the graphene oxide and the $(\text{NH}_4)_2\text{PtCl}_4$ solution. The graphene first layer was formed by reducing the graphene oxide (4 mg/mL) by CV scan from -1.4 to 0.3 V over one cycle. After the first cycle, the surface of the electrode was cleaned by gently dipping in the double distilled water, and the Pt^{+2} was reduced on the GR/GPE surface by dipping the surface in 0.1mM $(\text{NH}_4)_2\text{PtCl}_4$ solution by CV scan from -0.05 V to 0.3 over one cycle. The electrode surface again cleaned and the second layer of graphene was prepared under same conditions as the first layer was formed. The fabricated Pt NP_s sandwiched electrode mentioned as GR/Pt/GR/GPE.

4.3 Results and Discussions

4.3.1 Experimental Conditions Optimization

For the development of the sensitive sensors, all the possible conditions were tried to optimize for graphene oxide and the Pt^{+2} solutions for the miniaturization of the Pt NPs based reduced graphene oxide graphite pencil electrode. First of all, the layer sequence of the Pt NPs and the graphene was investigated. It has been observed, the graphene as the first layer was more efficient instead of Pt NPs. The maximum response of the sensor was observed for 0.2 mM dopamine when layer arrangement was GR/Pt/GR compared the other arrangements (Fig.4- 1). The Pt NPs were formed by the electrochemical reduction. The reduction window was optimized from -0.4 to 0.3 V for Pt^{+2} and the -0.05 to 0.3 V reduction window was observed best one due to highest response for dopamine. At higher reduction potential, the Pt NPs agglomeration could take place which could affect the sensor sensitivity.

The reduction scan rate for Pt^{+2} was optimized from 0.04 to 0.005 V/s and the best response was observed at 0.01 V/s. Similarly, various concentrations from 0.05 mM to 1 mM of $(\text{NH}_4)_2\text{PtCl}_4$ solutions were used for the electrochemical formation of Pt NPs on the GPE surface, and most suitable concentration was found 0.1 mM $(\text{NH}_4)_2\text{PtCl}_4$. At higher concentrations, possibly the bigger nanoparticles were being formed which also reduced the electrode sensitivity. All the optimized conditions of the Pt^{+2} electrochemical reduction were applied for the formation Pt NPs on the graphite pencil electrode surface. However, graphene oxide optimized conditions already described in detail [66].

4.3.2 Characterization of Synthesized Graphene Oxide and Fabricated Sensor

The characterization of synthesized graphene oxide was same as stated in sub section 3.3.1. The synthesized graphene oxide in 0.1 M acetate buffer was used for the fabrication of the graphene-based sensor. The interfacial behavior of the bare GPE, GR/GPE, and GR/Pt/GR/GPE was explored by the EIS. The impedance behavior was analyzed by measuring the impedance in 5 mM $K_3Fe(CN)_6/K_4Fe(CN)_6$ solution by dipping the surface of the bare or modified electrodes. In the case of bare GPE, a large semicircle has been observed, and quite a high charge transfer resistance was observed 2649 Ω (Fig. 4- 2 A, a). The charge transfer resistance (R_{ct}) was significantly reduced in the case of GR/GPE (Fig. 2Cc), and the GR/Pt/GR/GPE (Fig. 4- 2 A, b) and no semicircles were observed. The impedance studied has revealed the reduced graphene oxide and the Pt NPs sandwiched reduced graphene oxide layered sensor have effectively improved the surface charge transfer of the graphite pencil electrode. Similar behavior was observed when the various electrodes were explored by using cyclic voltammetry for 0.2 mM dopamine in 0.1 M PBS buffer (pH 5.5). In the case of bare GPE, a broad peak of dopamine was observed. The sensitivity of the bare electrode towards dopamine was poor as the small current was observed (Fig. 4- 2B, a). The sensitivity of the electrode was significantly improved by the electrochemically rGO on the surface of the GPE, and the sharp peak was observed for dopamine (Fig. 4- 2 B, b).

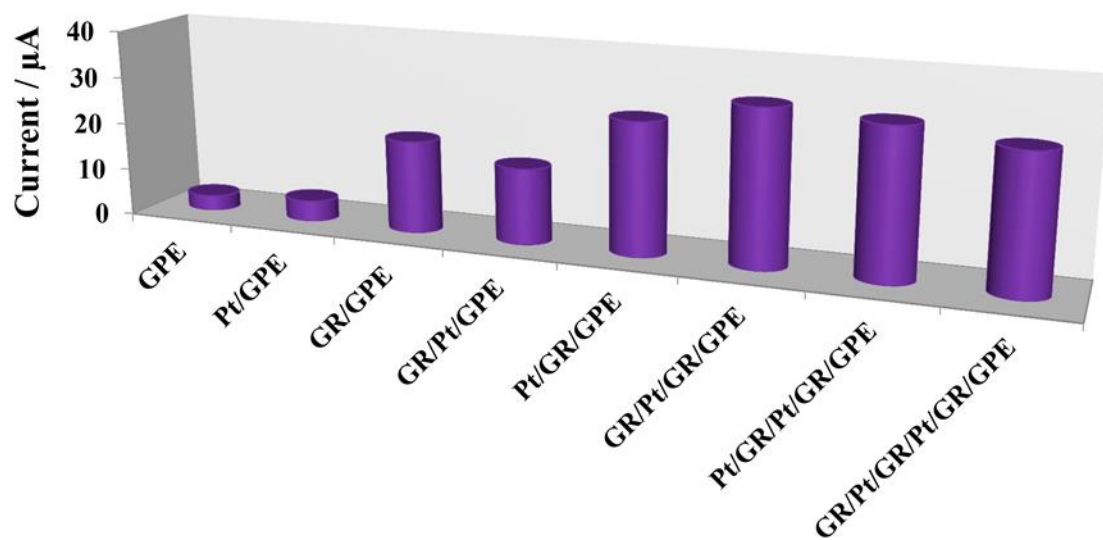


Figure 4- 1: The corresponding histogram for the oxidizing peak current of cyclic voltammograms for 0.2 mM dopamine in 0.1 M PBS (pH 6.80) at various modified electrode surfaces.

It has been observed the electrochemically formed NPs in between the layers of the reduced graphene oxide has a more useful impact on the sensitivity of the electrodes compared the other arrangements of the Pt NPs graphene nanocomposite. The enhancement in the current for oxidizing and reducing peak was observed for GR/Pt/GR/GPE compare GR/GPE and the bare GPE (Fig. 4- 2 Bc).

As the Pt NPs was between two layers of graphene, it may act as a spacer between two layers and may decrease the tendency of the graphene layers to be agglomerate and possibly in this way enhance the sensitivity of the sensor. Due to this reason, the outer layer of Pt NPs was not effective as the inner layer (Fig. 4- 1).

Moreover, the morphology of the surface was analyzed by using FE-SEM. The various FE-SEM images were recorded at 1 μm and 500 nm to observe the surface before and after various modifications (Fig. 4- 3). The FE-SEM images clearly revealed the formation of wrinkle-shaped graphene on the surface of the GPE (Fig. 4- 3b) while this layer was absent in the case of bare GPE (Fig. 4- 3a). Similarly, the sandwiched Pt NPs were also formed electrochemically between two layers of graphene. Around 10-50 nm in size Pt NPs between graphene layers could be observed in SEM images (Fig. 4- 3c). The tiny Pt NPs enhancing the sensitivity of the sensor due to their small size and also playing its role as a spacer between graphene layers. Due to the presence of Pt NPs in between the graphene layers, the Pt NPs are not clearly visible. The visibility of the Pt NPs was enhanced by using the backscattering electron beam (BSE), and SEM image has shown the uniform distribution of the Pt NPs in between the graphene layers (Fig. 4- 4).

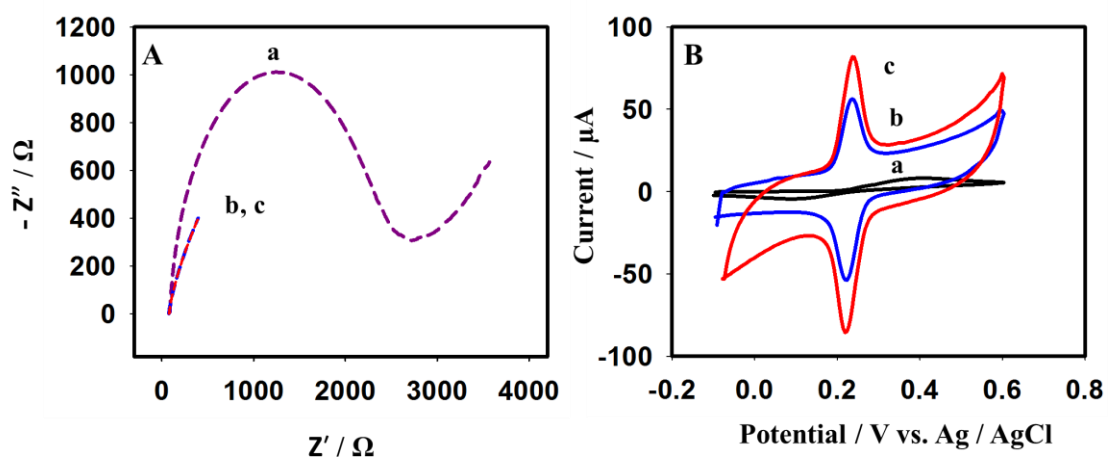


Figure 4- 2: (A) Nyquist plot of 5 mM $K_3Fe(CN)_6/K_4Fe(CN)_6$ in 0.1 M KCl solution at the (a) bare GPE, (b) GR/Pt/GR/GPE, and (c) GR/GPE by applying of 5 mV potential in the frequency range 100 to 0.01 Hz. (B) CVs of 0.2 mM DA in 0.1 M PBS buffer (pH 5.5) at the (a) bare GPE, (b) GR/GPE, and (c) GR/Pt/GR/GPE at scan rate 0.15 V/s. Inset B is the histogram of the oxidation peak current (OP) and reduction peak current (RP) on various electrode surfaces.

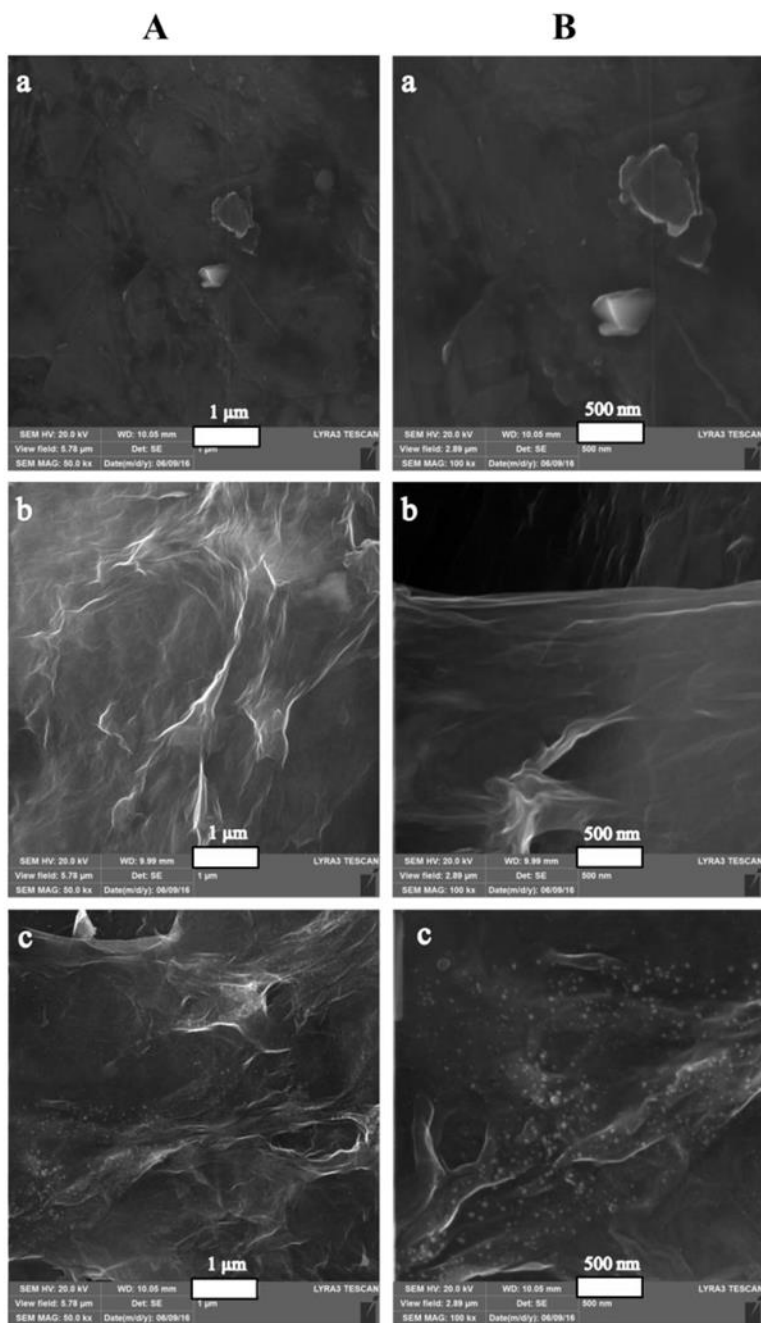


Figure 4- 3: FE-SEM images at two magnifications (A) 1 μm and (B) 500 nm of the (a) bare/GPE, (b) GR/GPE (c) GR/Pt/GR/GPE.

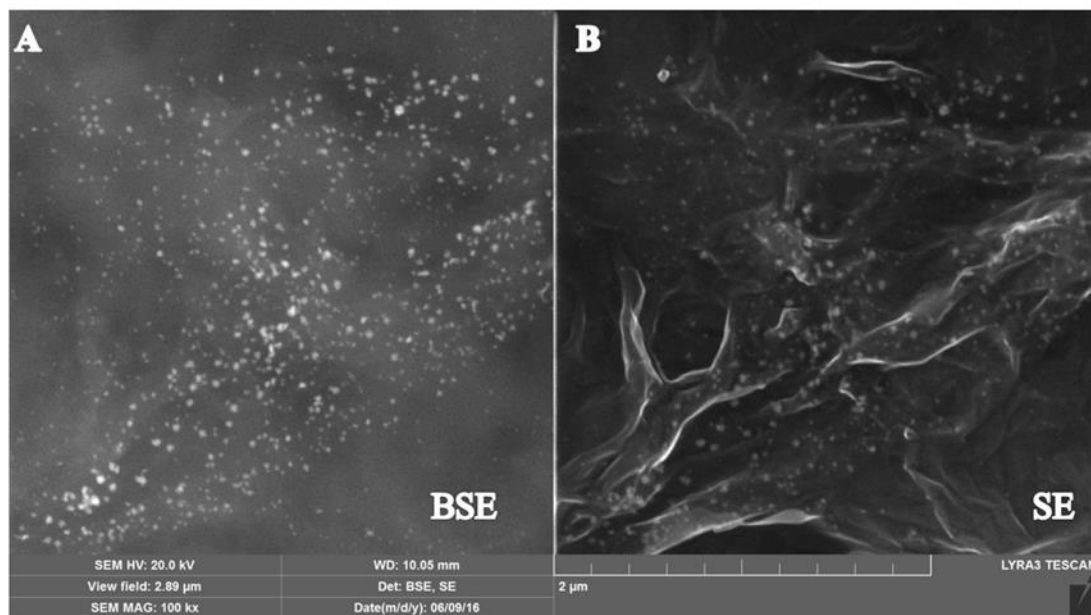


Figure 4- 4: FE-SEM image of GR/Pt/GR/GPE by using (A) back scattering electron beam (BSE) and (B) secondary electron beam (SE)

4.3.3 Scan Rate Study

The effect of scan rate of the cyclic voltammetry was also investigated on the fabricated sensors GR/GPE and GR/Pt/GR/GPE. The scan rate study was done by scanning the cyclic voltammetry on 0.2 mM dopamine in 0.1 M PBS buffer (pH 5.5). The different scan rates have shown a significant effect on the peak current of the dopamine (Fig. 4- 5 A and B). The ESA was calculated for the GR/GPE, and the Pt NPs sandwiched reduced graphene oxide sensor by using the Randles-Sevcik equation 1 [261]:

$$I_p = 2.69 \times 10^5 v^{1/2} n^{3/2} C D^{1/2} A \quad \mathbf{1}$$

The ESA was calculated for bare and modified electrode GR/GPE and GR/Pt/GR/GPE by scanning the CVs from 50 to 250 mV/s. The electroactive surface area was found 0.063 cm², 0.66 cm² and 0.81 cm² for bare GPE, GR/GPE and the GR/Pt/GR/GPE. The dopamine diffusion coefficient value was used 5.40 x 10⁻⁶ cm²s⁻¹ [267]. The huge electroactive surface area was observed for GR/GPE, and GR/Pt/GR/GPE compared bare GPE. The graphene layers have been effectively generated on the surface of the GPE by electrochemical reduction of the GO and significantly enhanced the electroactive surface area. The sandwiched Pt NPs in graphene layers further enhanced the electroactive surface area for dopamine. It is indicated the Pt NPs successfully embedded in graphene layers which were clear from the SEM images.

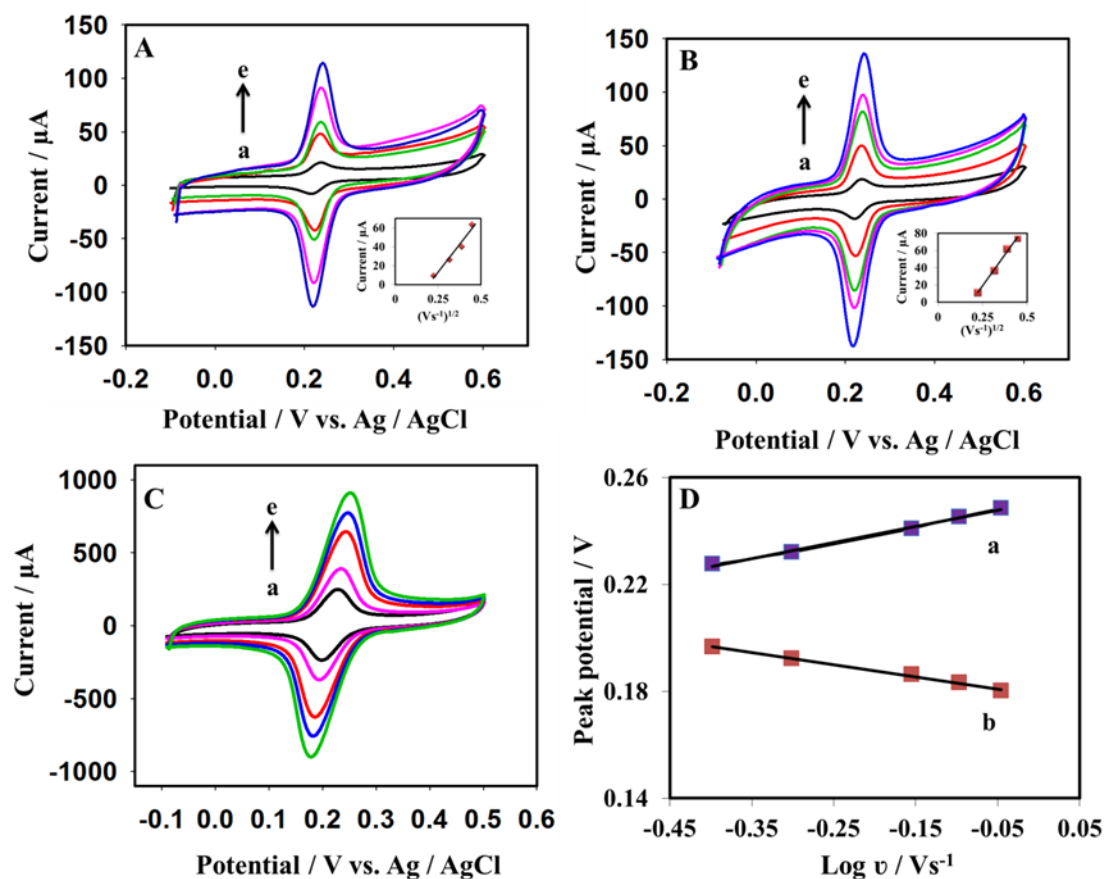


Figure 4- 5: Cyclic Voltammograms obtained from solution containing 0.2 mM dopamine in PBS buffer (0.1M, pH 5.5) using (A) GR/GPE and (B) GR/Pt/GR/GPE at scan rates of (a) 50, (b) 100, (c) 150, (d) 200 , (e) 250 mV/s. The insets in (A) and (B) shows the linear relationship between current and the square root of scan rates. (C) The cyclic voltammograms of 0.2 mM dopamine using GR/GPE at higher scan rate (a) 400, (b) 500, (c) 700, (d) 800, and (e) 900 mV/s. (D) The linear relationship between $\text{Log } v$ vs. (a) anodic and (b) cathodic peak potential obtained by cyclic voltammograms from 400 to 900 mV/s.

Further study for the GR/Pt/GR/GPE has shown at higher scan rate from 0.4 to 0.9 V; the linear relationship was obtained between peak potential shift and the logarithm of the scan rate (Log ν) for dopamine. In Fig. 4- 5 C, the positive and the negative peak shift could be observed for the anodic and the cathodic peak potential. Two straight line equations 2 and 3 were yielded for the anodic and the cathodic peak potentials, respectively:

$$E_{pa} \text{ (V)} = 0.0603 \log \nu + 0.2508 \quad (R^2 = 0.9945) \quad \mathbf{2}$$

$$E_{pc} \text{ (V)} = - 0.0453 \log \nu + 0.1786 \quad (R^2 = 0.9957) \quad \mathbf{3}$$

The slope of the anodic and the cathodic peak potential according to the Laviron's theory [28] are $2.3 RT/(1-\alpha)nF$ and $-2.3 RT/\alpha nF$, respectively. In slopes, α represents the charge transfer coefficient and its value was found using the following equation:

$$\log k_a/k_c = \log \alpha/1-\alpha \quad \mathbf{4}$$

The value of α calculated by using equation 4 was 0.57. Similarly, the value of k_s was found using another Laviron's [270] equation 5.

$$\log k_s = \alpha \log (1-\alpha) + (1-\alpha) \log \alpha - \log (RT/nF\nu) - \alpha (1-\alpha)nF\Delta E_p/2.3RT \quad \mathbf{5}$$

The value of k_s was found $8.99 \text{ s}^{-1} \pm 0.40$. The value of k_s is higher compared previously reported works 1.59 s^{-1} [297], 2.09 s^{-1} [298], and 1.63 s^{-1} [299]. The higher values of k_s of the sandwiched Pt NPs graphene layered modified GPE is indicated the fast charge transfer for the electrochemical reaction of dopamine.

Moreover, the surface coverage (Γ) [300] was calculated for dopamine by using equation 6 on the electrode surface of GR/GPE or GR/Pt/GR/GPE:

$$\Gamma = I_p 4RT/ n^2F^2Av \quad \mathbf{6}$$

The surface coverage was calculated for 1 mM dopamine for GR/GPE and the GR/Pt/GR/GPE. The surface coverage for GR/GPE and the GR/Pt/GR/GPE was found 7.107×10^{-10} and 8.909×10^{-10} . The bare GPE surface coverage was found 4.721×10^{-14} mol cm^{-2} . The huge increase in surface area coverage for GR/GPE compared bare surface was indicated the graphene has increased the electrode surface area. The surface coverage of the GPE was further improved by the Pt NPs sandwiched graphene layers.

4.3.4 pH Study of the Electrolyte

The pH effect was explored by using CV by varying the pH of the sensing medium from 5.0 to 7.5. The effect was analyzed for 0.5 mM DA in 0.1 M PBS buffer. The current variations were observed for dopamine with the changing of pH. It was increased as the pH increased from 5.0 to 5.5 and then continuously decreased as the pH is increased (Fig. 4- 6). Moreover, a negative peak shift observed with increasing pH which is indicated the protons are involved in the electrochemical reaction of DA on the electrode surface. It was also noted that at a lower pH from 5.5 the current was suddenly decreased, and peak broadness was also observed. A linear relation was found between pH and the peak potential. The slope was found - 57.5 mV/pH ($R^2 = 0.9918$) for pH 5.5 to 7.5 and - 63.2 mV/pH from pH 5.0 ($R^2 = 0.9855$) because at pH lower than 5.5 the peak became broad.

$$E \text{ vs. Ag/AgCl} = 579.3 - 57.5[\text{pH}] \quad (R^2 = 0.9918) \quad 7$$

The slope -57.5 mV/pH is very close to the theoretical slope -59 mV/pH (Eq. 7). It is revealed the same number of protons and electrons were taking part in the DA electrochemical reaction on the surface of GR/Pt/GR/GPE.

4.3.5 Optimization of Sensing Technique

Among the voltammetric technique, the SWV was found more sensitive for the sensing of dopamine, and it was selected for dopamine detection in the samples. The sensitivity of the developed sensor was tried to enhance by optimizing the various parameters of the SWV technique. First of all the amplitude was optimized, it was varied from 0.02 to 0.08 V for 20 μM dopamine in PBS (0.1 M, pH 5.5) (Fig. 4- 7A). The amplitude has shown significant impact on the peak current and maximum response was observed at 0.06 V and decreased with further increase. Similarly, the frequency was optimized from 20 to 90 Hz, and best response was observed at 80 Hz (Fig. 4- 7B). Frequency and adsorption time was optimized by using 10 μM dopamine in PBS buffer. The adsorption time has shown a significant effect on the peak current which is indicated the GR/Pt/GR/GPE has excellent capability of the adsorption of the dopamine. The current was increased sharply as the adsorption time and became almost constant after 120 s (Fig. 4- 7C). The optimized parameters were used for further study.

4.3.6 Detection of Dopamine, Reproducibility, and Limit of Detection

The various concentration of dopamine in the 0.1 M PBS buffer at pH 5.5 was detected by using the SWV optimized conditions including 0.06 V amplitude, 80 Hz frequency and 120 s adsorption times. The developed GR/Pt/GR/GPE was found very sensitive towards dopamine. The linear range was observed from 0.06 to 20 μM . A linear equation was yielded by the calibration curve: $I \text{ (mA)} = 0.2191 C_{\text{DA}} \text{ (}\mu\text{M)} + 0.0303$ with regression constant (R^2) 0.9991 (Fig. 4- 8).

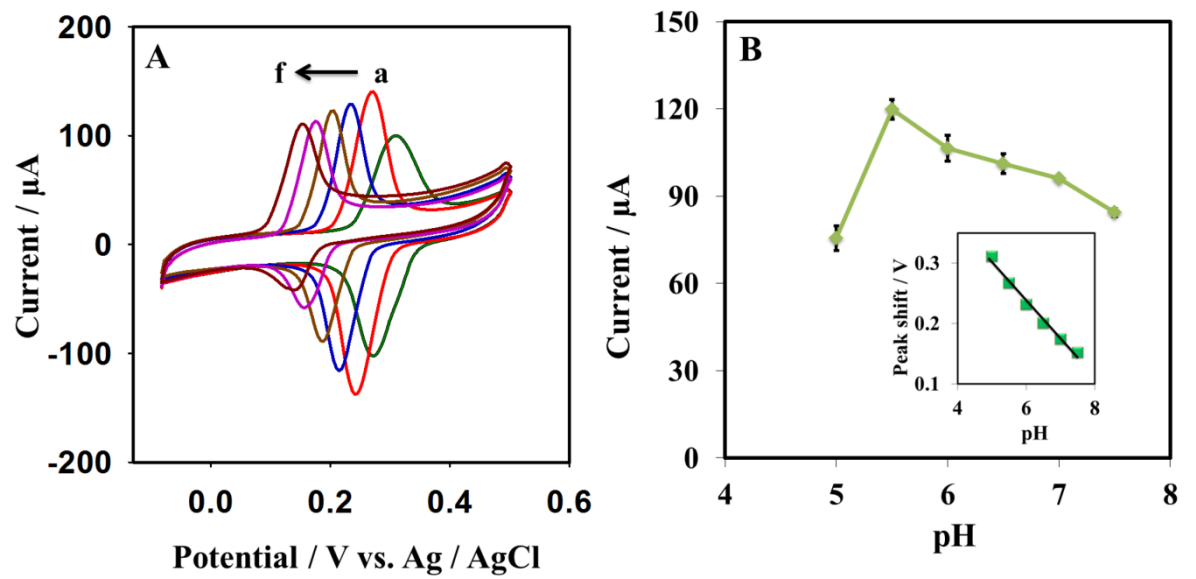


Figure 4- 6: (A) CVs obtained from solution containing 0.5 mM dopamine in 0.1 M PBS solution at various pH values (a) 5.0, (b) 5.5, (c) 6.0, (d) 6.5, (e) 7.0, (f) 7.5 pH at GR/Pt/GR/GPE. (B) Graphical representation of the peak current vs. pH for dopamine. Inset is showing the relationship between the pH and the oxidation peak potential.

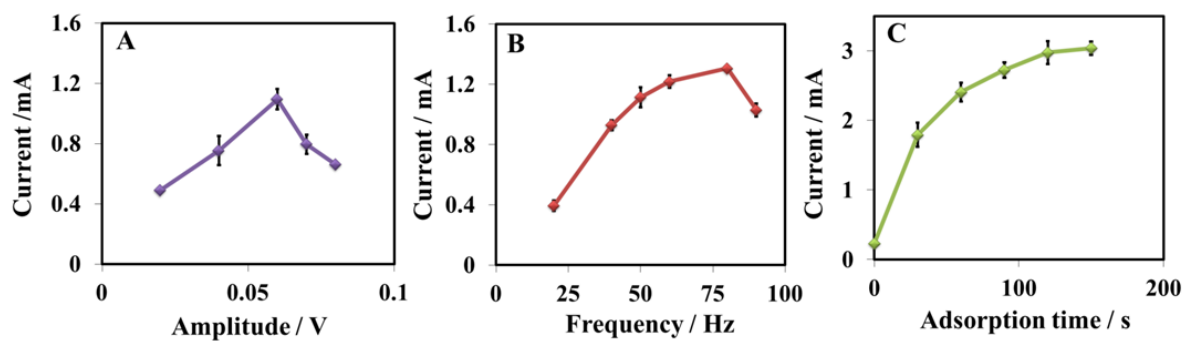


Figure 4- 7: Plots of the oxidation peak current of SWV vs. amplitude (A), frequency (B) collected at 20 μM and 10 μM dopamine, respectively (10 s adsorption time) and adsorption time (C) for 10 μM dopamine obtained from the SWVs in a PBS buffer (0.1 M, 5.5 pH)

A very low limit of quantification and detection was obtained 0.06 and 0.009 μM which indicated the biocompatibility of the Pt NPs sandwiched graphene layered sensor for the dopamine. Its sensitivity is much better or comparable with the previously reported work (Table 4- 1). It could be a promising candidate for the low-level sensing of dopamine.

The reproducibility of the sensor was evaluated by fabricating the five GR/Pt/GR/GPE sensors under the same set of conditions for the sensing of dopamine. The small current variation was observed, and the RSD of the fabricated sensor was found 5.49 %. The RSD value suggested that developed sensor reproducibility was quite satisfactory.

4.3.7 Real Sample Analysis and the Interferences Study

The GR/Pt/GR/GPE sensor was used for the sensing of DA in the real samples. The sensor was applied in the human urine sample. The dopamine was absent in the urine sample, and then the various concentration of dopamine was spiked 3, 5, 6 and 7 μM . The satisfactory recoveries were obtained in the range of 90.0 to 105% (Table. 4- 2). The response of the dopamine was also evaluated in the presence of higher concentration of 0.5 mM AA; the small current variation ± 3.80 was observed for 5 μM dopamine. The ten times greater concentration of the other interferences like alanine, adenine, glucose, l-methionine, and some ionic species Na^+ , K^+ , Ca^{+2} , Co^{+2} , and Cl^- has shown current variation in the range of ± 0.53 to $\pm 9.38\%$. The good recoveries and small current changes in the presence of interferences have shown the quite good accuracy of the sensor.

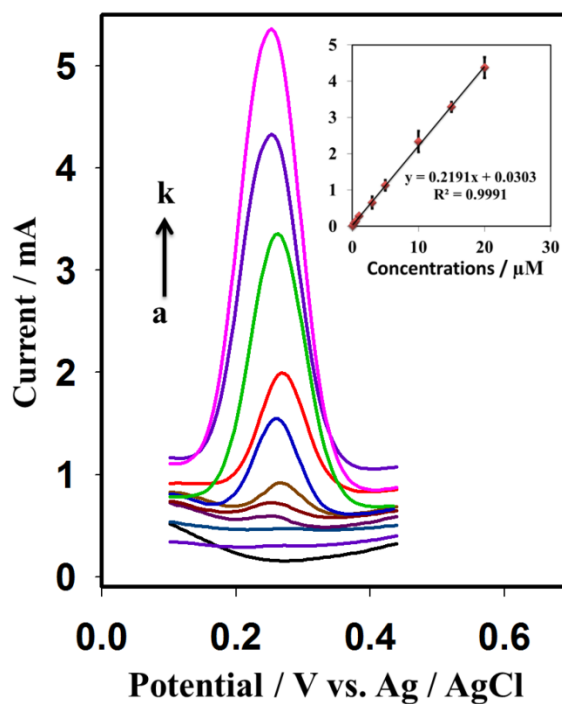


Figure 4- 8: SWVs of various concentration of dopamine in PBS buffer (0.1 M, pH 5.5) at (a) 0, (b) 0.06, (c) 0.08, (d) 0.3, (e) 0.5, (f) 1, (g) 3, (h) 5, (i) 10, (j) 15, (k) 20 μM . The inset shows the linear relationship between I (μA) and concentration. SWV parameters: amplitude 0.06 V, frequency 80 Hz and adsorption time 120s.

Table 4- 1: Comparison of the GR/Pt/GR/GPE with the reported graphene nanocomposite modified sensors

Sr#	Electrodes	Technique	Medium/pH	LOQ (μM)	LOD (μM)	Application	Ref.
1	GS@Mn ₃ O ₄ /Nf/GCE	Amperometry	0.1 M PB/4.5	1	0.08	Injection	[301]
2	PILs/PPy/GO/GCE	DPV	0.05 M PB/4.0	4	0.0733	NA	[302]
3	NiO-CuO/GR/GCE	SWV	0.1 M PB/8.0	0.5	0.167	Blood serum	[291]
4	N-G/NiTsPc/GCE	Amperometry	PB/7.4	0.1	0.1	NA	[303]
5	rGO-Cu ₂ O/GCE	DPV	0.1 M PBS/7.0	10	0.05	Human urine, blood	[292]
6	Fe ₃ O ₄ - NH ₂ @GS/GCE	DPV	0.1 M PB/7.0	0.2	0.126	Injection	[146]
7	GR-SnO ₂ /CILE	DPV	0.1 M PBS/6.0	0.5	0.13	Injection	[272]
8	Trp-GR/GCE	DPV	0.1 M PBS/7.0	0.5	0.29	Urine, serum, Injection	[160]
9	GR/GPE	DPV	0.01 M PBS/7.4	4	2.64		[249]
10	AgNW/rGO/SPCEs	LSV	0.1 M PB/7.4	40	0.26	NA	[304]
11	MgO/Gr/Ta	DPV	0.1 M PB/5.0	0.1	0.15	Human serum	[157]
12	CoTPP-CRGO/GCE	DPV	0.1 M PB/6.5	0.1	0.03	Urine, serum	[293]
13	mp-GR/GCE	DPV	0.1 M PB/6.5	4	1.5	Human serum	[276]
14	RGO-P5A/GCE	DPV	0.2 M HAc- NaAc/4.0	1	0.2	NA	[305]
15	Pd ₃ Pt ₁ /PDDA- RGO/GCE	DPV	0.1 M PB/7.4	4	0.04	Human urine, serum	[144]
16	Pt/RGO/GCE	DPV	0.1 M P/7.0	10	0.25	NA	[296]
17	GR/Pt/GR/GPE	SWV	PBS/5.5	0.06	0.009	Human urine	This work

Table 4- 2: Determination of DA in the human urine sample

Sr #	Found (μM)	Added (μM)	Recovered (μM)	% recovery
1	0	3	2.96	98.6
2	0	5	4.50	90.0
3	0	6	6.31	105
4	0	7	6.77	96.7

CHAPTER 5

A Cost-effective Disposable Graphene-modified Electrode Decorated with Alternating Layers of Au NPs for the Simultaneous Detection of Dopamine and Uric Acid in Human Urine

5.1 Introduction

Dopamine and uric acid are crucial biomolecules that normally co-occur in physiological fluids such as urine and serum [212]. Abnormal levels of DA and UA in the body could lead to numerous fatal diseases. The simultaneous detection of DA and UA is critical to characterizing the health condition of an individual. Dopamine belongs to the catecholamine family and acts as a vital neurotransmitter in the CNS [159, 306]. Dopamine also plays a major role in the hormonal and cardiovascular systems [307]. Abnormal dopamine levels in the body could cause serious conditions, including Parkinson's disease, schizophrenia, restless leg syndrome (RLS), and ADHD [126]. Uric acid is an important biomarker and is produced in the body by purine metabolism [207]. Abnormal levels of uric acid in the body could cause gout, hyperuricemia, and Lesch–Nyhan syndrome [176]. The extraordinary importance of dopamine and uric acid in the body underscores the importance of developing sensitive and reliable methods for their detection.

Several sensitive dopamine and uric acid detection approaches have been developed. Electrochemical methods are attractive over alternative methods due to their sensitivity, selectivity, rapid sensing capabilities, simple operation, and low cost [161]. The individual or concurrent detection of DA and UA using conventional electrodes has been difficult due to their electrochemical oxidation poor kinetics and overlapping oxidation potentials [133]. Conventional electrodes could not be used directly for the concurrent detection of DA and UA. The selectivity and sensitivity of the bare electrode surfaces may be improved using a variety of methods to overcome the overlapping oxidation potentials of dopamine and uric acid [181]. The literature describes the use of several

modified and complex materials for the simultaneous detection of dopamine and uric acid. Modified electrodes, such as NiCo-NPs-in-N/C modified GCE [33], PL-LEU/DNA/GCE [184], ZnO-Cu_xO-PPy/GCE [187], NiCo₂O₄/Nano-ZSM-5/GCE [308], and GNPs/PI_{max}/GCE [309] have been used for simultaneous detection.

Graphene has recently attracted attention for its extraordinary mechanical strength, high surface area, and electrical and thermal conductivity [241]. The interesting properties of graphene have inspired widespread exploration in the field of transparent conductors, energy storage devices, field emission displays, and chemical and biological sensing [25]. Graphene is potentially useful for the fabrication of electrochemical sensors due to its engagement in rapid electron transfer, its small charge transfer resistance, its large potential window, and its huge electroactive surface area [26]. Graphene-based sensors, including CTAB/rGO/ZnS/GCE [155], CTAB-GO/MWNT/GCE [310], and Pd₃Pt₁/PDDA-RGO/GCE, have been introduced for the concurrent detection of DA and UA. The electrocatalytic activity, biocompatibility, and excellent conductivity [281] of Au NPs have been combined with graphene to enhance the sensitivity and selectivity of electrodes. Previously studies of layered graphene and Au NP assemblies (GE/Au/GE/CFE) have fabricated these assemblies on carbon fiber electrodes. The sensitivity of this electrode was not very good. The limits of detection obtained from the GE/Au/GE/CFE assembly were 0.59 μM for dopamine and 12.6 μM for uric acid [311]. Wang et al. [161] fabricated an Au/RGO/GCE to improve the sensitivity of uric acid detection (1.8 μM), although this electrode's response to dopamine remained poor (1.4 μM). The uric acid-dopamine peak separation was 110 mV, less than that reported elsewhere. None of the aforementioned electrodes were disposable in the context of

dopamine and uric acid sensing. In most cases, complex steps were involved in fabricating the sensitive electrodes, and rendering the surfaces reusable remained a significant challenge. Dopamine easily fouled the surface, even after a single measurement. Regenerating the surface for a second measurement proved to be difficult.

In this work, we fabricated a disposable graphene nanocomposite electrode. Alternating Au NP and graphene layers were formed on a GPE surface through the direct electrochemical reduction of Au (III) or graphene oxide solutions. The fabrication of this arrangement provided a good electroactive surface area for the electrochemical reaction and was more facile and rapid compared to the casting methods commonly used to modify electrodes. We obtained significant peak separation and a low limit of detection compared to previous studies of Au and graphene for the concurrent detection of DA and UA. After each sensing measurement, the electrode surface could be renewed. To the best of our knowledge, this work constitutes the first attempt at fabricating a disposable electrode based on alternating Au NPs and graphene layers on a GPE surface for the concurrent detection of DA and UA. A low-cost single-use electrode, such as the GPE, provides a good alternative to the widely used GCE and CPE.

5.2 Materials and Methods

5.2.1 Reagents

Hydrogen tetrachloroaurate(III) hydrate was purchased from Sigma-Aldrich (USA). The rest of the chemicals are same as stated in 3.2.1 subsection.

5.2.2 Apparatus

The instrumentation and apparatus are same as stated in 3.2.2 subsection.

5.2.3 Fabrication of GR/Au/GR/Au/GPE Sensor

The optimized conditions for the modification material were used for the fabrication of the electrode for the simultaneous recognition of DA and UA. The graphene oxide modification conditions were already discussed in detail.[24] The 0.5 mM HAuCl₄ was prepared in 0.1M KNO₃ solution. The graphene oxide (4 mg/mL) was dispersed by sonicating in 0.1 M acetate buffer. The alternative layers of Au NPs were formed on the GPE surface by the electrochemical reduction of Au (III) by cyclic potential swept from -0.4 to 0.3 V at a scan rate of 10 mV over 1 cycle. After each Au NPs layer, the graphene layer was formed by the electrochemical reduction of graphene oxide by cyclic potential sweeping from -1.4 to 0.3 V over 1 cycle. After every layer, the modified electrode was washed gently three times by simply dipping in the double distilled water. The modified electrode was represented as GR/Au/GR/Au/GPE.

5.3 Results and Discussion

5.3.1 Characterization of the Synthesized Graphene Oxide

The characterization of synthesized graphene oxide was same as stated in sub section 3.3.1.

5.3.2 Optimization of the Conditions for Fabrication of a Sensitive Sensor

The sensitivity of the electrode was enhanced by optimizing the graphene and Au NP fabrication conditions from graphene oxide and HAuCl_4 , respectively. The optimal graphene conditions for preparing the GPE have been reported previously [66]. The concentration of HAuCl_4 was optimized over the range 0.05 to 1.5 mM. A maximum response was obtained at 0.5 mM (Fig. 5- 1). The optimal scan rate for the electrochemical reduction of Au^{+3} onto the GPE surface to form Au NPs was found to be 0.01 V/s (Fig. 5- 2). Different scan windows were analyzed, and a better response to dopamine and uric acid was observed using a CV scan window of -0.4 to 0.3 V for Au NPs formation on the electrode surface (Fig. 5- 3). A variety of electrolytes were analyzed, and KNO_3 was found to be effective for the incorporation of Au NPs onto the electrode surface (Fig. 5- 4).

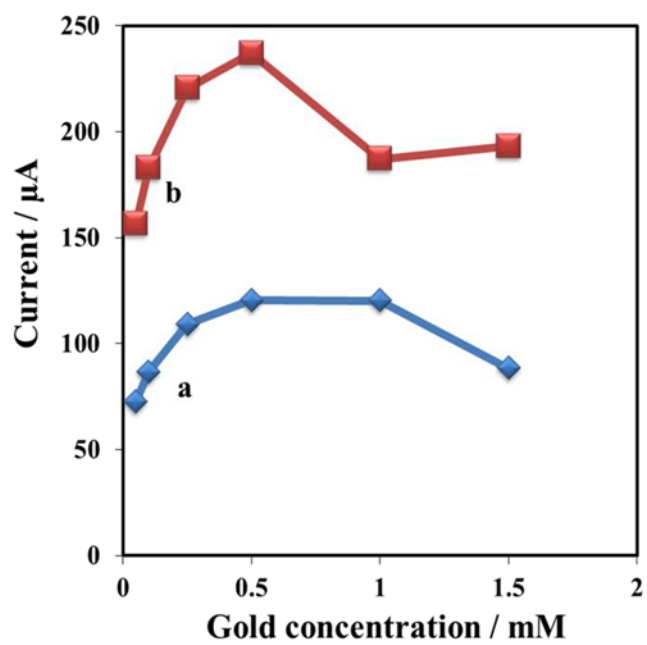


Figure 5- 1: The CVs oxidation peak current response for 0.5 mM dopamine (a) and uric acid (b) in 0.1 mM PBS at various concentration of HAuCl_4 .

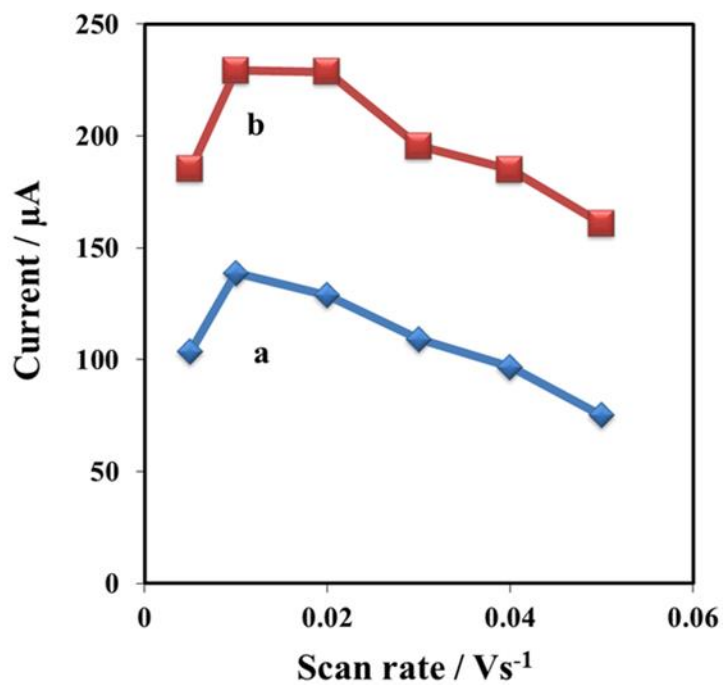


Figure 5- 2: The CVs oxidation peak current response for 0.5mM dopamine (a) and uric acid (b) in 0.1 mM PBS at various scan rate for the reduction of Au⁺³ on the electrode surface for Au NPs formation.

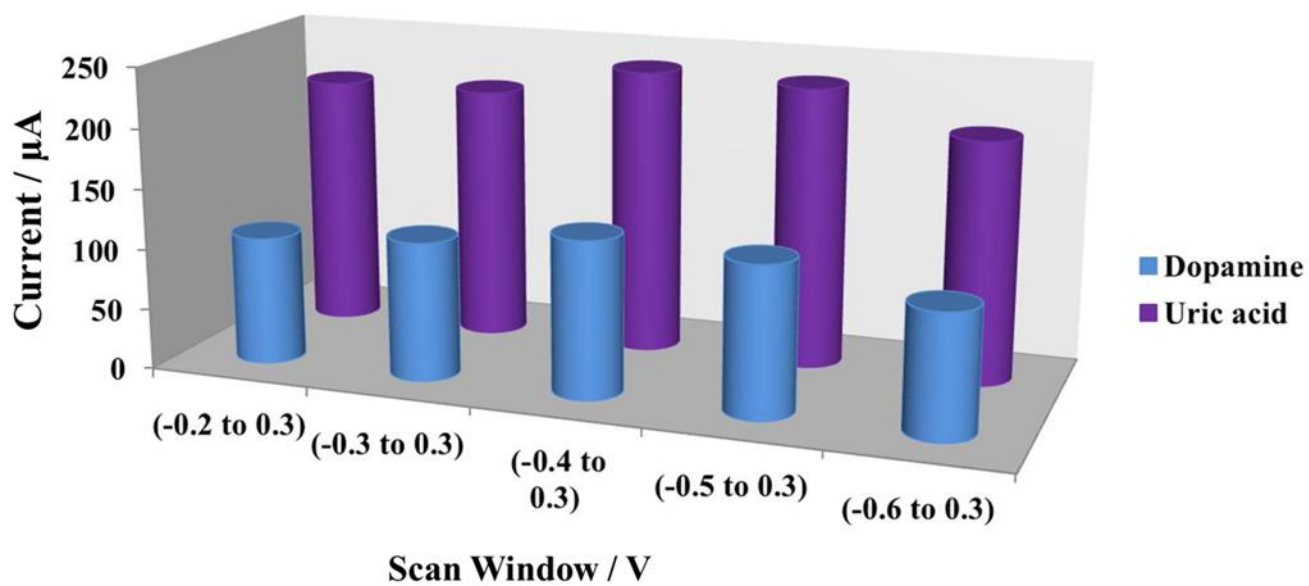


Figure 5- 3: The Scan window optimization for reduction of Au^{+3} for 0.5mM dopamine and uric acid in 0.1mM PBS

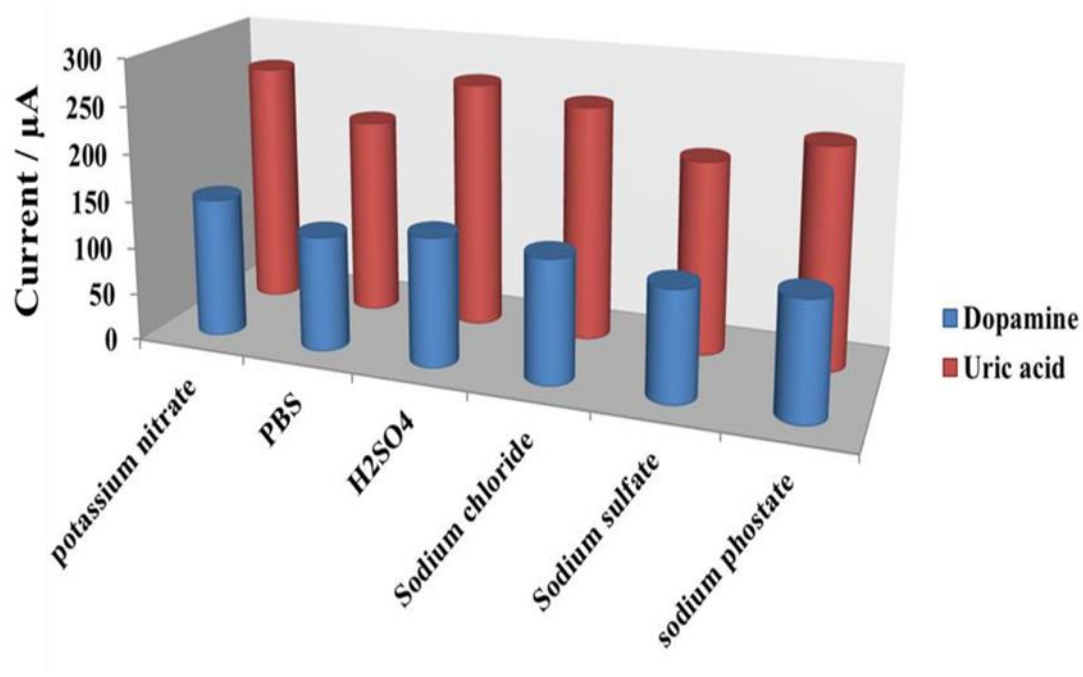


Figure 5- 4: The different electrolyte behavior for Au^{+3} reductions on GPE surface for 0.5 mM dopamine and uric acid in 0.1 mM PBS

5.3.3 Combination of Au NPs and Graphene Layers Patterned onto the Electrode Surface and Stepwise Morphological Characterization of the Sensing Surface

The layer arrangements on the GPE surface were characterized by miniaturizing a variety of Au NPs and graphene patterns on the GPE surface. CV scans were collected in the presence of a 0.2 mM dopamine and uric acid solution in 0.1 M PBS using different electrodes with a variety of layer combinations. An analysis of the different layers revealed that the sensor was more efficient for the concurrent detection of DA and UA if graphene comprised the outer layer and the Au NPs formed an inner layer on the electrode surface. Two combinations were found to provide the best responses: a sandwich scheme, in which the Au NPs formed an inner layer and the graphene formed an outer layer, GR/Au/GR/GPE (Fig. 5- 5), and alternating Au and graphene layers, in which the Au NPs were deposited as the first layer, GR/Au/GR/Au/GPE (Fig. 5- 5A). The GR/Au/GR/Au/GPE was selected for further study due to its slightly better response compared to GR/Au/GR/GPE. The various steps involved in fabricating the sensitive electrodes for the simultaneous measurement of dopamine and uric acid are presented in Scheme 1. The greater efficiency of the sensors fabricated with an outer graphene layer may have resulted from attractive forces between graphene and the dopamine and uric acid molecules.

The surface morphologies during GPE layer formation surface were analyzed in a stepwise fashion using field emission scanning electron microscopy. The graphene-modified electrode was fabricated on the GPE surface by reducing GO (4 mg/mL) under two cyclic voltammetry scans from -1.4 to 0.3 V.

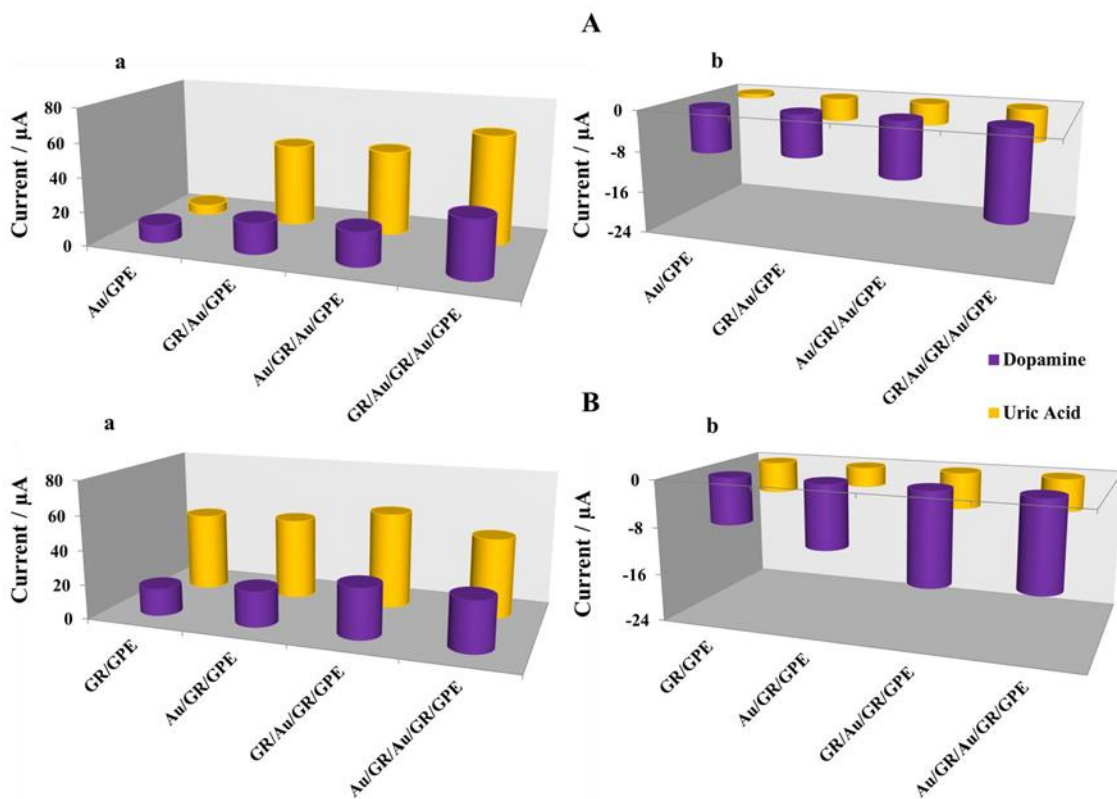
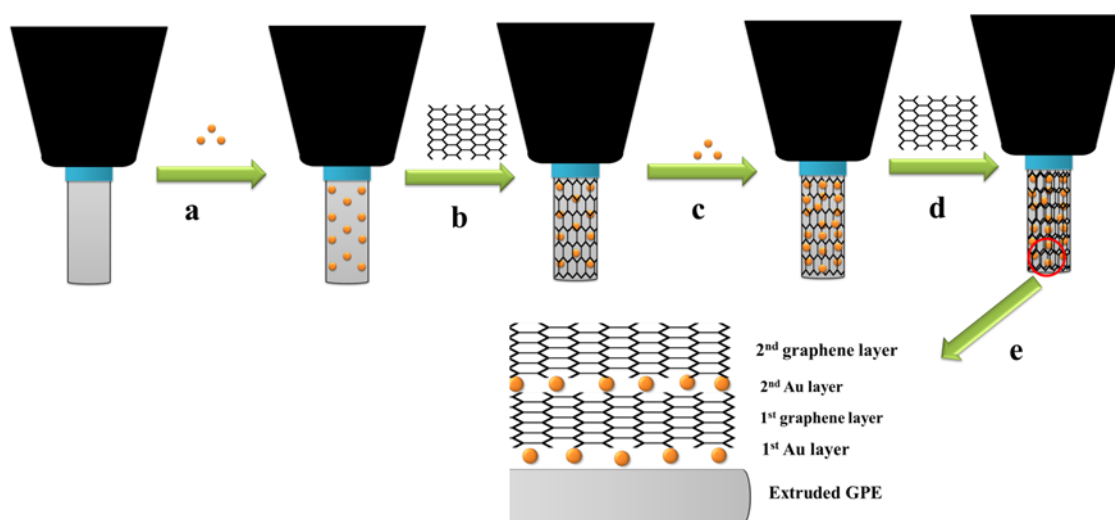


Figure 5- 5: Oxidizing (a) and reducing peak currents (b) obtained during collection of the 0.2 mM dopamine and uric acid cyclic voltammograms, for a starting layer of the Au NPs (A) or graphene (B) on the GPE surface



Scheme 1: Schematic representation of the stepwise fabrication of modified electrode: the electrochemical formation of Au NPs on GPE (a), formation of graphene layer on Au/GPE (b), second layer of Au on GR/Au/GPE (c), outer layer of GR on Au/GR/Au/GPE (d), and separate layer arrangements on the GPE surface (e).

The SEM images clearly revealed the formation of wrinkle-shaped graphene layers on the GPE surface (Fig. 5- 6b). No such layers were present on the bare GPE surface (Fig. 5- 6a). Stepwise SEM images of the surface were compared to reveal the morphological changes after each step fabrication process.

The first layer of Au NPs was deposited onto the GPE surface using a CV scan between – 0.4 and 0.3 V over 1 cycle. Well-distributed Au NPs were observed in the SEM image (Fig. 5- 7a). In the second electrode modification step, the graphene layer was formed by reducing GO, and the SEM images clearly revealed the presence of Au NPs beneath the graphene layer (Fig. 5- 7b). The second Au NPs layer was embedded in the first graphene layer (Fig. 5- 7c). Finally, the wrinkled and crumpled shape of the second graphene layer was formed by GO reduction (Fig. 5- 7d). The presence of Au NPs on the surface of the final modified electrode was confirmed by energy dispersive X-ray spectroscopy mapping. The spectrum confirmed the presence of Au on the GPE surface (Fig. 5- 8).

5.3.4 Electrochemical and Kinetics Study of the Modified Electrode

The CV scan rate effects were examined for the bare, GR/GPE, and GR/Au/GR/Au/GPE in the presence of a 5 mM $\text{K}_3\text{Fe}(\text{CN})_6/\text{K}_4\text{Fe}(\text{CN})_6$ solution in 0.1 M KCl. The scan rate was varied over the range 20 to 100 mVs^{-1} for the $\text{K}_3\text{Fe}(\text{CN})_6/\text{K}_4\text{Fe}(\text{CN})_6$ solution (Fig. 5- 9) and over the range 50 to 350 mVs^{-1} for the 0.2 mM uric acid and 1 mM dopamine solution (Fig. 5- 10).

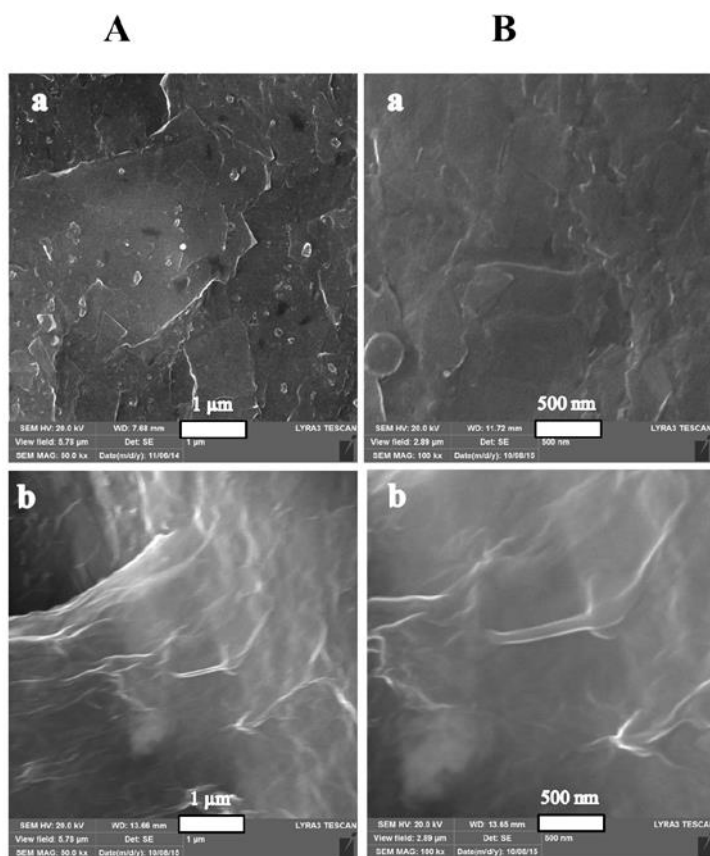


Figure 5- 6: FE-SEM images of the bare (a) and GR-GPE (b) at 1 μm (A) and 500 nm (B).

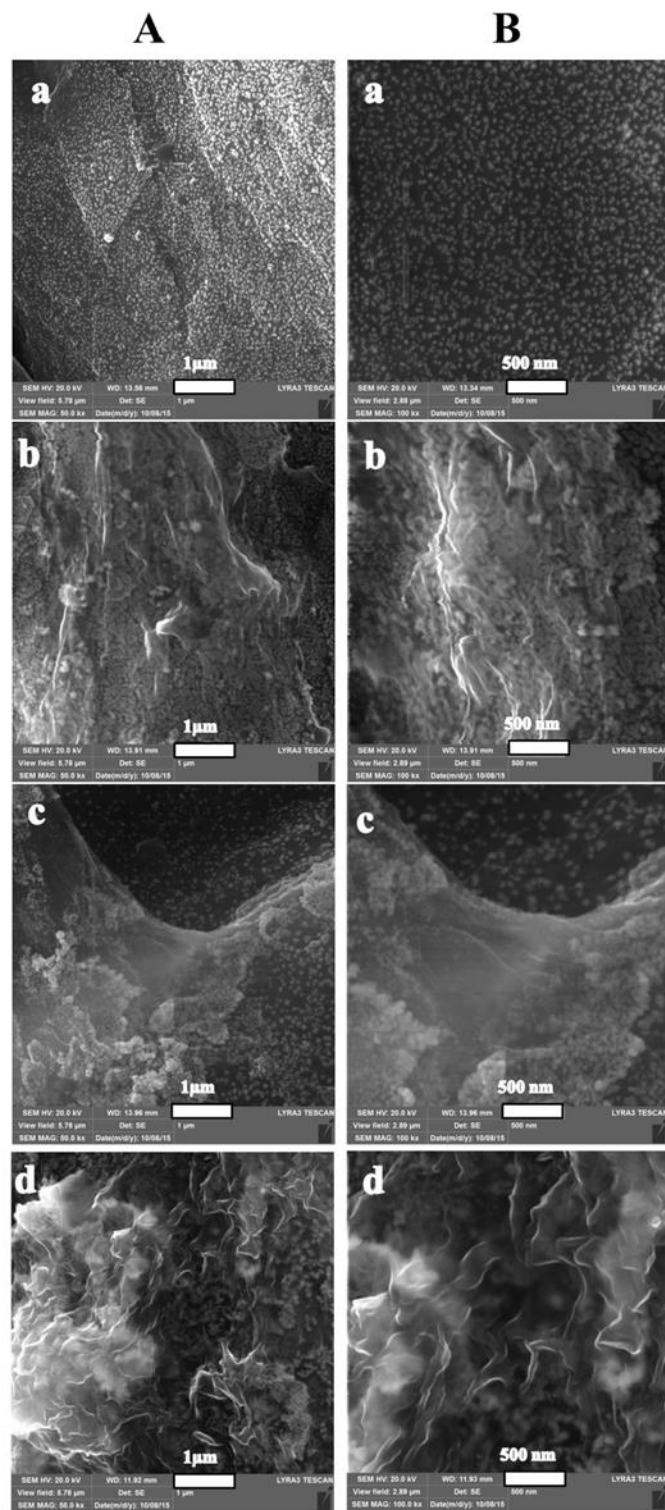


Figure 5- 7: FE-SEM images collected at two magnification values: 1 μm (A) or 500 nm (B), for the Au/GPE (a), GR/Au/GPE (b), Au/GR/Au/GPE (c), and GR/Au/GR/Au/GPE (d).

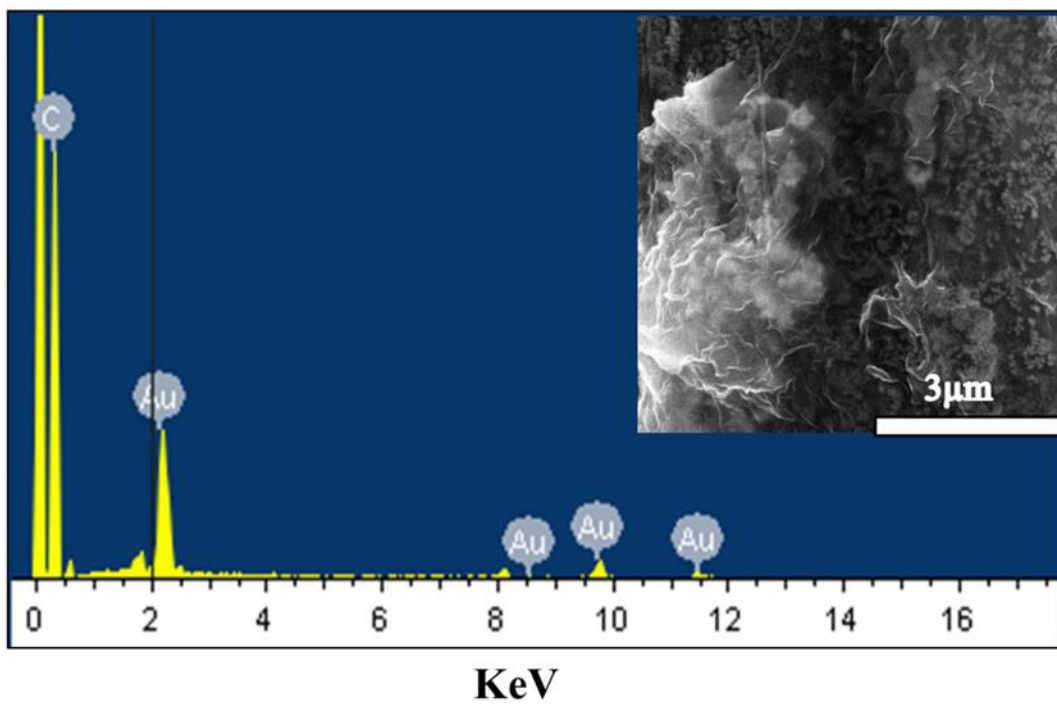


Figure 5- 8: EDX spectrum obtained from the GR/Au/GR/Au/GPE electrode.

The current increased as the scan rate increased. A linear relationship was observed between the square root of the scan rate and the peak current. At higher scan rates, the response of the bare electrode was not good compared to the modified electrodes. This result suggested that higher scan rates required the electrochemical reaction to reach completion in a shorter period of time, and the bare electrode surface could not support the fast charge transfer as well as the modified electrodes. The ESA was calculated for the bare, GR/GPE, and GR/Au/GR/Au/GPE electrodes using the Randles–Sevcik equation

$$I_p = 2.69 \times 10^5 \gamma^{1/2} D^{1/2} n^{3/2} C A, \quad 1$$

The ESA was calculated using a 5 mM $K_3Fe(CN)_6/K_4Fe(CN)_6$ solution in 0.1 M KCl for the bare, GR/GPE, and GR/Au/GR/Au/GPE. The graphene layer was found to be very effective at increasing the electroactive surface area. The electroactive surface area was further improved by the graphene and Au NPs layer arrangement on the GPE surface. The electroactive surface areas were 0.066 cm², 0.376 cm², and 0.518 cm² for the bare, GR/GPE, and GR/Au/GR/Au/GPE, respectively. The electroactive surface areas of the modified electrodes were also calculated for the 0.2 mM uric acid and 1 mM dopamine solutions in 0.1 M PBS buffer. The electroactive surface areas obtained for uric acid were 0.948 cm² and 1.21 cm², and those obtained for dopamine were 0.668 cm² and 0.7718 cm² on GR/GPE and GR/Au/GR/Au/GPE, respectively (Fig. 5- 10). The surface area study revealed that graphene efficiently increased the surface area, which was further improved by the alternating layers of graphene and Au NPs on the electrode surface.

The interfacial characteristics of the bare and the modified electrodes were further characterized by EIS. Figure 5- 9 D presents the EIS spectra of the bare GPE, Au/GPE, GR/GPE, and GR/Au/GR/Au/GPE. A large semicircle was observed in the case of the bare GPE. The large semicircle indicated a high interfacial resistance of approximately 2500 Ω . The Au NPs on the GPE surface effectively reduced the interfacial resistance to 18 Ω . The low resistance of the Au NPs significantly improved the conductance of the GPE. The graphene and Au NP combination yielded a fairly straight line in the EIS spectrum. The same was observed for the graphene-modified electrode, indicating that the graphene–Au NPs combination nearly overcame the charge transfer resistance.

The electrochemical properties of the various pencil graphite electrode surfaces were further investigated by recording the CVs in the presence of 0.5 mM DA and UA solutions in 0.1 M PBS. The response of the bare surface (Fig. 5-11a) during simultaneous detection was not sensitive at all. The dopamine and uric acid peak separation were very poor and insufficient for use in simultaneous sensing. The Au NPs on the GPE surface improved the sensitivity and peak separation slightly. The graphene layers (Fig. 5- 11c) provided significantly better peak separation and sensitivity. Furthermore, the alternating arrangements of Au NPs and graphene layers (Fig. 5- 11d) considerably enhanced the current compared to the bare GPE, Au NPs/GPE, and GR/GPE.

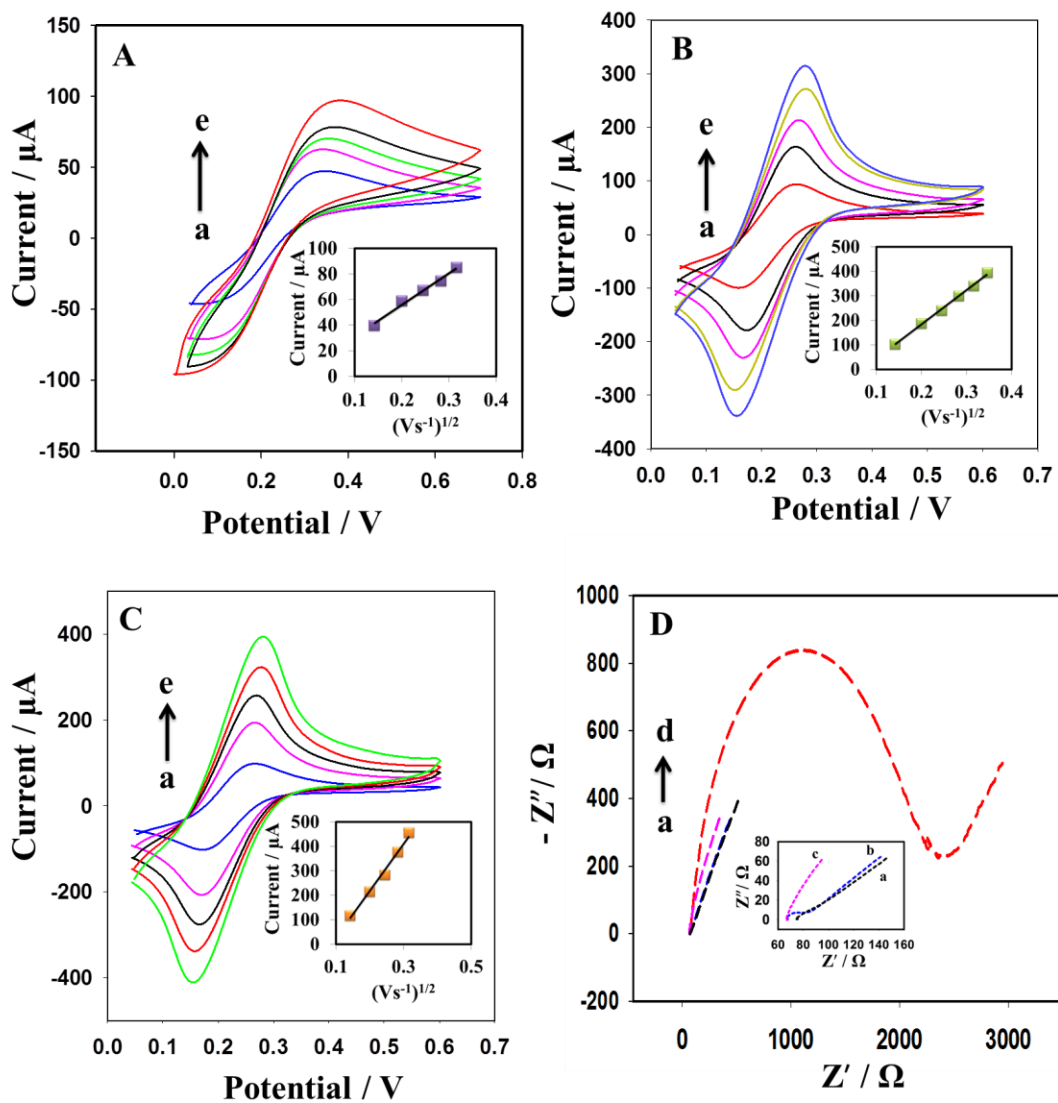


Figure 5- 9: Cyclic voltammograms obtained from a solution comprising 5 mM $\text{K}_3\text{Fe}(\text{CN})_6/\text{K}_4\text{Fe}(\text{CN})_6$ and 0.1 M KCl, using (A) the bare GPE, (B) GR/GPE, and (C) GR/Au/GR/Au/GPE at scan rates of (a) 20, (b) 40, (c) 60, (d) 80, or (e) 100 mVs^{-1} . The insets in (A), (B), and (C) reveal the linear relationship between the current and the square root of the scan rates. (D) EIS of the (a) GR/GPE, (b) Au/GPE, (c) GR/Au/GR/Au/GPE, and (d) bare GPE under an applied 5 mV potential over the frequency range 100 to 0.01 Hz in a KCl (0.1 M) solution comprising 5 mM $\text{K}_3\text{Fe}(\text{CN})_6/\text{K}_4\text{Fe}(\text{CN})_6$.

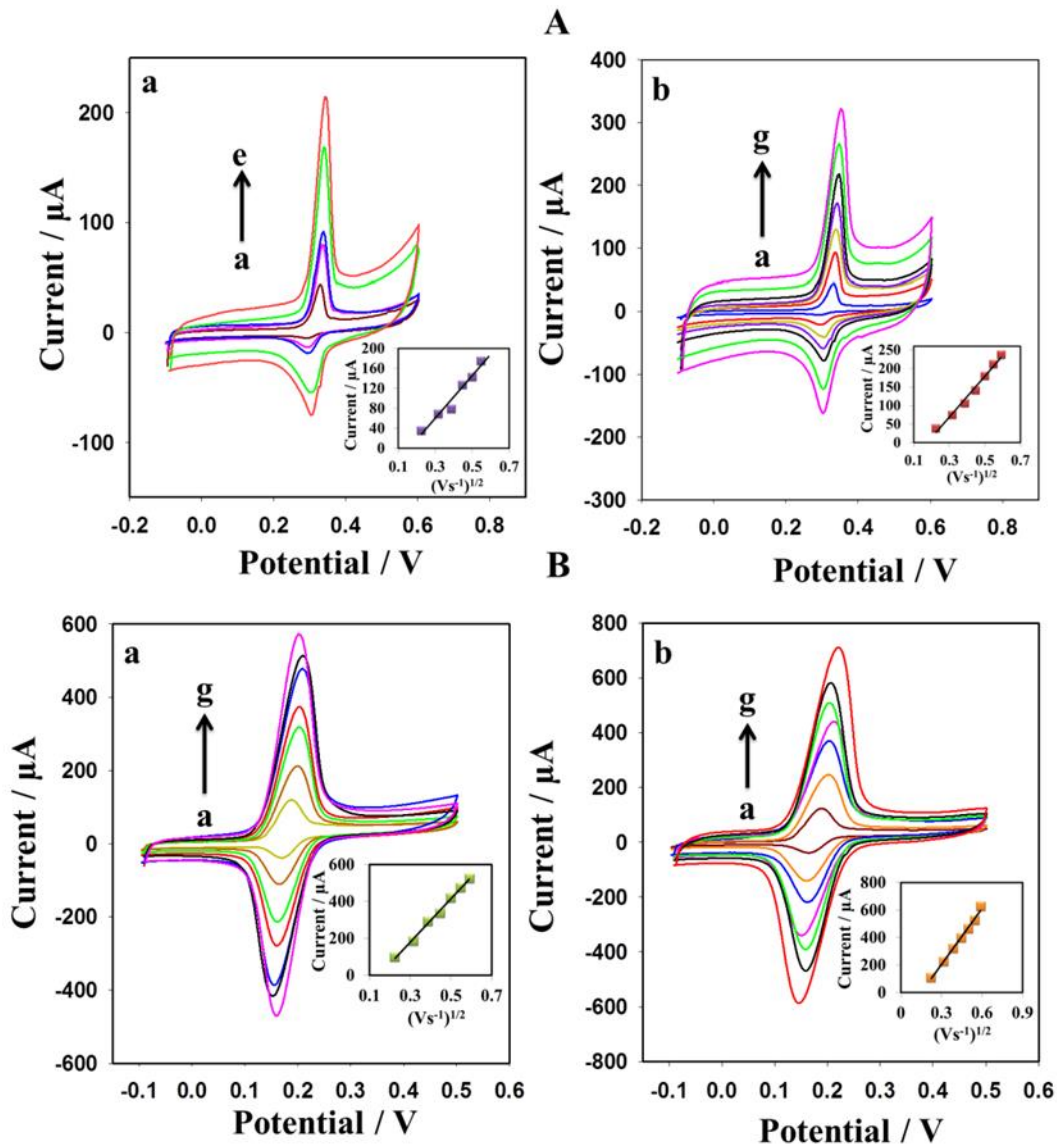


Figure 5- 10: Cyclic voltammograms were obtained from a solution comprising 0.2 mM uric acid (A) and 1 mM dopamine (B) in 0.1 M PBS. The responses of the GR/GPE to uric acid (Aa) at scan rates of 50 (a), 100 (b), 150 (c), 250 (d), and 300 mVs^{-1} (e). The responses of the GR/Au/GR/Au/GPE to uric acid (Ab) at scan rates of 50 (a), 100 (b), 150 (c), 200 (d), 250 (e), 300 (f), and 350 mVs^{-1} (g). The responses of the GR/GPE (Ba) and GR/Au/GR/Au/GPE (Bb) at scan rates of 50 (a), 100 (b), 150 (c), 200 (d), 250 (e), 300 (f), and 350 mVs^{-1} (g). The insets in (A) and (B) reveal the linear relationship between the current and the square root of the scan rate.

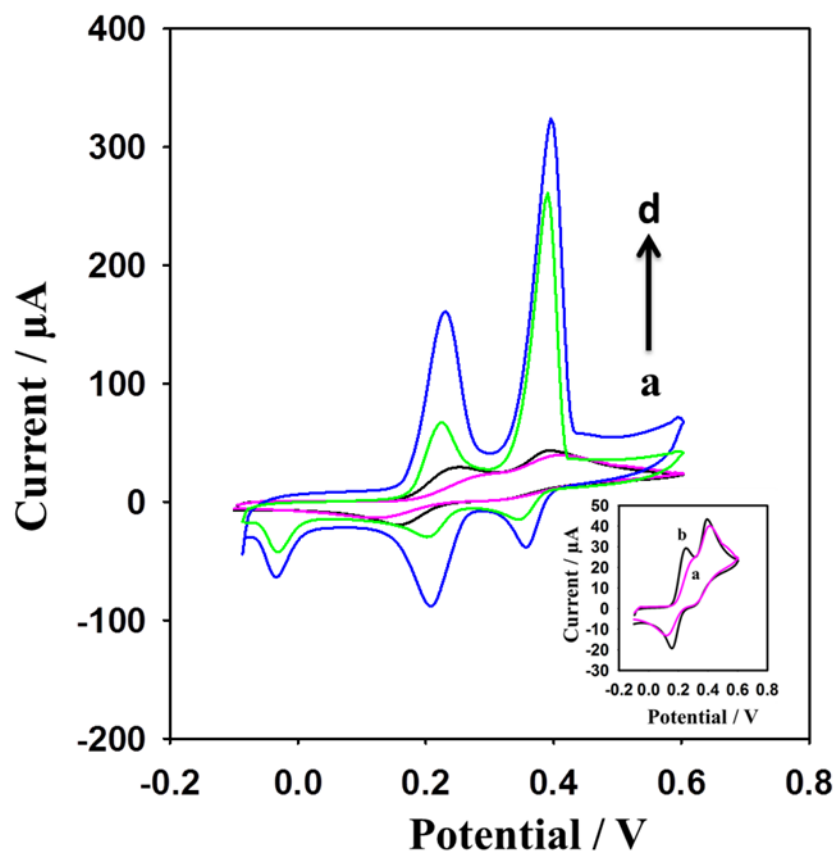


Figure 5- 11: CVs of the bare GPE (a), Au NPs/GPE (b), GR/GPE (c), and GR/Au/GR/Au/GPE in 0.1 M PBS containing 0.5 mM dopamine and uric acid

The electrode surface played a vital role in controlling the kinetics and reversibility of the electrochemical reactions [268]. The reversibility of the electrochemical reaction was examined by CV. The potential difference of the reversible reaction is expressed by equation 2.

$$\Delta E = E_{pa} - E_{pc} = 59/n, \quad 2$$

where ΔE (mV) is the peak potential difference between the anodic and cathodic peak potentials, E_{pa} (mV) is the anodic peak potential, E_{pc} (mV) is the cathodic peak potential, and n is the number of electrons taking part in the electrochemical reaction. An irreversible reaction yields only a single peak. The electrochemical reaction was reversible if the value of ΔE was $59/n$ mV and was quasi-reversible for a value exceeding $59/n$ mV. The ΔE values calculated using equation 2 were 31.0 mV for uric acid and 39.8 mV for dopamine. The calculated values of ΔE for dopamine and uric acid exceeded $2.3RT/nF$ or $59/n$ mV, indicating that the electrochemical reactions of dopamine and uric acid were quasi-reversible on the modified electrode surface. The values of n (number of electrons) for dopamine and uric acid were calculated (Eq. 2) to be 1.5 and 1.9, respectively. The experimental values of n indicated the involvement of two electrons in the electrochemical reactions of DA and UA on the GR/Au/GR/Au/GPE surfaces.

5.3.5 Study of pH

The effects of the PBS solution pH on the dopamine and uric acid detection were explored. The pH influence was investigated by varying the pH of the 0.1 M PBS solution from 5.0 to 7.5 in the presence of 0.5 mM dopamine and uric acid.

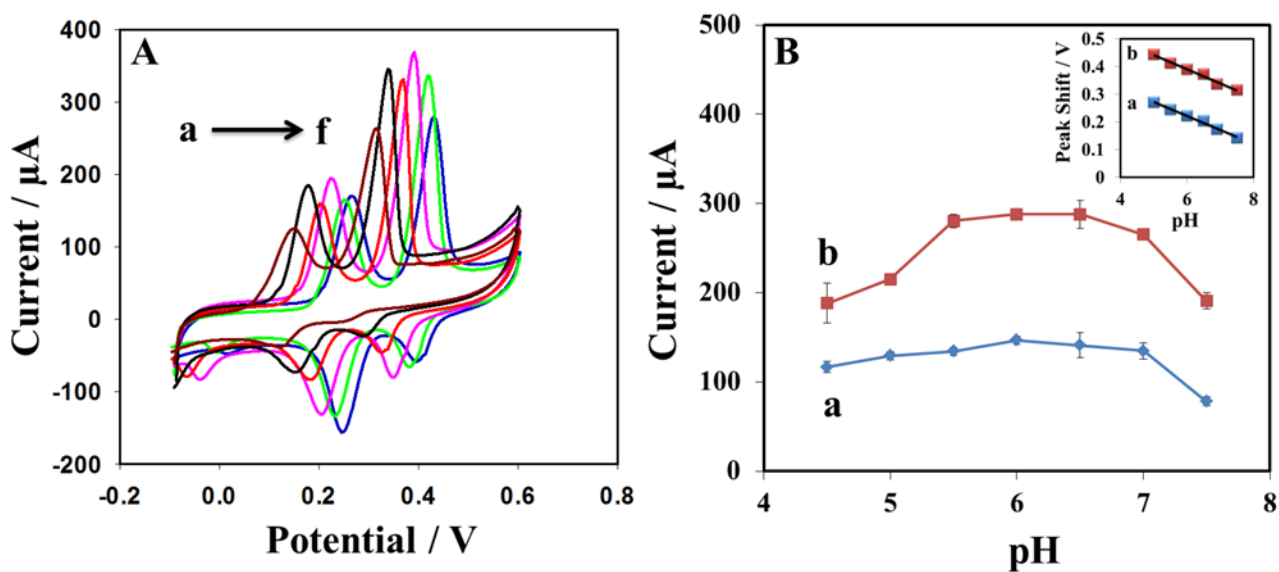


Figure 5- 12: (A) Cyclic voltammograms obtained from solutions comprising of 0.5 mM dopamine and uric acid in 0.1 M PBS at various pH values: (a) 7.5 pH, (b) 7.0 pH, (c) 6.5 pH, (d) 6.0 pH, (e) 5.5 pH, (f) 5.0 pH at GR/Au/GR/Au/GPE. (B) Graphical representation of the peak current vs. pH for uric acid (a) and dopamine (b). Inset: Relationship between the pH and the oxidation peak potential.

The effects of the PBS solution pH on the dopamine and uric acid detection were explored. The pH influence was investigated by varying the pH of the 0.1 M PBS solution from 5.0 to 7.5 in the presence of 0.5 mM DA and UA. The cyclic voltammograms obtained from the simultaneous measurements of DA and UA revealed the impact of pH on the current and on the oxidation and reduction peak potentials. The optimum response was obtained at a pH of 6.0. A negative peak shift was observed during the dopamine and uric measurements as the pH increased (Fig. 5- 12). The negative shift with increasing pH indicated the direct involvement of protons in the oxidation of the uric acid and dopamine. A linear relationship was observed between the peak shift potential and the pH of the medium for uric acid ($R^2 = 0.988$) and dopamine ($R^2 = 0.991$). The slope was found to be 51.3 mV/pH for uric acid (Eq. 3) and 50.6 mV/pH for dopamine (Eq. 4), in good agreement with the theoretical value of 59 mV/pH. These values for the slope revealed the participation of same numbers of protons and electrons in the electrooxidation of DA and UA. The transfer of two electrons and the mean involvement of two protons in the electrochemical reaction were calculated using Equation 2.

$$E \text{ vs. Ag/AgCl} = -0.0513 [\text{pH}] + 0.6991 \quad 3$$

$$E \text{ vs. Ag/AgCl} = -0.0506 [\text{pH}] + 0.5261 \quad 4$$

5.3.6 Optimization of the SWV

Different voltammetric techniques were applied for dopamine and uric acid detection. The SWV was found to be much more sensitive than the other techniques for dopamine and uric acid detection. The electrode sensitivity toward the analyte could be enhanced by

optimizing the SWV parameters. The amplitude displayed different effects on the dopamine and uric acid detection. The oxidation peak currents of both analytes increased as the amplitude increased to 0.04 V. The current subsequently decreased dramatically as the amplitude was increased in the presence of uric acid, whereas the current continued to increase in the presence of dopamine and then decreased beyond 0.06 V (Fig. 5- 13 A). The frequency was also found to impact the peak current. The maximum responses for DA and UA were observed at 50 Hz, and the current dropped at higher frequencies (Fig. 5- 13 B). The GR/Au/GR/Au/GPE electrode displayed excellent adsorption properties for dopamine and uric acid. The adsorption properties were improved by the presence of the graphene layer on the electrode surface. The π electron-rich system and the large surface area of the graphene-enhanced the adsorption of the analyte [312] as indicated by the sharp rise in the current as the adsorption time increased. The surface of the modified electrode became saturated at 120 s (Fig. 5- 13 C).

5.3.7 The Simultaneous Detection of DA and UA, Reproducibility, and the Detection Limit

The responses of the electrodes to dopamine and uric acid at the GR/Au/GR/Au/GPE surface were measured in the presence of various analyte concentrations. Well-resolved dopamine and uric acid peaks were observed at 0.232 and 0.383 V, respectively. The peak separation between dopamine and uric acid was 0.151 V. Linear responses during the simultaneous detection were attained for the concentration ranges 0.1 μ M and 25 μ M dopamine and 0.09 to 25 μ M uric acid (Fig. 5- 14 A). The LOD ($S/N = 3$) for dopamine and uric acid were 0.024 and 0.029 μ M, respectively. The detection and quantification limits achieved at the fabricated electrode were much better or comparable to the

corresponding limits reported previously for graphene and graphene nanocomposite electrodes (Table 5- 1).

The response of each analyte was considered while holding the other analyte concentrations constant (Fig. 5- 14B, 5- 14 C). The fabrication reproducibility was checked by fabricating five different GR/Au/GR/Au/GPEs under the same set of conditions. The RSD (n = 5) values for the simultaneous detection of DA and UA were found to be 7.56% and 3.07%, respectively.

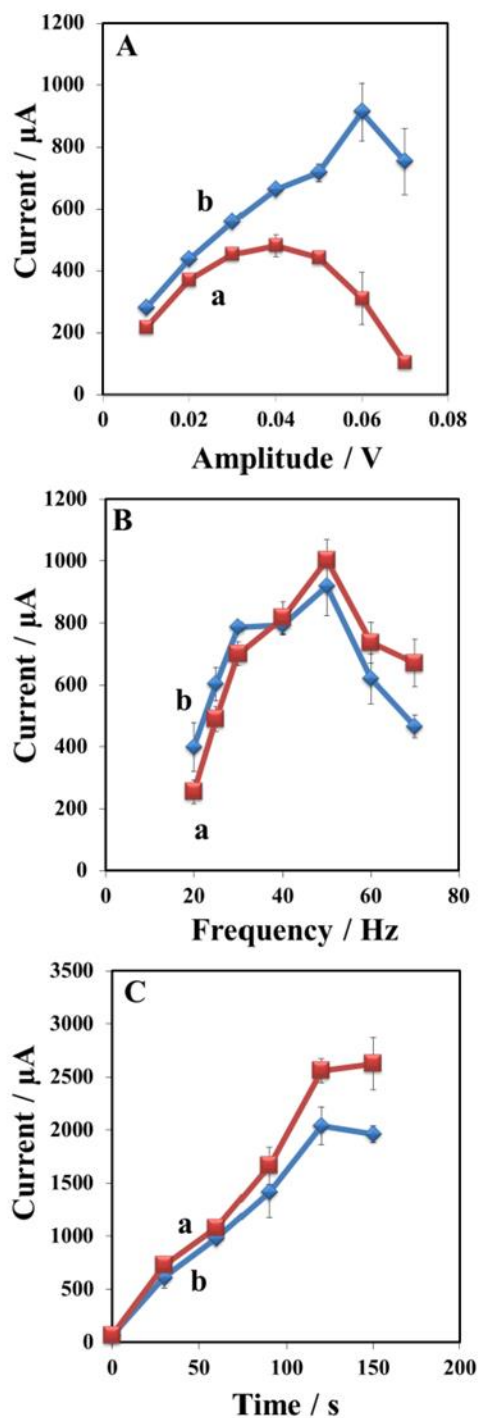


Figure 5- 13: Plots of the oxidation peak current vs. the (A) amplitude or (B) frequency, collected at $20\ \mu\text{M}$ after a 10 s adsorption time (C) adsorption time in the presence of $10\ \mu\text{M}$ (a) uric acid or (b) dopamine, obtained from the SWV in a PBS buffer (0.1 M, 6.0 pH).

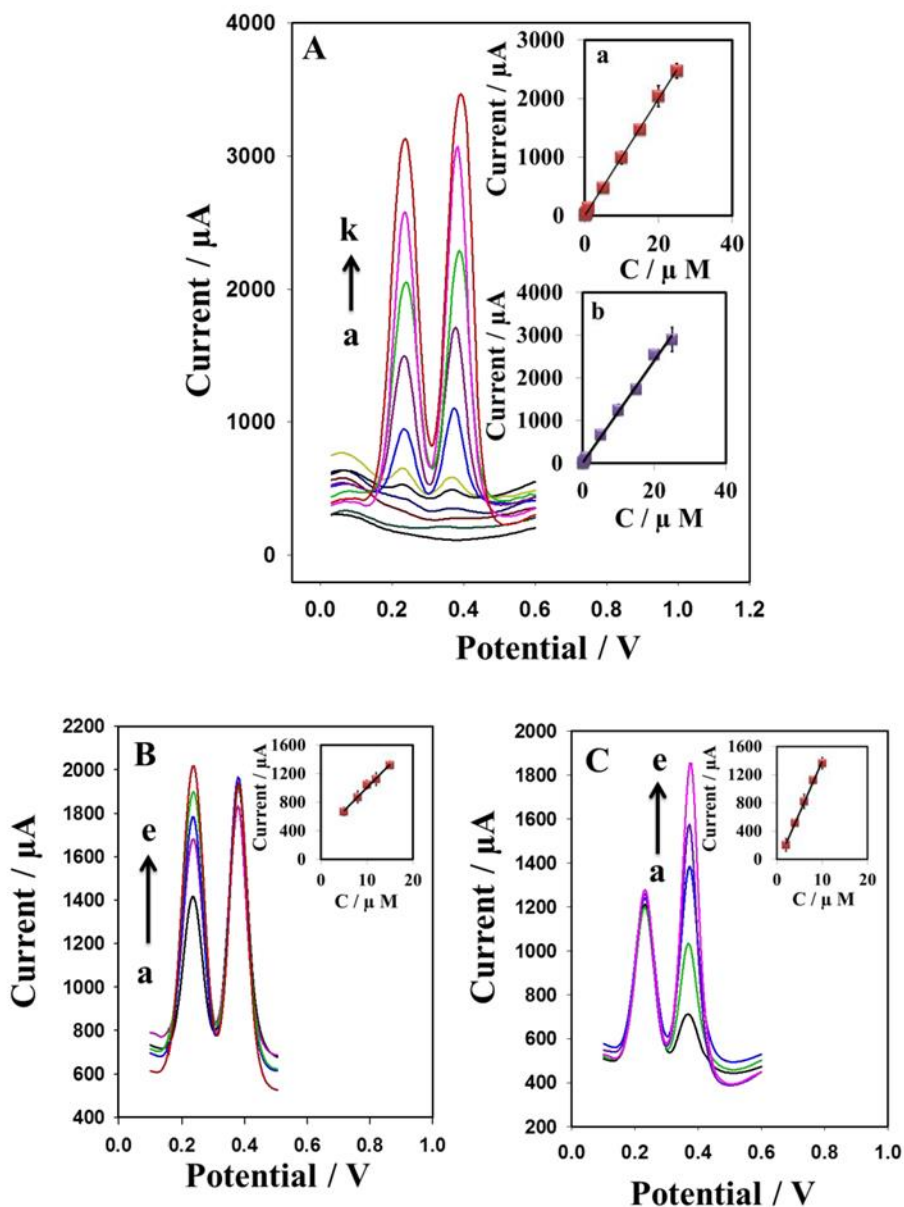


Figure 5- 14: Square wave voltammograms of (A) dopamine and uric acid at various concentrations: (a) 0, (b) 0.09, (c) 0.1, (d) 0.3, (e) 0.5, (f) 1, (g) 5, (h) 10, (i) 15, (j) 20, and (k) 25 μM . The inset shows the linear relationship between I (μA) and the concentration. (B) Dopamine concentrations: (a) 5, (b) 8, (c) 10, (d) 12, (e) 15 μM in the presence of 8 μM uric acid. (C) Uric acid concentrations: (a) 2, (b) 4, (c) 6, (d) 8, (e) 10 μM in the presence of 5 μM dopamine. The inset shows the linear relationship between I (μA) and the concentration (μM).

5.3.8 Comparison with Previously Described Graphene Composites and, Particularly, with Au NP Graphene Composites

The simultaneous detection of DA and UA was challenging, and several methods were introduced to improve the sensitivity of detection. A few literature reports have described the use of Au–graphene composites for this purpose. The GE/Au/GE layer arrangement was previously fabricated on a carbon fiber electrode. The limits of detection obtained using this electrode (0.59 for dopamine and 12.6 μM for uric acid) indicated that the arrangement was not very sensitive toward the analytes [311]. Another study examined a GCE modified with rGO and electrodeposited gold nanoplates, which yielded a LOD of 1.4 for dopamine and 1.8 μM for uric acid. The dopamine–uric acid peak separation was 110 mV [161]. A combination of Au NPs, β cyclodextrin, and graphene was used in another study to enhance the sensitivity of the GCE. The detection limits were significantly improved to 0.15 μM (dopamine) and 0.21 μM (uric acid), and the peak separation was increased to 120 mV [281]. Other graphene nanocomposites have been reported for the simultaneous recognition of DA and UA, as listed in Table 5- 1. In the present work, we found that the direct reduction of graphene oxide and Au(III) onto a disposable graphite pencil electrode surface was highly effective for the simultaneous sensing of DA and UA. The LOD was dramatically improved to 0.024 (dopamine) and 0.029 μM (uric acid) compared to previous studies, particularly compared to previous graphene–Au nanocomposite electrodes. The fabricated electrode is disposable and highly cost-effective, the modification method is facile compared the casting methods, which can require hours to obtain a dry electrode surface and further electrochemical treatments to enable the use of these electrode surfaces in sensing applications.

5.3.9 Actual Sample and Interference Studies

The fabricated GR/Au/GR/Au/GPE was used to sense DA and UA in a urine sample collected from a healthy person. The level of UA in urine is high; therefore, the sample was diluted to bring the value into the linear detection range of the fabricated electrode. The urine sample was not treated in any other way prior to conducting the measurements. The dopamine and uric acid concentrations were obtained using standard addition methods. The urine samples were spiked with 2, 4, or 8 μM DA and UA. Recoveries in the range of 93–109% were obtained (Table 5- 2). The RSD ($n = 3$) values were less than 8.1%. The modified electrode detection properties were examined for potential interference from other urine components. Good recoveries of the dopamine and uric acid concentrations in the urine sample indicated that the electrode efficiently coped with interference from other substances present in the actual urine sample. The biomolecule that interfered the most with the simultaneous measurements of DA and UA was AA. DA and UA measurements were obtained in the presence of 1 mM AA, and current variations of 7.0% for dopamine and 9.3% for uric acid were obtained. The presence of 0.1 mM fructose, alanine, phenylalanine, and methionine revealed variations of 0.9–14% for dopamine and 1–10% for uric acid.

Table 5- 1: Comparison of the fabricated electrochemical sensor with previously reported graphene modified sensors

Sr#	Electrodes	Analyte	Technique	Medium /pH	Linear range	LOQ	LOD	Peak separation (mV)	Ref.
1	Au/RGO/GCE	DA UA	DPV	0.1M PBS/ 7.0	6.8 – 41, 8.8 – 53	6.8, 8.8	1.4, 1.8	110	[161]
2	GE/Au/GE/CFE	DA UA	DPV	0.1M PBS/7.0	0.59 – 43.96, 12.6 – 413.62	0.59, 12.6	0.59, 12.6	-	[311]
3	AuNPs/ β CD/GR/ GCE	DA UA	SWV	0.10 M NaH ₂ PO ₄ -HCl/2.0	0.5 – 150, 0.5 – 60	0.5, 0.5	0.15, 0.21	120	[281]
4	AuNCs/AGR/ MWCNT/GCE	DA UA	SWV	0.1 M PBS/7.0	1.0 – 210, 5.0 – 100	1, 5	0.08, 0.1	140	[156]
5	RGO/PAMAM/ MWCNT/AuNP/ GCE	DA UA	DPV	0.1 M PBS/4.0	10 – 320, 1 – 114	10, 1	3.3, 0.33	120	[158]
6	rGO/MB/AuNPs /GCE	DA UA	DPV	PBS/7.4	–	-	0.15, 0.25	132	[313]
7	Pd ₃ Pt ₁ /PDDA- RGO/GCE	DA UA	DPV	0.1 M PBS/7.4	4 – 200, 4 – 400	4, 4	0.04, 0.1	116	[144]
8	CoTPP- CRGO/GCE	DA UA	DPV	0.1 M PBS/6.5	0.1 – 12, 0.5 – 40	0.1, 0.5	0.03, 0.15	140	[293]
9	MgO/Gr/TaE	DA UA	DPV	0.1 M PBS/5.0	0.1 – 7, 1 – 70	0.1, 1	0.15, 0.12	147	[157]
10	CTAB- GO/MWCNT/ GCE	DA UA	DPV	0.1 M PBS/7.0	5 – 500, 3 – 60	5, 3	1.5, 1.0	70	[310]
11	AgNW/rGO/ SPCEs	DA UA	LSV	0.1 M PBS/7.4	40 – 450, 35 – 300	40, 35	0.26, 0.30	125	[304]

12	AgNPs/rGO/ GCE	DA UA	LSV	PB/3.5	10 – 800, 10 – 800	10, 10	5.4, 8.2	124	[137]
13	Trp-GR/GCE	DA UA	DPV	0.1 M PBS/7.0	0.5 – 110, 10 – 1000	0.5, 10	0.29, 1.24	120	[160]
14	CTAB/rGO/ZnS/ GCE	DA UA	DPV	0.1 M PB/7.0	1 – 500, 1 – 500	1, 1	0.5, 0.4	100	[155]
15	GR/Au/GR/Au/ GPE	DA UA	SWV	0.1 M PBS/6.0	0.1 – 25, 0.09 – 25	0.1, 0.09	0.024 , 0.029	151	This work

Table 5- 2: Determination of dopamine and uric acid in the human urine sample

Analyte	Found (μM)	Added (μM)	Recovered (μM)	Recovery (%)	RSD
Dopamine					
	0	2	2.18	109	8.08
	0	4	3.71	93	1.54
	0	8	7.48	93.5	5.54
Uric acid					
	4	2	1.88	94.1	5.55
	4	4	4.07	101	4.11
	4	8	7.76	97	3.37

CHAPTER 6

Single Step Electrochemically Fabricated Optimized Extended Graphene-methylene Blue Layered Nanocomposite Modified Disposable Cost-effective Graphite Pencil Electrode for the Simultaneous Sensitive Sensing of DA, UA, and L-tyrosine in Human Urine

6.1 Introduction

The sensing of small biomolecules is always interesting to clinical laboratories for assessment of the health condition and the monitoring of treatment direction of the under observation patients. Dopamine, uric acid, and L-tyrosine have significant importance in the physiological fluid and considered as crucial biomarkers. Dopamine is a vital neurotransmitter and hormone in the body. It is contributing to the feelings, learning, mood, attention and behavior. The role of dopamine is obvious in renal, nervous and cardiovascular systems [13]. Its abnormal level could raise some serious problems such as Parkinson's disease, schizophrenia, and Huntington [15]. Uric acid is the oxidation by-product of the purine metabolism. Abnormal level of uric acid in the human body fluid is the indication of some severe diseases such as hyperuricemia, gout and the Lesch-Nyhan syndrome [20, 209]. L-tyrosine is crucial amino acid and acting as a precursor for dopamine, epinephrine, and norepinephrine [2]. L-tyrosine is also acting as a precursor for thyroid hormone and melanin [3]. Tyrosinemia is initiated due to a higher concentration of L-tyrosine and the lower concentration result into alkaptonuria and albinism. L-tyrosine in urine is considered a biomarker for certain cancers and its 50 % high concentration compared to normal in urine indicated the possibility of cancer.

Graphene after isolation in 2004, it is widely being considered in the various fields. It is fascinating two-dimensional sp^2 hybridized honeycomb like one atom-thick carbon material [314]. Graphene emerged as more prominent among other two-dimensional materials due to its diverse applications in different fields. Due to its promising behavior, it is being investigated in the field of transparent conductors, solar cells, batteries, fuel cells, field emission display and electrochemical sensors [25, 241]. It has gained great

attraction in the field of electrochemical sensing due to rapid charge transfer, extremely low resistance, and wide potential window [26].

The polymers of highly oriented dyes have the capability to exhibit outstanding photochemical and catalytic properties. The dyes are practically being applied and investigated for enzyme immobilization, light emitting diodes, batteries, electrochemical devices and electrode modifications [315]. Methylene blue is a dye which belongs to heterocyclic aromatic compounds and provides a blue solution in water. Methylene blue is a highly conjugated positive charge molecule and could act as electron actuator [316]. The long-term stable polymethylene blue films could be obtained simply by commonly used electropolymerization [315].

Graphene is used in the development of numerous sensitive sensors for sensing of various analytes. The sensitivity of the sensors could be further improved using graphene in combination with other nanomaterials. The metal-graphene, metal oxide-graphene, and polymer based graphene nanocomposite are used in the development of sensors, optical devices and as a catalyst [317]. Polymethylene blue graphene composite is also showing interesting behavior on the surface of various electrode systems. The PMB-GR/CILE was used for sensitive sensing of dopamine [318]. Similarly, the dopamine grafted graphene oxide/poly(methylene blue) on glassy carbon electrode surface was used for dopamine sensing [18]. NADH was also determined using Graphene/Poly(methylene blue)/AgNPs Composite on Paper [316] and Graphene/Methylene Blue Nanocomposite Thin Films on Au electrode [320].

As the sensors are the major recognition methods for the direct and indirect monitoring of various biomarkers. However, the sensitivity, selectivity and sometimes costs are the major factors and the hurdles to developing disposable sensors for monitoring. Graphite pencil electrode is a developing electrode. Graphite pencil is commonly used for writing purposes. In past few years, it is being explored in the field of electrochemistry as the working electrode. It is applied for the sensing of numerous analytes by activating its surface with nanomaterial [209, 24, 294, 66]. It is being recognized due to disposability, low cost, facile modification, control of exposed surface area and easy availability. Various methods are being explored to enhance its sensitivity to make it a valuable tool in the field of electrochemical sensing. In this work, we have first time modified GPE with extended MB-GR layers. The synergistic effect of MB and GR has significantly improved the sensitivity of the GPE. The formation of extended and intensive wrinkled shaped layers of MB-GR assisted to achieve huge electroactive area compared to GR/GPE. The interaction of the MB and GR is very fast and GPE modification process takes short time which imparts the sensor disposable characteristics. To avoid surface fouling due to electrochemical byproducts after a single use, the new surface could be fabricated in few minutes. MB-GR/GPE was applied for the simultaneous sensing of dopamine, uric acid, and the L-tyrosine. Well-separated peaks were observed. The ascorbic acid which is problematic for the simultaneous sensing of DA and UA has shown no effect. The developed sensor behaved well in the human urine sample.

6.2 Materials and Methods

6.2.1 Reagents

The materials and reagents are same as stated in 3.2.1 subsection.

6.2.2 Apparatus

The instrumentation and apparatus are same as stated in 3.2.2 subsection.

6.2.3 Preparation of Modified GPE

The pencil electrode modification was done by GO or MB+GO. Prior to modification the GO (2mg/mL) and MB-GO (0.5 mM MB+ 2mg/mL GO) was dispersed in double distilled water. The MB-GO was reduced on the GPE surface by sweeping electrode potential from -1.4 to 0.5 V over 5 cycles using scan rate 0.03 Vs^{-1} . The modified surface was gently washed by dipping twice in the double distilled before analysis to remove adsorbs MB-GO from the surface.

6.3 Results and Discussion

6.3.1 Optimization of Various Parameters for Effective Reduction of MB-GO on GPE

GPE is highly cost-effective sensor but issue with its surface sensitivity like other bare electrodes. The surface sensitivity was improved by direct electrochemical reduction of MB-GO composite on the GPE surface. To achieve optimum surface sensitivity, the various possible parameters were optimized. The several concentrations of GO and the MB solution were mixed to get an optimum response. The sensor response was observed for the simultaneous sensing of DA, UA and the L-tyrosine. The maximum response was observed when the concentration of the MB-GO composite containing 0.5 mM MB and the 2 mg mL^{-1} GO. The reaction time of the MB and the GO was analyzed as this factor could affect the sensor sensitivity and the stability. The reaction time has shown no effect on the sensor sensitivity. Almost a constant current response was observed for 0.5 mM dopamine, uric acid and L-tyrosine. This study revealed, the interaction between GO and

MB is spontaneous which contribute to the development of disposable sensor. It facilitates the fast fabrication of the sensor.

Later on, the electrochemical reduction parameters of MB+GO on the GPE surface were optimized. Cyclic voltammetry was used for the reduction of MB+GO. First of all, the scan rate for reduction of composite effect the sensitivity of the sensor and 0.03 V/s was found most effective for composite reduction. The optimum scan window for reduction of the composite was found -1.4 to 0.5 V. Finally, the number of scans for the reduction of the MB+GO composite were optimized which is crucial for the control of the thickness of the layers and provide the higher sensitivity to the GPE.

The response was found maximum when reduction cycles were five and a further increase in reduction cycles sharply affect the response of the sensor. The sensitivity of the sensor was decreased. It may be due to an increase of the layer thickness and agglomeration of the layers which nastily affect the sensitivity of the sensor. Various buffer medium such as phosphate buffer (PB), phosphate buffer saline (PBS), acetate buffer and tris-EDTA were analyzed for the analytes. The PBS buffer has shown a great impact on the peak currents of analytes. The possible great effect is due to the high conductance effect of the medium as it contained a lot of salts (Fig. 6- 1).

6.3.2 Characterization by FE-SEM and Raman Spectroscopy

The surfaces of the bare GPE and modified GPE were investigated by FE-SEM and the Raman spectroscopy. The FE-SEM images have shown particular changes on the surface of GPE after each modification step.

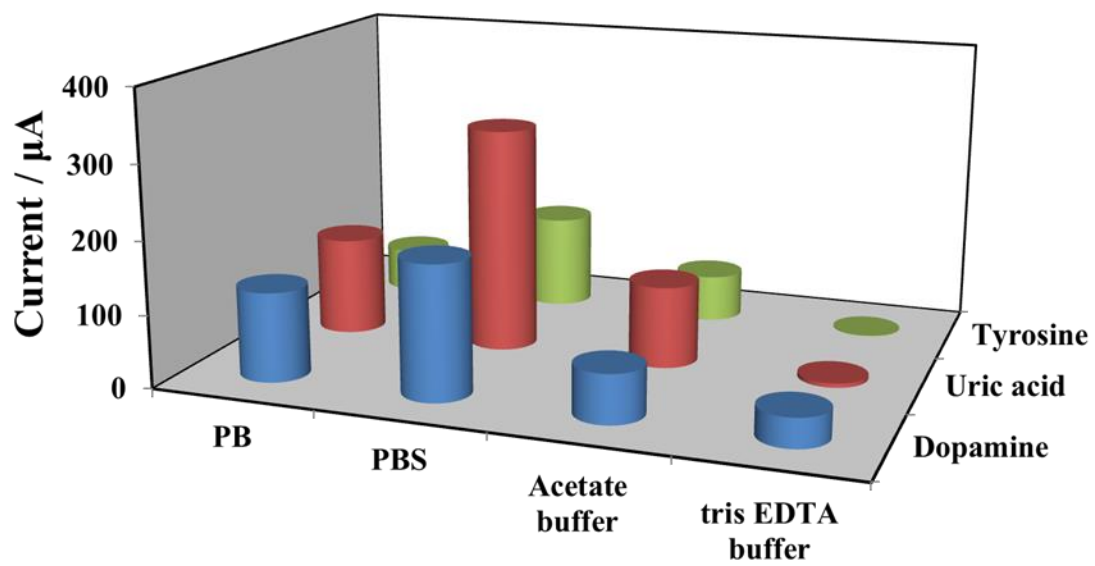


Figure 6- 1: Effect of different sensing medium for 0.5 mM Dopamine, uric acid, and L-tyrosine on MB-GR/GPE.

MB, GO and MB-GO were reduced on the surface of GPE by similar fashion and under the same set of conditions. The bare and the MB/GPE surface have not shown any kind of layers on the surface (Fig. 6- 2a&b). However, the roughness on the bare surface could be observed. Graphene layers could be observed on the surface of GR/GPE with few wrinkles (Fig. 6- 2c). An amazing behavior of reduction of MB-GO could be observed on the surface of GPE. Very fine and intensive wrinkled layers of MB-GR could be observed on the surface of MB-GR/GPE. It seems graphene oxide more effectively reduced on the surface of GPE in the presence of MB and extensive wrinkles is a clear indication of a sharp increase in surface area of the electrode surface. Moreover, these layers are coming out of the surface and giving little bit 3D extension (Fig. 6- 2d).

Further, the modified surfaces were explored by Raman spectroscopy. The Raman spectra of bare GPE have shown an expected weak D-band and strong G-band. The 2D band appeared at 2707 cm^{-1} (Fig. 6- 3a). Although graphene Raman spectra should be similar to graphite it's generally contained defects due to which strong D band is observed. It is also an indication of the graphene layers formed on the surface of GPE. In the Raman spectra of GR/GPE, the strong D and G band appeared and 2D band could be observed (Fig. 6- 3b). Similar Raman spectra like GR/GPE were observed for MB-GR/GPE but the intensity of D and G band was dramatically enhanced.

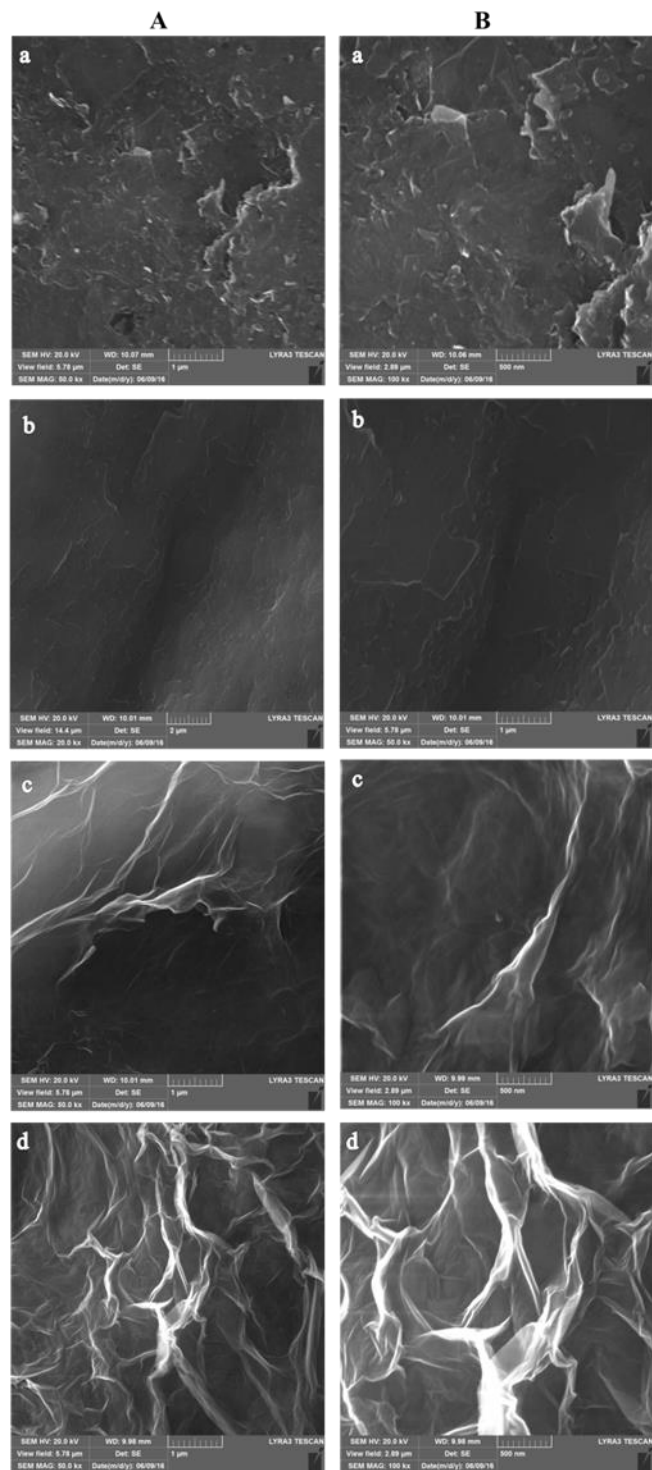


Figure 6- 2: FE-SEM images at two magnification (A) 1 μ m and (B) 500 nm (a) bare/GPE, (b) MB/GPE, (c) GR/GPE, (d) MB-GR/GPE.

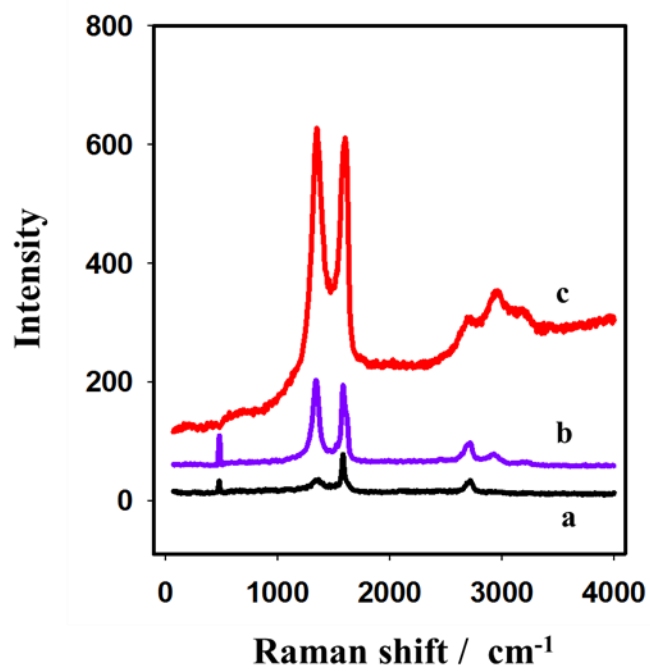


Figure 6- 3: Raman spectra of (a) bare GPE (b) GR/GPE, and (c) MB-GR/GPE.

6.3.3 Electrochemical Investigation of the GPE Surface and its Interaction with MB-GO

The scan rate effect was studied on the GR/GPE and the MB-GR/GPE. The modified surfaces were investigated for the targeted analytes such as DA, UA, and L-tyrosine. The scan rate was varied from 0.05 to 0.25 v for 0.2 mM dopamine and uric acid using cyclic voltammetry (Fig. 6- 4 A, A', B, B'). Similarly, it was varied from 0.01 to 0.1v for 0.5 mM L-tyrosine (Fig. 6- 4 C, C'). As the scan rate increased, the current was increased for the same concentration of the analytes. However, the current enhancement was much greater for the MB-GR/GPE compared GR/GPE. The behavior of the uric acid changed on the surface of MB-GR/GPE. The reversible peak of the uric acid became more prominent. The ESA was calculated for the GR/GPE and the MB-GR/GPE using equation 1:

$$I_p = 2.69 \times 10^5 v^{1/2} n^{3/2} C D^{1/2} A, \quad 1$$

The enormous rise in ESA was observed when MB-GO reduced on the GPE surface compared GO reduction. The electroactive surface area of dopamine, uric acid and L-tyrosine was increased from 0.141, 0.453 and 0.0445 (GR/GPE) to 2.353, 1.43 and 0.299 cm² (MB-GR/GPE) (Fig. 6- 4). This immense enhancement in the electroactive surface area of GPE by MB-GR compared GR could also be observed from FE-SEM images. A great number of wrinkles and extended surface could be observed compared GR/GPE where few wrinkles could be observed. Possibly, these wrinkles and extended 3D surface playing great role in the enhancement of the ESA.

The basic purpose of the modification is to overcome the charge transfer resistance of the bare GPE surface. The surface resistances were analyzed by the electrochemical impedance spectroscopy (EIS). EIS spectra were scanned from 0.01 to 100 kHz in 0.1 M KCl solution containing 5 mM $K_3Fe(CN)_6/K_4Fe(CN)_6$. Generally, two portions could be observed in the Nyquist plots. The linear part at lower frequency relates to diffusion control process while the semicircle part at higher frequency describes the electron transfer limited process. A large semicircle could be observed in the case of bare GPE. The semicircle of the GPE reduced by applying GR and it was almost disappeared for MB-GR/GPE (Fig. 6- 5A). The impedance result has shown the MB-GR facilitate the GPE surface for fast charge transfer for simultaneous sensing of DA, UA, and L-tyrosine. The CVs were recorded for the 0.2 mM dopamine, uric acid and 0.5 mM L-tyrosine using bare GPE (Fig 6- 5Ba), MB/GPE (Fig 6- 5Bb), GR/GPE (Fig. 6- 5Bc) and MB-GR/GPE (Fig. 6- 5 Bd). The bare GPE although showing the peaks of the analytes but the peak current was very weak and the peaks are not well separated and broad which affects the selectivity of the sensor in the presence of other electroactive species. MB/GPE was also found insensitive. The peak separation and the current were improved by the graphene layer on the GPE. However, the MB-GR layer on the GPE has dramatically enhanced the peak current and the improved the peak separation of the dopamine, uric acid and l-tyrosine (Fig 6- 5B). Surface analysis of the GPE is revealed, the MB-GR layers were successfully formed on the GPE surface and improved its sensitivity and selectivity compared GR or MB alone on the GPE. This disposable sensor could be proved a valuable tool for the simultaneous sensing.

6.3.4 Study of pH Effect

The pH effect was evaluated for 0.2 mM dopamine, uric acid, and 0.4 mM L-tyrosine in 0.1 M PBS buffer medium using cyclic voltammetric scans. The negative peak shift was observed for dopamine, uric acid, and L-tyrosine as the pH increased from 5.0 to 7.0. The peak shift was observed by changing pH from 5.0 to 7.0 for dopamine, uric acid, and L-tyrosine from 241 to 126 mV, 409 to 250 mV, and 701 to 546 mV, respectively. A linear relation was observed between peak shift and the pH change with regression constant (R^2) 0.9963, 0.9968 and 0.9966 for dopamine, uric acid, and L-tyrosine, respectively (Fig. 6- 6). The slop for dopamine, uric acid and L-tyrosine was -57.1 mV/pH (Eq. 2), -62.6 mV/pH (Eq. 3), and -60.6 mV/pH (Eq. 4), respectively. pH has shown some effect on the peak current of the analytes. The best response was observed at pH 6.0 and for further study, the same pH was used.

$$E \text{ vs. Ag/AgCl} = 526.4 - 57.1[\text{pH}] \quad (R^2 = 0.9963) \quad 2$$

$$E \text{ vs. Ag/AgCl} = 721.9 - 62.6[\text{pH}] \quad (R^2 = 0.9968) \quad 3$$

$$E \text{ vs. Ag/AgCl} = 999.9 - 60.6[\text{pH}] \quad (R^2 = 0.9966) \quad 4$$

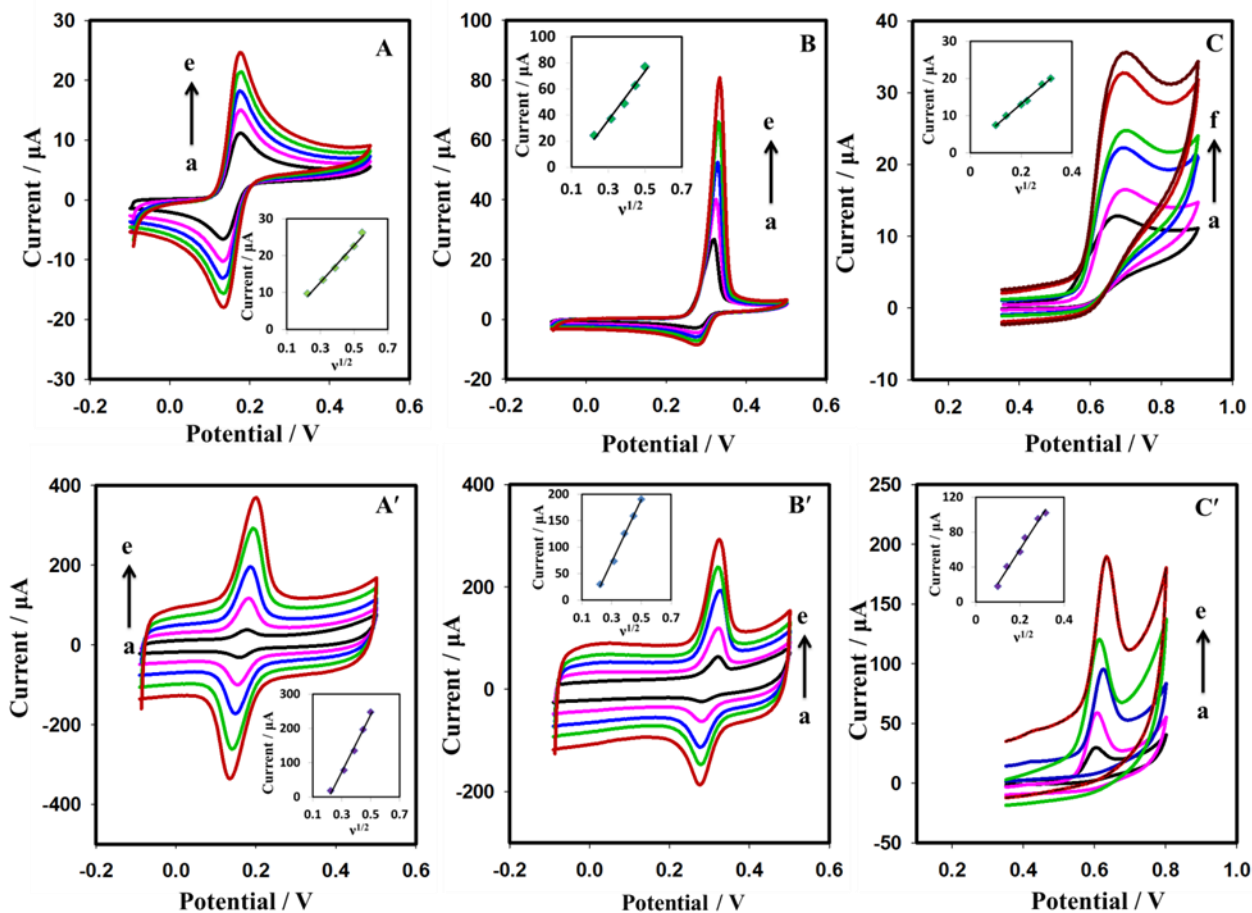


Figure 6- 4: Cyclic Voltammograms were acquired using (A, B, C) GR/GPE and (A', B', C') MB-GR/GPE from 0.1 M PBS solution comprising 0.2 mM (A, A') dopamine (B, B') Uric acid at scan rates of (a) 0.05, (b) 0.1, (c) 0.15, (d) 0.2, and (e) 0.25 v. The response of 0.5 mM L-tyrosine (C, C') at scan rates of (a) 0.01 (b) 0.02, (c) 0.04, (d) 0.05, (e) 0.08, and (f) 0.1 v. The insets in (A, A', B, B', and C, C') has shown the linear relationship between current and the square root of the scan rates

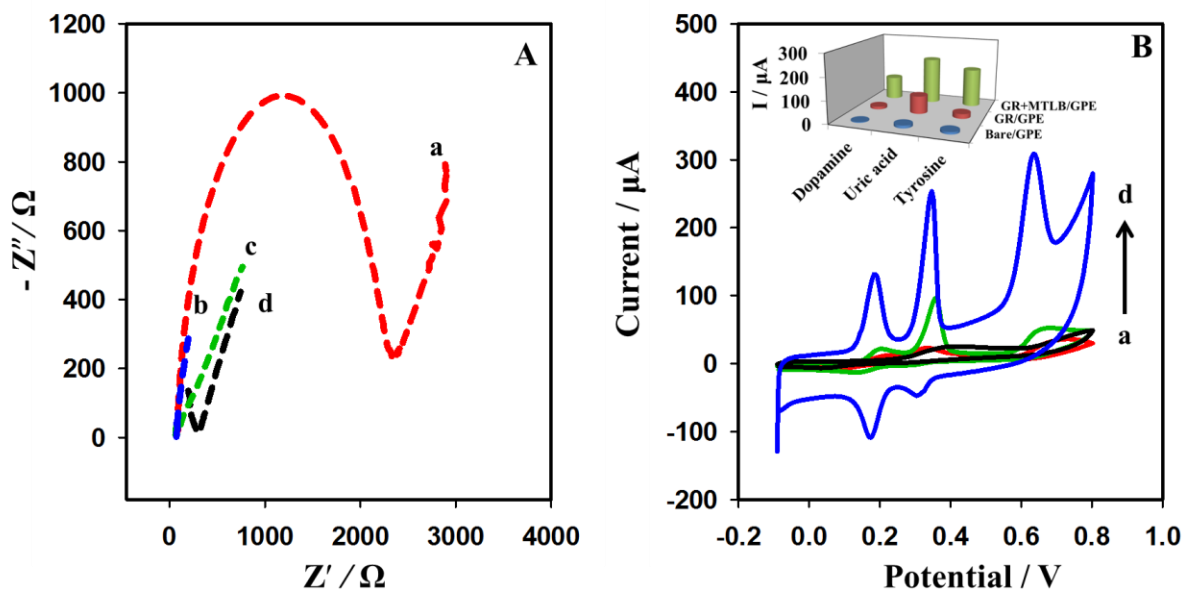


Figure 6- 5: (A) Nyquist plot of 5 mM $\text{K}_3\text{Fe}(\text{CN})_6/\text{K}_4\text{Fe}(\text{CN})_6$ in 0.1 M KCl solution on (a) bare-GPE, and (b) MB-GR/GPE (c) GR/GPE, and (d) MB/GPE upon application of frequency range from 0.01 Hz to 100 kHz. (B) CVs of (a) bare GPE, (b) MB/GPE, (c) GR/GPE, (d) MB-GR/GPE were recorded at 0.1 V/s in 0.1M PBS solution containing 0.2 mM dopamine, uric acid and 0.5 mM L-tyrosine.

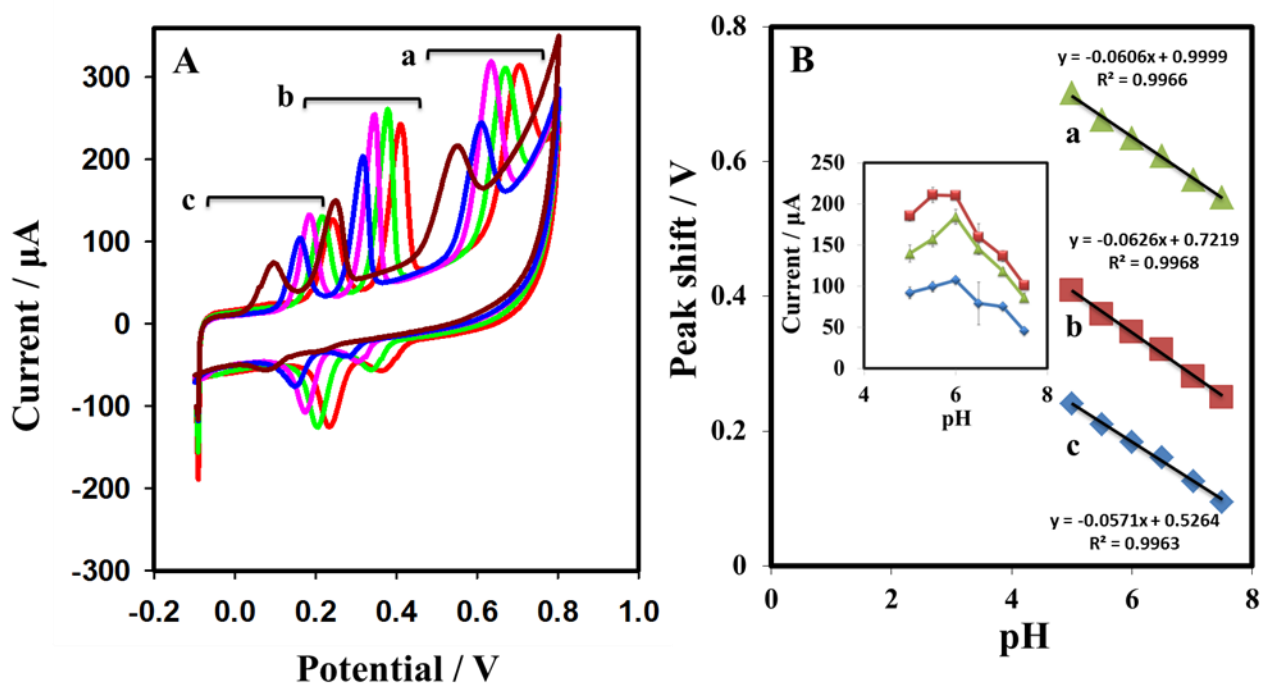


Figure 6- 6: (A) Cyclic voltammograms in 0.1 M PBS solution containing 0.4 mM (Aa) L-tyrosine, 0.2 mM (Ab) uric acid and (Ac) dopamine at various pH values from 5 to 7.0 at MB-GR/GPE. (B) The graph indicated the relationship between pH and peak current of (Ba) L-tyrosine, (Bb) uric acid, and (Bc) dopamine. Inset is showing the relationship between the peak potential and pH of the sensing medium

6.3.5 Optimization of the Sensing Technique

Prior to going for optimization of sensing techniques, the various voltammetric techniques were scanned for dopamine, uric acid, and L-tyrosine. The best response was obtained by square wave voltammetry (SWV). The sensitivity of the sensor was further improved by optimizing the various parameters of square wave voltammetry. First of all, amplitude was optimized and best response was observed at 50 mV (Fig. 6- 7A). The frequency was also shown a great impact on the peak current and optimum response was observed at 50 Hz (Fig. 6- 7B). At the end, the adsorption time was optimized. The adsorption time was optimized for 5 μ M DA, UA and 40 μ M L-tyrosine in 0.1 M PBS. The sensor has shown the great capability of adsorption for dopamine and uric acid. The current was continuously increased as the adsorption time increased till 150s and after that current almost became constant (Fig. 6- 7C). However, the SWV parameters have shown less effect on the L-tyrosine compared dopamine and uric acid.

6.3.6 Simultaneous Sensing of Dopamine, Uric Acid, L-Tyrosine, Limit of Detection, and Reproducibility

The MB-GR/GPE sensor was used for the concurrent sensing of DA, UA, and L-tyrosine in 0.1 M PBS sensor. The well-resolved peaks of dopamine, uric acid, and L-tyrosine were observed at 0.167, 0.307 and 0.626 V. The peak separation between dopamine and uric acid, dopamine and L-tyrosine, uric acid and L-tyrosine was found 140 mV, 459 mV, and 319 mV, respectively.

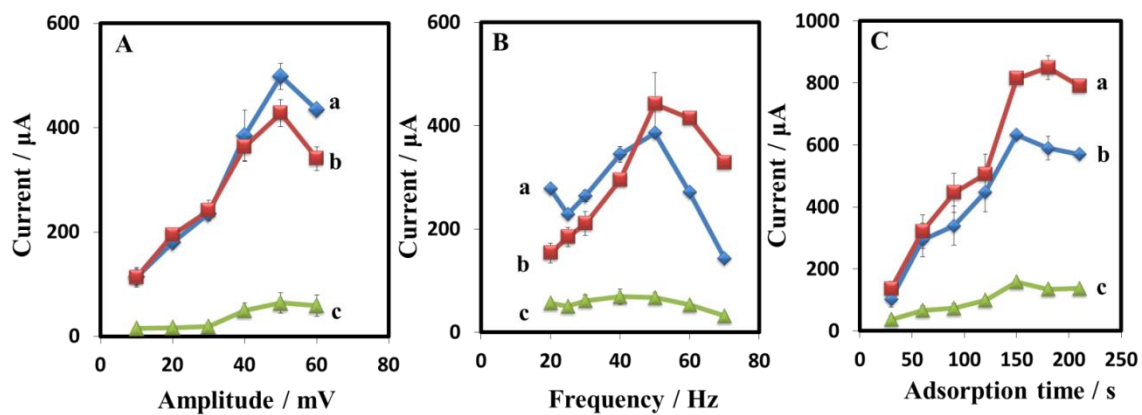


Figure 6- 7: Plots of the oxidation peak current vs. (A) amplitude scanned for 20 μM dopamine, uric acid and 40 μM L-tyrosine, (B) frequency scanned for 10 μM dopamine, uric acid and 20 μM L-tyrosine, (C) adsorption time for 5 μM dopamine, uric acid and 40 μM L-tyrosine obtained in PBS buffer (0.1 M, 6.0 pH) using square wave voltammetry.

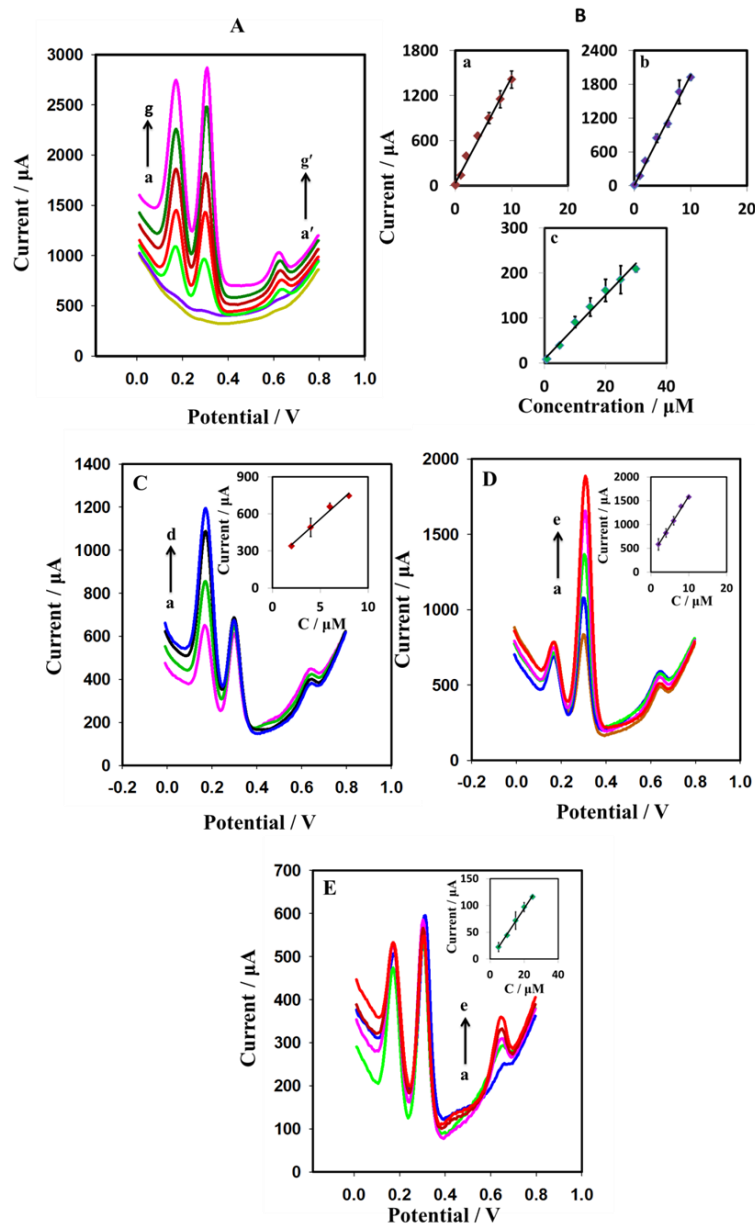


Figure 6- 8: Square wave voltammograms of (A) dopamine, uric acid at various concentrations: (a) 0.05, (b) 0.1, (c) 2, (d) 4, (e) 6, (f) 8, (g) 10 μM , and L-tyrosine (a') 0.7, (b') 0.9, (c') 10, (d') 15, (e') 20, (f') 25, (g') 30 μM . The (B) graphs show the linear relationship between I (μA) and the concentration of (Ba) dopamine, (Bb) uric acid and (Bc) L-tyrosine. (C) Dopamine concentrations: (a) 2, (b) 4, (c) 6, (d) 8 μM in the presence of 4 μM uric acid and 20 μM L-tyrosine. (D) Uric acid concentrations: (a) 2, (b) 4, (c) 6, (d) 8, (e) 10 μM in the presence of 2 μM dopamine and 20 μM L-tyrosine. (E) L-tyrosine concentrations: (a) 10, (b) 15, (c) 20, (d) 25 μM in the presence of 2 μM dopamine and uric acid. The inset in (C), (D) and (E) shows the linear relationship between I (μA) and the concentrations (μM).

The peak separations among the targeted analytes were sufficient for the simultaneous sensing. The various concentrations of the analytes were tried to find out the linear range on the developed disposable sensor. The sensor was found extremely sensitive for dopamine and uric acid. The linear ranges for dopamine and uric acid were observed from 0.05 to 10 μM (Fig 6- 8 A, Bab). The linear range for L-tyrosine was found 0.7 to 30 μM (Fig 6- 8 A, Bc). The response of dopamine (Fig. 6- 8C), uric acid (Fig 6- 8D), and L-tyrosine (Fig 6- 8E) was considered by varying the concentration of the analytes while keeping the concentration of the other two analytes constant. A linear response to the current and varying analytes concentrations was observed while a small change in current was observed for the constant concentration analytes. The developed disposable sensor could be used for simultaneous and the individual sensing of DA, UA, and L-tyrosine.

Furthermore, the sensor was evaluated on the term of reproducibility. Six different MB-GR/GPE sensors were fabricated under the same set of conditions. The developed sensors were used for the simultaneous analysis of DA, UA, and L-tyrosine. The RSD values were found 4.02, 5.44 and 6.72 % for dopamine, uric acid, and L-tyrosine, respectively.

6.3.7 Distinguish Characteristics of MB-GR/GPE over other Graphene-Based Sensors

Graphene is continuously being explored in the field of electrochemical sensing of dopamine, uric acid, and l-tyrosine. LOQ was achieved by Graphene/NiOH/GCE was 0.12 and 0.46 μM for DA and UA, respectively [159]. GO was doped with graphitic carbon nitride nanosheets and LOD was achieved 0.096 and 0.228 μM for DA and UA, respectively. The LOD found for dopamine and uric acid by Ag NPs/rGO/GCE was 5.4

and 8.2 μM , respectively [137]. In another work, the Pd and Pt NPs were used for fabrication of Pd₃Pt₁/PDDA-RGO/GCE and LOD for DA and UA was achieved 0.04 and 0.1 μM [144]. Methylene blue was also being used for sensing of various electroactive molecules. PMB-GR on CILE was found effective for sensing of dopamine [318]. H. Han et al cast rGO/MB/AuNPs/GCE nanocomposite on the GCE and used for the concurrent sensing of AA, DA, and UA. The detection limit for DA and UA was found 0.15 and 0.25 μM , respectively. The peak separation between dopamine and uric acid was 132 mV [313]. We tried to develop highly sensitive, very low cost, facile surface renewable and fast fabrication time to achieve the ultimate target of disposability using graphite pencil electrode. GPE is more suitable and highly cost-effective for the direct electrochemical reduction of MB-GR due to its elongated shape, roughness, and porous behavior. It gave more stable and highly effective layer of MB-GR for simultaneous sensing of dopamine, uric acid, and L-tyrosine. The limit of detection was achieved 0.015, 0.027, 0.247 μM , respectively. The peak separation between dopamine and uric acid was found 140 mV which more than rGO/MB/AuNPs/GCE and many other graphene-based sensors. Moreover, no precious metals such as Au or Pt NPs were used to achieve high sensitivity. Due to short fabrication time, it could be used as a single-use electrode which made it foul free electrode. The comparison of the developed electrode with other graphene modified electrodes could be observed in Table 6- 1.

Table 6- 1: Comparison of MB-GR/GPE with reported graphene-based sensors

Sr#	Modified electrode	Analyte	Sensing technique	Sensing medium	Linear range	LOQ	LOD	Application	Ref.
1	H-GO/GCE	DA UA	DPV	B – R/pH 6.0	0.5 – 40, 0.5 – 50,	0.5, 0.5		Urine & serum samples	[154]
2	pCu ₂ O NS- rGO/GCE	DA UA	DPV	0.1 M PB/pH 7.0	0.05 – 109.0, 1.0 – 138.0,	0.05, 1	0.015 0.112	-	[321]
3	GF@NiCo ₂ O ₄	DA UA	DPV	0.1 M PBS/pH 7.0	1 – 13, 10 – 26	1, 10	0.1, 0.2	Urine & serum samples	[322]
4	RGO-ZnO/GCE	DA UA	DPV	0.1 M PB/pH 6.0	3 – 330, 1 – 70,	3, 1	1.08, 0.33	Urine & plasma samples	[323]
5	GR/Au/GR/Au/ GPE	DA UA	SWV	0.1 M PBS/pH 6.0	0.1 – 25, 0.09 – 25,	0.1, 0.09	0.024 , 0.029	Urine sample	[209]
6	MoS ₂ /rGO/GCE	DA UA	DPV	0.1 M PB/pH 7.0	5 – 545, 25 – 2745	5, 25	0.05, 0.46	Serum sample	[152]
7	3DGH- AuNPs/GCE	DA UA	DPV	0.01 M PB/ pH 7.0	0.2 – 30, 1 – 60	0.2, 1	0.002 6, 0.005	Urine sample	[139]
8	Porous graphene/GCE	DA UA	DPV	0.1 M PB/pH 6.8	0.2 – 8, 1 – 60,	0.2, 1	0.2, 1	-	[324]
9	AuNCs/AGR/MW CNT/GCE	DA UA	SWVs	0.1 M PB/pH 7.0	1.0 – 210, 5.0 – 100,	1.0, 5.0	0.08, 0.1	Urine sample	[156]
10	rGO/MB/AuNPs/ GCE	DA UA	DPV	PBS/7.4			0.15, 0.25		[313]

10	Trp-GR/GC	DA UA	DPV	0.1 M PB/pH 7.0	0.5 – 110, 10 – 1000,	0.5, 10	0.29, 1.24	Injection, Urine & serum samples	[160]
11	RGO-PAMAM- MWCNT- AuNP/GCE	DA UA	DPV	0.1 M PB/pH 4.0	10 – 320, 1.0 – 114,	10, 1.0	3.33, 0.33	-	[158]
12	MB-GR/GPE	DA UA	SWV	0.1 M PBS/pH	0.05 – 10, 0.05 – 10,	0.05, 0.05		Urine sample	This work

6.3.8 Application and Interference Study

The sensor capability for simultaneous sensing of dopamine, uric acid, and L-tyrosine was done in the presence of various potential interferences. The interferences were studied for 4 μM dopamine, uric acid and 20 μM L-tyrosine. Ascorbic acid is considered major interfering agent in the sensing of dopamine and uric acid. The dopamine, uric acid, and L-tyrosine were measured in the presence of high concentration of ascorbic acid (0.5mM) and current variation was observed 2.78, 1.30 and 7.07%, respectively. The response of dopamine was also observed in the presence of 50 μM other potential interferences such as alanine, phenylalanine, L-methionine, glucose, and fructose. The current variation was observed $\pm 0.8 - 3.5$, $\pm 1.9 - 12.5$, $\pm 2.8 - 11\%$ for dopamine, uric acid, and L-tyrosine, respectively. A small variation of current of the targeted analytes observed in the presence of interferences.

MB-GR/GPE was applied in the real human urine sample for the simultaneous sensing of DA, UA, and L-tyrosine. Human urine contained a huge concentration of uric acid. The urine sample was diluted to bring it in the linear range and a sharp peak of uric acid was observed in the unspiked sample. However, the urine sample was not treated chemically prior to analysis. Standard addition method was used for the determination of analyte concentrations in the human urine. The urine sample was spiked with 2, 4, 6 μM dopamine and uric acid. In a similar way, the 10, 15 and 20 μM of L-tyrosine was spiked in the urine sample to find out the accuracy of the sensor. The recoveries of the dopamine, uric acid, and L-tyrosine were found in the range of 91 to 107% (Table 6- 2). A satisfactory recovery in the presence of real samples was indicated that developed sensor could be used for the quantitative analysis of DA, UA, and L-tyrosine.

Table 6- 2: Determination of dopamine, uric acid and L-tyrosine by MB-GR/GPE in the human urine sample

Sr #	Found	Spiked	Recovered	Percent recovery
Dopamine				
1	0	2	2.139	106.96
2	0	4	3.656	91.38
3	0	6	6.309	105.15
Uric acid				
1	2.99	2	2.063	103.16
2	2.99	4	3.787	
3	2.99	6	6.553	109.31
L-tyrosine				
1	0	10	9.197	91.97
2	0	15	13.925	92.83
4	0	20	20.159	100.79

CHAPTER 7

CONCLUSION

In this work, a number of electrochemical methods were introduced for the individual and simultaneous sensing of dopamine, uric acid, and L-tyrosine. The graphite pencil electrode (GPE) was used as a working electrode. The GPE is very cost effective and readily available, as it is widely being used for writing purposes. The graphite pencil electrode surface sensitivity was enhanced using graphene as a modifying material. For this purpose, first of all, graphene oxide was chemically synthesized. The synthesized graphene oxide was characterized by FTIR and Raman spectroscopy. The morphological and electrochemical investigations of the bare and modified GPE surfaces were investigated using FE-SEM, impedance spectroscopy, and voltammetry.

The GO was reduced directly on the GPE surface using an electrochemical method. The graphene layer on the GPE surface displayed an enhanced electroactivity towards L-tyrosine, dopamine and uric acid which at a low oxidation potential. The direct reduction of IM-GO was faster and sensitive compared to the w-GO on GPE surface. The IM-rGO modified GPE has exhibited a huge electroactive surface area, and provided an excellent linear response over the range of 0.4 to 30 μM ($R^2 = 0.998$), 0.2 – 22 μM ($R^2 = 0.996$) and 0.8 - 60 μM ($R^2 = 0.9995$) for dopamine, uric acid and L-tyrosine. The enhanced signals of the analytes on the electrode indicated that the existence of the graphene on the surface of the graphite pencil electrode significantly improved the electrode's conductivity, improved the detection limits to 0.095, 0.037, 0.07 μM (S/N=3) for dopamine, uric acid and L-tyrosine, respectively. The modification took around five minutes; hence, it is the fastest modification method among the so far reported similar ones. The presence of interfering species did not affect the sensitivity of the GR-modified

GPE. The reproducibility studies indicated that the electrode fabrication process yielded a uniform clean electrode, which could be modified easily.

Furthermore, an extremely sensitive surface was fabricated based on the Pt NPs sandwiched graphene layered modified GPE. The fabrication of the sensor is very facile, and the inherent character of the GPE gave it a disposable character. The presence of Pt NPs in the graphene layers significantly enhanced the electrocatalytic oxidation of the dopamine. The fabricated sensor was found very sensitive compared to other sensors for dopamine detection with a limit of detection of 9 nM. The sensor response was linear from 0.06 to 20 μM ($R^2 = 0.9991$). The value of α and k_s was found 0.57 and 8.99 s^{-1} , respectively. The developed sensor has shown a high sensitivity, fast charge transfer response, facile fabrication, good reproducibility and at the same time is disposable. These characteristics make it a unique and promising candidate for sensing a trace level of dopamine.

The sensitivity of the GPE was further improved using alternating layer arrangements of Au NPs and graphene. It was used for the concurrent detection of DA and UA. The improvement in the electrode sensitivity after modification indicated that the graphene oxide and Au(III) GPE surface was reduced efficiently at the GPE surface. All electrode fabrication parameters were optimized to obtain the best possible response for the simultaneous measurement of DA and UA. The linear range for dopamine and uric acid detection was identified. The LOQ and LOD were lower than or that comparable to the corresponding values reported previously for graphene-based electrodes. The advanced electrochemical sensor provided a good recovery of DA and UA in a human urine

sample. The sensor displayed an excellent sensitivity and selectivity, and a good electrocatalytic activity and reproducibility.

Finally, the combination of methylene blue (MB) and graphene oxide was used to attain a conductive polymer reduced graphene oxide combination on the GPE surface. The MB-GR extended wrinkle shape layers fabricated on the surface of GPE by the spontaneous interaction of GO and MB. These extended wrinkle-shaped layers of MB-GR on GPE have extensively enhanced the electroactive surface area of GPE compared to GR-GPE. The developed sensor has shown linear range from 0.05 – 10 μM for dopamine and uric acid while for L-tyrosine observed from 0.7 – 30 μM . Very low limit of detection was achieved by MB-GR/GPE. The peak separations between DA-UA, UA-Tyr, and DA-Tyr were observed 140 mV, 319 mV, and 459 mV, respectively. The fabricated sensor has the capability to cope with potential interferences. The real sample applications have shown satisfactory recoveries of dopamine, uric acid and L-tyrosine in human urine in the range of 91 to 107%. Due to low cost, facile fabrication and very low limit of detection, the methylene blue and reduced graphene oxide modified graphite pencil electrode could be proved a valuable tool for simultaneous sensing of DA, UA, and L-tyrosine.

The developed modified GPE surfaces have shown high sensitivity, fast charge transfer response, facile fabrication, and good reproducibility. Moreover, all the modified surfaces could be used as disposable surfaces due to the fast modification process. These characteristics made the graphene and graphene nanocomposite modified GPE a unique and promising candidate for trace level quantification of dopamine, uric acid, and L-tyrosine as individual analytes or in a mixture.

References

- [1] G.-P. Jin, X.-Q. Lin, The electrochemical behavior and amperometric determination of tyrosine and tryptophan at a glassy carbon electrode modified with butyrylcholine, *Electrochem. Commun.* 6 (2004) 454–460.
- [2] A. Carlsson, M. Lindqvist, Dependence of 5-HT and catecholamine synthesis on concentrations of precursor amino-acids in rat brain, *Arch. Pharmacol.* 303 (1978) 157–164.
- [3] A. Slominski, R. Paus, Towards defining receptors for L-tyrosine and L-dopa, *Mol. Cell. Endocrinol.* 99 (1994) C7–C11.
- [4] C.C. Mabry, Joseph, C. Denniston, T.L. Nelson, C.D. Son, Maternal Phenylketonuria — A cause of mental retardation in children without the metabolic defect, *N Engl J Med* . 269 (1963) 1404–1408.
- [5] A. Sava, I. Barisone, D. Di Mauro, G. Fumagalli, C. Sala, Modulation of nicotinic acetylcholine receptor turnover by tyrosine phosphorylation in rat myotubes, *Neurosci. Lett.* 313 (2001) 37–40.
- [6] M. Miranda, C. Ligas, F. Amicarelli, E.D. Alessandro, F. Brisdelli, O. Zarivi, et al., Sister chromatid exchange (SCE) rates in human melanoma cells as an index of mutagenesis, *Mutagenesis.* 12 (1997) 233–236.
- [7] S. Meyers, Use of neurotransmitter precursors for treatment of depression, *Altern. Med. Rev.* 5 (2000) 64–71.
- [8] S. Hao, Y. Avraham, O. Bonne, E.M. Berry, Separation-induced body weight loss, impairment in alternation behavior, and autonomic tone: effects of tyrosine, *Pharmacol. Biochem. Behav.* 68 (2001) 273–281.
- [9] G.G. Huang, J. Yang, Development of infrared optical sensor for selective detection of tyrosine in biological fluids., *Biosens. Bioelectron.* 21 (2005) 408–18.
- [10] G.A. Molnar, Z. Wagner, L. Marko, T. Koszegi, M. Mohas, B. Kocsis, et al., Urinary ortho-tyrosine excretion in diabetes mellitus and renal failure : Evidence for hydroxyl radical production, *Kidney Int.* 68 (2005) 2281–2287.

- [11] R. Nie, X. Bo, H. Wang, L. Zeng, L. Guo, Chiral electrochemical sensing for tyrosine enantiomers on glassy carbon electrode modified with cysteic acid, *Electrochem. Commun.* 27 (2013) 112–115.
- [12] Z. Guo, M.-L. Seol, M.-S. Kim, J.-H. Ahn, Y.-K. Choi, J.-H. Liu, et al., Sensitive and selective electrochemical detection of dopamine using an electrode modified with carboxylated carbonaceous spheres., *Analyst.* 138 (2013) 2683–90.
- [13] L. Goldberg, Cardiovascular and renal actions of dopamine: Potential clinical applications, *Pharmacol. Rev.* 24 (1972) 1–29.
- [14] K. Jackowska, P. Kryszynski, New trends in the electrochemical sensing of dopamine., *Anal. Bioanal. Chem.* 405 (2013) 3753–3771.
- [15] A. Galvan, T. Wichmann, Pathophysiology of parkinsonism., *Clin. Neurophysiol.* 119 (2008) 1459–74.
- [16] S.H. Kollins, J.S. March, Advances in the pharmacotherapy of attention-deficit/hyperactivity disorder., *Biol. Psychiatry.* 62 (2007) 951–953.
- [17] T. Peik-See, A. Pandikumar, H. Nay-Ming, L. Hong-Ngee, Y. Sulaiman, Simultaneous electrochemical detection of dopamine and ascorbic acid using an iron oxide/reduced graphene oxide modified glassy carbon electrode., *Sensors (Basel).* 14 (2014) 15227–15243.
- [18] N.D. Volkow, G.-J. Wang, J.S. Fowler, D. Tomasi, F. Telang, Addiction: beyond dopamine reward circuitry., *Proc. Natl. Acad. Sci. U. S. A.* 108 (2011) 15037–15042.
- [19] R.N. Goyal, V.K. Gupta, A. Sangal, N. Bachheti, Voltammetric determination of uric acid at a fullerene-C60-modified glassy carbon electrode, *Electroanalysis.* 17 (2005) 2217–2223.
- [20] W.L. Nyhan, Lesch-Nyhan Disease, *Nucleosides, nucleotides and nucleic acids.* 27 (2008) 559–563.
- [21] A. Costa, I. Iguala, J. Bedini, L. Quinto, I. Conget, Uric acid concentration in subjects at risk of type 2 diabetes mellitus: Relationship to components of the

metabolic syndrome, *Metabolism*. 51 (2002) 372–375.

- [22] J.S. R. G. Robles, F. Villabla, O. G. Albarran, O. Gomez, A. Rabano, L.M. Ruilope, A. Hurtado, ORALS : Theme II : Why is there an epidemic of end stage renal disease ? and the progression of renal failure in an experimental model of type II diabetes, *Am. J. Hypertens*. 13 (2000) 36–37.
- [23] A. Dekanski, J. Stevanović, R. Stevanović, B. Ž Nikolić, V. M Jovanović, Glassy carbon electrodes I . Characterization and electrochemical activation, *Carbon N. Y.* 39 (2001) 1195–1205.
- [24] A. Kawde, N. Baig, M. Sajid, Graphite pencil electrodes as electrochemical sensors for environmental analysis : a review of features , developments , and applications, *RSC Adv*. 6 (2016) 91325–91340.
- [25] Y. Liu, X. Dong, P. Chen, Biological and chemical sensors based on graphene materials., *Chem. Soc. Rev.* 41 (2012) 2283–2307.
- [26] S. Wu, Q. He, C. Tan, Y. Wang, H. Zhang, Graphene-based electrochemical sensors., *Small*. 9 (2013) 1160–1172.
- [27] M. Rahman, N. Siraj, K. Kim, J. Lee, Selective detection of L-tyrosine in the presence of ascorbic acid, dopamine, and uric acid at poly(thionine)-modified glassy carbon electrode, *J. Electroanal. Chem.* 754 (2015) 87–93.
- [28] Y. Zhang, W. Lei, Y. Xu, X. Xia, Q. Hao, Simultaneous detection of dopamine and uric acid using a poly (L-lysine)/graphene oxide modified electrode, *Nanomaterials*. 178 (2016) 1–17.
- [29] J. Tashkhourian, M. Daneshi, S. Nami-Ana, Simultaneous determination of tyrosine and tryptophan by mesoporous silica nanoparticles modified carbon paste electrode using H-point standard addition method, *Anal. Chim. Acta*. 902 (2016) 89–96.
- [30] A.A. Ensafi, A. Arabzadeh, H. Karimi-Maleh, Simultaneous determination of dopamine and uric acid by electrocatalytic oxidation on a carbon paste electrode using pyrogallol red as a mediator, *Anal. Lett.* 43 (2010) 1976–1988.
- [31] K.S. Prasad, G. Muthuraman, J. Zen, The role of oxygen functionalities and edge

plane sites on screen-printed carbon electrodes for simultaneous determination of dopamine, uric acid and ascorbic acid, *Electrochem. Commun.* 10 (2008) 559–563.

- [32] J. Ping, J. Wu, Y. Wang, Y. Ying, Simultaneous determination of ascorbic acid, dopamine and uric acid using high-performance screen-printed graphene electrode., *Biosens. Bioelectron.* 34 (2012) 70–76.
- [33] X. Zhang, W. Yan, J. Zhang, Y. Li, W. Tang, Q. Xu, NiCo-embedded in hierarchically structured N-doped carbon nanoplates for the efficient electrochemical determination of ascorbic acid, dopamine, and uric acid, *RSC Adv.* 5 (2015) 65532–65539.
- [34] M. Sajid, M.K. Nazal, M. Mansha, A. Alsharaa, S.M.S. Jillani, C. Basheer, Chemically modified electrodes for electrochemical detection of dopamine in the presence of uric acid and ascorbic acid: A review, *TrAC - Trends Anal. Chem.* 76 (2016) 15–29.
- [35] K.P. Gong, Y.M. Yan, M.N. Zhang, L. Su, S.X. Xiong, L.Q. Mao, Electrochemistry and electroanalytical applications of carbon nanotubes: A review, *Anal. Sci.* 21 (2005) 1383–1393.
- [36] M. Trojanowicz, Analytical applications of carbon nanotubes: a review, *TrAC - Trends Anal. Chem.* 25 (2006) 480–489.
- [37] V. Datsyuk, M. Kalyva, K. Papagelis, J. Parthenios, D. Tasis, A. Siokou, et al., Chemical oxidation of multiwalled carbon nanotubes, *Carbon N. Y.* 46 (2008) 833–840.
- [38] D. Vairavapandian, P. Vichchulada, M.D. Lay, Preparation and modification of carbon nanotubes: Review of recent advances and applications in catalysis and sensing, *Anal. Chim. Acta.* 626 (2008) 119–129.
- [39] D. Tasis, N. Tagmatarchis, A. Bianco, M. Prato, Chemistry of carbon nanotubes, *Chem. Rev.* 106 (2006) 1105–1136.
- [40] T. Saito, K. Matsushige, K. Tanaka, Chemical treatment and modification of multi-walled carbon nanotubes, *Phys. B Condens. Matter.* 323 (2002) 280–283.

- [41] J.J. Gooding, Nanostructuring electrodes with carbon nanotubes: A review on electrochemistry and applications for sensing, *Electrochim. Acta.* 50 (2005) 3049–3060.
- [42] C.E. Banks, R.G. Compton, New electrodes for old: from carbon nanotubes to edge plane pyrolytic graphite, *Analyst.* 131 (2006) 15–21.
- [43] R. R. Moore, A. Craig E. Banks, R.G. Compton, Basal plane pyrolytic graphite modified electrodes: comparison of carbon nanotubes and graphite powder as electrocatalysts, *Anal. Chem.* 76 (2004) 2677–2682.
- [44] C.E. Banks, T.J. Davies, G.G. Wildgoose, R.G. Compton, Electrocatalysis at graphite and carbon nanotube modified electrodes: edge-plane sites and tube ends are the reactive sites., *Chem. Commun.* 10 (2005) 829–841.
- [45] C.E. Banks, R.R. Moore, T.J. Davies, R.G. Compton, S.P. Road, Investigation of modified basal plane pyrolytic graphite electrodes: definitive evidence for the electrocatalytic properties of the ends of carbon nanotubes, *Chem. Commun.* 2 (2004) 1804–1805.
- [46] K. Balasubramanian, M. Burghard, Biosensors based on carbon nanotubes, *Anal. Bioanal. Chem.* 385 (2006) 452–468.
- [47] H. Dai, Carbon Nanotubes: Synthesis, integration, and properties, *Acc. Chem. Res.* 35 (2002) 1035–1044.
- [48] J. Wang, Carbon-nanotube based electrochemical biosensors: A review, *Electroanalysis.* 17 (2005) 7–14.
- [49] A. Ural, Y. Li, H. Dai, Electric-field-aligned growth of single-walled carbon nanotubes on surfaces, *Appl. Phys. Lett.* 81 (2002) 3464–3466.
- [50] S. Talapatra, S. Kar, S.K. Pal, R. Vajtai, L. Ci, P. Victor, et al., Direct growth of aligned carbon nanotubes on bulk metals:, *Nat. Nanotechnol.* 1 (2006) 112–116.
- [51] J. Manso, M.L. Mena, P. Yáñez-Sedeño, J. Pingarrón, Electrochemical biosensors based on colloidal gold–carbon nanotubes composite electrodes, *J. Electroanal. Chem.* 603 (2007) 1–7.

- [52] R.H. Baughman, A.A. Zakhidov, W.A. de Heer, W. Liang, S.P. Frank, P. Poncharal, et al., Carbon nanotubes--the route toward applications., *Science*. 297 (2002) 787–792.
- [53] M. Yang, Y. Yang, Y. Liu, G. Shen, R. Yu, Platinum nanoparticles-doped sol-gel/carbon nanotubes composite electrochemical sensors and biosensors, *Biosens. Bioelectron*. 21 (2006) 1125–1131.
- [54] J. Wang, M. Musameh, Carbon nanotube/teflon composite electrochemical Sensors and Biosensors, *Anal. Chem*. 75 (2003) 2075–2079.
- [55] C. Wang, R. Yuan, Y. Chai, S. Chen, Y. Zhang, F. Hu, et al., Non-covalent iron(III)-porphyrin functionalized multi-walled carbon nanotubes for the simultaneous determination of ascorbic acid, dopamine, uric acid and nitrite, *Electrochim. Acta*. 62 (2012) 109–115.
- [56] M. Noroozifar, M. Khorasani-Motlagh, R. Akbari, M. Bemanadi Parizi, Simultaneous and sensitive determination of a quaternary mixture of AA, DA, UA and Trp using a modified GCE by iron ion-doped natrolite zeolite-multiwall carbon nanotube., *Biosens. Bioelectron*. 28 (2011) 56–63.
- [57] E.B. Bahadır, M.K. Sezgintürk, Applications of graphene in electrochemical sensing and biosensing, *TrAC Trends Anal. Chem*. 76 (2016) 1–14.
- [58] R. Zhang, W. Chen, Recent advances in graphene-based nanomaterials for fabricating electrochemical hydrogen peroxide sensors, *Biosens. Bioelectron*. (2016).
- [59] D. Chen, H. Feng, J. Li, Graphene oxide : Preparation , functionalization , and electrochemical applications, *Chem. Rev*. 112 (2012) 6027–6053.
- [60] J. Ping, Y. Zhou, Y. Wu, V. Papper, S. Boujday, R.S. Marks, et al., Recent advances in aptasensors based on graphene and graphene-like nanomaterials, *Biosens. Bioelectron*. 64 (2015) 373–385.
- [61] M. Zhou, Y. Zhai, S. Dong, Electrochemical sensing and biosensing platform based on chemically reduced graphene oxide., *Anal. Chem*. 81 (2009) 5603–5613.
- [62] X. Xiao, P.R. Miller, R.J. Narayan, S.M. Brozik, D.R. Wheeler, I. Brener, et al.,

- Simultaneous detection of dopamine , ascorbic acid and uric acid at lithographically-defined 3D graphene electrodes, *Electroanalysis*. 26 (2014) 52–56.
- [63] V. Singh, D. Joung, L. Zhai, S. Das, S.I. Khondaker, S. Seal, Graphene based materials: Past, present and future, *Prog. Mater. Sci.* 56 (2011) 1178–1271.
- [64] J. William S. Hummers, R.E. Offeman, Preparation of graphitic oxide, *J. Am. Chem. Soc.* 80 (1958) 1339.
- [65] S.K. Vashist, J.H.T. Luong, Recent advances in electrochemical biosensing schemes using graphene and graphene-based nanocomposites, *Carbon N. Y.* 84 (2015) 519–550.
- [66] N. Baig, A.-N. Kawde, A novel, fast and cost effective graphene-modified graphite pencil electrode for trace quantification of L-tyrosine, *Anal. Methods*. 7 (2015) 9535–9541.
- [67] L. Li, F. Yan, G. Xue, Preparation of a porous conducting polymer film by electrochemical synthesis-solvent extraction method, *J. Appl. Polym. Sci.* 91 (2004) 303–307.
- [68] D.E. Labaye, C. Jérôme, V.M. Geskin, P. Louette, R. Lazzaroni, L. Martinot, et al., Full Electrochemical synthesis of conducting polymer films chemically grafted to conducting surfaces, *Langmuir*. 18 (2002) 5222–5230.
- [69] R.-M. Latonen, C. Kvarnström, A. Ivaska, Electrochemical preparation of oligo(azulene) on nanoporous TiO₂ and characterization of the composite layer, *J. Appl. Electrochem.* 40 (2010) 1583–1591.
- [70] R.J. Waltman, J. Bargon, Electrically conducting polymers: a review of the electropolymerization reaction, of the effects of chemical structure on polymer film properties, and of applications towards technology, *Can. J. Chem.* 64 (1986) 76–95.
- [71] J.V. Grazulevicius, P. Strohhriegl, J. Pielichowski, K. Pielichowski, Carbazole-containing polymers: synthesis, properties and applications, *Prog. Polym. Sci.* 28 (2003) 1297–1353.

- [72] M. Quinto, A.J. Bard, Polymer films on electrodes: Part 29. Electropolymerized poly(7,14-diphenylacenaphtho[1,2-k]fluoranthene): Electrochemistry and conductance of a novel electrochromic hydrocarbon ladder polymer film, *J. Electroanal. Chem.* 498 (2001) 67–74.
- [73] M.A. Del Valle, F.R. Díaz, M.E. Bordini, T. Pizarro, R. Córdova, H. Gómez, et al., Polythiophene, polyaniline and polypyrrole electrodes modified by electrodeposition of Pt and Pt+Pb for formic acid electrooxidation, *J. Appl. Electrochem.* 28 (1998) 943–946.
- [74] L. Zeng, Z. Le, J. Xu, H. Liu, F. Zhao, S. Pu, Electrochemical polymerization of 9-phenylcarbazole in mixed electrolytes of boron trifluoride diethyl etherate and sulfuric acid, *J. Mater. Sci.* 43 (2008) 1135–1143.
- [75] K.C. Persaud, Polymers for chemical sensing, *Mater. Today.* 8 (2005) 38–44.
- [76] A.G. MacDiarmid, Synthetic metals: a novel role for organic polymers, *Synth. Met.* 125 (2001) 11–22.
- [77] J.D. Stenger-Smith, Intrinsically electrically conducting polymers. Synthesis, characterization, and their applications, *Prog. Polym. Sci.* 23 (1998) 57–79.
- [78] M. Gerard, A. Chaubey, B.D. Malhotra, Application of conducting polymers to biosensors, *Biosens. Bioelectron.* 17 (2002) 345–359.
- [79] A. Michalska, J. Dumańska, K. Maksymiuk, Lowering the detection limit of ion-selective plastic membrane electrodes with conducting polymer solid contact and conducting polymer potentiometric sensors, *Anal. Chem.* 75 (2003) 4964–4974.
- [80] X. Yang, A. Liu, Y. Zhao, H. Lu, Y. Zhang, W. Wei, et al., Three-dimensional macroporous polypyrrole-derived graphene electrode prepared by the hydrogen bubble dynamic template for supercapacitors and metal-free catalysts, *ACS Appl. Mater. Interfaces.* 7 (2015) 23731–23740.
- [81] M. Raicopol, C. Andronescu, R. Atasiei, A. Hanganu, A.M. Manea, I. Rau, et al., Synthesis of conducting azopolymers by electrochemical grafting of a diazonium salt at polypyrrole electrodes, *Synth. Met.* 206 (2015) 84–91.
- [82] K.E. Feldman, D.C. Martin, Functional conducting polymers via thiol-ene

chemistry., *Biosensors*. 2 (2012) 305–317.

- [83] C. Tengstedt, W. Osikowicz, W.R. Salaneck, I.D. Parker, C.-H. Hsu, M. Fahlman, Fermi-level pinning at conjugated polymer interfaces, *Appl. Phys. Lett.* 88 (2006) 0535021–0535023.
- [84] J. Janata, M. Josowicz, Conducting polymers in electronic chemical sensors, *Nat. Mater.* 2 (2003) 19–24.
- [85] J.L. Bredas, G.B. Street, Polarons, bipolarons, and solitons in conducting polymers, *Acc. Chem. Res.* 18 (1985) 309–315.
- [86] Z.H. Wang, E.M. Scherr, A.G. MacDiarmid, A.J. Epstein, Transport and EPR studies of polyaniline: A quasi-one-dimensional conductor with three-dimensional “metallic” states, *Phys. Rev. B.* 45 (1992) 4190–4202.
- [87] A.G. Macdiarmid, A.J. Epstein, Secondary doping: A new concept in conducting polymers, *Macromol. Symp.* 98 (1995) 835–842.
- [88] K. Low, C.B. Horner, C. Li, G. Ico, W. Bosze, N. V. Myung, et al., Composition-dependent sensing mechanism of electrospun conductive polymer composite nanofibers, *Sensors Actuators B Chem.* 207 (2015) 235–242.
- [89] C.M. Hangarter, N. Chartuprayoon, S.C. Hernández, Y. Choa, N. V. Myung, Hybridized conducting polymer chemiresistive nano-sensors, *Nano Today.* 8 (2013) 39–55.
- [90] P. Kumar, S. Saravanan, K. Ranjith, P.C. Ramamurthy, D–A–D-structured conducting polymer-modified electrodes for detection of lead(II) ions in water, *J. Appl. Electrochem.* 44 (2014) 133–139.
- [91] C.A. Lindino, M. Casagrande, A. Peiter, C. Ribeiro, Poly(o-methoxyaniline) modified electrode for detection of lithium ions, *Quim. Nova.* 35 (2012) 449–453.
- [92] D. Wei, A. Ivaska, Applications of ionic liquids in electrochemical sensors, *Anal. Chim. Acta.* 607 (2008) 126–135.
- [93] M.J. Shiddiky, A.A. Torriero, Application of ionic liquids in electrochemical sensing systems, *Biosens. Bioelectron.* 26 (2011) 1775–1787.

- [94] D.R. MacFarlane, N. Tachikawa, M. Forsyth, J.M. Pringle, P.C. Howlett, G.D. Elliott, et al., Energy applications of ionic liquids, *Energy Environ. Sci.* 7 (2014) 232–250.
- [95] A. Abo-hamad, M. Abdulhakim, M. Hayyan, I. Juneidi, M. Ali, Ionic liquid-carbon nanomaterial hybrids for electrochemical sensor applications : A review, *Electrochim. Acta.* 193 (2016) 321–343.
- [96] M. Opallo, A. Lesniewski, A review on electrodes modified with ionic liquids, *J. Electroanal. Chem.* 656 (2011) 2–16.
- [97] T.D. Ho, C. Zhang, L.W. Hantao, J.L. Anderson, Ionic liquids in analytical chemistry: Fundamentals, advances, and perspectives, *Anal. Chem.* 86 (2014) 262–285.
- [98] C.B. Jacobs, M.J. Peairs, B.J. Venton, Review: Carbon nanotube based electrochemical sensors for biomolecules., *Anal. Chim. Acta.* 662 (2010) 105–27.
- [99] R.H. Baughman, A.A. Zakhidov, W.A. de Heer, Carbon nanotubes--the route toward applications., *Science.* 297 (2002) 787–792.
- [100] L.-C. Jiang, W.-D. Zhang, A highly sensitive nonenzymatic glucose sensor based on CuO nanoparticles-modified carbon nanotube electrode., *Biosens. Bioelectron.* 25 (2010) 1402–1407.
- [101] Y. Zhao, Y. Gao, D. Zhan, H. Liu, Q. Zhao, Y. Kou, et al., Selective detection of dopamine in the presence of ascorbic acid and uric acid by a carbon nanotubes-ionic liquid gel modified electrode., *Talanta.* 66 (2005) 51–57.
- [102] C.-L. Sun, C.-T. Chang, H.-H. Lee, J. Zhou, J. Wang, T.-K. Sham, et al., Microwave-assisted synthesis of a core-shell MWCNT/GONR heterostructure for the electrochemical detection of ascorbic acid, dopamine, and uric acid., *ACS Nano.* 5 (2011) 7788–7795.
- [103] S.M. Ghoreishi, M. Behpour, S. Mousavi, A. Khoobi, F.S. Ghoreishi, Simultaneous electrochemical determination of dopamine, ascorbic acid and uric acid in the presence of sodium dodecyl sulphate using a multi-walled carbon nanotube modified carbon paste electrode, *RSC Adv.* 4 (2014) 37979–37984.

- [104] C. Dekker, Carbon nanotubes As molecular quantum wires, *Phys. Today*. 52 (1999) 22–28.
- [105] B. Xu, Q. Song, H. Wang, Simultaneous determination of ascorbic acid, dopamine, and uric acid based on double-walled carbon nanotubes/choline-modified electrode, *Anal. Methods*. 5 (2013) 2335–2342.
- [106] B. Zhang, D. Huang, X. Xu, G. Alemu, Y. Zhang, F. Zhan, et al., Simultaneous electrochemical determination of ascorbic acid, dopamine and uric acid with helical carbon nanotubes, *Electrochim. Acta*. 91 (2013) 261–266.
- [107] S. Zhu, H. Li, W. Niu, G. Xu, Simultaneous electrochemical determination of uric acid, dopamine, and ascorbic acid at single-walled carbon nanohorn modified glassy carbon electrode., *Biosens. Bioelectron.* 25 (2009) 940–943.
- [108] J. Prasek, J. Drbohlavova, J. Chomoucka, J. Hubalek, O. Jasek, V. Adam, et al., Methods for carbon nanotubes synthesis—review, *J. Mater. Chem.* 21 (2011) 15872–15884.
- [109] Z. Shi, Y. Lian, F.H. Liao, X. Zhou, Z. Gu, Y. Zhang, et al., Large scale synthesis of single-wall carbon nanotubes by arc-discharge method, *J. Phys. Chem. Solids*. 61 (2000) 1031–1036.
- [110] A.A. Puretzky, D.B. Geohegan, X. Fan, S.J. Pennycook, In situ imaging and spectroscopy of single-wall carbon nanotube synthesis by laser vaporization, *Appl. Phys. Lett.* 76 (2000) 182–184.
- [111] N. Braidy, M. El Khakani, G. Botton, Single-wall carbon nanotubes synthesis by means of UV laser vaporization, *Chem. Phys. Lett.* 354 (2002) 88–92.
- [112] J. Kong, A.M. Cassell, H. Dai, Chemical vapor deposition of methane for single-walled carbon nanotubes, *Chem. Phys. Lett.* 292 (1998) 567–574.
- [113] M. Kumar, Y. Ando, Chemical vapor deposition of carbon nanotubes: A review on growth mechanism and mass production, *J. Nanosci. Nanotechnol.* 10 (2010) 3739–3758.
- [114] I.A. Novoselova, N.F. Oliinyk, S.V. Volkov, A.A. Konchits, I.B. Yanchuk, V.S.

Yefanov, et al., Electrolytic synthesis of carbon nanotubes from carbon dioxide in molten salts and their characterization, *Phys. E Low-Dimensional Syst. Nanostructures*. 40 (2008) 2231–2237.

- [115] H. Bi, Y. Li, S. Liu, P. Guo, Z. Wei, C. Lv, et al., Carbon-nanotube-modified glassy carbon electrode for simultaneous determination of dopamine, ascorbic acid and uric acid: The effect of functional groups, *Sensors Actuators B Chem.* 171-172 (2012) 1132–1140.
- [116] Z. Dursun, B. Gelmez, Simultaneous determination of ascorbic acid, dopamine and uric acid at Pt nanoparticles decorated multiwall carbon nanotubes modified GCE, *Electroanalysis*. 22 (2010) 1106–1114.
- [117] H. Filik, A.A. Avan, S. Aydar, Simultaneous detection of ascorbic acid, dopamine, uric acid and tryptophan with Azure A-interlinked multi-walled carbon nanotube/gold nanoparticles composite modified electrode, *Arab. J. Chem.* 9 (2016) 471–480.
- [118] W. Zhang, R. Yuan, Y.-Q. Chai, Y. Zhang, S.-H. Chen, A simple strategy based on lanthanum–multiwalled carbon nanotube nanocomposites for simultaneous determination of ascorbic acid, dopamine, uric acid and nitrite, *Sensors Actuators B Chem.* 166-167 (2012) 601–607.
- [119] K. Deng, X. Li, H. Huang, A glassy carbon electrode modified with a nickel(II) norcorrole complex and carbon nanotubes for simultaneous or individual determination of ascorbic acid, dopamine, and uric acid, *Microchim. Acta.* 183 (2016) 2139–2145.
- [120] S. Yan, X. Li, Y. Xiong, M. Wang, L. Yang, X. Liu, et al., Simultaneous determination of ascorbic acid, dopamine and uric acid using a glassy carbon electrode modified with the nickel(II)-bis(1,10-phenanthroline) complex and single-walled carbon nanotubes, *Microchim. Acta.* 183 (2016) 1401–1408.
- [121] H. Li, Y. Wang, D. Ye, J. Luo, B. Su, S. Zhang, et al., An electrochemical sensor for simultaneous determination of ascorbic acid, dopamine, uric acid and tryptophan based on MWNTs bridged mesocellular graphene foam nanocomposite., *Talanta*. 127 (2014) 255–261.
- [122] K.C. Lin, J.Y. Huang, S.M. Chen, Simultaneous determination of ascorbic acid, dopamine, uric acid and hydrogen peroxide based on co-immobilization of PEDOT and FAD using multi-walled carbon nanotubes, *Anal. Methods*. 6 (2014)

8321–8327.

- [123] L.V. da Silva, F.A.S. Silva, L.T. Kubota, C.B. Lopes, P.R. Lima, E.O. Costa, et al., Amperometric sensor based on carbon nanotubes and electropolymerized vanillic acid for simultaneous determination of ascorbic acid, dopamine, and uric acid, *J. Solid State Electrochem.* 20 (2016) 2389–2393.
- [124] B. Habibi, M.H. Pournaghi-Azar, Simultaneous determination of ascorbic acid, dopamine and uric acid by use of a MWCNT modified carbon-ceramic electrode and differential pulse voltammetry, *Electrochim. Acta.* 55 (2010) 5492–5498.
- [125] S. Kochmann, T. Hirsch, O.S. Wolfbeis, Graphenes in chemical sensors and biosensors, *Trends Anal. Chem.* 39 (2012) 87–113.
- [126] B. Yang, H. Wang, J. Du, Y. Fu, P. Yang, Y. Du, Direct electrodeposition of reduced graphene oxide on carbon fiber electrode for simultaneous determination of ascorbic acid, dopamine and uric acid, *Colloids Surfaces A Physicochem. Eng. Asp.* 456 (2014) 146–152.
- [127] H. Wang, F. Ren, C. Wang, B. Yang, D. Bin, K. Zhang, et al., Simultaneous determination of dopamine, uric acid and ascorbic acid using a glassy carbon electrode modified with reduced graphene oxide, *RSC Adv.* 4 (2014) 26895–26901.
- [128] P.K. Aneesh, S.R. Nambiar, T.P. Rao, A. Ajayaghosh, Electrochemically synthesized partially reduced graphene oxide modified glassy carbon electrode for individual and simultaneous voltammetric determination of ascorbic acid, dopamine and uric acid, *Anal. Methods.* 6 (2014) 5322–5330.
- [129] D. Zhang, L. Li, W. Ma, X. Chen, Y. Zhang, Electrodeposited reduced graphene oxide incorporating polymerization of L -lysine on electrode surface and its application in simultaneous electrochemical determination of ascorbic acid , dopamine and uric acid, *Mater. Sci. Eng. C.* 70 (2017) 241–249.
- [130] C. Liu, K. Wang, S. Luo, Y. Tang, L. Chen, Direct electrodeposition of graphene enabling the one-step synthesis of graphene-metal nanocomposite films, *Small.* 7 (2011) 1203–1206.
- [131] H. Zhang, P. Gai, R. Cheng, L. Wu, X. Zhang, J. Chen, Self-assembly synthesis of a hierarchical structure using hollow nitrogen-doped carbon spheres as spacers to

separate the reduced graphene oxide for simultaneous electrochemical determination of ascorbic acid, dopamine and uric acid, *Anal. Methods*. 5 (2013) 3591–3600.

- [132] S.M. Li, S.Y. Yang, Y.S. Wang, C.H. Lien, H.W. Tien, S.T. Hsiao, et al., Controllable synthesis of nitrogen-doped graphene and its effect on the simultaneous electrochemical determination of ascorbic acid, dopamine, and uric acid, *Carbon N. Y.* 59 (2013) 418–429.
- [133] Z.-H. Sheng, X.-Q. Zheng, J.-Y. Xu, W.-J. Bao, F.-B. Wang, X.-H. Xia, Electrochemical sensor based on nitrogen doped graphene: Simultaneous determination of ascorbic acid, dopamine and uric acid, *Biosens. Bioelectron.* 34 (2012) 125–131.
- [134] T.-Q. Xu, Q.-L. Zhang, J.-N. Zheng, Z.-Y. Lv, J. Wei, A.-J. Wang, et al., Simultaneous determination of dopamine and uric acid in the presence of ascorbic acid using Pt nanoparticles supported on reduced graphene oxide, *Electrochim. Acta.* 115 (2014) 109–115.
- [135] X. Wang, M. Wu, W. Tang, Y. Zhu, L. Wang, Q. Wang, et al., Simultaneous electrochemical determination of ascorbic acid, dopamine and uric acid using a palladium nanoparticle/graphene/chitosan modified electrode, *J. Electroanal. Chem.* 695 (2013) 10–16.
- [136] S.-M. Li, Y.-S. Wang, S.-T. Hsiao, W.-H. Liao, C.-W. Lin, S.-Y. Yang, et al., Fabrication of a silver nanowire-reduced graphene oxide-based electrochemical biosensor and its enhanced sensitivity in the simultaneous determination of ascorbic acid, dopamine, and uric acid, *J. Mater. Chem. C* 3 (2015) 9444–9453.
- [137] B. Kaur, T. Pandiyan, B. Satpati, R. Srivastava, Simultaneous and sensitive determination of ascorbic acid, dopamine, uric acid, and tryptophan with silver nanoparticles-decorated reduced graphene oxide modified electrode., *Colloids Surf. B. Biointerfaces.* 111 (2013) 97–106.
- [138] C. Wang, F. Ye, H. Wu, Y. Qian, Depositing Au nanoparticles onto graphene sheets for simultaneous electrochemical detection ascorbic acid, dopamine and uric acid, *Int. J. Electrochem. Sci.* 8 (2013) 2440–2448.
- [139] Q. Zhu, J. Bao, D. Huo, M. Yang, C. Hou, J. Guo, et al., 3D Graphene hydrogel – gold nanoparticles nanocomposite modified glassy carbon electrode for the simultaneous determination of ascorbic acid , dopamine and uric acid, *Sensors*

Actuators B Chem. 238 (2017) 1316–1323.

- [140] H. Imran, P.N. Manikandan, V. Dharuman, Facile and green synthesis of graphene oxide by electrical exfoliation of pencil graphite and gold nanoparticle for non-enzymatic simultaneous sensing of ascorbic acid, dopamine and uric acid, RSC Adv. 5 (2015) 63513–63520.
- [141] L.-X. Chen, J.-N. Zheng, A.-J. Wang, L.-J. Wu, J.-R. Chen, J.-J. Feng, Facile synthesis of porous bimetallic alloyed PdAg nanoflowers supported on reduced graphene oxide for simultaneous detection of ascorbic acid, dopamine, and uric acid, Analyst. 140 (2015) 3183–3192.
- [142] J. Jiang, X. Du, Sensitive electrochemical sensors for simultaneous determination of ascorbic acid, dopamine, and uric acid based on Au@Pd-reduced graphene oxide nanocomposites., Nanoscale. 6 (2014) 11303–11309.
- [143] W. He, H. Jiang, Y. Zhou, S. Yang, X. Xue, Z. Zou, et al., An efficient reduction route for the production of Pd-Pt nanoparticles anchored on graphene nanosheets for use as durable oxygen reduction electrocatalysts, Carbon N. Y. 50 (2012) 265–274.
- [144] J. Yan, S. Liu, Z. Zhang, G. He, P. Zhou, H. Liang, et al., Simultaneous electrochemical detection of ascorbic acid, dopamine and uric acid based on graphene anchored with Pd-Pt nanoparticles., Colloids Surf. B. Biointerfaces. 111 (2013) 392–397.
- [145] Y.-L. Xie, J. Yuan, H.-L. Ye, P. Song, S.-Q. Hu, Facile ultrasonic synthesis of graphene/SnO₂ nanocomposite and its application to the simultaneous electrochemical determination of dopamine, ascorbic acid, and uric acid, J. Electroanal. Chem. 749 (2015) 26–30.
- [146] D. Wu, Y. Li, Y. Zhang, P. Wang, Q. Wei, B. Du, Sensitive electrochemical sensor for simultaneous determination of dopamine, ascorbic acid, and uric acid enhanced by amino-group functionalized mesoporous Fe₃O₄@graphene sheets, Electrochim. Acta. 116 (2014) 244–249.
- [147] H. Wang, H. Feng, J. Li, Graphene and graphene-like layered transition metal dichalcogenides in energy conversion and storage, Small. 10 (2014) 2165–2181.
- [148] H. Bagheri, N. Pajoohehpour, B. Jamali, S. Amidi, A. Hajian, H. Khoshafar, A

novel electrochemical platform for sensitive and simultaneous determination of dopamine, uric acid and ascorbic acid based on Fe₃O₄-SnO₂-Gr Ternary nanocomposite, *Microchem. J.* 131 (2017) 120–129.

- [149] J. Huang, L. Ye, X. Gao, H. Li, J. Xu, Z. Li, Molybdenum disulfide-based amplified fluorescence DNA detection using hybridization chain reactions, *J. Mater. Chem. B.* 3 (2015) 2395–2401.
- [150] J. Ge, E.C. Ou, R.Q. Yu, X. Chu, A novel aptameric nanobiosensor based on the self-assembled DNA-MoS₂ nanosheet architecture for biomolecule detection, *J. Mater. Chem. B.* 2 (2014) 625–628.
- [151] S. Su, J. Chao, D. Pan, L. Wang, C. Fan, Electrochemical sensors using two-dimensional layered nanomaterials, *Electroanalysis.* 27 (2015) 1062–1072.
- [152] L. Xing, Z. Ma, A glassy carbon electrode modified with a nanocomposite consisting of MoS₂ and reduced graphene oxide for electrochemical simultaneous determination of ascorbic acid, dopamine, and uric acid, *Microchim. Acta.* 183 (2016) 257–263.
- [153] M.H. Parvin, Simultaneous Determination of Ascorbic Acid, Dopamine and Uric Acid, at a Graphene Paste Electrode Modified with Functionalized Graphene Sheets, *Electroanalysis.* 27 (2015) 1394–1402.
- [154] H.L. Zou, B.L. Li, H.Q. Luo, N.B. Li, A novel electrochemical biosensor based on hemin functionalized graphene oxide sheets for simultaneous determination of ascorbic acid, dopamine and uric acid, *Sensors Actuators B Chem.* 207 (2015) 535–541.
- [155] Y.J. Yang, One-pot synthesis of reduced graphene oxide/zinc sulfide nanocomposite at room temperature for simultaneous determination of ascorbic acid, dopamine and uric acid, *Sensors Actuators B Chem.* 221 (2015) 750–759.
- [156] A.A. Abdelwahab, Y.-B. Shim, Simultaneous determination of ascorbic acid, dopamine, uric acid and folic acid based on activated graphene/MWCNT nanocomposite loaded Au nanoclusters, *Sensors Actuators B Chem.* 221 (2015) 659–665.
- [157] L. Zhao, H. Li, S. Gao, M. Li, S. Xu, C. Li, et al., MgO nanobelt-modified graphene-tantalum wire electrode for the simultaneous determination of ascorbic

acid, dopamine and uric acid, *Electrochim. Acta.* 168 (2015) 191–198.

- [158] S. Wang, W. Zhang, X. Zhong, Y. Chai, R. Yuan, Simultaneous determination of dopamine, ascorbic acid and uric acid using a multi-walled carbon nanotube and reduced graphene oxide hybrid functionalized by PAMAM and Au nanoparticles, *Anal. Methods.* 7 (2015) 1471–1477.
- [159] T.E.M. Nancy, V.A. Kumary, Synergistic electrocatalytic effect of graphene/nickel hydroxide composite for the simultaneous electrochemical determination of ascorbic acid, dopamine and uric acid, *Electrochim. Acta.* 133 (2014) 233–240.
- [160] Q. Lian, Z. He, Q. He, A. Luo, K. Yan, D. Zhang, et al., Simultaneous determination of ascorbic acid, dopamine and uric acid based on tryptophan functionalized graphene., *Anal. Chim. Acta.* 823 (2014) 32–39.
- [161] C. Wang, J. Du, H. Wang, C. Zou, F. Jiang, P. Yang, et al., A facile electrochemical sensor based on reduced graphene oxide and Au nanoplates modified glassy carbon electrode for simultaneous detection of ascorbic acid, dopamine and uric acid, *Sensors Actuators B Chem.* 204 (2014) 302–309.
- [162] W. Zhang, Y. Chai, R. Yuan, S. Chen, J. Han, D. Yuan, Facile synthesis of graphene hybrid tube-like structure for simultaneous detection of ascorbic acid, dopamine, uric acid and tryptophan, *Anal. Chim. Acta.* 756 (2012) 7–12.
- [163] S. Ramakrishnan, K.R. Pradeep, A. Raghul, R. Senthilkumar, M. Rangarajan, N.K. Kothurkar, One-step synthesis of Pt-decorated graphene–carbon nanotubes for the electrochemical sensing of dopamine, uric acid and ascorbic acid, *Anal. Methods.* 7 (2015) 779–786.
- [164] E. Kharlampieva, V. Kozlovskaya, S.A. Sukhishvili, Layer-by-layer hydrogen-bonded polymer films: From fundamentals to applications, *Adv. Mater.* 21 (2009) 3053–3065.
- [165] E. Michael, G. Lyons, *Electroactive polymer electrochemistry part 2: Methods and applications*, Springer, 1996.
- [166] L.C. Clark, C. Lyons, Electrode systems for continuous monitoring in cardiovascular surgery, *Ann. N. Y. Acad. Sci.* 102 (1962) 29–45.

- [167] A. Ensafi, M. Taei, T. Khayamian, A. Arabzadeh, Highly selective determination of ascorbic acid, dopamine, and uric acid by differential pulse voltammetry using poly(sulfonazo III) modified glassy carbon electrode, *Sensors Actuators B Chem.* 147 (2010) 213–221.
- [168] M.D. Rubianes, G.A. Rivas, Highly selective dopamine quantification using a glassy carbon electrode modified with a melanin-type polymer, *Anal. Chim. Acta.* 440 (2001) 99–108.
- [169] D.-W. Wang, F. Li, J. Zhao, W. Ren, Z.-G. Chen, J. Tan, et al., Fabrication of graphene/polyaniline composite paper via in situ anodic electropolymerization for high-performance flexible electrode., *ACS Nano.* 3 (2009) 1745–1752.
- [170] A. Rana, A. Kawde, Open-circuit electrochemical polymerization for the sensitive detection of phenols, *Electroanalysis.* 28 (2016) 898–902.
- [171] F. Darain, S.-U. Park, Y.-B. Shim, Disposable amperometric immunosensor system for rabbit IgG using a conducting polymer modified screen-printed electrode, *Biosens. Bioelectron.* 18 (2003) 773–780.
- [172] M. Albareda-Sirvent, A. Merkoçi, S. Alegret, Configurations used in the design of screen-printed enzymatic biosensors. A review, *Sensors Actuators B Chem.* 69 (2000) 153–163.
- [173] K. Norrman, A. Ghanbari-Siahkali, N.B. Larsen, 6 Studies of spin-coated polymer films, *Annu. Reports Sect. "C" (Physical Chem.* 101 (2005) 174–201.
- [174] G. Harsányi, Polymer films in sensor applications: a review of present uses and future possibilities, *Sens. Rev.* 20 (2000) 98–105.
- [175] C. Zhao, L.-Y. Li, M.-M. Guo, J. Zheng, Functional polymer thin films designed for antifouling materials and biosensors, *Chem. Pap.* 66 (2012) 323–339.
- [176] P. Kalimuthu, S.A. John, Electropolymerized film of functionalized thiadiazole on glassy carbon electrode for the simultaneous determination of ascorbic acid, dopamine and uric acid, *Bioelectrochemistry.* 77 (2009) 13–18.
- [177] P. Kalimuthu, S.A. John, Simultaneous determination of ascorbic acid, dopamine, uric acid and xanthine using a nanostructured polymer film modified electrode.,

Talanta. 80 (2010) 1686–1691.

- [178] H. Yao, Y. Sun, X. Lin, Y. Tang, L. Huang, Electrochemical characterization of poly(eriochrome black T) modified glassy carbon electrode and its application to simultaneous determination of dopamine, ascorbic acid and uric acid, *Electrochim. Acta.* 52 (2007) 6165–6171.
- [179] R. Zhang, G.-D. Jin, D. Chen, X.-Y. Hu, Simultaneous electrochemical determination of dopamine, ascorbic acid and uric acid using poly(acid chrome blue K) modified glassy carbon electrode, *Sensors Actuators B Chem.* 138 (2009) 174–181.
- [180] L. Lin, J. Chen, H. Yao, Y. Chen, Y. Zheng, X. Lin, Simultaneous determination of dopamine, ascorbic acid and uric acid at poly (Evans Blue) modified glassy carbon electrode, *Bioelectrochemistry.* 73 (2008) 11–17.
- [181] A.A. Ensafi, M. Taei, T. Khayamian, A differential pulse voltammetric method for simultaneous determination of ascorbic acid, dopamine, and uric acid using poly (3-(5-chloro-2-hydroxyphenylazo)-4,5-dihydroxynaphthalene-2,7-disulfonic acid) film modified glassy carbon electrode, *J. Electroanal. Chem.* 633 (2009) 212–220.
- [182] M. Mazloun-Ardakani, M.A. Sheikh-Mohseni, A. Benvidi, Electropolymerization of thin film conducting polymer and its application for simultaneous determination of ascorbic acid, dopamine and uric acid, *Electroanalysis.* 23 (2011) 2822–2831.
- [183] X. Zheng, X. Zhou, X. Ji, R. Lin, W. Lin, Simultaneous determination of ascorbic acid, dopamine and uric acid using poly(4-aminobutyric acid) modified glassy carbon electrode, *Sensors Actuators B Chem.* 178 (2013) 359–365.
- [184] X. Zheng, Y. Guo, J. Zheng, X. Zhou, Q. Li, R. Lin, Simultaneous determination of ascorbic acid, dopamine and uric acid using poly(L-leucine)/DNA composite film modified electrode, *Sensors Actuators B Chem.* 213 (2015) 188–194.
- [185] Y. Wang, C. Bi, Simultaneous electrochemical determination of ascorbic acid, dopamine and uric acid using poly (tyrosine)/functionalized multi-walled carbon nanotubes composite film modified electrode, *J. Mol. Liq.* 177 (2013) 26–31.
- [186] G. Zhang, P. He, W. Feng, S. Ding, J. Chen, L. Li, et al., Carbon nanohorns/poly(glycine) modified glassy carbon electrode: Preparation,

characterization and simultaneous electrochemical determination of uric acid, dopamine and ascorbic acid, *J. Electroanal. Chem.* 760 (2016) 24–31.

- [187] K. Ghanbari, N. Hajheidari, ZnO–Cu_xO/polypyrrole nanocomposite modified electrode for simultaneous determination of ascorbic acid, dopamine, and uric acid, *Anal. Biochem.* 473 (2015) 53–62.
- [188] K. Ghanbari, N. Hajheidari, Simultaneous electrochemical determination of dopamine, uric acid and ascorbic acid using silver nanoparticles deposited on polypyrrole nanofibers, *J. Polym. Res.* 22 (2015) 152. doi:10.1007/s10965-015-0797-0.
- [189] C. Wang, X. Zou, X. Zhao, Q. Wang, J. Tan, R. Yuan, Cu-nanoparticles incorporated overoxidized-poly(3-amino-5-mercapto-1,2,4-triazole) film modified electrode for the simultaneous determination of ascorbic acid, dopamine, uric acid and tryptophan, *J. Electroanal. Chem.* 741 (2015) 36–41.
- [190] C. Wang, R. Yuan, Y. Chai, Y. Zhang, F. Hu, M. Zhang, Au-nanoclusters incorporated 3-amino-5-mercapto-1,2,4-triazole film modified electrode for the simultaneous determination of ascorbic acid, dopamine, uric acid and nitrite., *Biosens. Bioelectron.* 30 (2011) 315–319.
- [191] Y. Zhang, W. Ren, S. Zhang, Simultaneous determination of epinephrine, dopamine, ascorbic acid and uric acid by polydopamine-nanogold composites modified electrode, *Int. J. Electrochem. Sci.* 8 (2013) 6839–6850.
- [192] S. Palanisamy, Polydopamine supported gold nanoclusters for sensitive and simultaneous detection of dopamine in the presence of excess ascorbic acid and uric acid, *Electrochim. Acta.* 138 (2014) 302–310.
- [193] E.A. Khudaish, K.Y. Al-Ajmi, S.H. Al-Harhi, A solid-state sensor based on ruthenium (II) complex immobilized on polytyramine film for the simultaneous determination of dopamine, ascorbic acid and uric acid, *Thin Solid Films.* 564 (2014) 390–396.
- [194] S. Yu, C. Luo, L. Wang, H. Peng, Z. Zhu, Poly(3,4-ethylenedioxythiophene)-modified Ni/silicon microchannel plate electrode for the simultaneous determination of ascorbic acid, dopamine and uric acid., *Analyst.* 138 (2013) 1149–1155.

- [195] D. Zheng, J. Ye, L. Zhou, Y. Zhang, C. Yu, Simultaneous determination of dopamine, ascorbic acid and uric acid on ordered mesoporous carbon/nafion composite film, *J. Electroanal. Chem.* 625 (2009) 82–87.
- [196] Y. Li, H. Lin, H. Peng, R. Qi, C. Luo, A glassy carbon electrode modified with MoS₂ nanosheets and poly(3,4-ethylenedioxythiophene) for simultaneous electrochemical detection of ascorbic acid, dopamine and uric acid, *Microchim. Acta.* 183 (2016) 2517–2523.
- [197] Y.-T. Shieh, Y.-A. Chen, R.-H. Lin, T.-L. Wang, C.-H. Yang, Temperature responsive carbon nanotubes/poly(N-isopropylacrylamide)-modified electrodes for electrochemical selective determination of dopamine, uric acid, and ascorbic acid, *Colloid Polym. Sci.* 290 (2012) 1451–1456.
- [198] P. Manivel, M. Dhakshnamoorthy, A. Balamurugan, N. Ponpandian, D. Mangalaraj, C. Viswanathan, Conducting polyaniline-graphene oxide fibrous nanocomposites: preparation, characterization and simultaneous electrochemical detection of ascorbic acid, dopamine and uric acid, *RSC Adv.* 3 (2013) 14428–14437.
- [199] M.U. Anu Prathap, R. Srivastava, Tailoring properties of polyaniline for simultaneous determination of a quaternary mixture of ascorbic acid, dopamine, uric acid, and tryptophan, *Sensors Actuators B Chem.* 177 (2013) 239–250.
- [200] X. Zheng, Y. Guo, J. Zheng, X. Zhou, Q. Li, R. Lin, Simultaneous determination of ascorbic acid, dopamine and uric acid using poly(L-leucine)/DNA composite film modified electrode, *Sensors Actuators B Chem.* 213 (2015) 188–194.
- [201] X. Liu, X. Ou, Q. Lu, J. Zhang, S. Chen, S. Wei, Electrochemical sensor based on overoxidized dopamine polymer and 3,4,9,10-perylenetetracarboxylic acid for simultaneous determination of ascorbic acid, dopamine, uric acid, xanthine and hypoxanthine, *RSC Adv.* 4 (2014) 42632–42637.
- [202] C. Xiao, X. Chu, Y. Yang, X. Li, X. Zhang, J. Chen, Hollow nitrogen-doped carbon microspheres pyrolyzed from self-polymerized dopamine and its application in simultaneous electrochemical determination of uric acid, ascorbic acid and dopamine., *Biosens. Bioelectron.* 26 (2011) 2934–2939.
- [203] A. Safavi, N. Maleki, O. Moradlou, F. Tajabadi, Simultaneous determination of dopamine, ascorbic acid, and uric acid using carbon ionic liquid electrode., *Anal. Biochem.* 359 (2006) 224–229.

- [204] X. Niu, W. Yang, H. Guo, J. Ren, F. Yang, J. Gao, A novel and simple strategy for simultaneous determination of dopamine, uric acid and ascorbic acid based on the stacked graphene platelet nanofibers/ionic liquids/chitosan modified electrode, *Talanta*. 99 (2012) 984–988.
- [205] A. Afraz, A.A. Rafati, M. Najafi, Optimization of modified carbon paste electrode with multiwalled carbon nanotube/ionic liquid/cauliflower-like gold nanostructures for simultaneous determination of ascorbic acid, dopamine and uric acid, *Mater. Sci. Eng. C*. 44 (2014) 58–68.
- [206] A.A. Rafati, A. Afraz, A. Hajian, P. Assari, Simultaneous determination of ascorbic acid, dopamine, and uric acid using a carbon paste electrode modified with multiwalled carbon nanotubes, ionic liquid, and palladium nanoparticles, *Microchim. Acta*. 181 (2014) 1999–2008.
- [207] Z. Temoçin, Modification of glassy carbon electrode in basic medium by electrochemical treatment for simultaneous determination of dopamine, ascorbic acid and uric acid, *Sensors Actuators B Chem*. 176 (2013) 796–802.
- [208] S.S. Shankar, B.E.K. Swamy, B.N. Chandrashekar, K.J. Gururaj, Sodium dodecyl benzene sulfate modified carbon paste electrode as an electrochemical sensor for the simultaneous analysis of dopamine, ascorbic acid and uric acid: A voltammetric study, *J. Mol. Liq*. 177 (2013) 32–39.
- [209] N. Baig, A.-N. Kawde, A cost-effective disposable graphene-modified electrode decorated with alternating layers of Au NPs for the simultaneous detection of dopamine and uric acid in human urine, *RSC Adv*. 6 (2016) 80756–80765.
- [210] L.Y. Haofan Sun, J. Chao, X. Zuo, S. Su, X. Liu, C. Fan, L. Wang, Gold nanoparticle-decorated MoS₂ nanosheets for simultaneous detection of ascorbic acid, dopamine and uric acid, *RSC Adv*. 4 (2014) 27625–27629.
- [211] D. Zhao, D. Fan, J. Wang, C. Xu, Hierarchical nanoporous platinum-copper alloy for simultaneous electrochemical determination of ascorbic acid, dopamine, and uric acid, *Microchim Acta*. 182 (2015) 1345–1352.
- [212] M. Li, W. Guo, H. Li, W. Dai, B. Yang, Electrochemical biosensor based on one-dimensional MgO nanostructures for the simultaneous determination of ascorbic acid, dopamine, and uric acid, *Sensors Actuators B. Chem*. 204 (2014) 629–636.

- [213] A.-M. O'Carroll, C.J. Fowler, J.P. Phillips, I. Tobbia, K.F. Tipton, The deamination of dopamine by human brain monoamine oxidase, *Naunyn. Schmiedebergs. Arch. Pharmacol.* 322 (1983) 198–202.
- [214] J.L. Ponchon, R. Cesuglio, F. Gonon, M. Jouvet, J.F. Pujol, Normal pulse polarography with carbon fiber electrodes for in vitro and in vivo determination of catecholamines, *Anal. Chem.* 51 (1979) 1483–1486.
- [215] Z. Wang, Q. Liang, Y. Wang, G. Luo, Carbon nanotube-intercalated graphite electrodes for simultaneous determination of dopamine and serotonin in the presence of ascorbic acid, *J. Electroanal. Chem.* 540 (2003) 129–134.
- [216] K. Starke, W. Reimann, A. Zumstein, G. Hertting, Effect of dopamine receptor agonists and antagonists on release of dopamine in the rabbit caudate nucleus in vitro, *Naunyn. Schmiedebergs. Arch. Pharmacol.* 305 (1978) 27–36.
- [217] J.-H. Kim, J.M. Auerbach, J.A. Rodríguez-Gómez, I. Velasco, D. Gavin, N. Lumelsky, et al., Dopamine neurons derived from embryonic stem cells function in an animal model of Parkinson's disease, *Nature.* 418 (2002) 50–56.
- [218] H.C. Fischer, W.C. Chan, Nanotoxicity: the growing need for in vivo study, *Curr. Opin. Biotechnol.* 18 (2007) 565–571.
- [219] A. Aggarwal, M. Hu, I. Fritsch, Detection of dopamine in the presence of excess ascorbic acid at physiological concentrations through redox cycling at an unmodified microelectrode array., *Anal. Bioanal. Chem.* 405 (2013) 3859–3869.
- [220] M.K. Zachek, P. Takmakov, B. Moody, R.M. Wightman, G.S. McCarty, Simultaneous decoupled detection of dopamine and oxygen using pyrolyzed carbon microarrays and fast-scan cyclic voltammetry., *Anal. Chem.* 81 (2009) 6258–6265.
- [221] M.K. Zachek, J. Park, P. Takmakov, R.M. Wightman, G.S. McCarty, Microfabricated FSCV-compatible microelectrode array for real-time monitoring of heterogeneous dopamine release., *Analyst.* 135 (2010) 1556–1563.
- [222] J.D. Fernstrom, M.H. Fernstrom, Tyrosine, phenylalanine, and catecholamine

synthesis and function in the brain., *J. Nutr.* 137 (2007) 1539S–1547S

- [223] L. Jiang, S. Gu, Y. Ding, D. Ye, Z. Zhang, F. Zhang, Amperometric sensor based on tricobalt tetroxide nanoparticles-graphene nanocomposite film modified glassy carbon electrode for determination of tyrosine., *Colloids Surf. B. Biointerfaces.* 107 (2013) 146–51.
- [224] Y. Fan, J.-H. Liu, H.-T. Lu, Q. Zhang, Electrochemistry and voltammetric determination of L-tryptophan and L-tyrosine using a glassy carbon electrode modified with a Nafion/TiO₂-graphene composite film, *Microchim. Acta.* 173 (2011) 241–247.
- [225] Q. Xu, S.-F. Wang, Electrocatalytic oxidation and direct determination of L-tyrosine by square wave voltammetry at multi-wall carbon nanotubes modified glassy carbon electrodes, *Microchim. Acta.* 151 (2005) 47–52.
- [226] C. Li, Voltammetric determination of tyrosine based on an L-serine polymer film electrode., *Colloids Surf. B. Biointerfaces.* 50 (2006) 147–51.
- [227] M. Arvand, T.M. Gholizadeh, Simultaneous voltammetric determination of tyrosine and paracetamol using a carbon nanotube-graphene nanosheet nanocomposite modified electrode in human blood serum and pharmaceuticals., *Colloids Surf. B. Biointerfaces.* 103 (2013) 84–93.
- [228] J.-B. He, G.-P. Jin, Q.-Z. Chen, Y. Wang, A quercetin-modified biosensor for amperometric determination of uric acid in the presence of ascorbic acid., *Anal. Chim. Acta.* 585 (2007) 337–43.
- [229] N.M. Felitsyn, G.N. Henderson, M.O. James, P.W. Stacpoole, Liquid chromatography-tandem mass spectrometry method for the simultaneous determination of delta-ALA, tyrosine and creatinine in biological fluids., *Clin. Chim. Acta.* 350 (2004) 219–230.
- [230] S. Bouchet, E. Chauzit, D. Ducint, N. Castaing, M. Canal-Raffin, N. Moore, et al., Simultaneous determination of nine tyrosine kinase inhibitors by 96-well solid-phase extraction and ultra performance LC/MS-MS., *Clin. Chim. Acta.* 412 (2011) 1060–1067.

- [231] M.C. Sanfeliu Alonso, L. Lahuerta Zamora, J. Martínez Calatayud, Determination of tyrosine through a FIA-direct chemiluminescence procedure., *Talanta*. 60 (2003) 369–376.
- [232] M. Lee, H. Nohta, Y. Umegae, Y. Ohkura, Assay for tyrosine hydroxylase by high-performance liquid chromatography with fluorescence detection., *J. Chromatogr.* 415 (1987) 289–296.
- [233] D.I. Sánchez-Machado, B. Chavira-Willys, J. López-Cervantes, High-performance liquid chromatography with fluorescence detection for quantitation of tryptophan and tyrosine in a shrimp waste protein concentrate., *J. Chromatogr. B. Analyt. Technol. Biomed. Life Sci.* 863 (2008) 88–93.
- [234] M. Sa, L. Ying, A.-G. Tang, L.-D. Xiao, Y.-P. Ren, Simultaneous determination of tyrosine, tryptophan and 5-hydroxytryptamine in serum of MDD patients by high performance liquid chromatography with fluorescence detection., *Clin. Chim. Acta.* 413 (2012) 973–977.
- [235] G. Neurauter, S. Scholl-Bürgi, A. Haara, S. Geisler, P. Mayersbach, H. Schennach, et al., Simultaneous measurement of phenylalanine and tyrosine by high performance liquid chromatography (HPLC) with fluorescence detection., *Clin. Biochem.* 46 (2013) 1848–1851.
- [236] X. Mo, Y. Li, A. Tang, Y. Ren, Simultaneous determination of phenylalanine and tyrosine in peripheral capillary blood by HPLC with ultraviolet detection., *Clin. Biochem.* 46 (2013) 1074–1078.
- [237] C. Bayle, N. Siri, V. Poinso, M. Treilhou, E. Caussé, F. Couderc, Analysis of tryptophan and tyrosine in cerebrospinal fluid by capillary electrophoresis and “ball lens” UV-pulsed laser-induced fluorescence detection., *J. Chromatogr. A.* 1013 (2003) 123–130.
- [238] Y. Huang, X. Jiang, W. Wang, J. Duan, G. Chen, Separation and determination of L-tyrosine and its metabolites by capillary zone electrophoresis with a wall-jet amperometric detection., *Talanta*. 70 (2006) 1157–1163.
- [239] Y. Tao, X. Zhang, J. Wang, X. Wang, N. Yang, Simultaneous determination of cysteine, ascorbic acid and uric acid by capillary electrophoresis with electrochemiluminescence, *J. Electroanal. Chem.* 674 (2012) 65–70.

- [240] M. Pumera, Graphene-based nanomaterials and their electrochemistry., *Chem. Soc. Rev.* 39 (2010) 4146–4157.
- [241] Y. Shao, J. Wang, H. Wu, J. Liu, I.A. Aksay, Y. Lin, Graphene Based Electrochemical Sensors and Biosensors: A Review, *Electroanalysis.* 22 (2010) 1027–1036.
- [242] M. Pumera, Graphene in biosensing, *Mater. Today.* 14 (2011) 308–315.
- [243] A.S. Razavian, S.M. Ghoreishi, A.S. Esmaily, M. Behpour, L.M. a. Monzon, J.M.D. Coey, Simultaneous sensing of L-tyrosine and epinephrine using a glassy carbon electrode modified with nafion and CeO₂ nanoparticles, *Microchim. Acta.* 181(2014) 1947-1955.
- [244] A. Babaei, S. Mirzakhani, B. Khalilzadeh, A Sensitive Simultaneous Determination of Epinephrine and Tyrosine using an Iron(III) Doped Zeolite-Modified Carbon Paste Electrode, *J. Braz. Chem. Soc.* 20 (2009) 1862–1869.
- [245] T. Madrakian, E. Haghshenas, A. Afkhami, Simultaneous determination of tyrosine, acetaminophen and ascorbic acid using gold nanoparticles/multiwalled carbon nanotube/glassy carbon electrode by differential pulse voltammetric method, *Sensors Actuators B Chem.* 193 (2014) 451–460.
- [246] C. Quintana, S. Suárez, L. Hernández, Nanostructures on gold electrodes for the development of an l-tyrosine electrochemical sensor based on host–guest supramolecular interactions, *Sensors Actuators B Chem.* 149 (2010) 129–135.
- [247] G. Zhao, Y. Qi, Y. Tian, Simultaneous and direct determination of tryptophan and tyrosine at boron-doped diamond electrode, *Electroanalysis.* 18 (2006) 830–834.
- [248] S.B. Revin, S.A. John, Selective determination of L-tyrosine in the presence of ascorbic and uric acids at physiological pH using the electropolymerized film of 3-amino-5-mercapto-1,2,4-triazole, *Sensors Actuators B Chem.* 161 (2012) 1059–1066.
- [249] Y.-R. Kim, S. Bong, Y.-J. Kang, Y. Yang, R.K. Mahajan, J.S. Kim, et al., Electrochemical detection of dopamine in the presence of ascorbic acid using graphene modified electrodes., *Biosens. Bioelectron.* 25 (2010) 2366–2369.

- [250] X. Ma, M. Chao, Z. Wang, Electrochemical detection of dopamine in the presence of epinephrine, uric acid and ascorbic acid using a graphene-modified electrode, *Anal. Methods*. 4 (2012) 1687–1692.
- [251] Y. Wang, Y. Li, L. Tang, J. Lu, J. Li, Application of graphene-modified electrode for selective detection of dopamine, *Electrochem. Commun.* 11 (2009) 889–892.
- [252] S.-Q. Liu, W.-H. Sun, F.-T. Hu, Graphene nano sheet-fabricated electrochemical sensor for the determination of dopamine in the presence of ascorbic acid using cetyltrimethylammonium bromide as the discriminating agent, *Sensors Actuators B Chem.* 173 (2012) 497–504.
- [253] B. Yu, D. Kuang, S. Liu, C. Liu, T. Zhang, Template-assisted self-assembly method to prepare three-dimensional reduced graphene oxide for dopamine sensing, *Sensors Actuators B Chem.* 205 (2014) 120–126.
- [254] Z. Zhuang, J. Li, R. Xu, D. Xiao, Electrochemical detection of dopamine in the presence of ascorbic acid using Overoxidized polypyrrole / graphene modified electrodes, *Int. J. Electrochem. Sci.* 6 (2011) 2149–2161.
- [255] S. Pruneanu, A.R. Biris, F. Pogacean, C. Socaci, M. Coros, M.C. Rosu, et al., The influence of uric and ascorbic acid on the electrochemical detection of dopamine using graphene-modified electrodes, *Electrochim. Acta.* 154 (2015) 197–204.
- [256] Y. Xue, H. Zhao, Z. Wu, X. Li, Y. He, Z. Yuan, The comparison of different gold nanoparticles/graphene nanosheets hybrid nanocomposites in electrochemical performance and the construction of a sensitive uric acid electrochemical sensor with novel hybrid nanocomposites., *Biosens. Bioelectron.* 29 (2011) 102–108.
- [257] Z. Zhang, J. Yin, Sensitive detection of uric acid on partially electro-reduced graphene oxide modified electrodes, *Electrochim. Acta.* 119 (2014) 32–37.
- [258] R. Akanda, M. Sohail, A. Aziz, A. Kawde, Recent advances in nanomaterial-modified pencil graphite electrodes for electroanalysis, *Electroanalysis.* (2016) 408–424.
- [259] M. Abdul Aziz, A.-N. Kawde, Gold nanoparticle-modified graphite pencil electrode for the high-sensitivity detection of hydrazine., *Talanta.* 115 (2013) 214–221.

- [260] F.Y. Ban, S.R. Majid, N.M. Huang, H.N. Lim, Graphene oxide and its electrochemical performance, *Int. J. Electrochem. Sci.* 7 (2012) 4345–4351.
- [261] P. Rattanarat, A. Suea-Ngam, N. Ruecha, W. Siangproh, C.S. Henry, M. Srisa-Art, et al., Graphene-polyaniline modified electrochemical droplet-based microfluidic sensor for high-throughput determination of 4-aminophenol, *Anal. Chim. Acta.* 925 (2016) 51–60.
- [262] J. Kudr, L. Richtera, L. Nejd, K. Xhaxhiu, P. Vitek, B. Rutkay-Nedecky, et al., Improved electrochemical detection of zinc ions using electrode modified with electrochemically reduced graphene oxide, *Materials (Basel).* 9 (2016) 31.
- [263] Y. Fang, E. Wang, Electrochemical biosensors on platforms of graphene., *Chem. Commun. (Camb).* 49 (2013) 9526–9539.
- [264] X. Tang, Y. Liu, H. Hou, T. You, Electrochemical determination of L-tryptophan, L-tyrosine and L-cysteine using electrospun carbon nanofibers modified electrode., *Talanta.* 80 (2010) 2182–2186.
- [265] G.-P. Jin, X. Peng, Q.-Z. Chen, Preparation of novel arrays silver nanoparticles modified polyrutin coat-paraffin-impregnated graphite electrode for tyrosine and tryptophan's oxidation, *Electroanalysis.* 20 (2008) 907–915.
- [266] J. Okuno, K. Maehashi, K. Matsumoto, K. Kerman, Y. Takamura, E. Tamiya, Single-walled carbon nanotube-arrayed microelectrode chip for electrochemical analysis, *Electrochem. Commun.* 9 (2007) 13–18.
- [267] E. Colín, S.C.- Avendaño, M.T. Ramírez, M. Romero-Romo, M. Palomar-Pardave, On the electrochemical oxidation of dopamine, ascorbic acid and uric acid onto a bare carbon paste electrode from a 0.1 M NaCl aqueous solution at pH 7, *Int. J. Electrochem. Sci.* 7 (2012) 6097–6105.
- [268] T. Ndlovu, O.A. Arotiba, S. Sampath, R.W. Krause, B.B. Mamba, Reactivities of modified and unmodified exfoliated graphite electrodes in selected redox systems, *Int. J. Electrochem. Sci.* 7 (2012) 9441–9453.
- [269] J.M.-G. Griselle Hernández-Cancel, Damaris Suazo-Dávila, K.G. María Rosado-González, Liz M. Díaz-Vázquez, Chemically glycosylation improves the stability of an amperometric horseradish peroxidase biosensor, *Anal. Chim. Acta.* 854 (2015) 129–139.

- [270] W. Zhu, T. Chen, X. Ma, H. Ma, S. Chen, Highly sensitive and selective detection of dopamine based on hollow gold nanoparticles-graphene nanocomposite modified electrode, *Colloids Surfaces B Biointerfaces*. 111 (2013) 321–326.
- [271] L.N. Qu, J. Wu, X.Y. Sun, M.Y. Xi, W. Sun, Application of multi-walled carbon nanotube modified carbon ionic liquid electrode for the voltammetric: detection of dopamine, *J. Chinese Chem. Soc.* 57 (2010) 701–707.
- [272] W. Sun, X. Wang, Y. Wang, X. Ju, L. Xu, G. Li, et al., Application of graphene–SnO₂ nanocomposite modified electrode for the sensitive electrochemical detection of dopamine, *Electrochim. Acta*. 87 (2013) 317–322.
- [273] Y.J. Yang, One step electrosynthesis of polyacrylamide crosslinked by reduced graphene oxide and its application in the simultaneous determination of dopamine and uric acid, *Electrochim. Acta*. 146 (2014) 23–29.
- [274] J. Tang, L. Zhang, Y. Liu, J. Zhou, G. Han, W. Tang, Gold nanoparticles- β -cyclodextrin-chitosan-graphene modified glassy carbon electrode for ultrasensitive detection of dopamine and uric acid, *Electroanalysis*. 26 (2014) 2057–2064.
- [275] S. Qi, B. Zhao, H. Tang, X. Jiang, Determination of ascorbic acid, dopamine, and uric acid by a novel electrochemical sensor based on pristine graphene, *Electrochim. Acta*. 161 (2015) 395–402.
- [276] X. Zhu, Y. Liang, X. Zuo, R. Hu, X. Xiao, J. Nan, Novel water-soluble multi-nanopore graphene modified glassy carbon electrode for simultaneous determination of dopamine and uric acid in the presence of ascorbic acid, *Electrochim. Acta*. 143 (2014) 366–373.
- [277] F. Zhang, Z. Wang, Y. Zhang, Z. Zheng, C. Wang, Y. Du, et al., Simultaneous electrochemical determination of uric acid, xanthine and hypoxanthine based on poly(L-arginine)/graphene composite film modified electrode., *Talanta*. 93 (2012) 320–5.
- [278] F.C. Koch, A new method uric acid, *J Biol Chem*. 130 (1939) 443–454.
- [279] M. H. Town et al., Uric Acid, *J. Clin. Chem. Clin. Biochem*. 23 (1985) 591–599.

- [280] Y. Zhao, X. Yang, W. Lu, H. Liao, Uricase based methods for determination of uric acid in serum, *Microchim Acta*. 164 (2009) 1–6.
- [281] X. Tian, C. Cheng, H. Yuan, J. Du, D. Xiao, S. Xie, et al., Simultaneous determination of L-ascorbic acid, dopamine and uric acid with gold nanoparticles- β -cyclodextrin-graphene-modified electrode by square wave voltammetry., *Talanta*. 93 (2012) 79–85.
- [282] J. Song, J. Qiao, S. Shuang, Y. Guo, C. Dong, Synthesis of neutral red covalently functionalized graphene nanocomposite and the electrocatalytic properties toward uric acid, *J. Mater. Chem.* 22 (2012) 602 – 608.
- [283] Y. Li, G. Ran, W.J. Yi, H.Q. Luo, N.B. Li, A glassy carbon electrode modified with graphene and poly(acridine red) for sensing uric acid, *Microchim. Acta*. 178 (2012) 115–121.
- [284] M. Wang, L. Bai, L. Zhang, G. Sun, X. Zhang, S. Dong, A microporous silk carbon–ionic liquid composite for the electrochemical sensing of dopamine, *Analyst*. 141 (2016) 2447–2453.
- [285] H. Kim, T. Kim, S. Hong, H. Kim, Direct detection of tetrahydrobiopterin (BH₄) and dopamine in rat brain using liquid chromatography coupled electrospray tandem mass spectrometry., *Biochem. Biophys. Res. Commun.* 419 (2012) 632–637.
- [286] A. Yildirim, M. Bayindir, Turn-on Fluorescent Dopamine Sensing Based on in Situ Formation of Visible Light Emitting Polydopamine Nanoparticles, *Anal. Chem.* 86 (2014) 5508 –5512.
- [287] P. Kanyong, S. Rawlinson, J. Davis, Simultaneous electrochemical determination of dopamine and 5-hydroxyindoleacetic acid in urine using a screen-printed graphite electrode modified with gold nanoparticles, *Anal. Bioanal. Chem.* (2016) 1–9.
- [288] L. Mercante, A. Pavinatto, L. Iwaki, V. Scagion, V. Zucolotto, O. Oliveira, L. Mattoso, D. Correa, Electrospun polyamide 6/poly(allylamine hydrochloride) nanofibers functionalized with carbon nanotubes for electrochemical detection of dopamine, *ACS Appl. Mater. Interfaces*. 7 (2015) 4784–4790.

- [289] S. Reddy, B. Swamy, H. Jayadevappa, CuO nanoparticle sensor for the electrochemical determination of dopamine, *Electrochim. Acta.* 61 (2012) 78–86.
- [290] X. Huang, Z. Yin, S. Wu, X. Qi, Q. He, Q. Zhang, Q. Yan, F. Boey, H. Zhang, Graphene-based materials: synthesis, characterization, properties, and applications., *Small.* 7 (2011) 1876–1902.
- [291] B. Liu, X. Ouyang, Y. Ding, L. Luo, D. Xu, Y. Ning, Electrochemical preparation of nickel and copper oxides-decorated graphene composite for simultaneous determination of dopamine, acetaminophen and tryptophan, *Talanta.* 146 (2016) 114–121.
- [292] R. Sivasubramanian, P. Biji, Preparation of copper (I) oxide nanohexagon decorated reduced graphene oxide nanocomposite and its application in electrochemical sensing of dopamine, *Mater. Sci. Eng. B.* 210 (2016) 10–18.
- [293] K. Deng, J. Zhou, X. Li, Noncovalent nanohybrid of cobalt tetraphenylporphyrin with graphene for simultaneous detection of ascorbic acid, dopamine, and uric acid, *Electrochim. Acta.* 114 (2013) 341–346.
- [294] A. Kawde, M. Aziz, N. Baig, Y. Temerk, A facile fabrication of platinum nanoparticle-modified graphite pencil electrode for highly sensitive detection of hydrogen peroxide, *J. Electroanal. Chem.* 740 (2015) 68–74.
- [295] D. Zhao, G. Yu, K. Tian, C. Xu, A highly sensitive and stable electrochemical sensor for simultaneous detection towards ascorbic acid, dopamine, and uric acid based on the hierarchical nanoporous PtTi alloy., *Biosens. Bioelectron.* 82 (2016) 119–126.
- [296] T. Xu, Q. Zhang, J. Zheng, Z. Lv, J. Wei, A. Wang, J. Feng, Simultaneous determination of dopamine and uric acid in the presence of ascorbic acid using Pt nanoparticles supported on reduced graphene oxide, *Electrochim. Acta.* 115 (2014) 109–115.
- [297] F. Gao, X. Cai, X. Wang, C. Gao, S. Liu, F. Gao, Q. Wang, Highly sensitive and

selective detection of dopamine in the presence of ascorbic acid at graphene oxide modified electrode, *Sensors Actuators, B Chem.* 186 (2013) 380–387.

- [298] T. See, A. Pandikumar, H. Ming, L. Ngee, Y. Sulaiman, Simultaneous electrochemical detection of dopamine and ascorbic acid using an iron oxide/reduced graphene oxide modified glassy carbon electrode, *Sensors (Basel)*. 14 (2014) 15227–15243.
- [299] W. Wang, Y. Cheng, L. Yan, H. Zhu, G. Li, J. Li, W. Sun, Highly sensitive electrochemical sensor for dopamine with a double-stranded deoxyribonucleic acid/gold nanoparticle/graphene-modified electrode, *Anal. Methods*. 7 (2015) 1878–1883.
- [300] G. Cancel, D. Dávila, J. Guzmán, K.G. M. González, L. Vázquez, K. Griebenow, Chemically glycosylation improves the stability of an amperometric horseradish peroxidase biosensor, *Anal. Chim. Acta*. 854 (2015) 129–139.
- [301] G. He, D. Wu, G. Xiao, Electrochemical detection of dopamine in the presence of ascorbic acid using GS @ Mn₃O₄/nafion film modified electrode at a low working potential, *Int. J. Electrochem. Sci.* 10 (2015) 10093–10103.
- [302] H. Mao, J. Liang, H. Zhang, Q. Pei, D. Liu, S. Wu, Y. Zhang, X. Song, Poly(ionic liquids) functionalized polypyrrole/graphene oxide nanosheets for electrochemical sensor to detect dopamine in the presence of ascorbic acid, *Biosens. Bioelectron.* 70 (2015) 289–298.
- [303] H. Xu, J. Xiao, L. Yan, L. Zhu, B. Liu, An electrochemical sensor for selective detection of dopamine based on nickel tetrasulfonate phthalocyanine functionalized nitrogen-doped graphene nanocomposites, *J. Electroanal. Chem.* 779 (2016) 92–98.
- [304] S. Li, Y. Wang, S. Hsiao, W. Liao, C. Lin, S. Yang, H. Tien, C. Ma, C. Hu, Fabrication of a silver nanowire-reduced graphene oxide-based electrochemical biosensor and its enhanced sensitivity in the simultaneous determination of ascorbic acid, dopamine, and uric acid, *J. Mater. Chem. C*. 3 (2015) 9444–9453.
- [305] X. Liu, W. Wang, X. Li, C. Li, L. Qin, J. Sun, S. Kang, Preparation of per-

hydroxylated pillar[5]arene decorated graphene and its electrochemical behavior, *Electrochim. Acta.* 210 (2016) 720-728.

- [306] L. Yang, D. Liu, J. Huang, T. You, Simultaneous determination of dopamine, ascorbic acid and uric acid at electrochemically reduced graphene oxide modified electrode, *Sensors Actuators B Chem.* 193 (2014) 166–172.
- [307] H. Zhang, Q. Huang, Y. Huang, F. Li, W. Zhang, C. Wei, et al., Graphitic carbon nitride nanosheets doped graphene oxide for electrochemical simultaneous determination of ascorbic acid, dopamine and uric acid, *Electrochim. Acta.* 142 (2014) 125–131.
- [308] B. Kaur, B. Satpati, R. Srivastava, Synthesis of NiCo₂O₄/Nano-ZSM-5 nanocomposite material with enhanced electrochemical properties for the simultaneous determination of ascorbic acid, dopamine, uric acid and tryptophan, *New J. Chem.* 39 (2015) 1115–1124.
- [309] C. Wang, R. Yuan, Y. Chai, S. Chen, F. Hu, M. Zhang, Simultaneous determination of ascorbic acid, dopamine, uric acid and tryptophan on gold nanoparticles/overoxidized-polyimidazole composite modified glassy carbon electrode, *Anal. Chim. Acta.* 741 (2012) 15–20.
- [310] Y.J. Yang, W. Li, CTAB functionalized graphene oxide/multiwalled carbon nanotube composite modified electrode for the simultaneous determination of ascorbic acid, dopamine, uric acid and nitrite, *Biosens. Bioelectron.* 56 (2014) 300–306.
- [311] J. Du, R. Yue, F. Ren, Z. Yao, F. Jiang, P. Yang, et al., Simultaneous determination of uric acid and dopamine using a carbon fiber electrode modified by layer-by-layer assembly of graphene and gold nanoparticles, *Gold Bull.* 46 (2013) 137–144.
- [312] S. Ge, F. Lan, F. Yu, J. Yu, Applications of graphene and related nanomaterials in analytical chemistry, *New J. Chem.* 39 (2015) 2380–2395.
- [313] H. Han, D. Pan, X. Wu, Q. Zhang, H. Zhang, Synthesis of graphene / methylene blue / gold nanoparticles composites based on simultaneous green reduction , in situ growth and self-catalysis, *J Mater Sci.* 49 (2014) 4796–4806.
- [314] Y. Song, Y. Luo, C. Zhu, H. Li, D. Du, Y. Lin, *Biosensors and Bioelectronics*

Recent advances in electrochemical biosensors based on graphene two-dimensional nanomaterials, *Biosens. Bioelectron.* 76 (2016) 195–212.

- [315] I.H. Kaplan, K. Dağci, M. Alanyalıoğlu, Nucleation and growth mechanism of electropolymerization of methylene blue: The effect of preparation potential on poly(methylene blue) structure, *Electroanalysis*. 22 (2010) 2694–2701.
- [316] E. Topçu, K. Dağci, M. Alanyalıoğlu, Free-standing graphene/poly(methylene blue)/AgNPs composite paper for electrochemical sensing of NADH, *Electroanalysis*. 28 (2016) 2058–2069.
- [317] L. Cao, Y. Liu, B. Zhang, L. Lu, In situ controllable growth of Prussian blue nanocubes on reduced graphene oxide: Facile synthesis and their application as enhanced nanoelectrocatalyst for H₂O₂ reduction, *ACS Appl. Mater. Interfaces*. 2 (2010) 2339–2346.
- [318] W. Sun, Y. Wang, Y. Zhang, X. Ju, G. Li, Z. Sun, Poly(methylene blue) functionalized graphene modified carbon ionic liquid electrode for the electrochemical detection of dopamine, *Anal. Chim. Acta*. 751 (2012) 59–65.
- [319] D.B. Gorle, M.A. Kulandainathan, Electrochemical sensing of dopamine at the surface of a dopamine grafted graphene oxide/poly(methylene blue) composite modified electrode, *RSC Adv*. 6 (2016) 19982–19991.
- [320] N. Barkoula, B. Alcock, N. Cabrera, T. Peijs, Fatigue properties of highly oriented polypropylene tapes and all-polypropylene composites, *Polym. Polym. Compos.* 16(2008)101–113.
- [321] L. Mei, J. Feng, L. Wu, J. Chen, L. Shen, Y. Xie, et al., A glassy carbon electrode modified with porous Cu₂O nanospheres on reduced graphene oxide support for simultaneous sensing of uric acid and dopamine with high selectivity over ascorbic acid, *Microchim. Acta*. (2016) 2039–2046.
- [322] W. Cai, J. Lai, T. Lai, H. Xie, J. Ye, *Sensors and Actuators B: Chemical* Controlled functionalization of flexible graphene fibers for the simultaneous determination of ascorbic acid, dopamine and uric acid, *Sensors Actuators B Chem.* 224 (2016) 225–232.
- [323] X. Zhang, Y. Zhang, L. Ma, *Sensors and Actuators B: Chemical* One-pot facile fabrication of graphene-zinc oxide composite and its enhanced sensitivity for

simultaneous electrochemical detection of ascorbic acid , dopamine and uric acid, *Sensors Actuators B. Chem.* 227 (2016) 488–496.

- [324] Y. Wang, Y. Huang, B. Wang, T. Fang, J. Chen, C. Liang, Three-dimensional porous graphene for simultaneous detection of dopamine and uric acid in the presence of ascorbic acid, *J. Electroanal. Chem.* 782 (2016) 76–83.

Vitae

Name :NADEEM BAIG |

Nationality :PAKISTANI |

Date of Birth :2/1/1984|

Email :nadeembaig@kfupm.edu.sa|

Address :KFUPM, student housing|

Academic Background :

B.S Chemistry (4-year program) Institute of Chemistry, University of Punjab, Lahore
Pakistan, 2008.

M.Phil. in Applied Chemistry, University of Engineering and Technology, Lahore
Pakistan. 2012.

Ph.D. in Chemistry, King Fahd University for Petroleum & Minerals, Dhahran, Saudi
Arabia, 2017 |

List of ISI Journal publications:

1. A. Kawde, M. Aziz, **N. Baig**, and Y. Temerk, “A facile fabrication of platinum nanoparticle-modified graphite pencil electrode for highly sensitive detection of hydrogen peroxide”, **Journal of Electroanalytical Chemistry**, 740 , 68-74, **2015**
2. M. Sajid, M. Ilyas, C. Basheer, M. Tariq, M. Daud, **N. Baig**, F. Shehzad “Impact of nanoparticles on human and environment: review of toxicity factors, exposures, control strategies, and future prospects” **Environmental Science and Pollution Research**, 22 4122-4143, **2015**
3. **N. Baig**, and A. Kawde “A novel, fast and cost effective graphene-modified graphite pencil electrode for trace quantification of l –tyrosine” **Analytical Methods**, 7, 9535-9541, **2015**
4. **N Baig**, and A. Kawde “A cost-effective disposable graphene-modified electrode decorated with alternating layers of Au NPs for the simultaneous detection of dopamine and uric acid in human urine” **RSC. Advances**, 6, 80756-80765, **2016**

5. A. Kawde, **N Baig**, and M. Sajid “Graphite pencil electrodes as electrochemical sensors for environmental analysis: a review of features, developments, and applications” **RSC. Advances**, 6, 91325-91340, **2016**
6. M. Altaf, S. Ahmad, A Kawde, **N. Baig**, A. Alawad, S. Altuwaijri, H. Stoeckli-Evans and A. Isab “Synthesis, structural characterization, electrochemical behavior and anticancer activity of gold(III) complexes of meso-1,2-di(1-naphthyl)-1,2-diaminoethane and tetraphenyl porphyrin” **New J. Chem.**, 40, 8288-8295, **2016**.
7. A. Kawde, M. Aziz, M. El-Zohri, **N. Baig**, N. Odewunmi “Cathodized Gold Nanoparticle-modified Graphite Pencil Electrode for Non-enzymatic Sensitive Voltammetric Detection of Glucose” **Electroanalysis**, 29, **2017**.

Filed Patents:

1. A. Kawde and **N. Baig** “Method for detecting l-tyrosine by using graphene-modified graphite pencil electrode system” **Application Ref # 449909US8**
2. A. Kawde and **N. Baig** and “A graphite electrode comprising electrochemically reduced graphene oxide and methods thereof” **Application Ref#471382US8**

Conferences:

1. **N. Baig**, and A. Kawde “Graphene-based single use cost-effective electrochemical sensors for monitoring of electroactive biomarkers in human body” **Chemindex, 2016**.
2. **N. Baig**, and A. Kawde “A single step fast and facile fabrication of the single use cost-effective reduced graphene oxide sensor for sensitive and selective determination of dopamine” **Research poster day KFUPM (Chemistry, 2016)**